Isolation, structures and properties of anthocyanins and wine pigments

by

Robert E. Asenstorfer

10 January 2001

Thesis submitted for the degree of

Doctor of Philosophy

University of Adelaide

Department of Horticulture, Viticulture and Oenology

Abstract

This study concerns the structures, equilibrium distributions and formation of pigments found in red wine. A revision of the macroscopic ionisation and hydration of malvidin-3-glucoside, and a determination of these constants for malvidin-3-(*p*-coumaryl)glucoside, and the wine pigment, vitisin A were made using a combination of high voltage electrophoresis (HVPE) and UV-visible spectroscopy.

The estimated ionisation constants of malvidin-3-glucoside are 1.76, 5.36, and 8.31 for pKa_1, pKa_2 and pKa_3 respectively, whilst the hydration constants are 2.66 and 5.90 for pK_{H1} and pK_{H2} respectively. The absorbance maximum of the flavylium ion is 518 nm, the hemiketal/chalcone is 276 nm and the quinonoidal dianion is 595 nm. The absorbance maxima of the quinonoidal anion are 444 nm and 578 nm. The measurement of the anthocyanin-bound glucose was used to determine the anthocyanin concentrations in solution. These were then used to provide an estimate of the molar absorption coefficient for the malvidin-3-glucoside at pH 0.0 in aqueous solution of 27 958 (± 500).

The ionisation constants of malvidin-3-(*p*-coumaryl)glucoside are 0.94, 4.45, and 8.66 for pKa_1, pKa_2 and pKa_3 respectively, whilst the hydration constants are 3.01 and 5.90 for pK_{H1} and pK_{H2} respectively. The absorbance maximum of the flavylium ion is 523 nm, the quinonoidal base is 5.28 nm, the hemiketal/chalcone is 281 nm, and the quinonoidal dianion is 594 nm. The absorbance maxima of the quinonoidal anion are 448 and 580 nm. The molar absorption coefficient of the malvidin-3-(*p*-coumaryl)glucoside flavylium ion at pH 0.0 in aqueous solution is 25 683 (± 233).

The estimated ionisation constants of vitisin A are 0.97, 3.56, 5.38 and 8.84 for pKa_1, pKa_2, pKa_3 and pKa_4 respectively, whilst the hydration constants were 4.37, 7.58 for pK_{H1} and pK_{H2} respectively. The absorbance maximum of the flavylium ion is 513 nm, the quinonoidal base is 498 nm, the hemiketal/chalcone is 503 nm, and the quinonoidal trianion is 599 nm. The molar absorption coefficient of the vitisin A flavylium ion at pH 0.0 in aqueous solution is 24 863 (± 1 807). The pKa and pK_H estimates as well as additional information from infra red analysis suggest that at wine pH vitisin A has a three ringed structure viz. malvidin-3-glucoside-4-(2-keto propionic acid).

Another important aspect of this study was an investigation of C4-substituted wine pigments. Vitisin A was used as a model compound in a study to gain an understanding of the mechanisms involved in the formation of these pigments during wine making. Vitisin A may be synthesised from pyruvate and malvidin-3-glucoside in the presence of an oxidant. The crucial time of vitisin A synthesis was during fermentation when there was a maximum concentration of both pyruvate and oxidant. The nature of the oxidant present in the wine during fermentation remains unknown.

A new method was developed for the isolation of C4-substituted pigments from wine and grape marc extracts which was based on the reactivity of anthocyanins with bisulphite ion to form anionic bisulphite addition products. Anthocyanins were partitioned according to their resistance to bisulphite addition using cation exchange chromatography. With this method the presence of several C4-substituted pigments in wines was confirmed.

Contents

List of Tables

Chapter 1

Chapter 2

Chapter 3

Chapter 4

Chapter 5

Chapter 6

Chapter 7

Chapter 8

List of Figures

Chapter 1

Chapter 2

Chapter 3

Chapter 4

Chapter 5

Chapter 6

Chapter 7

Chapter 8

Appendix B

Appendix C

Acknowledgments

Thanks to my principal supervisor Dr Graham Jones, and my co-supervisors, Mr Patrick Iland and Dr Elizabeth Waters for their helpful advice and guidance.

Dr Max Tate is gratefully acknowledged for his many suggestions, especially regarding the determination of pK values by HVPE and spectroscopic method.

I wish to acknowledge the help from the people at the AWRI especially, Dr Leigh Francis, Dr Weis Cynkar and Mariola Kwiatkowski for the help with the GG assays. Special thanks to Yoji Hayasaka for performing the mass spectrometry.

Thanks to David Botting, Patrick Iland, Anita Oberholster, Renata Ristic and Dr Andrew Markides for their help with the wine making. Thanks also to John Gray for advice with the measurement of the organic acids and sugars. I would also like to acknowledge the contribution made by Peter Asenstorfer for his technical assistance.

This project was funded by the Grape and Wine Research and Development Corporation and the Australian Research Committee.

Declaration

This thesis describes my research carried out in the Department of Horticulture, Viticulture and Oenology, the University of Adelaide and contains no material which has been accepted for the award of any other degree or diploma in any University. To the best of my knowledge this thesis contains no material previously published or written by any other person except where due reference is made in the text.

I give my consent for a copy of this thesis, when deposited in the Library of the University of Adelaide, to be available for loan and photocopying.

Robert Asenstorfer

List of publications arising from this thesis

Refereed Journals

Asenstorfer, R. E., Morgan, A. L., Hayasaka, Y., Sedgley, M., and Jones G. P. (2001) "A simple purification procedure for plant anthocyanins." *Phytochem. Anal.* (submitted)

Asenstorfer, R. E., Tate, M. E., and Jones, G. P. (2001) "Red wine colour, anthocyanin charge equilibria and pKas by electrophoresis." *J. Chem. Soc. Perkin II* (to be submitted)

Asenstorfer, R. E., Tate, M. E., Iland, P. G., Waters, E. J. and Jones, G. P. (2001) "Spectroscopic investigations of wine pigments. I. Malvidin-3-*O*-glucoside and malvidin-3-*O*-(6-*p*-coumaryl)glucoside." *J. Chem. Soc. Perkin II* (to be submitted)

Asenstorfer, R. E., Hayasaka, Y, Waters, E. J. and Jones, G. P. (2001) "Structures and isolation of red wine pigments" *J. Agric. Food Chem.* (submitted)

Asenstorfer, R. E., Iland, P. G., Markides, A. and Jones, G. P. (2001) " Synthesis of vitisin A during the wine making process." *Aust. J. Grape Wine Res.* (to be submitted)

Non-refereed conference and other publications

Jones, G. P., and Asenstorfer R. E. (1997) "Development of anthocyanin-derived pigments in young red wine." Proceedings ASVO Oenology Seminar: Phenolics and extraction, Wine titles, Adelaide, pp 33-37

Jones, G. P., Asenstorfer, R. E., Iland, P. G. and Waters, E. J. (1998) "Colour, phenolics and tannins in wine." Proceedings of the Tenth Australian Wine Industry Technical Conference Eds Blair, Sas, Hayes and Høj, Wine titles, Adelaide, pp 109-112

Asenstorfer, R. E., Cynkar, W., Francis, I. L. and Jones, G. P. (1999) "Determination of the extinction co-efficient of malvidin-3-glucose." Proceedings of the Tenth Australian Wine Industry Technical Conference eds Blair, Sas, Hayes and Høj Wine titles Adelaide p p 258

Asenstorfer, R. E., Hayasaka, Y., Iland, P. G. and Jones, G. P. (1999) "Isolation and purification of the wine pigment-vitisin A." Proceedings of the Tenth Australian Wine Industry Technical Conference eds Blair, Sas, Hayes and Høj, Wine titles Adelaide p p 258-259

Asenstorfer, R. E., Hayasaka, Y., Iland, P. G., Lambert, S. G., and Jones, G. P. (1999) "Wine phenolics: The development of pigments in red wine." Proceedings of the 1999 Conference of the New Zealand Society for Viticulture and Oenology, Auckland, Ed. G. Steans pp 83-87

Chapter 1

Literature Review

Introduction

A significant proportion of the colour of young red wine is derived from the anthocyanins extracted from the skin of red wine grapes (Ribéreau-Gayon, 1973). As time proceeds the importance of these grape anthocyanins in the expression of red wine colour declines and the pigment composition becomes progressively more complex (Somers and Vérette, 1988). Maintenance of wine colour is achieved by conversion of the extracted grape anthocyanins to more stable pigments (Somers, 1971).

It was originally proposed that the stable pigments in aged red wine consisted of polymeric pigments (Somers, 1971), resulting from the complexation of grape anthocyanins with other flavonoid phenolic compounds. However, a newly discovered group of non-polymeric grape anthocyanin derivatives are now thought to contribute to this pool of stable pigments (Fulcrand *et al.,* 1996b; Fulcrand *et al.,* 1998; Bakker and Timberlake, 1997; Bakker *et al.,* 1997). The importance of these wine pigments to colour stability merits further investigation.

Anthocyanins

The anthocyanins extracted from *Vitis vinifera* grapes are glycosides and the anthocyanin aglycones are generally referred to as the 2-phenylbenzopyrylium cations, or flavylium ions. The anthocyanins present in grapes and wine are derived from five aglycones; delphinidin, petunidin, malvidin, cyanidin and paeonidin (Ribéreau-Gayon, 1973; Figure 1.1).

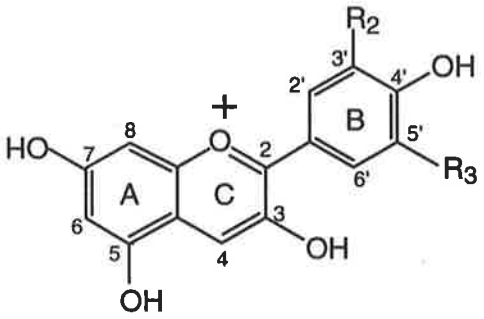

R_2=OH, R_3=H	Cyanidin
R_2=OH, R_3=OH	Delphinidin
R_2=OCH_3, R_3=H	Paeonidin
R_2=OCH_3, R_3=OH	Petunidin
R_2=OCH_3, R_3=OCH_3	Malvidin

Figure 1.1: Structures of the anthocyanin aglycones.

These polycyclic aromatic anthocyanidin structures may be present in the anthocyanin constituents as 3-mono-glycosides, or acylated heterosides. The acylated anthocyanins have either *p*-coumaric acid (Somers, 1966; Bakker and Timberlake, 1985), caffeic acid (Somers, 1966; Wulf and Nagel, 1978) or acetic acid (Fong *et al.*, 1971; Dallas and Laureano, 1994b) esterified with the hydroxyl on the sixth carbon of a glucose molecule (Hrazdina and Franese, 1974; Gueffroy *et al.*, 1971). Malvidin-3-glucoside (oenin) and its acylated derivatives account for 60-90% of total anthocyanins in *V. vinifera* grapes, usually with malvidin-3-glucoside as the dominant form (Bakker and Timberlake, 1985).

Various methods have been used to isolate malvidin-3-glucoside and malvidin-3-(*p*-coumaryl)glucoside. Willstätter and Zollinger (1916) were able to extract gram quantities of malvidin glucoside by extracting grape skins using dilute sulphuric acid, and subsequently extracting the dilute sulphuric acid solution with isoamyl alcohol. Although, Willstätter and

Zollinger (1916), and Levy *et al.,* (1931) were able to show that anthocyanin chlorides can then be crystallised from the isoamyl alcohol with diethyl ether, a superior crystallisation was achieved using a methanol solution.

Willstätter and Zollinger (1916) and Levy and Robinson (1931) report that differential partitioning of anthocyanins is obtained by washing the isoamyl alcohol with different concentrations of dilute hydrochloric acid. Thus, by extracting solutions of differing pH with isoamyl alcohol, it was possible to purify different anthocyanins from a mixture. Preliminary investigations for this thesis showed that if grape skins are extracted using 1% sulphur dioxide (SO_2) solution, and this solution was then extracted with isoamyl alcohol, the *p*-coumaryl derivative is preferentially extracted. However, the diethylether-induced precipitation of malvidin-3-glucoside from an alcoholic solution is favoured over the precipitation of the *p*-coumaryl derivative, and therefore malvidin-3-glucoside must be removed to obtain a pure sample of malvidin-3-(*p*-coumaryl)glucoside.

Structural transformations and the effect of pH

The colour intensity and hue of a wine depends on many factors, including the structure and concentration of the anthocyanins (Mazza and Miniati, 1993), the pH of the wine, and the concentration of sulphur dioxide and co-pigments (Somers and Vérette, 1988). The presence of hydroxyl groups, methoxyl groups, sugars, and acylated sugars in the structure of the anthocyanins also affects their colour intensity and stability.

Anthocyanins in aqueous solutions can donate protons and therefore act as Brønsted acids. Generally, the flavylium cation (A^+) is only stable at pH values lower than three (Brouillard and Cheminat, 1988). With increasing pH, the flavylium ion can either lose a proton to produce quinonoidal base structures (A_5, A_7, A_4'), or can hydrate to create the hemiketals (B_2 or B_2') and water-4-adduct (B_4). The hemiketals tautomerise and isomerise into the chalcones (C_{cis} and C_{trans}).

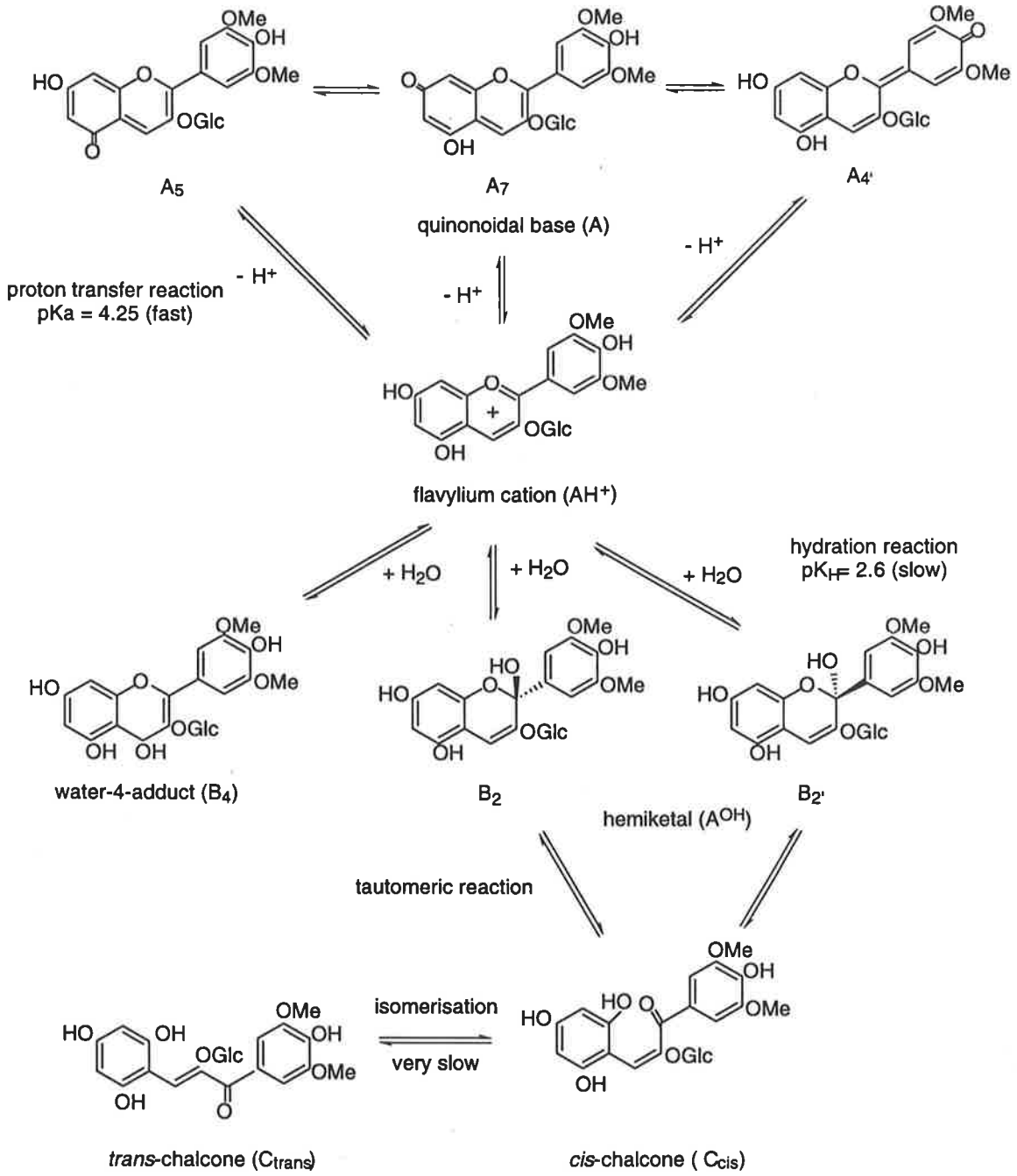

Figure 1.2: pH dependent equilibria of malvidin glucoside

(Cheminat and Brouillard, 1986; pK values from Brouillard and Delaporte, 1977).

In slightly acidic aqueous solutions, such as wine (pH 3.2 - 3.8), Cheminat and Brouillard, (1986; Figure 1.2), showed that malvidin glucoside exists as an equilibrium mixture of seven different structures including the flavylium ion (A^+), the quinonoidal base (A), the water 4 adduct (B_4), two isomers of the hemiketal, the *cis*-chalcone (C_{cis}) and *trans*-chalcone (C_{trans}). The three tautomers A_5, A_7, $A_{4'}$ exist in a very fast equilibrium (Cheminat and Brouillard, 1986) and therefore may be considered as a single quinonoidal base.

The elucidation of the structural transformations that the malvidin glucoside undergoes in aqueous conditions is important for the understanding of the colour of red wine. Furthermore, the ionisation and solvated states of anthocyanins in wine (pH 3.2 - 3.8) will determine the rates for the reactions that these compounds may participate. The Brønsted apparent ionisation constant, or pKa, supplies an estimate of the pH where significant concentrations of the flavylium ion and quinonoidal base concentrations co-exist. Similarly the apparent hydration constant, pK_H, provides a measure of the pH where significant concentrations of the hemiketal and water-4-adduct co-exist (Figure 1.2). The best estimates for the ionisation constants (pKa values) for malvidin-3-glucoside have been derived by Brouillard and Delaporte (1977) using temperature jump experiments. These authors derived a pKa value of 4.25.

Use of high voltage paper electrophoresis (HVPE) to determine ionisation constants

In their classic text, Rossotti and Rossotti (1961) outlined the application of electrophoresis to the determination of stability constants by observing the migration of one or more species. Markakis (1960) and Harborne (1989) have shown that anthocyanins exhibit some degree of electrophoretic mobility, however the possibility of proton equilibria in anthocyanins using this method has not been previously reported. Whilst high voltage paper electrophoresis (HVPE) has been principally used for the study of pH dependent metal ligand equilibria (Jokl, 1964a,b and 1972), the determination of ionisation constants by HVPE has been used by Tate (1981), Tate *et al.* (1982), Ryder *et al.* (1984) and Donner (1997). The method is capable of estimating the unknown ionisation constants of low molecular weight species by studying their electrophoretic mobility profile as a function

of pH. A good correlation of HVPE determined pKa values with the literature values has been determined for a number of compounds including; adenine, adenosine, 5'-adenosine monophosphate, 5'-adenosine diphosphate and 5'-adenosine triphosphate (Tate, 1981). An advantage of HVPE is that pKa estimates are based on molecular charge and do not rely on spectroscopic methods.

Another advantage of HVPE is that the concentrations used are similar to the concentrations of pigments found in wine. One of the problems using spectroscopic methods to determine pKa values is that relatively low concentrations are used, ie to determine a pKa value of malvidin-3-glucoside utilising temperature jump experiments, Brouillard and Delaporte (1977) used concentrations of 0.9×10^{-5} mol dm^{-3}. Young wines contain 0.95 - 7.2 gL^{-1} of total anthocyanin or $1.9 - 14.6 \times 10^{-3}$ mol dm^{-3} malvidin-3-glucoside equivalents (Somers, 1982) which is considerably greater than the concentration used b y Brouillard and Delaporte (1977). However, concentrations of 1×10^{-3} mol dm^{-3} are achievable using HVPE (Tate, 1981).

Estimation of hydration constants

The reactivity of anthocyanins is determined by the relative concentration of the various forms. The exact proportion of these forms depends not only on pH but also the structure of the anthocyanin (Timberlake and Bridle, 1967a; Mazza and Brouillard, 1987; Brouillard and Lang, 1990). The hydration and ionisation constants for malvidin-3-glucoside have been determined (Brouillard and Delaporte, 1977; Figure 1.2), however little is known regarding the values of these constants for either malvidin-3-(acetyl)glucoside or malvidin-3-(*p*-coumaryl)glucoside. Furthermore, Brouillard and Cheminat, (1988), Pina, (1998) and Cabrita *et al.* (2000) have speculated that anthocyanins show some stability at high pH (pH 8 - 10), This suggests that a dehydration of anthocyanins may occur at high pH, and therefore a second pK_H may be proposed. A spectroscopic study of malvidin-3-glucoside, that includes a pH range greater than 5 will supply a pH when this dehydration reaction occurs. Good estimates of the Brønsted apparent ionisation and hydration constants are important to ascertain the relative proportion of the various states of these anthocyanins in wine and ultimately to understand factors that influence the colour of wine.

Proton transfer reactions are fast reactions and therefore the formation of the quinonoidal base from the flavylium ion can be considered as a fast reaction. Brouillard and Delaporte (1977) estimated the deprotonation reaction rate to be 4.7×10^{4} s^{-1}. The competing reaction is the formation of the hemiketal. This reaction requires addition of water and is thought to be a slow reaction (Brouillard and Dubois, 1977). Using pH jump experiments, Brouillard and Delaporte (1977) determined rates constants of 0.95 (± 0.1) x 10^{-2} s^{-1}, and, 8.5 (± 0.1) x 10^{-2} s^{-1} or, half lives ($t_{1/2}$) of 72.95 s, and 8.15 s for the hydration of malvidin-3-glucoside flavylium ion at 4°C and 25°C, respectively. The difference in reaction rates may be used to obtain the spectrum of malvidin-3-glucoside at wine pH (3.2 - 3.8) in the absence of hydration.

Modern computing techniques coupled with a diode array spectrometer allows the measurement of a spectrum for a very short time period. This diode array spectrometer may be coupled with a flow cell similar to those used in HPLC apparatus. By pumping two solutions through the flow cell, the spectra of the resulting mixture may be obtained. The aim of this procedure is to minimise the retention time in the cell, and measure the spectra of only the species that form rapidly. Thus a solution containing the malvidin-3-glucoside flavylium ion was mixed with a buffered solution to obtain a pH of approximately 3.6. The difference in reaction rates between the ionisation and hydration will allow the measurement the spectrum and verify that it is the flavylium ion that contributes to the colour of wine.

Quantification of anthocyanins and the use of molar absorption coefficients

It is possible to estimate the concentration of an anthocyanin in a solution from its absorbance at a particular wavelength using the Beer-Lambert relationship,

$$\text{Absorbance} = \varepsilon l c \qquad \text{(Equation 1.1)}$$

where ε is the molar absorption coefficient, l is the pathlength in cm, c is the concentration in mol dm^{-3}. The advantage of using molar absorption coefficients is that this approach provides a relatively simple method for the quantification of anthocyanins. To obtain a good estimate for the concentration of an anthocyanin it is necessary of have the anthocyanin in a single state. Malvidin-3-glucoside, for example, exists primarily as the flavylium cation at pH < 0.5 (Timberlake, 1980). Niketic-Aleksic and Hrazdina (1972) estimated the concentration of malvidin-3-glucoside in grape juice and wine by acidifying the solution to pH 1, measuring the absorbance at 520 nm and using a molar absorption coefficient at 28 000. However, molar absorption coefficients estimates found in the literature may vary (Table 1.1).

Table 1.1: Values for the molar absorbance coefficient (ε) of malvidin-3-glucoside in water (H_2O) and methanol (MeOH) as reported by the indicated authors.

Author	Wavelength	Solvent	ε
Bakker *et al.* (1986)	520	H_2O	28 000
Nagel and Wulf (1979)	520	H_2O	27 455
Brouillard and Delaporte (1977)	520	H_2O	27 000
Somers and Evans (1977)	520	H_2O	26 455
Niketic-Aleksic and Hrazdina (1972)	520	H_2O	28 000
Koeppen and Basson (1966)	538	MeOH	29 500
Nagel and Wulf (1979)	539	MeOH	33 700

For the estimation of the molar absorption coefficient a pure sample is required. This usually requires a dehydration stage. The oxygen catalysed degradation of anthocyanins may occur. It is therefore proposed to use the glycosyl-glucose assay (Iland *et al.,* 1996) as a new approach for the estimation of the anthocyanin concentration. The glycosyl-glucose assay measures the concentration of glucose in solution, and therefore avoids dehydration and possibility of oxidation.

Co-pigmentation and self association

In 1916, Willstäter and Zollinger reported that when tannin was added to a solution of oenin chloride the colour intensified substantially. However, it was Robinson and Robinson (1931) who first proposed the effect of co-pigmentation, and their work showed that the most frequently occurring co-pigments for anthocyanins are tannins and flavone derivatives. Associated with the co-pigmentation of anthocyanins, there is an increase in colour intensity (hyperchromic effect) and a shift of the maximum absorbance towards longer wavelengths (bathochromic shift; Mazza and Miniatti, 1993). Mazza and Brouillard (1990) found that hydrophobic interactions are important forces in bringing the pigment and co-pigment in close contact, and this phenomenon is characteristic of aqueous solutions. The complexation is dominated by van der Waals interactions and hydrophobic effects in the aqueous medium resulting in π-π stacking of anthocyanin and co-pigment molecules (Liao *et al.,* 1992). The anthocyanin stabilisation is explained by strong attractive interactions between the different 'π' systems driven in the aqueous medium by hydrophobic effects. The main role of the co-pigment is that of controlling the extent of hydration reaction between the flavylium cation and the colourless hemiketal (Mazza and Miniati, 1993). Mistry *et al.* (1991) found that different co-pigments stabilise different forms of the anthocyanin. This suggests that the electron donating capacity of a phenolic co-substrate is also of importance in the preferential stabilisation of the anhydrobase (Asen *et al.,* 1972; Scheffeldt and Hradzdina, 1978).

Self association and intra-molecular co-pigmentation are special forms of co-pigmentation. Self association, is where an increase in pigment concentration is associated with a greater

than expected increase in colour (Asen *et al.*, 1972; Hoshino *et al.*, 1981). Intra-molecular co-pigmentation occurs when structural groups are covalently bonded to the anthocyanin unit. These groups form an intra-molecular π-π complex and thereby contribute to the colour intensity and stability of the anthocyanin (van Buren *et al.*, 1968; Brouillard, 1981). Furthermore, intramolecular co-pigmentation is associated with anthocyanins containing two or more aromatic acyl groups (Brouillard, 1981). There is no evidence that mono-acylated monoglucosides such as malvidin-3-(*p*-coumaryl)glucoside can participate in intra-molecular co-pigmentation.

Wine pigments

Wine pigments are derived from grape anthocyanins, and are formed either during fermentation or during the maturation process. These are newly identified compounds and their relative importance to wine remains unknown. There are six major wine pigments that have been identified (Fulcrand *et al.*, 1996b; Bakker and Timberlake, 1997; Fulcrand *et al.*, 1998), and all of these have malvidin-3-glucoside as part of their structure. Benabdeljalil (1998; 2000) has identified several other minor wine pigments.

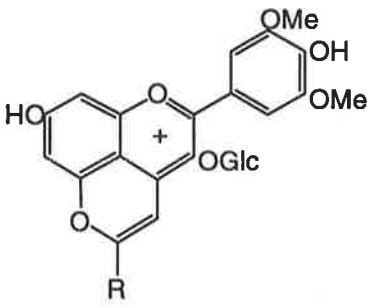

Figure 1.3: Basic structure of C-4 vinyl wine pigments.

The structure of C-4 vinyl wine pigments (Figure 1.3) is based on that of grape anthocyanins with a fourth ring attached to carbons 4 and 5. The carbon covalently bonded to the carbon 4 of the anthocyanin influences not only resistance to the formation of the bisulphite addition product but also production of the hemiketal (Timberlake and Bridle, 1967b). These types of compounds are also resistant to oxidation (Timberlake and Bridle, 1968). Thus as the wine matures and the grape derived anthocyanins degrade, it is expected that the importance of the contribution of C4-substituted anthocyanins to the colour of the wine will increase.

Pigments A and B

Fulcrand *et al.* (1996b) have described two anthocyanins that are formed by the covalent binding of either malvidin 3-mono-glucoside, or malvidin-3-(6-*p*-coumaryl)mono-glucoside, with *p*-vinylphenol (Fulcrand *et al.*, 1996b). The *p*-vinylphenol adduct of malvidin-3-*O*-glucoside is called pigment A while the *p*-coumaryl product is named pigment B. The structure yields two flavylium mesomeric forms; malvidin type and pelargonidin (Figure 1.4). Fulcrand *et al.* (1996b) suggest that pelargonidin form dominates, however the whole will act as a single chromophore.

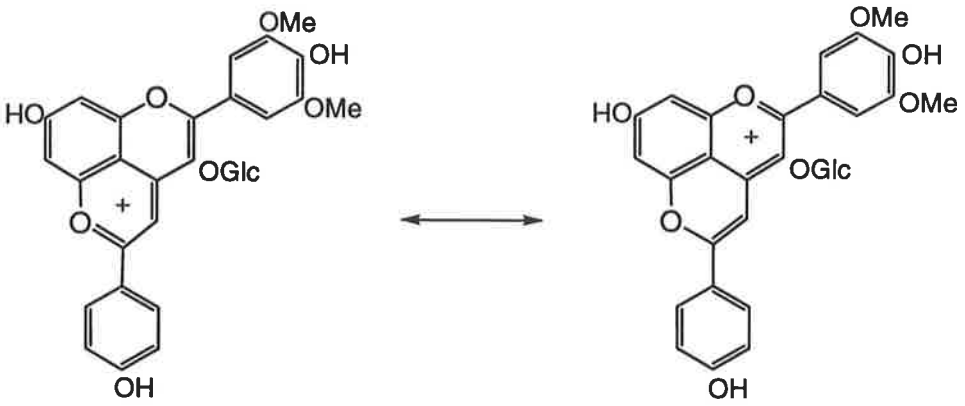

Figure 1.4: Mesomeric forms of pigment A (malvidin-3-glucoside bound with *p*-vinyl-phenol; Fulcrand *et al.*, 1996b).

In an early study of the production of vinyl phenols in beer, it was shown that *p*-vinyl-phenol is synthesised during the first three days of fermentation, and then at day 3 to 4 *p*-vinylphenol is reduced into *p*-ethylphenol (Figure 1.5; Steinke and Paulson, 1964). In wine Baumes *et al.* (1986) provided evidence that the yeast initially forms the *p*-vinylphenol, and the malo-lactic bacteria reduce the *p*-vinylphenol to form the *p*-ethyl phenol. However, *Saccharomyces cerevisiae* (Chatonnet *et al.*, 1993; Chatonnet *et al.*, 1997), *Lactobacillus plantarum* (Cavin *et al.*, 1993), *L. brevis* (Cavin *et al.*, 1993) and *Pedicoccus* sp. (Cavin *et*

al., 1993) are all capable of synthesising both *p*-vinylphenol and *p*-ethylphenol. *Leuconostoc oenos,* the major malo-lactic acid bacterium added to wine, only synthesises very small quantities of *p*-vinylphenol (Chatonnet *et al.,* 1995). Furthermore, procyanidins inhibit the production of volatile phenols by *S. cerevisiae, L. plantarum* and *L. brevis* (Chatonnet *et al.,* 1997) and therefore under normal red wine making conditions the levels of either *p*-vinylphenol or *p*-ethyl phenol in red wine should be low. However, the spoilage organisms *Brettanomyces/Dekkera* sp., which are usually associated with poor hygiene, are the main organisms responsible for the development of the volatile phenolic character in red wines (Chatonnet *et al.,* 1997). The final concentrations of Pigments A and B depend on the fermentation conditions, the level of procyanidins and the presence of certain spoilage organisms.

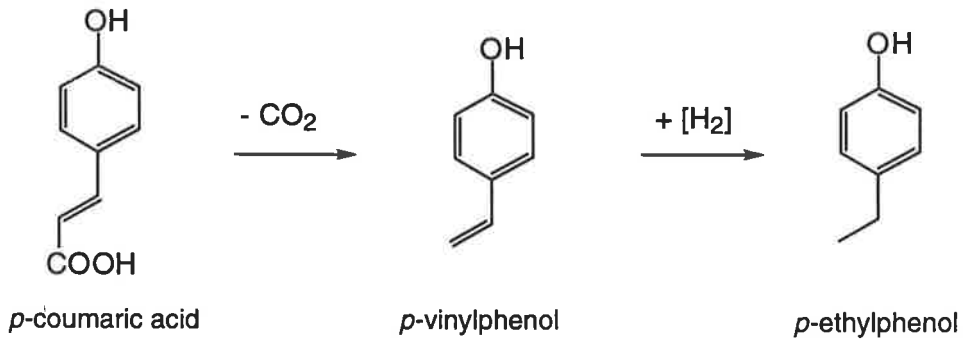

p-coumaric acid *p*-vinylphenol *p*-ethylphenol

Figure 1.5: Suggested pathway for the formation of *p*-vinylphenol. The synthesis involves two steps. The decarboxylation of *p*-coumaric acid to synthesise *p*-vinylphenol, and then the reduction of *p*-vinylphenol into *p*-ethylphenol.

Vitisins A and B

Bakker and Timberlake (1997) identified vitisin A and vitisin B (Figure 1.6, 1.9) as well as the acetyl-glycosides vitisin AX and BX in red fortified wine. Vitisin B is the simplest of the wine pigments. Bakker and Timberlake (1997) proposed that vitisins form during wine maturation. Furthermore, these authors proposed that although the concentration of vitisins

in wine is quite low these compounds are able to make a significant contribution to the wine colour because of their resistance to hydration reactions.

The structure for vitisin A (Figure 1.6a) was initially described by Bakker and Timberlake (1997) and Bakker *et al.* (1997). However, since the original publication of the structure of vitisin A, Cheynier *et al.* (1997a) proposed that the structure of vitisin A should be revised. In 1998, Fulcrand *et al.* published a description of the pyruvate adduct of malvidin-3-glucoside (Figure 1.6b) with identical properties to vitisin A. Since then Romero and Bakker (1999) were able to synthesise vitisin A from malvidin-3-glucoside and pyruvic acid. In this thesis, vitisin A will be used to describe the two possible structural isomers (Figure 1.6).

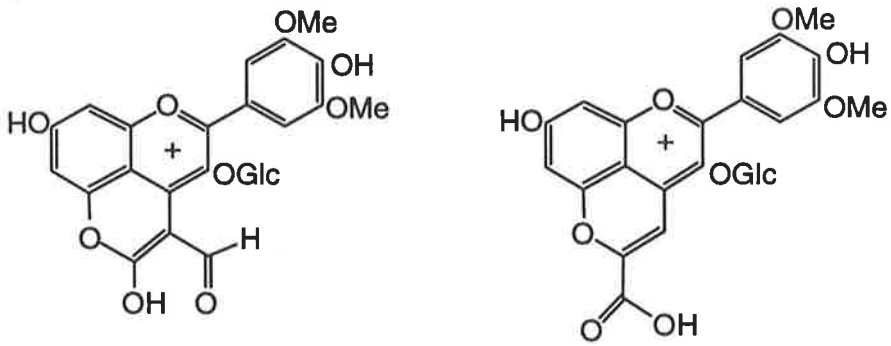

Figure 1.6: Structure of vitisin A (1.6a) as proposed by Bakker and Timberlake (1997) and (1.6b) as proposed by Cheynier (1997a).

The structure of vitisin A (Figure 1.6a) as proposed by Bakker and Timberlake (1997), and Bakker *et al.* (1997), is based mainly on data from both nuclear magnetic resonance (H^1 and C^{13} NMR) and fast atom bombardment mass spectrophotometry (FAB-MS). From the synthetic material, Cheynier *et al.* (1997a) and Fulcrand *et al.* (1998) described the alternative isomer (Figure 1.6b) using electrospray mass spectrometry (ES-MS), proton NMR and C^{13} NMR. The similarities between the UV-visible spectra, proton and C^{13} NMR the two isomers make it difficult to differentiate by these conventional methods.

Cheynier *et al.* (1997 a,b) proposed that the pyruvate adduct (Figure 1.6b) can be detected in the negative ion mode of the ion spray mass spectrometry, and therefore has a carboxylic acid functional group. However, using the Hammet and Taft equations, according to the methods outlined by Perrin *et al.* (1981), for the estimation of the pKa of the equivalent protons (Figure 1.8), the pKa values for these two alternative isomers is expected to be very similar (Appendix B).

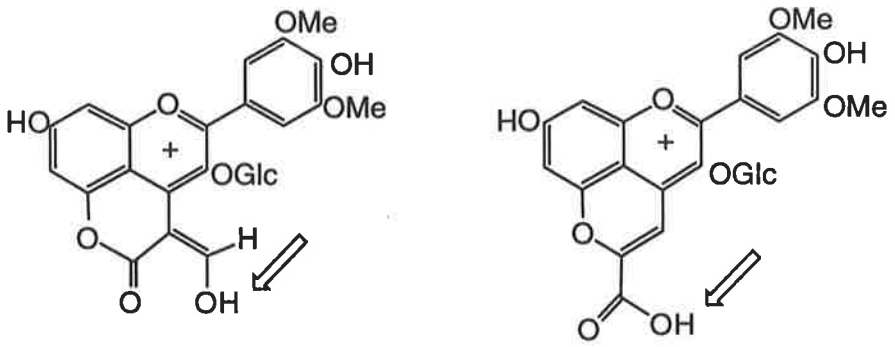

Figure 1.7: Equivalent protons of the two structural tautomers of vitisin A.

An important difference between these isomers is that the mass spectrum of the pyruvic acid adduct (Figure 1.6b; Cheynier *et al.*, 1997a,b; Fulcrand *et al.*, 1998) in the negative ion mode loses a component with a mass unit of 44 which corresponds to the loss of a carboxylic acid. Whilst the negative ion mass spectrum for isomer (Figure 1.6a) as proposed by Bakker and Timberlake (1997), and Bakker *et al.* (1997) has not been published, a loss of 44 mass units is not expected.

Another method that may be used to differentiate between the two proposed structures is infra-red spectroscopy. The region 1800-1600 cm^{-1} is considered the carbonyl region of the mid infra-red spectrum and the absence of other bands in this region makes it easy to study the carbonyl vibrational frequency (Josien *et al.*, 1953). The two structural tautomers are expected to have different carbonyl frequencies and therefore mid infra-red spectroscopy may be used to obtain further information regarding the structure of vitisin A.

The isolation of vitisin A from wine in sufficient quantities for a detailed chemical analysis has proven difficult. Bakker and Timberlake, (1997) and Bakker *et al.* (1997) were able to

isolate small quantities from wine using an acidified hydrophobic reverse phase (Sephadex LH 20) column. Spagna and Pifferi (1992) were able to achieve good separation of anthocyanins from other pigments using the cation exchange material, sulphoxyethyl cellulose. Charge differences between malvidin-3-glucoside and vitisin A as proposed by Cheynier *et al.* (1997a) may be exploited by utilising sulphoxyethyl cellulose as a semi-preparative step to improve the yield of vitisin A.

In this thesis, a preliminary survey of the pigments in wine identified a bisulphite resistant pigment (Figure 1.8). This pigment had identical UV-visible and mass spectral characteristics as vitisin A. Experiments were conducted to confirm the structure of this compound including the comparison of this pigment with the synthetic product of malvidin-3-glucoside and pyruvic acid (Fulcrand *et al.*, 1998). Moreover, the calculation of the molar absorbance coefficient using the glycosyl-glucose assay, protonation constants using high voltage paper electrophoresis and hydration constants using spectroscopic methods provided additional information regarding the structure of this pigment.

Vitisin A has been synthesised from malvidin-3-glucoside and pyruvic acid in model solutions (Cheynier *et al.*, 1997a; Benabdeljalil, 1998; Fulcrand *et al.*, 1998; Romero and Bakker, 1999). Pyruvic acid is formed by yeast during the fermentation process, and pyruvate accumulation occurs during the stationary phase of fermentation (Michnick *et al.*, 1997). It is therefore proposed that this pyruvate is available for the synthesis of vitisin A. Furthermore, pyruvate may be bound in the form of a bisulphite addition product (Burroughs, 1981). Slow release of pyruvate during maturation may also enable continued synthesis of vitisin A. Therefore, an investigation of the synthesis of vitisin A during the wine making process is desirable.

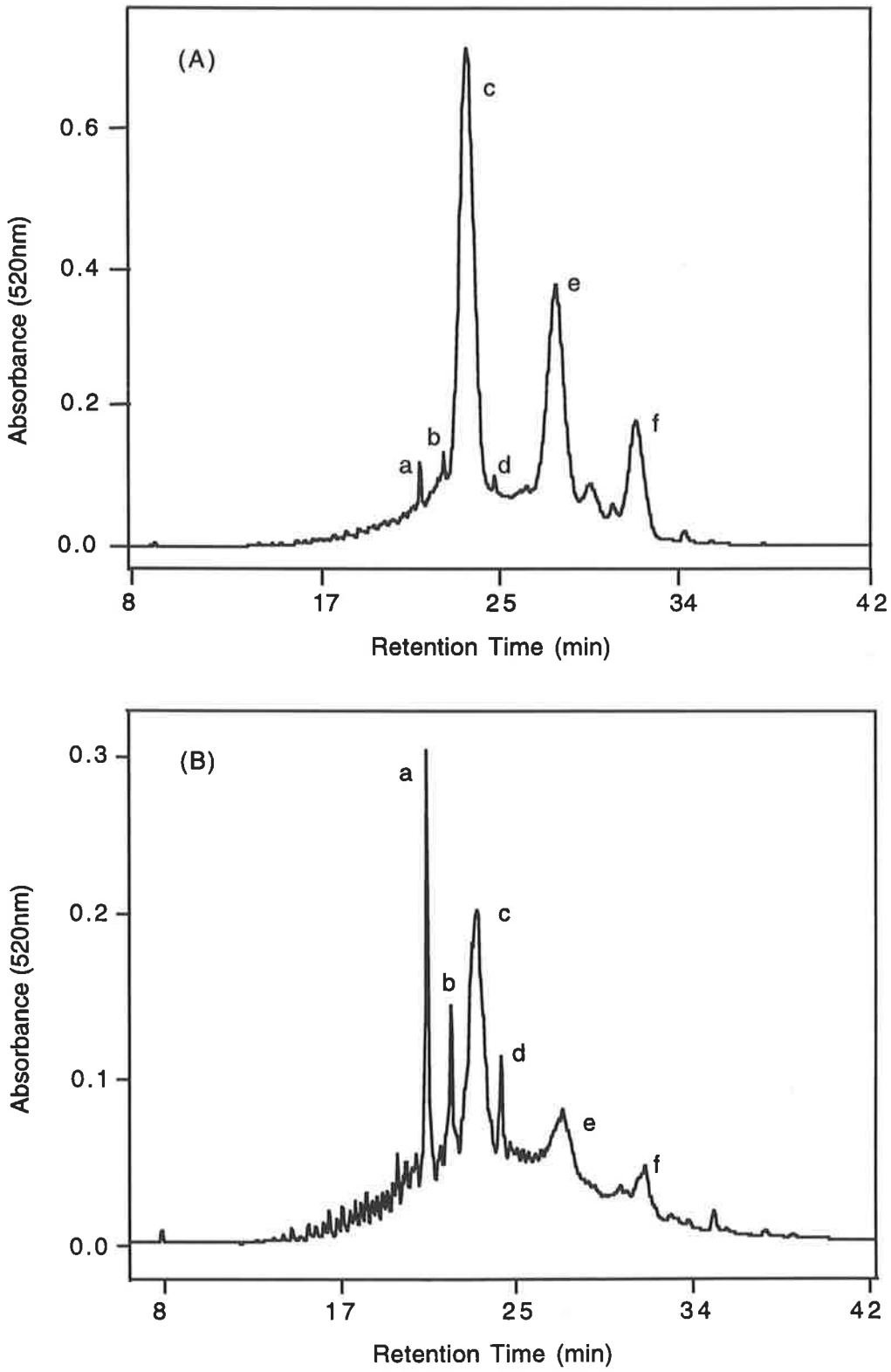

Figure 1.8: HPLC chromatograms of wines made from *Vitis vinifera* cv. Shiraz; (A) young wine (approx 2 months), (B) 2 year old wine (no malo-lactic fermentation). The peaks are (a) vitisin A, (b) acetyl-vitisin A, (c) malvidin-3-glucoside, (d) *p*-coumaryl-vitisin A, (e) malvidin-3-(acetyl)glucoside and (f) malvidin-3-(*p*-coumaryl)glucoside. (The HPLC technique is described in Chapter 2)

The structure of vitisin B (Figure 1.9) was described by Bakker and Timberlake (1997) using NMR data. and they considered that this compound was an acetaldehyde-adduct of malvidin glucoside. Vitisin BX is the acetylated glycoside of vitisin B. Bakker and Timberlake (1997) synthesised vitisin B in model solutions from malvidin-3-glucoside in the presence of acetaldehyde and white wine extract. The mechanism of vitisin B type pigment formation from anthocyanins and acetaldehyde was first proposed by Cheynier *et al.* (1997b). The structure of vitisin B was confirmed by hemisynthesis from malvidin-3-glucoside and acetaldehyde (Benabdeljalil, 1998; Benabdeljalil *et al.*, 2000). Within wine, acetaldehyde participates in a number of reactions and therefore it is difficult to estimate the potential for this reactant to participate in the formation of vitisin B.

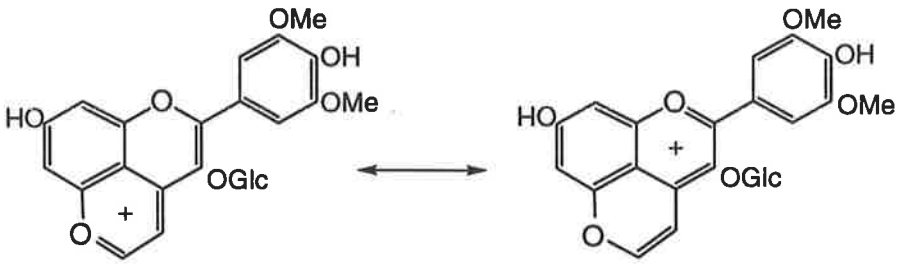

Figure 1.9: Structure of vitisin B as proposed by Bakker and Timberlake (1997).

Minor wine pigments

Benabdeljalil (Benabdeljalil, 1998; Benabdeljalil *et al.*, 2000) synthesised a series of pigments that included the acetone, the 2-oxo-glutarate (α-keto-glutarate) and 3-hydroxybutan-2-one adducts of malvidin-3-glucoside (Figure 1.10). Using mass spectrometry, Benabdeljalil (Benabdeljalil, 1998; Benabdeljalil *et al.*, 2000) also detected the acetone adducts in grape marc extracts. There is no reason to believe that either the 2-oxo-glutarate or the 3-hydroxybutan-2-one adducts cannot form in wine.

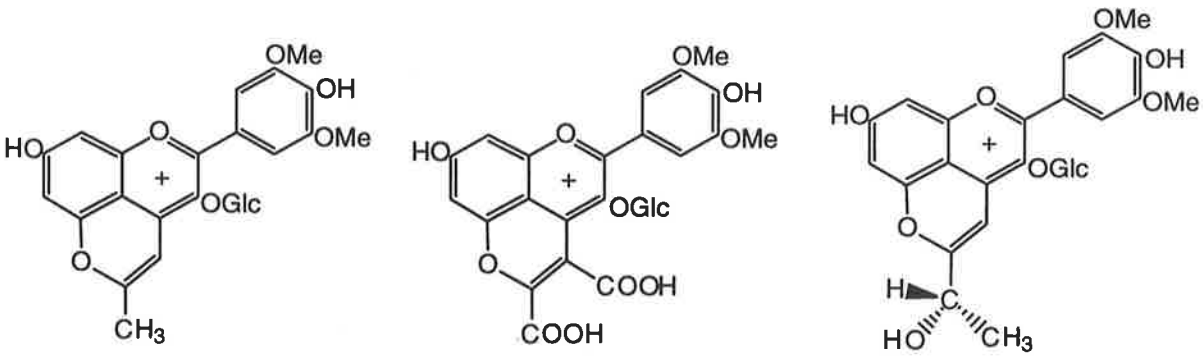

1.10a **1.10b** **1.10c**

Figure 1.10: Structures of the minor wine pigments; (1.10a) acetone adduct of malvidin-3-glucoside, (1.10b), 2-oxo-glutarate adduct of malvidin-3-glucoside and (1.10c) 3-hydroxybutan-2-one adduct of malvidin-3-glucoside as proposed by Benabdeljalil (1998).

Polymeric pigments

Somers (1971) found that the concentration of anthocyanins steadily declines during wine aging, and these anthocyanins are replaced by more stable polymeric pigments. The structures of these pigments in wine have not been determined (Johnson and Morris, 1996). To date, a knowledge of these polymeric pigments has remained mainly theoretical; however a brief resume of the different proposals is appropriate. The addition of anthocyanins to either catechins or procyanidins is thought to come about by two main mechanisms; one with and one without acetaldehyde. In wine, the levels of acetaldehyde are relatively low, and therefore, it has been proposed that both acetaldehyde bridging and non-acetaldehyde bridging reactions occur simultaneously Baranowski and Nagel (1983).

Non-acetaldehyde bridging reactions

The mechanism proposed by Somers (1971; Figure 1.11), involves the direct reaction of the anthocyanin with the catechin. This is similar, in principle, to the method for the formation of procyanidins in plants. Plant procyanidins are formed from flavan-3,4-diols and catechins (Kristiansen, 1984). The link between the monomers is called an interflavan bond. By analogy with plant procyanidins, Somers (1971) proposed the linking of the C4 carbon of the anthocyanin with either the C6 or C8 positions of the flavan-3-ol via an interflavan bond.

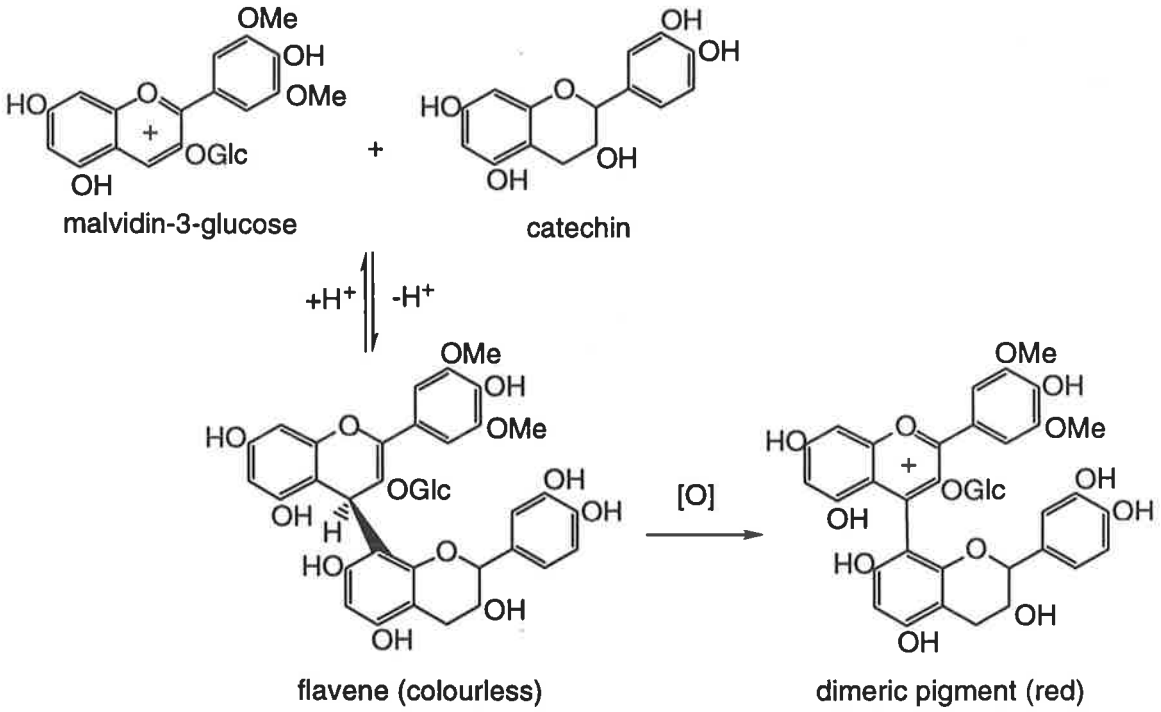

Figure 1.11: Method of malvidin-3-glucoside and catechin coupling via the interflavan bond to yield a dimeric pigment as proposed by Somers (Allen, 1996).

Jurd (1969) proposed a polymeric pigment formed where either the catechin flaven-3-en-ol or carbonium ion reacts with the anthocyanin flavene at the 6 or 8 position followed b y oxidation. Using a combination of mass spectrometry and thiolysis, Remy *et al.* (2000) have detected the presence of such anthocyanin derived pigments where catechin is linked to the C-6 or C-8 positions of malvidin-3-glucoside. These authors propose that the catechin carbonium ion reacts with the hemiketal and subsequent dehydration to form the pigment.

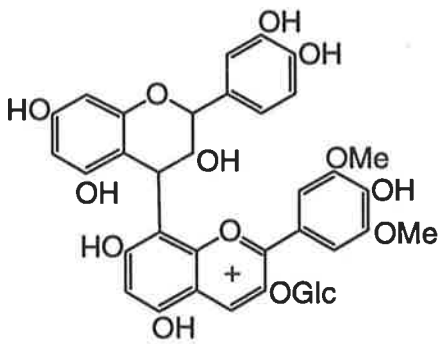

Figure 1.12: Polymeric pigment as identified by Remy *et al.*, (2000)

Acetaldehyde-bridging reactions

It is proposed that acetaldehyde acts as an intermediary for tannin/anthocyanin condensation by a Baeyer type reaction (phenol-formaldehyde-Novolak) in which CH-CH_3 (ethyl) bridges are formed between phloroglucinol rings (Timberlake and Bridle, 1967a; Somers, 1971; Haslam, 1980; Bakker *et al.*, 1993), in a similar mechanism to that when acetaldehyde acts as an intermediary in flavan-3-ol condensation (Fulcrand *et al.*, 1996a; Figure 14).

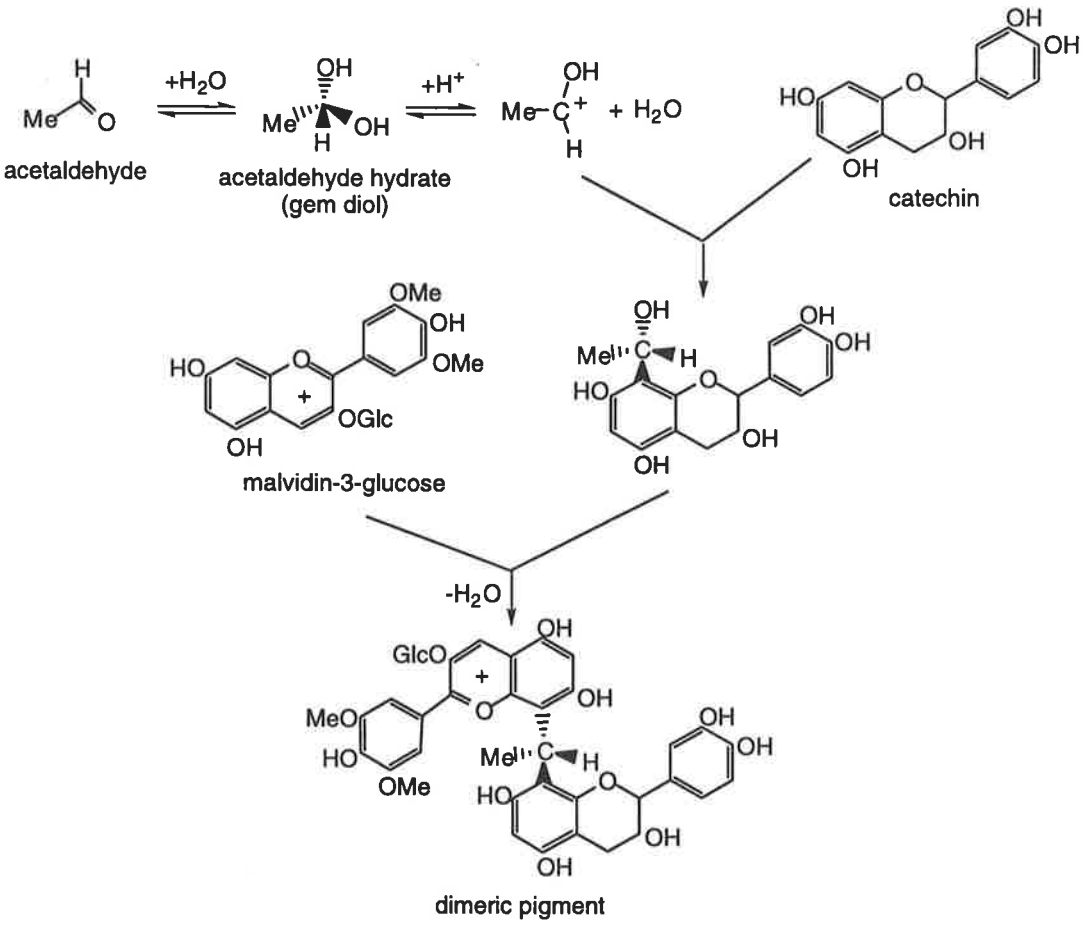

Figure 1.13: Pathway for the condensation of malvidin-3-glucoside and catechin using an acetaldehyde bridge to create a pigmented dimer (Adapted from Timberlake and Bridle, 1967a).

García-Viguera *et al.* (1994) have clearly shown that malvidin glucoside and catechin in the presence of acetaldehyde rapidly form a polymer in model solutions. Furthermore, it is has

been proposed that the initial dimer has a ethyl bridge between the two flavonoid molecules in the C8 positions (Escribano-Bailón *et al.*, 1996), although Dournel (cited by Mazza and Miniati, 1993) reported that ethyl bridges occur with the same probability between C8/C8, C8/C6, and C6/C6 positions. Using a combination of liquid chromatography and mass spectroscopy, and Cheynier *et al.* (1997c) and Revilla *et al.* (1999) identified ethyl-bridged malvidin-catechin dimers and malvidin-catechin trimers in red wine.

With the discovery of the vitisins, there has been interest in similar types of pigments containing a vinyl linkage between the anthocyanin and catechin moieties. In this thesis, these pigments were called C-4 vinyl pigments to differentiate this group of pigments from the other polymeric pigments described. Using model solutions, Francia-Aricha *et al.* (1997) have synthesised a compound, B2-III (Figure 1.14), from acetaldehyde, malvidin-3-glucoside and procyanidin B2. This compound has spectroscopic and chromatographic properties similar to compounds found in wine and therefore these authors have concluded that their compound is likely to be present in wine.

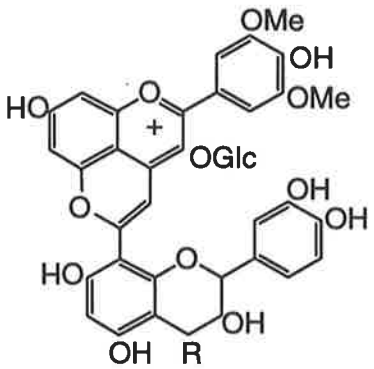

Figure 1.14: Proposed structure of B2-III (Francia-Aricha *et al.*, 1997; R = epicatechin).

The reaction of acetaldehyde with catechin, or procyanidins, can yield vinyl type compounds. The mechanism for the formation of the vinyl bridged pigments is thus thought to be via vinyl catechin or vinyl procyanidin intermediates. These compounds contain an A ring that is analogous to *p*-vinylphenol (Figure 1.15). Therefore it can be proposed that

these vinyl intermediates react with malvidin-3-glucoside in a similar way as *p*-vinylphenol addition to form pigment A.

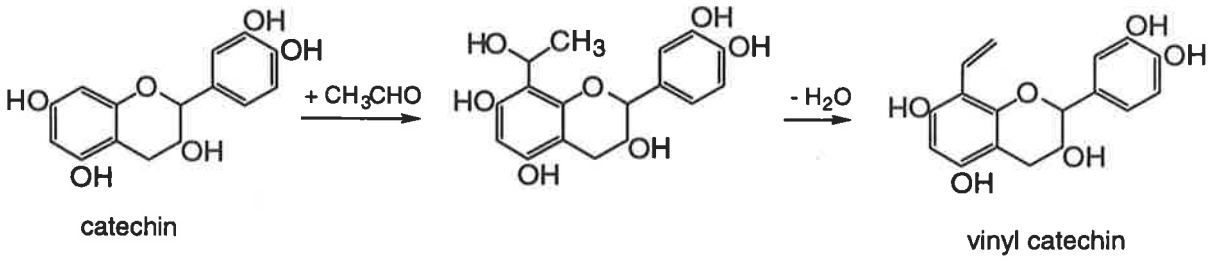

catechin

vinyl catechin

Figure 1.15: Proposed mechanism for the formation of vinyl catechin from the addition of acetaldehyde to catechin.

Bisulphite addition as a method for isolating complex wine pigments

In solution, sulphur dioxide hydrates to form the bisulphite anion. Anthocyanins combine with the bisulphite ions to give a stable, colourless, addition products. Nucleophilic addition of the bisulphite ion, HSO_3^-, to the flavylium (2-phenylbenzopyrylium) cation results in the formation of a σ-complex of the Meisenheimer type (Brouillard and Hage-Chahine, 1980). Using proton (^1H), carbon (^{13}C) and sulphur (^{33}S) nuclear magnetic resonance (NMR) spectroscopy Berké *et al.* (1998) established that the bisulphite ion adds to the 4 position. The bisulphite addition occurs in a conjugate fashion (Timberlake and Bridle, 1967a), to yield chromen-4-sulphonic acid (Figure 1.16).

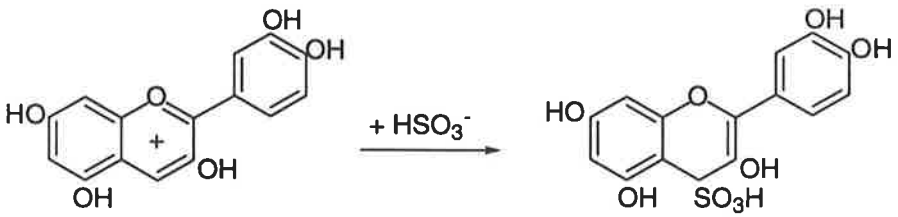

cyanidin chromen-4-sulphonic acid

Figure 1.16: Addition of the bisulphite ion to cyanidin to produce chromen-4-sulphonic acid.

Somers (1971) considered that the polymeric pigments have catechin or procyanidin groups directly linked to the C4 position of the anthocyanin. The recent isolation of C4-substituted pigments from wine (Bakker and Timberlake, 1997; Bakker *et al.*, 1997; Fulcrand *et al.*, 1996a) and grape marc (Fulcrand *et al.*, 1998; Benabdeljalil, 1998) further suggests that C4-substitution may be an important feature of the larger pigments. While the non-substituted C4 anthocyanins react with bisulphite to form the colourless addition products, the C4-substituted anthocyanins are bisulphite resistant (Timberlake and Bridle, 1968). By analogy, it is therefore proposed that the non-substituted C4 polymeric pigments are able to react readily with the bisulphite ion, while the C4-substituted anthocyanins are resistant to bisulphite addition. Thus, by utilising this difference in

reactivity, bisulphite addition has the potential of providing new methods for the isolation of pigments from wine.

The formation of anionic hydroxy sulphonic acids from ketones and aldehydes can be considered to be analogous to the formation of the anthocyanin-bisulphite addition product (Figure 1.17). Using paper ionophoresis and capillary electrophoresis, Theander (1957) and Aguin *et al.* (1993) showed that neutral aldehydes in the presence of bisulphite form strong acids that were anionic under the conditions used. Therefore, by adapting the methods of Theander (1957) and Aguin *et al.* (1993) it may be possible to develop anion exchange as a method for the isolation of anthocyanin type compounds.

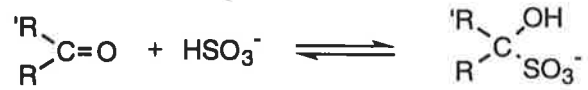

Figure 1.17: Formation of hydroxy sulphonic acid (Theander, 1957).

Furthermore, while bisulphite addition products are considered to be stable compounds (Adams and Woodman, 1973), the bisulphite anthocyanin equilibria are pH dependent (Burroughs, 1975). A better knowledge of the bisulphite and anthocyanin equilibrium, will allow the development of new methods for the isolation of wine pigments. The isolation and identification of these pigments will provide a basis for future research.

Chapter 2

Materials and Methods

Materials

All solvents were of analytical grade except the isoamyl alcohol which was bulk grade supplied by Ajax Chemicals. Specific reagents chemicals and buffers used were analytical grade and supplied by BDH Chemicals Ltd., (Poole, England) unless indicated.

The malvidin-3-glucoside standard for HPLC was supplied by Carl Roth GmbH and Co (Karlsruhe, Germany).

The C18 chromatography material was supplied by Alltech Associates (Deerfield, Illinios, USA) except for the Sep-Pak Classic cartridges which were supplied by Waters Corporation, (Milford, Massachusetts, USA). The sulphoxyethyl-cellulose material and Sephadex LH 20 were supplied by Sigma (Castle Hill, NSW, Australia).

For wine making the grapes used were *Vitis vinifera* cv. Shiraz and unless otherwise indicated were sourced from a commercial vineyard at Lyndoch, South Australia. The chemicals used for the wine making were all food grade.

Methods for isolation and purification

Malvidin-3-glucoside

Approximately 100 g of Shiraz grape skins were extracted with 200 mL of isoamyl alcohol for 48 h at 25°C. The isoamyl alcohol was decanted from the skins, and the skins washed with a further 200 mL of isoamyl alcohol. These two fractions were combined and the isoamyl alcohol volume reduced to approximately 200 mL by rotary evaporating at 60°C utilising water as an azeotrope. The solution was cooled to room temperature, and diethyl ether added until the solution became cloudy (opaque). This solution was allowed to stand at 4°C for 12 h, during which time a precipitate formed. The isoamyl alcohol was decanted from the precipitate. The volume of the decanted isoamyl alcohol was further reduced, and the procedure for precipitation repeated.

Each precipitate was suspended in a minimal volume of slightly acidified methanol (0.1%. HCl) and the solutions combined. Diethyl ether was added to the methanol solution until the solution became opaque. The methanol/diethyl ether solution was cooled for 12 h during which time a precipitate formed. The crystals were removed from the solution by centrifugation for 10 min. The crystals were then resuspended in a minimal volume of acidified methanol, precipitated with diethyl ether and isolated using centrifugation. This procedure was repeated twice. The purity of the material from the final crystallisation was analysed using the HPLC method described below. It was considered compounds containing no more than 10% impurities were adequate for future analyses.

Malvidin-3-(*p*-coumaryl)glucoside

Approximately 100 g of skins obtained from Shiraz grapes sourced from Eden Valley, South Australia, were extracted using 1% sulphur dioxide solution at 80°C for 1 h. Isoamyl alcohol was used to extract the malvidin-3-(*p*-coumaryl)glucoside from the solution by cold liquid/liquid separation in a separating funnel. The crude extract was washed three times

with isoamyl alcohol. Because malvidin-3-glucoside is preferentially precipitated from solution, it must be removed to obtain a pure sample of malvidin-3-(*p*-coumaryl)glucoside. Therefore the isoamyl alcohol extract was washed with 1% sulphur dioxide solution three times to remove any malvidin-3-glucoside present in the isoamyl alcohol. The isoamyl alcohol solution was concentrated by rotary evaporation using water as an azeotrope. When sufficiently concentrated the isoamyl alcohol was cooled to 4°C, a small amount of HCl (approx 0.5 mL/litre) added and then diethyl ether added until cloudy. After approximately 12 h, the malvidin-3-(*p*-coumaryl)glucoside precipitate was separated by centrifugation as described above. The separated precipitate was dissolved in 5 mL methanol and 45 mL water added. This solution was then cleaned using a 25 g C18 column (30 x 25 mm) to remove some minor impurities identified by HPLC. The resultant methanolic malvidin-3-(*p*-coumaryl)glucoside was further purified by repeated crystallisation from methanol. Each crystallisation was monitored using HPLC and a purity greater than 90% was considered sufficient for future analyses.

Vitisin A

Approximately 11.25 litres of four year old wine made from Shiraz, sourced from the Riverland, South Australia, was concentrated using both rotary evaporation and reverse phase C18 chromatography. The C18 column consisted of 50 g of material loaded in a 100 mm Buchner funnel with diatomaceous earth as supporting material. The material retained on this column was eluted using methanol. The methanol eluent (wine concentrate) was further concentrated using rotary evaporation until almost dryness and then water was added to give a volume of 200 mL.

Approximately 50 mL of the above wine concentrate was loaded onto a sulphoxyethyl-cellulose column (40 x 200 mm) prepared according to the method outlined by Spagna and Pifferi (1992). Vitisin A and its acetyl form were eluted from the column using 10% methanol. The column was cleaned using 2 L of 2 mol dm^{-3} NaCl and 50% (v/v) aqueous methanol. The method was repeated four times.

Methanol was removed from the crude vitisin extract by rotary evaporation. The material dissolved into water and then loaded onto a C18 column (Buchner funnel). The pigment was eluted with methanol, and further concentrated using rotary evaporation. The extract was then applied to a Sephadex LH 20 (32.5 x 540 mm) column. Vitisin A was eluted as the first coloured band with a 10% (v/v) aqueous methanol solution. This band was concentrated using a 25 g reverse phase C18 column (30 x 25 mm). The pigment was eluted from the C18 column using methanol.

Using preparative reverse phase thin layer chromatography (TLC) plates (KC 18; Whatman, Clifton, New Jersey, USA) the vitisin A pigment was isolated using 50% (v/v) aqueous methanol. A band at R_f 0.59 was eluted from the plate using a solution of 50% (v/v) aqueous methanol and 0.1 mol dm^{-3} HCl. The methanol was evaporated and the compound was purified using a C18 cartridge (Sep-Pak Classic). The purity of vitisin A was checked using HPLC, and the sample analysed using mass spectrometry by direct injection.

A second method was developed whereby the methanol from a concentrate of crude vitisin A was evaporated and water added until there was approximately 5-10% (v/v) aqueous methanol. This solution was loaded onto a prepared C18 column (170 x 30 mm). The column was washed with water and then eluted with 25% (v/v) aqueous methanol. The first coloured band was collected, and the purity of vitisin A was analysed using HPLC.

Wine pigments

Using the same wine sample that was used for the isolation of vitisin A, after the fraction containing vitisin A was eluted from the column using 10% (v/v) aqueous methanol, the wine pigment retained on the sulphoxyethyl cellulose column was removed using a solution of 2 mol dm^{-3} NaCl and 50% (v/v) aqueous methanol (Figure 2.1). The use of concentrated acid was intentionally avoided to prevent acid hydrolysis, and therefore the cationic or hydrophobic material retained on the column was removed using a solution of 2 mol dm^{-3} NaCl and 50% (v/v) aqueous methanol.

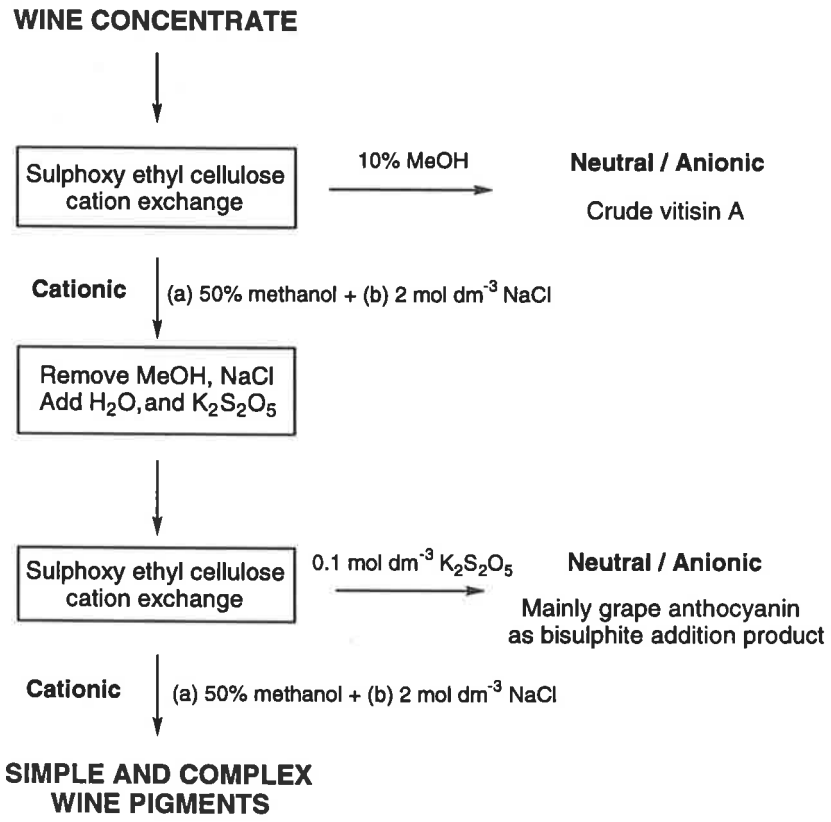

Figure 2.1: Scheme of method for isolation of wine pigments

The methanol was evaporated and any NaCl present removed using a C18 column (Buchner funnel). The pigment retained on the C18 was eluted with methanol. The methanol was rotary evaporated to almost dryness, and the pigment dissolved in 500 mL of 0.1 mol dm^{-3} potassium metabisulphite solution. A sulphoxyethyl cellulose cation exchange was prepared as before and the pigment solution (approximately 100 mL) was loaded onto this column. The grape anthocyanins existing primarily as the anionic bisulphite addition product were eluted from the column using a 0.1 mol dm^{-3} potassium metabisulphite solution. The pigment that was retained on the column was removed using a solution of 2 mol dm^{-3} NaCl and 50% methanol. From this solution, the methanol was evaporated and any salt present removed using the C18 material as described previously.

Purification of the crude pigment extract could be further achieved using preparative TLC. The crude pigment extract was applied to a plate prepared using silica gel without binder (Merck Darmstadt, Germany) and separated using 70% (v/v) aqueous propanol. The red band at R_f 0.8 was eluted using a 10% (v/v) aqueous methanol solution. The solution was centrifuged, filtered through a 0.45 µm filter and any silica remaining removed using a C18 (Sep-Pak Classic) cartridge. The pigment samples eluted from the C18 columns with methanol and subsequently were concentrated using rotary evaporation for analysis by HPLC and mass spectrometry.

This general procedure was repeated using a commercial sample of concentrated grape marc extract supplied by Tarac (Nuriootpa, South Australia). The aqueous grape marc extract was applied directly to the sulphoxyethyl cellulose column without any prior preparation.

Quantification using HPLC

Anthocyanins and wine pigments

The HPLC apparatus was a Waters (Waters 501 pump, wisp auto-sampler 710B; Waters Corporation, Milford, Massachusetts, USA) system equipped with a diode array detector (Waters diode array 996). The column was a reverse phase C18 column (250 x 4 mm Licrosphere 100; Merck, Darmstadt, Germany) and was protected by a C18 (NovaPak; Waters) guard column. The elution conditions consisted of a binary solvent system. Solvent A was dilute HCl (pH 2.4) and solvent B was 80% acetonitrile solution acidified using concentrated HCl to pH 2.1. A flow rate of 0.6 mL min^{-1} and, column temperature of 30°C was used. The linear gradient consisted of 0% to 100% solvent B over 50 min. The elution was monitored at 254 nm and UV-visible spectra were recorded from 200 to 600 nm. The wines were filtered using a 0.45 μm syringe filter (Schleicher und Schuell GmbH, Dassel, Germany). The data was analysed with Waters Software Millennium (Version 3.05). The purity of the anthocyanin was determined using per cent peak area integration at 280 nm.

In the wine samples where there were a mixture of pigments, it was no longer possible to use peak area integration for the estimation of the malvidin-3-glucoside concentration due to interference from other pigments. Thus, the concentration of malvidin-3-glucoside was calculated using tangential peak height. The concentration of vitisin A was estimated using peak area and expressed as mg/L malvidin-3-glucoside equivalents. Purified malvidin glucoside was used for the determination of the standard curves and the calculations were performed using the Waters Software Millennium (Version 2.15.01).

Pyruvate, malate, glucose and fructose

Quantification of pyruvate and malate was based on HPLC methods outlined by Frayne (1986), and Schneider *et al.* (1987). Separation was achieved using two organic acid analysis columns (Aminex ion exclusion, HPX-87H, 300 x 7.8 mm; Biorad Laboratories,

Richmond, California, USA) in series with a guard column (Microguard, 40 x 4.6 mm, Cation-H; Biorad Laboratories). The buffer used was 3.24 x 10^{-3} mol dm^{-3} H_2SO_4 and the column temperature was 65°C. The HPLC (Waters 501 pump, wisp auto-sampler 710B) was run using a flow rate of 0.6 mL min^{-1}. The wines were diluted 1/10 using distilled water and then filtered using a 0.45 µm syringe filter (Schleicher und Schuell GmbH). Pyruvic and malic acids were monitored using a diode array detector (Waters 996) at 214 nm and the concentration estimated using peak height. Glucose and fructose were monitored using a refractive index (RI) detector (Model 410 Differential refractometer; Waters) and this concentration estimated using peak heights. Analytical grade standards were used for the determination of the retention times and standard curves and the calculations were performed using the Waters Software Millennium (Version 2.15.01).

Quantification using glycosyl-glucose (G-G) assay

The anthocyanin glucose concentration was estimated using the glycosyl-glucose (G-G) assay (Iland *et al.*, 1996). To determine G-G, 2 mL of solution containing the anthocyanin was diluted 10 fold and the pH adjusted to approximately pH 2. The diluted and pH adjusted anthocyanin solution was then passed through a pretreated C18 (Sep-Pak Classic) cartridge to remove and free glucose. The anthocyanin glucosides were eluted from the C18 cartridge with 5 mL ethanol. A portion (0.2 mL) of this eluent was diluted in 4 mL of 1 mol dm^{-3} HCl and the absorbance measured. Aliquotes of the remaining eluent (0.8 mL) were hydrolysed using 2.2 mL of 1.5 mol dm^{-3} H_2SO_4 at 100 °C for 1 hour to release the glucose. To remove the anthocyanidin and non-glucose anthocyanin breakdown products, 3 mL of the hydrolysate was passed through a pretreated C18 (Sep-Pak Classic) cartridge. The first 1 mL of each solution was discarded and the remainder collected for glucose analysis. The D-glucose concentration was measured using a hexokinase/glucose-6-phosphate dehydrogenase enzyme assay kit (Boehringer Mannheim, Germany).

Estimation of molar absorbance coefficients

Malvidin-3-glucoside

All molar absorbance coefficients were estimated at 520 nm because wine colour is measured at this wavelength. The molar absorbance coefficient of malvidin-3-glucoside in aqueous solution was estimated using malvidin-3-glucoside isolated by the method described previously. Five aqueous solutions, with absorbances of 1.580, 3.620, 4.020, 4.100, and 4.720 at 520 nm, were made up from an initial malvidin glucoside stock solution. The glycosyl-glucose (G-G) concentration and the absorbance at 520 nm in 1 mol dm^{-3} HCl (pH 0.0) in replicate of each solution was measured. The G-G assays were performed at the Australian Wine and Research Institute according to the methods outlined above. The measurements at 520 nm were made on a 20 fold dilution of the sample solution, which gave an absorbance in the range between 0 and 1 whilst the G-G assays were made on the undiluted solutions.

To observe the effect of ethanol on the molar absorbance coefficient of malvidin-3-glucoside, the absorbance at 520 nm, the maximum absorbance and the wavelength of the maximal absorbance were measured for solutions containing 19.64 µmol dm^{-3} malvidin-3-glucoside and varying concentrations of acidified ethanol (0.1 mol dm^{-3} HCl). These solutions contained 0%, 5%, 10%, 15%, 20%, 25%, 30%, 40%, 50%, 75%, and 90% (v/v) aqueous ethanol. These absorbance measures were performed using a Perkin Elmer (Lambda 5) spectrometer. The spectra of malvidin-3-glucoside in both water and 90% (v/v) aqueous ethanol were obtained using a Cary 1 spectrometer (Varian Optical Instruments, Melbourne, Australia). The spectra were transferred to Grams/32 Spectral Notebase Software (Version 4.01; Galactic Industries Corp., USA) for publishing.

Malvidin-3-(*p*-coumaryl)glucoside

Using malvidin-3-(*p*-coumaryl)glucoside isolated by the method described previously a series of six solutions were made. These solutions had absorbances of 11.04, 11.16,

11.96, 13.76, 14.96 and 15.40 (1 mol dm^{-3} HCl) at 520 nm. The G-G concentrations were measured for each solution.

The molar absorbance coefficient in acidified ethanol was calculated using of a standard solution of 48.6 µmol dm^{-3} malvidin-3-(*p*-coumaryl)glucoside. The standard solution was diluted (1/4000) in 90% (v/v) acidified ethanol (1 mol dm^{-3} HCl). The spectra of eight replicates were measured on a Cary 1 UV-visible spectrometer.

The absorbance of a series of 21.2 µmol dm^{-3} solutions of malvidin-3-(*p*-coumaryl)glucoside of 0.02, 0.065, 0.225, 0.35, 0.6, and 1.1 mol dm^{-3} HCl were measured at 520 nm to determine the effect of pH on the molar absorbance coefficient. The pH values were calculated from the HCl concentration.

Solutions of 18.55 µmol dm^{-3} malvidin-3-(*p*-coumaryl)glucoside in 0%, 10%, 20%, 30%, 40%, 50%, 60%, 70%, 80%, and 90% (v/v) aqueous ethanol and 0.2 mol dm^{-3} HCl mixtures were analysed to determine the maximum absorbance and wavelength of maximal absorbance. These measures were performed using a Lambda 5 (Perkin Elmer) spectrometer in a 10 mm pathlength cell. This experiment was repeated to obtain spectra for publication using 32 µmol dm^{-3} malvidin-3-(coumaryl)glucoside at pH 0.0, and 90% (v/v) aqueous ethanol and 0.2 mol dm^{-3} HCl on a Cary 1 UV-visible spectrometer. The spectra were exported to Grams/32 Spectral Notebase software.

Vitisin A

The molar absorbance coefficient of vitisin A was estimated using the material isolated as described previously. Two replicate samples with an absorbance of 1.020 at 520 nm were used to determine the molar absorbance coefficient of vitisin A utilising the G-G assay as described previously. The effect of ethanol on the absorbance of vitisin A was analysed using a series of 15.1 µmol dm^{-3} solutions. The methods used for ethanol addition were as for malvidin-3-(*p*-coumaryl)glucoside. To minimise the presence of hydrated forms the initial solution was adjusted to pH 0.0.

Determination of the quinonoidal base spectrum of malvidin-3-glucoside using the continuous flow method

An Ocean Optics Inc. (Florida, USA) diode array spectrometer (Model 52 000) was coupled to a flow-through cell. A flow-through cell from a Waters HPLC absorbance detector (Model 441) was mounted in a holder customised by Lastek Pty. Ltd. (Adelaide, Australia). The spectra obtained from the spectrometer were collected using Spectra Array software (Lastek Pty. Ltd.; Adelaide, Australia) on a Microbits personal computer (Pentium MMX200 processor using Win 95 operating system). Transmission spectra were measured for 63 x 10^{-3} s and an average of 100 spectra was taken. Resultant spectral information were exported to Grams/32 software (Galactic Industries Corp.; New Hampshire, USA) and subsequently smoothed. The spectra were scaled according to the dilution.

A citrate/phosphate buffer solution pH 6.4 (Solution A) was prepared from 179 mL 0.1 mol dm^{-3} citric acid and 321 mL 0.2 mol dm^{-3} dibasic sodium phosphate (Na_2HPO_4; Gomori, 1955). A second solution, Solution B, consisted of 164.4 μmol dm^{-3} malvidin-3-glucoside in dilute HCl (pH 0.7). Solution C was dilute HCl (pH 0.7). For calibration of the spectrometer and obtaining approximate flow rates, the indicator methyl red was used instead of malvidin-3-glucoside.

Two separate pumps were used to pump the buffer (Pump A; Waters 590 pump max flow rate 50 mL min^{-1}) and the malvidin-3-glucoside (Pump B; Waters 501 pump max flow rate 10 mL min^{-1}). The two solutions were mixed in a low volume T-piece. The Waters HPLC pumps were piston pumps, the flow rates were not constant and therefore a dampener was placed in line to minimise flow rate change. The flow-through cell has a internal volume of 8 μL with approximately 2 μL of tubing prior to the cell making a total mixing volume of 10 μL. Relatively high flow rates gave a short mixing time allowing for the

observation of the spectrum over a very short time interval. The relative mixing time provides an indication of the reaction rate. The pH of the solution was measured after mixing using a FET pH meter (pH Boy-P2; Shindigen, Japan). The mean temperature after mixing was 30°C.

To obtain a spectrum of malvidin-3-glucoside at pH 0.7, pump A was used to pump buffer solution C at a rate of 26.8 mL min^{-1} and pump B to pump the malvidin-3-glucoside (solution B) at the rate of 2 mL min^{-1}. To record the spectrum of malvidin-3-glucoside at pH 4.2 pump A was used to pump the buffer solution A at a rate of 8 mL min^{-1} and pump B to pump malvidin-3-glucoside (solution B) at the rate of 8 mL min^{-1}. The spectra were recorded as described above.

Estimation of ionisation constants using high voltage paper electrophoresis (HVPE)

Calculations

The loss of a proton by a polyprotic acid $(H_nB)^m$ of charge m, may be depicted by,

$$(H_nB)^m \rightleftharpoons (H_{n-1}B)^{m-1} + H^+ \qquad \text{(Equation 2.1)}$$

where m is an integer and n is the maximum number of dissociable protons. The Brønsted macroscopic ionisation constant ${}^{B}K_a$, for the first ionisation of this polyprotic acid may be represented by,

$${}^{B}K_a = \frac{[H_{n-1}B].\{H\}}{[H_nB]} \qquad \text{(Equation 2.2)}$$

where the species concentrations are expressed in square brackets ([]), the H^+ activity with braces ({}). The charges and species parentheses have been omitted for clarity.

The mobility relative to a standard of the first ionisation product, $H_{n-1}B$, is m_1 and the relative mobility of the fully protonated acid, H_nB, is m_0 (Tate, 1981). At pH values where the ionisation of H_nB is incomplete, the net relative mobility, $\bar{m}$, of the equilibrium mixture of the acid, m_0, and its ionisation product, m_1, is determined by the sum of the respective mobilities and partial molar fractions of the acid and its ionisation product (Tate, 1981). Thus the relative electrophoretic mobility for a single ionisation can be represented by,

$$\bar{m} = m_0 \cdot \frac{[H_nB]}{[H_nB] + [H_{n-1}B]} + m_1 \cdot \frac{[H_{n-1}B]}{[H_nB] + [H_{n-1}B]} \qquad \text{(Equation 2.3)}$$

By substituting Equation 2.2 into Equation 2.3 and rearranging, the Brønsted macroscopic ionisation constant, ${}^{B}K_a$, may be derived from any of the following linear equations;

$$\frac{1}{\{H\}} = \frac{1}{{}^{B}K_a} \cdot \frac{(\bar{m} - m_0)}{(m_1 - \bar{m})} \qquad \text{(Equation 2.4)}$$

$$\bar{m} = m_0 + {}^{B}K_a \cdot \frac{(m_1 - \bar{m})}{\{H\}} \qquad \text{(Equation 2.5)}$$

$$\bar{m} = m_1 + \frac{1}{{}^{B}K_a} \cdot \{H\} \cdot (m_0 - \bar{m}) \qquad \text{(Equation 2.6)}$$

where the H^+ activity, $\{H\}$, is equal to the antilogarithm of the negative value of the measured pH, ie $\{H\} = 10^{-pH}$ (Tate, 1981). The most accurate values of the pKa are always obtained in the pH range corresponding to the pKa itself and if data is used from pH values greater than ± 1.0 pH units outside the pKa range, then the error will increase (Tate, pers. com.). In regions of overlapping pH buffers, and in buffered solutions of low and high pH, where electrophoretic data that covers the pKas of interest is difficult to obtain the single plateau approach (ie Equations 2.4 and 2.5) can be used.

However, it should be noted that Equation 2.4 is not valid when $\bar{m} = m_1$ because

$${}^{B}K_a \cdot \frac{(m_1 - \bar{m})}{\{H\}} = 0 \qquad \text{(Equation 2.7)}$$

and therefore $\bar{m} = m_0$. Thus any value that can be used as an estimate m_1, can not be used as a estimate of $\bar{m}$ to obtain a valid estimate of the ${}^{B}K_a$, ie there must be a statistical difference between m_1 and $\bar{m}$. This is similar in Equation 2.5 whereby it is not valid when $\bar{m} = m_0$. Linear transformations of the data can also bias estimates of the pKa. It is therefore preferable to fit the predicted mobility ($\bar{m}_P$) curve (Tate, 1981) directly to the data;

$$\bar{m}_P = \frac{m_o + m_1 \cdot 10^{pH-pK_1} + m_2 \cdot 10^{2pH-pK_1-pK_2} + \ldots\ldots}{1 + 10^{pH-pK_1} + 10^{2pH-pK_1-pK_2} + \ldots\ldots} \qquad \text{(Equation 2.8)}$$

Whether or not the constants overlap, the predicted mobility ($\bar{m}_P$) can be estimated at each pH by Equation 2.8. For a single ionisation, only the first two terms of the multiplicand and the divisor are required. Similarly, for three or more ionisations Equation 2.8 can be expanded to include the appropriate addition terms.

One of the disadvantages of using paper electrophoresis for the determination of macroscopic pKa values is that discontinuities occur between buffers. It is therefore not always possible to obtain a continuous mobility profile across all buffers. Another limitation for the use of HVPE for macroscopic pKa calculations is that it is a laborious method when compared with normal spectroscopic methods. It is therefore preferable to consider each buffer separately rather than attempting the time consuming process to obtain a smooth mobility profile across the entire pH range.

It should be noted that the mathematical model used (Equation 2.8) is constrained by the number of variables, and therefore a a slight deviation of the experimental data from the theoretical curve may occur due to the experimental effects. These effects may include the buffer ion concentration and pH related changes in adsorbtion to the paper.

Apparatus

The HVPE apparatus is based on the immersed strip method, where the electrophoretogram is immersed in an inert liquid, which is used to dissipate the heat. The device is a modification by Tate (1968) of the simple solvent cooled system of Markham and Smith (1951, 1952). The coolant used in this case is tetrachloroethylene. Additional cooling is provided by a water cooling coil to maintain an operating temperature of approximately 25°C.

Method for the estimation of ionisation constants

The buffers, times and voltages used are outlined in (Table 2.1). The oxalate buffer was made by mixing 0.1 mol dm^{-3} oxalic acid and 0.1 mol dm^{-3} sodium oxalate (Sigma). The

citrate buffer was made up using 0.05 mol dm-3 trisodium citrate (Sigma) and 0.05 mol dm^{-3} citric acid. The phosphate/ oxalate buffer was made using 0.05 mol dm^{-3} sodium pyrophosphate and 0.05 mol dm^{-3} oxalic acid adjusted using sodium hydroxide. All other pH values were measured using a Activon Model 210 (Thornleigh, NSW, Aust.) pH meter calibrated and checked against in the appropriate pH range using 0.2 mol dm^{-3} HCl (pH 0.7), pH 4, 7, and 10 buffers (BDH). The times and voltages for each buffer used varied (Table 2.1).

Table 2.1: Parameters used in HVPE measurements.

pH	Buffer	Volts (V)	Amps (mA)	Power (mW)	Time (min)
1.4 - 4.5	oxalate	1850	80	150	30
2.6 - 8.0	citrate	2000	75	150	45
7.0 -10.4	phosphate/oxalate	1500	100	150	60

The electrophoretogram consisted of chromatography paper (number 1; Whatman). All relative mobilities (Rm_{OG}) were compared to Orange G (1-phenylazo-2-naphthol-3,5-disulphonate) as the anionic standard and fructose as the neutral standard. The position of fructose was revealed using a silver nitrate stain (Trevelyan *et al.*, 1950). All runs were done in duplicate and the average relative mobility calculated.

It was not possible to estimate any pKa values for either the citrate or phosphate buffers because the malvidin-3-(*p*-coumaryl)glucoside adsorbs to the paper under these conditions. Therefore the range of the oxalate buffer was extended to include pH values from 1.2 to 4.9, so that both pKa_1 and pKa_2 could be calculated using this buffer.

Once the electrophoretic mobilities were calculated, graphs were drawn and the predicted mobility curve (Equation 2.8) was fitted using MacCurveFit version 1.4 (Kevin Raner Software, Australia). Error estimates and regression estimates were calculated by the MacCurveFit software.

Estimation of hydration constants using UV-visible spectrophotometry

Calculations

The UV-visible spectroscopic method for calculation of pKa values depends on the determination of the ratio of molecular to ionised species in a series of non-absorbing buffers. For this purpose the spectrum of each of the species is first determined and a wavelength is chosen at which the greatest difference between the absorbances of two species is observed (Albert and Serjeant, 1971). The Grams software allows for post processing of the data and therefore the optimal wavelengths can be determined after the experiment has been conducted. The wavelength chosen at which there is greatest difference between the absorbances between the two species is called the analytical wavelength.

From the earlier discussion on electrophoretic determination of the pKa, Equation 2.2 stated that the first Brønsted macroscopic ionisation constant may be represented by,

$$^{B}K_a = \frac{[H_{n-1}B].\{H\}}{[H_nB]} \qquad \text{(Equation 2.2)}$$

Furthermore, the equilibrium of the flavylium ion with the hemiketal (pseudobase) in the presence of water may be written as,

$$AH^+ + H_2O \rightleftharpoons A^{OH} + H^+ \qquad \text{(Equation 2.9)}$$

where AH^+ the flavylium ion, is A^{OH} is the hemi-ketal. Therefore, the equilibrium constant for hemiketal (pseudobase) formation can be estimated using,

$$K_H = \frac{[A^{OH}].\{H\}}{[AH^+]} \qquad \text{(Equation 2.10)}$$

which is analogous to the pKa of a Brønsted acid (Perrin *et al.*, 1981). The hydration constant, pK_H, is the hydrogen ion concentration when A^{OH} and AH^+ are present in equal amounts.

However, for malvidin-3-glucoside the hemiketal is in equilibrium with the *cis*-chalcone and the *trans*-chalcone. The base catalysed tautomeric reaction for the hemiketal and *cis*-chalcone is rapid and it is not possible using normal spectral techniques to differentiate between the two (Brouillard and Lang, 1990). It is generally thought that the *cis*-chalcone to *trans*-chalcone isomerisation is a slow reaction (k_i = 4.5 x 10^{-5} s^{-1} or $t_{1/2}$ = 4.28 h; Brouillard and Delaporte, 1977), and therefore unless long equilibration times are allowed the contribution of the trans-chalcone to the pK_H is negligible. Whilst, Pina (1998) suggests that the concentration of the *trans*-chalcone for malvidin-3,5-diglucoside is non-negligible and therefore may influence the macroscopic pK_H calculated, it was considered here that the rate of isomerisation was too slow for a significant effect on the hydration constant. Furthermore, previous estimates of the pK_H for malvidin-3-glucoside compare the concentration of the flavylium ion, and the combined concentrations of the hemiketal and *cis*-chalcone (Brouillard and Lang, 1990). Thus, the pK_H for malvidin-3-glucoside must be estimated using,

$$K_{H1} = \frac{([A^{OH}]+[C_{cis}]).\{H\}}{[AH^+]} \qquad \text{(Equation 2.11)}$$

At a sufficiently high pH, the hemiketal may dehydrate and ionise to form the quinonoidal anion.

$$A^{OH} \rightleftharpoons A^- + H_2O + H^+ \qquad \text{(Equation 2.12)}$$

Again the rapid equilibrium between the hemiketal and *cis*-chalcone (C_{cis}) must be considered. Therefore, the macroscopic hydration constant (K_H) for this can be calculated using,

$$K_{H2} = \frac{[A^-].\{H\}}{([A^{OH}]+[C_{cis}])} \qquad \text{(Equation 2.13)}$$

Again this is analogous to the pKa of a Brønsted acid. The pK_H is the pH when there is an equal concentration of A^- plus C_{cis}, and A^{OH}. Thus, for the following discussion for the calculation of pKa and pK_H values spectroscopically with regard to the determination of pK_{H1}, $[H_nB]$ can be replaced by $[A^{OH}]+[C_{cis}]$ and $[H_{n-1}B]$ by $[AH^+]$ and for the determination of pK_{H2}, $[A^-]$ can be replaced by $[H_{n-1}B]$ and $[A^{OH}]+[C_{cis}]$ by H_nB.

The calculation of the pKa or pK_H values of a two component system using spectroscopic data was initially considered. Once the spectra of two species had been obtained, the pKa or pK_H could be estimated from the absorbance for a series of pH values intermediate between the optimal pH values for the two species. The ratio of $[H_nB]$ to $[H_{n-1}B]$ could be calculated at a particular analytical wavelength in a two component system because the ratio of the two species depended solely upon the pH at which the solution was optically measured. If it is assumed that Beer's Law is obeyed for both species, the observed absorbance, $\bar{d}$, at the analytical wavelength will be due to the sum of the absorbances of the two species, d_0 and d_1, (Albert and Serjeant, 1971; Equation 2.17).

$$\bar{d} = d_0 + d_1 \qquad \text{(Equation 2.14)}$$

The absorbance of either component is related to its molar concentration C by a general expression $d = \varepsilon.t.C$ where ε is the molar absorbance coefficient of the particular species and t is the optical pathlength of the cell. The terms ε_0 and ε_1 are the molar absorbance coefficients of the pure ionised and molecular species respectively which are directly related to the optical densities obtained when their charged state is an integral.

The concentration of the ionised species in the mixture is $F_0.C$ where F_0 is the fraction ionised and hence its contribution to the observed absorbance is $\varepsilon_0.F_0.C.t$, ie,

$$d_0 = \varepsilon_0.F_0.C.t \qquad \text{(Equation 2.15)}$$

If the same cell pathlength is used throughout,

$$\bar{d} = (\varepsilon_0.F_0 + \varepsilon_1.F_1)C \qquad \text{(Equation 2.16)}$$

where $\varepsilon = d/C$. However,

$$\varepsilon_0 = \frac{d_0}{C_0.t} \qquad \text{(Equation 2.17)}$$

and substituting into equation (2.15) and re-arranging,

$$F_0 = \frac{C_0}{C} \qquad \text{(Equation 2.18)}$$

where C is the total concentration, ie $C = [H_nB] + [H_{n-1}B]$ and C_0 is the concentration of the ionised species , ie $C_0 = [H_nB]$. Therefore,

$$F_o = \frac{[H_nB]}{[H_nB] + [H_{n-1}B]} \qquad \text{(Equation 2.19)}$$

Similarly the contribution of the molecular species to the observed absorbance of the mixture is $\varepsilon_1.F_1.C.t$ where F_1 is the fraction present in the molecular form.

$$F_1 = \frac{[H_{n-1}B]}{[H_nB] + [H_{n-1}B]} \qquad \text{(Equation 2.20)}$$

The final absorbance, $\bar{d}$, is equal to the contribution of the absorbances of the fractional concentrations F_0 and F_1 of each of the species,

$$\bar{d} = d_0.F_0 + d_1.F_1 \qquad \text{(Equation 2.21)}$$

Thus, the relative density for a single ionisation can be represented by,

$$\bar{d} = d_0.\frac{[H_nB]}{[H_nB] + [H_{n-1}B]} + d_1.\frac{[H_{n-1}B]}{[H_nB] + [H_{n-1}B]} \qquad \text{(Equation 2.22)}$$

By substituting Equation 2.2 into Equation 2.22, the Brønsted macroscopic ionisation can be derived by the following linear equations;

$$\frac{1}{\{H\}} = \frac{1}{{}^{B}K_a} . \frac{(\bar{d} - d_0)}{(d_1 - \bar{d})} \qquad \text{(Equation 2.23)}$$

$$\bar{d} = d_0 + {}^{B}K_a . \frac{(d_1 - \bar{d})}{\{H\}} \qquad \text{(Equation 2.24)}$$

$$\bar{d} = d_1 + \frac{1}{{}^{B}K_a} . \{H\} . (d_0 - \bar{d}) \qquad \text{(Equation 2.25)}$$

Equation 2.25 can be rewritten as,

$$pKa = pH + \log \frac{(d_1 - \bar{d})}{(\bar{d} - d_0)} \qquad \text{(Equation 2.26)}$$

From Equation 2.26, it is also possible to predict the absorbance, d_p, at any particular wavelength in a two component system using the following equation;

$$d_p = \frac{d_o + d_1 . 10^{pH - pK_1}}{1 + 10^{pH - pK_1}} \qquad \text{(Equation 2.27)}$$

Equation 2.27 is analogous to Equation 2.8, and therefore for multiple pKa value it possible to extend this equation;

$$d_p = \frac{d_o + d_1 . 10^{pH - pK_1} + d_2 . 10^{2pH - pK_1 - pK_2} + ...}{1 + 10^{pH - pK_1} + 10^{2pH - pK_1 - pK_2} + ...} \qquad \text{(Equation 2.28)}$$

The application of Equation 2.28 to UV-visible spectroscopic data allow for the calculation of macroscopic pK values.

As was noted previously for the determination of protonation constants using HVPE, the mathematical model used, ie Equation 2.28, is constrained by the number of variables. Therefore a a slight deviation of the experimental data from the theoretical curve may occur due to the experimental effects.

Malvidin-3-glucoside

The macroscopic hydration constant (pK_H) of malvidin-3-glucoside was estimated using two 10 mL equimolar solutions (37.35 mol dm^{-3}) that were prepared at pH 0.7 (0.2 mol dm^{-3} HCl) and pH 7.0 (0.2 mol dm^{-3} trisodium citrate). The citrate buffer was titrated using the acidified solution to obtain a series of spectra of malvidin-3-glucoside ranging from pH 7.0 to pH 0.7. This was repeated by titrating an equimolar solution malvidin-3-glucoside (37.35 µmol dm^{-3}) in 0.1 mol dm^{-3} pyrophosphate (pH 9.4), with the acidified malvidin-3-glucoside solution (pH 0.7) to pH 4.1. The solution of malvidin-3-glucoside, pH 9.4, was also titrated with a small amount (1-3 µL per mL) of 20% sodium hydroxide solution to obtain spectra up to pH 10.6. The pH values were obtained using a FET pH meter (pH Boy-P2; Shindigen, Japan). Spectra of each of these solutions were recorded using a Cary 1 spectrometer (Varian) in 1 mL 10 mm pathlength cell. The temperature of the cell was approximately 25°C. The spectra were post processed on a Microbits personal computer using Grams software. A program was written in Array Basic to calculate the absorbances at specific analytical wavelengths (See Appendix 1). The analytical wavelengths chosen for the estimation of the macroscopic pK values were 520 nm, 440 nm and 575 nm.

Malvidin-3-(*p*-coumaryl)glucoside

The methods used for the estimation of the hydration constant of malvidin-3-(*p*-coumaryl)glucoside were similar to those described for malvidin-3-glucoside. Solutions of 32 µmol dm^{-3} malvidin-3-(*p*-coumaryl)glucoside were used. To obtain spectra at pH values less than 0.8, 32 µmol dm^{-3} solutions were prepared in HCl solutions, and pH was estimated using the concentration of HCl. Spectra were recorded using a Cary 1 spectrometer (Varian) in 1 mL 10 mm pathlength cell. Three analytical wavelengths were used to estimate the pKa and pK_H values. The wavelengths used were 575, 520 and 360 nm.

Vitisin A

The hydration constant of vitisin A was estimated using the methods developed for malvidin-3-glucoside. The two buffer systems used were, 0.2 mol dm^{-3} citrate (pH 0.7 - 7.8) and 0.1 mol dm^{-3} pyrophosphate (pH 2.2 - 10.3). The three analytical wavelengths used for the determination of the pK values were 510 nm, 544 nm and 599 nm.

Mass spectrometry

Direct injection

The ionspray mass spectra of the compounds were obtained using an API-300 mass spectrometer with an ionspray interface (PE Sciex, Thornhill, Ontario, Canada). The ion spray and orifice potentials were 5.5 kV and 30 V for the positive ion mode and -4.5 kV and -30 V for the negative ion mode, respectively. The curtain (nitrogen) and nebuliser (air) gases were set at 8 and 10 units, respectively. The isolated compound was introduced into the mass spectrometer by a flow injector (8125, Rheodyne, Cotati, CA) with a 5 µL sample loop connected to the ion sprayer. The injected solution was delivered by 50% acetonitrile acidified with 2.5% acetic acid at a rate of 5 µL min^{-1}, using a syringe pump (Cole-Parmer, Niles, IL, USA).

Liquid chromatography mass spectrometry (LC-MS)

The sample was injected using the flow injector with a 5 µL loop and delivered to a C18 reversed phase HPLC column (2 x 150 mm, Nova-Pak, Waters) at a flow rate of 100 µL/min using the syringe pump. The column was equilibrated in a mixture of 90% Solvent A [2.5% (v/v) aqueous acetic acid] and 10% Solvent B [2.5% acetic acid in 90% aqueous acetonitrile (v/v)]. The anthocyanins were eluted from the cartridge by a gradient of Solvent B from 10%, 70% in the first 60 min and from 70% to 100% from 60 min to 70 min. All data of mass spectra were processed using Bio-Multiview software 1.2ß3 (PE Sciex).

Ionspray mass spectrometry via desalting trap

Ionspray mass spectrometry was also performed by direct injection via a desalting trap. Twenty µL of the sample was loaded onto the desalting trap cartridge (Michrom BioResources, Auburn, CA, USA) by a dual-syringe pump (140B Solvent Delivery Systems, Applied Biosystems, Foster City, CA, USA) at a rate of 100 µL/min through the

flow injector. Anthocyanins was eluted from the cartridge by a binary solvent system consisting of solvent A (2.5% acetic acid) and solvent B (2.5% acetic acid in 90% acetonitrile) at a rate of 10 μL/min after the cartridge had been washed with 2.5% acetic acid at a rate of 100 μL/min for 5 min. A linear gradient of 0 to 100% of solvent B over 30 min was used. The eluent from the cartridge was directly delivered to the ionspray mass spectrometer.

Methods of synthesis

Acetylation of vitisin A

The peracetylation of vitisin A was achieved by adding approximately 1 mg of vitisin A to 1 mL of acetic anhydride with 0.1% concentrated perchloric acid added. The mixture was allowed to stand for 2 h at room temperature and then slowly diluted by pouring over approximately 50 g of crushed ice. The acetylated product was extracted from the aqueous solution using 50 mL chloroform in a separation funnel. The chloroform was evaporated and the acetylated product resuspended in 100 µL methanol for mass spectral determination. The acetylated form of vitisin A was identified using direct injection ES/MS, and LC/MS.

Synthesis of vitisin A

This method was adapted from by Fulcrand *et al.* (1998). A solution of 10% ethanol and 2% formic acid was made. To 10 mL of this solution approximately 2 mg of malvidin-3-glucoside (isolated using methods described previously) and 100 mg sodium pyruvate (BDH) were added. This was stirred at room temperature for 6 h.

Two variations of this synthesis were attempted. The synthesis was first performed under nitrogen gas for 8 h at room temperature to limit the effect of oxygen. The synthesis of vitisin A was also executed in the presence of oxygen, with 0.6 mg/mL copper sulphate ($CuSO_4$) added to catalyse the reaction and improve the yield. The experiment was conducted over 4 h at room temperature.

Infra-red spectroscopy

The infra red spectra of malvidin-3-glucoside, *p*-hydroxyphenylpyruvate, pyruvic acid and vitisin A were obtained using diffuse reflectance. Methanolic solutions of malvidin-3-glucoside and vitisin A were dried in the presence of a few milligrams of potassium chloride. Samples of *p*-hydroxyphenylpyruvate and pyruvic acid were dissolved into water and then dried in the presence of a few milligrams of potassium chloride. The samples were then finely ground and loaded into a Harrick sample holder (diameter of 11 mm and a depth of 1 mm; Model DRA-SX3; Harrick Scientific Corp., USA). To obtain the spectra, a double beam dispersive infra-red spectrometer (Model PE 983G; Perkin-Elmer, England) fitted with a Harrick praying mantis diffuse reflectance attachment (Model 3SP; Harrick Scientific Corp., USA) operating in double beam mode was used. The spectrometer was linked to a personal computer and controlled through a modified PE983G emulator-controller (MDS engineering Associates, USA).

The sample compartment was continually purged throughout the duration of sample collection using a circulatory drier (Model CD3; Bodenseewerk Perkin-Elmer & Co GmbH, W. Germany). The diffuse reflectance data was recorded as % transmission using Grams/386 II software (Galactic Industries Corp, USA). The data was then converted to absorbance units.

Wine making methods

Synthesis of vitisin A during fermentation

Shiraz grapes at a maturity of 23.6 °Brix were made into four 20 kg replicate wines. After crushing 250 mg/L diammonium phosphate (DAP) and, 250 mg/L of yeast (*Saccharomyces cerevisiae* strain EC1118; Lavin) were added and the pH was adjusted to pH 3.57. The musts were fermented at approximately 18°C. The wines were plunged after each sampling. The sampling was finished at 177 h.

The rate of the fermentation was monitored by measuring the total soluble solids using a digital refractometer (Model BRX-242; Erma Inc., Japan). Samples were taken every 2 h for the first 54 h. At 54 h, the ferment was at approximately 18 °Brix, and it was estimated that the ferment was proceeding at its maximum rate. At this stage, drop plates were used to estimate yeast cell numbers (Hills, 1999). After this the sampling rate varied according to the fermentation rate as determined by the °Brix. Samples were measured for the concentration of vitisin A, malvidin-3-glucoside, glucose, fructose and pyruvic acid using the HPLC method described previously. The completion of fermentation [<0.25% (w/v) reducing sugar] was estimated using Clinitest tablets(Miles Australia Pty Ltd., Mulgrave, Victoria, Australia).

Measurement of oxygen concentration during fermentation and its relationship to the formation of vitisin A

Frozen grapes, picked previously at a maturity of 23.6 °Brix and divided into three replicates 3.2 kg lots were defrosted and crushed. After crushing 100 mg/L diammonium phosphate, 40 mg/L potassium metabisulphite and 170 mg/L yeast (EC1118, Lavin) were

added. Samples were taken every 8 h and the concentration of malvidin-3-glucoside, pyruvic acid, and vitisin A was measured. The dissolved oxygen concentration of these samples was measured using the method described below. When the wines were near to completion, they were pressed, and placed in 2 litre bottles with air locks and allowed to finish. Samples were taken for the measurement of vitisin A formation after pressing.

Formation of vitisin A in wine post fermentation

A series of 11 wines were made using a standard procedure from *Vitis vinifera* cv. Shiraz grapes collected from different regions in South Australia. These wines were representative of the 1997 vintage. Approximately 10 kg of the grapes were crushed. After crushing 80 mg/L diammonium phosphate (DAP), and 50 mg/L potassium metabisulphite per litre were added. The pH of the juice was adjusted to approximately pH 3.4 using tartaric acid. The yeast, (*Saccharomyces cerevisiae,* EC1118) was added at the rate of 170 mg/L. The juice was then fermented on skins, and the wines were plunged 3 times per day for 7 days. At the end of this period the wines were pressed using a diaphragm type press. Following pressing, the wines were allowed to stand for 7 days to finish fermentation. After the completion of fermentation the wines were racked, cold settled and bottled.

Samples of wines were obtained after cold stabilisation (time zero) and at the end of six months of aging at room temperature (approximately 20°C). The wines were analysed for malvidin-3-glucoside, vitisin A and pyruvic acid using HPLC. The concentration of bound pyruvate was calculated using the method described below.

Effect of sulphur dioxide as an oenological treatment on the formation of vitisin A during maturation

A total of 12 wines were made from 20 kg lots of Shiraz grapes. The grapes had a maturity of 24.6 °Brix. The experiment was a factorial design with three replicates of four treatments. The treatments consisted of a control and three different levels of sulphur

dioxide added; 50, 100 and 200 mg/L. The wines were made in the standard procedure (above) except that prior to crushing different levels of sulphur dioxide were added.

After fermentation and pressing, 10 mL samples were taken for determination of the concentration of malvidin-3-glucoside, vitisin A and pyruvic acid using HPLC. On 100 mL samples the free and bound sulphur dioxide concentrations were calculated using the aspiration method outlined by Iland *et al.* (1993).

For continued analysis, samples were taken and bottled at the end of fermentation prior to the inoculation with malolactic bacteria. These samples consisted of 10 x 100 mL bottles. Because the bisulphite levels were very low, 1 mmol dm^{-3} of sodium azide per 100 mL of wine was added to prevent spoilage. These samples were stored at approximately 20°C. At each sampling period a new 100 mL bottle was opened for the analysis of malvidin-3-glucoside, vitisin A and pyruvic acid. The concentration of malic acid was also measured to monitor the progress of malolactic fermentation.

Samples were taken at regular intervals during malolactic fermentation to measure vitisin A and malvidin-3-glucoside concentration. After completion of malolactic fermentation, 6 x 100 mL portions were stored in bottles for continued analyses. These samples were kept at approximately 20°C. Again at each sampling period a new 100 mL bottle was opened for the analysis.

Calculations used in winemaking analysis

Determination of bound pyruvate

Using the method outlined by Burroughs (1975) it is possible to calculate the proportion of metabisulphite bound pyruvate compared with total pyruvate present in wine. This is performed using the concentration of free sulphur dioxide and the concentration of total pyruvate as measured by HPLC.

The concentration of free sulphur dioxide $[SO_2]$ can be calculated from the relative concentration of anthocyanin bisulphite addition product using,

$$[SO_2] = K_{SO2} \cdot \frac{[ASO_3^-]}{[A]} \qquad \text{(Equation 2.29)}$$

where $[ASO_3^-]$ is the concentration of bisulphite bound to anthocyanin (ie, sulphur dioxide bleached anthocyanin) and $[A]$ is the concentration of free monomeric anthocyanin. The free sulphur dioxide can be estimated using,

$$[SO_2] = K_{SO2} \cdot \frac{(a_1 - a_0)}{(a_0 - a_2)} \qquad \text{(Equation 2.30)}$$

where K_{SO2} is 6×10^{-5} (between pH 2.5 and 4.0), a_0, is a measure of the concentration of coloured anthocyanin in wine (ie, absorbance at 520 nm of untreated wine), a_1 total anthocyanin in wine (ie, absorbance at 520 nm of wine with free sulphur dioxide removed) and a_2 is the non-bleachable pigment in wine (ie, absorbance at 520 nm of wine with free sulphur dioxide added) (Burroughs, 1975).

According to the law of mass action the apparent equilibrium constant of pyruvate, K_P, can be calculated using;

$$K_P = \frac{[SO_2].[P-p]}{[p]} \qquad \text{(Equation 2.31)}$$

where $[SO_2]$ is the concentration of free SO_2 in any form, $[p]$ is the molecular concentration of the undissociated pyruvate/bisulphite (bound pyruvate), and $[P]$ is the total concentration of the pyruvate (both free and bound pyruvate) (Burroughs and Sparks, 1973a). Rearranging this equation gives the concentration of bound pyruvate $[P_B]$;

$$[P_B] = [P] - \frac{[SO_2]}{K_P + [SO_2]} \qquad \text{(Equation 2.32)}$$

where K_P equals 1.82×10^{-4} at pH 3.6 (Burroughs and Sparks, 1973b,c).

Estimation of oxygen concentration

The apparent oxygen concentration in the wine was measured using a oxygen meter, (Digital Oxygen System Model 10; Rank Brothers Ltd., Cambridge, England) equipped with a semi permeable membrane that was selective for oxygen. The meter measures the apparent oxygen concentration by the reduction of oxygen. A series of single electron reduction reactions may be proposed for this reduction reaction,

$$O_2 + H^+ + e^- \rightarrow HOO^{\cdot} \qquad \text{(Equation 2.33)}$$

$$HOO^{\cdot} + e^- + H^+ \rightarrow H_2O_2 \qquad \text{(Equation 2.34)}$$

$$H_2O_2 + e^- + H^+ \rightarrow H_2O + OH^{\cdot} \qquad \text{(Equation 2.35)}$$

$$OH^{\cdot} + e^- + H^+ \rightarrow H_2O \qquad \text{(Equation 2.36)}$$

however the precise stoichiometry of the electrode reaction may depend on various factors including the nature of the electrode, and the applied voltage (Beechey and Ribbons, 1972). Beechey and Ribbons (1972) advise that operationally the electrode reaction is not important, but a consistency of the electrode reaction and sensitivity to that reaction is important. Any reactive species capable of passing through the membrane and participating in the reduction reactions at the electrode (Equation 2.33 - 2.36) will interfere with the oxygen concentration measured.

The meter calibration was performed using an indirect method that utilises the ability of sodium dithionite to react rapidly with dissolved oxygen to produce anaerobic conditions (Beechey and Ribbons, 1972). A known standard of 0.1 mol dm^{-3} citric acid, 0.2 mol dm^{-3} $NaHPO_4$ and 1% sodium dodecyl sulphate (SDS) solution at 25°C containing 25.5 mg/L oxygen was used to calibrate the meter (S_1). One to 2 mg of sodium dithionite was used to remove the oxygen from the standard solution to give a zero value (S_0). The meter was standardised for each analysis. The wine was measured using the oxygen meter (W_1), and then dithionite was added to give the value of the wine without oxygen (W_0). The apparent oxygen concentration was then estimated using the equation,

$$O_{2\ apparent} = \frac{W_1 - W_0}{S_1 - S_0} \times 25.5\ mgL^{-1} \qquad \text{(Equation 2.37)}$$

Mathematical calculations for curve fitting and statistical comparisons

To enable comparisons between the production of vitisin A and malvidin-3-glucoside extraction, pyruvic acid production and sugar degradation a mathematical description is useful. For a true comparison, a single type of curve is required. The logistic function is relatively simple and is characterised by an initial lag phase followed by rapid growth and a final asymptote (De Sapio 1978; Figure 2.2). The logistic equation of the general form;

$$y = \frac{K}{1 + ce^{-Kkt}} + b \qquad \text{(Equation 2.38)}$$

where y is the concentration, t is the time, K is the difference between the final and the initial concentrations, b is the initial concentration and k and c are both constants.

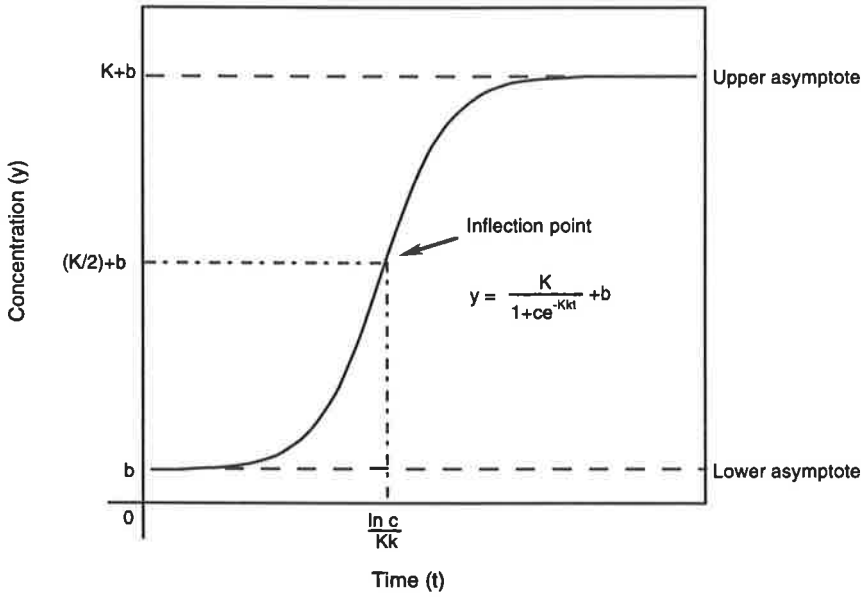

Figure 2.2: The graph of the logistic function $y = K/(1+ce^{-Kkt})$. The inflection point is at $t = (\ln c)/Kk$, and at this point there is a maximum increase in the concentration. The logistic model starts at a relatively slow rate at $t = 0$, then proceeds faster and faster until the point of inflection is reached. From this point the rate decreases as the concentration increases and approaches a maximum limit (Adapted from De Sapio, 1978).

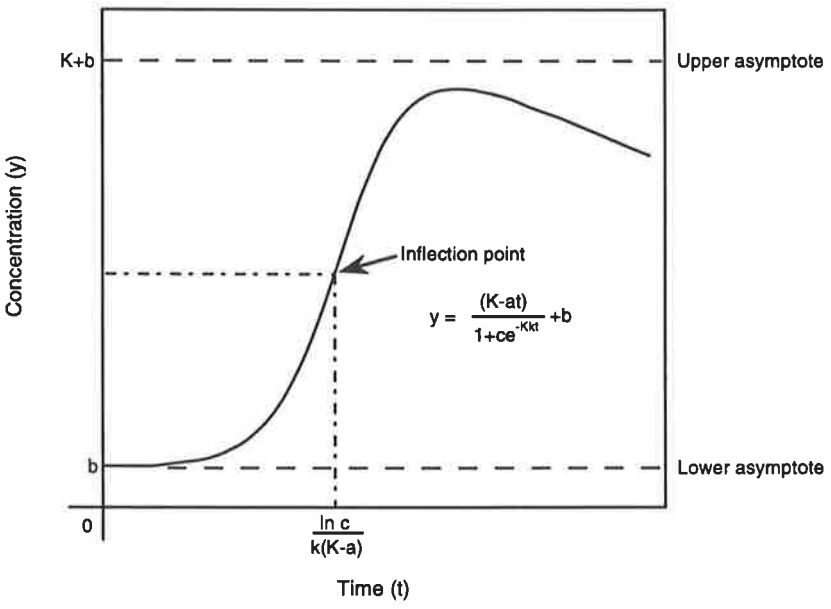

Figure 2.3: The graph of the modified logistic function $y = (K-at)/(1+ce^{-Kkt})$. The inflection point is at $t = (\ln c)/(K-a)k$, and at this point there is a maximum increase in the concentration. This function is similar to the logistic function (Figure 5.1). It starts at a relatively slow rate at $t = 0$, then proceeds faster and faster until the point of inflection is reached. From this point the rate decreases as the concentration increases, and approaches a maximum concentration limit. After the maximum limit is reached, the concentration declines.

The time when the maximum rate (t_m) of the increase in concentration occurs is at the point of inflection,

$$t_m = \frac{\ln c}{kK} \qquad \text{(Equation 2.39)}$$

The asymptote for the pyruvate curve is not parallel to the baseline and therefore the logistic equation was modified to,

$$y = \frac{(K - at)}{(1 + ce^{-Kkt})} + b \qquad \text{(Equation 2.40)}$$

(see Figure 2.3). The point of inflection, or the maximum slope of the curve, provides an estimate of the time when the fastest rate of change in concentration occurs (t_m). This is defined by,

$$t_m = \frac{\ln c}{k(K - a)} \qquad \text{(Equation 2.41)}$$

To fit the logistic curve to the glucose and fructose data, a transformation was required. This transformation calculated the relative glucose utilisation (G_u) using the equation,

$$G_u = 1 - \frac{[G]}{[G_0]} \qquad \text{(Equation 2.42)}$$

where [G] was the glucose concentration and [G_0] was the initial glucose concentration. The fructose data was similarly transformed to give the relative fructose utilisation (F_u).

When the modified logistic equation (Equation 2.40) was fitted to the experimental data some variables were defined. The initial concentrations of malvidin-3-glucoside were estimated to equal zero (ie, b = 0). Furthermore, the transformations of glucose and fructose concentrations meant that, by definition, the initial relative glucose utilisation and initial relative fructose utilisation equalled zero (ie, b = 0), and the height of the asymptote

equalled one (ie, $K = 1$), and the slope of the asymptote equalled zero (ie, $a = 0$). All other estimates were provided by the curve fitting program MacCurvefit version 1.4 (Kevin Raner Software, Australia).

Statistical analyses

Statistical analyses were performed using JMP software version 3.1.6 (SAS Institute Inc., Cary, North Carolina, USA).

Estimation of the oxidative stability of vitisin A

Model wine solution was made using a saturated potassium hydrogen tartrate in 10% (v/v) aqueous ethanol adjusted to pH 3.6 using tartaric acid. Two 25 mL solutions were made up using malvidin-3-glucoside and vitisin A to give absorbances of approximately 1.0 at 520 nm. For the model wine solution (pH 3.6) a much higher concentration of malvidin-3-glucoside (265 mg/L) than vitisin A (28.8 mg/L malvidin-3-glucoside equivalents) was required to give a similar absorbance. The solutions kept in open containers were allowed to oxidise gradually at room temperature (approximately 20°C). The concentrations were measured at regular intervals using HPLC.

The stability constants of malvidin-3-glucoside and vitisin A, as a first-order reaction may be solved using,

$$[A] = [A_0]e^{-kt} \qquad \text{(Equation 2.43)}$$

where $[A_0]$ is the initial concentration and $[A]$ is the concentration at time t, and k is the rate constant for a first order reaction. The data was transformed using the formula,

$$\ln\frac{[A]}{[A_0]} = -kt \qquad \text{(Equation 2.44)}$$

and the rate constant, k, determined by the slope. The error assocated with rate constant was estimated using MacCurvefit version 1.4 (Kevin Raner Software, Australia). Once the rate constant k was calculated then the half lives were estimated using,

$$t_{1/2} = \frac{\ln 2}{k} \qquad \text{(Equation 2.45)}$$

Preliminary survey of the longevity of vitisin A in wine

A series of wines from 1958 - 1998 were analysed for malvidin-3-glucoside and vitisin A using HPLC. These wines were made from Shiraz grapes sourced from a single vineyard. The wines were made using traditional methods and stored under optimal conditions. Although the vintages may be different, it was proposed that this series may provide an indication as to the persistence of these anthocyanins over an extended period. Stability constants were estimated using Equation 2.44 for vitisin A and malvidin-3-glucoside.

Separation and identification of anthocyanin bisulphite addition products using HVPE

Method for bisulphite adduct separation

The use of bisulphite addition as a method for isolation of anthocyanins was initially investigated using HVPE. The buffer system used was 100 mmol dm^{-3} potassium metabisulphite (pH 4.2). The samples were run for 45 min at 1400 V and 150 mA. The papers were dried and fumed with concentrated hydrochloric acid to indicate the position of the anthocyanins. The anthocyanin mobilities were compared with Orange G, Xylene cyanol and fructose. The anthocyanins were both observed under visible and UV (254 and 325 nm) light. The grape skin extracts showed two major coloured bands. These compounds present in these bands were identified using a combination of preparative paper electrophoresis (described below), HPLC and mass spectrometry. The electrophoretic mobilities of the grape anthocyanins were compared with the pigments present in a series of wine samples. The wines were directly applied to the electrophoretogram without prior treatment.

Preparative paper electrophoresis

Chromatography paper (Number 3; Whatman) was used to separate samples according to the procedure above to obtain fractions for further identification by mass spectrometry. A metabisulphite buffer (0.1 mol dm^{-3} pH 4.2) was used for the separation. The run time was 60 min at 1400 V and 150 mA. Two bands Rm_{OG} 0.39 and 0.33 were eluted with 0.1 mol dm^{-3} metabisulphite buffer. The metabisulphite solutions were cleaned using a C18 reverse phase cartridge (Sep-Pak Classic). The bisulphite was displaced using water and the retained anthocyanins were then eluted with methanol. The anthocyanin fraction was filtered using 0.45 µm filter and identified using HPLC and electro spray mass spectrometry by direct injection.

The pH stability of the bisulphite addition complex

A series of titrations were performed on the anthocyanin extracts containing bisulphite to provide an estimate of the bisulphite addition product pH stability. A crude extract of anthocyanins were made by extracting 1.5 g Shiraz grape skins in 30 mL methanol. The extract was filtered and the skins were re-extracted with 30 mL methanol to give 60 mL of crude extract consisting primarily of malvidin-3-glucoside. A series of 100 mL solutions were made containing 20 mL of the crude methanolic extract, and aqueous potassium metabisulphite. Each of solutions had a final metabisulphite concentration of 0.001 mol dm^{-3}, 0.01 mol dm^{-3} and 0.1 mol dm^{-3}.

Twenty five mL aliquots of each of the three anthocyanin-extract solutions were titrated using a drop wise addition of 1 mmol dm^{-3} HCl. The pH and the absorbance at 520 nm were monitored during this addition. Similarly, 0.1 mmol dm^{-3} NaOH was added to the 25 mL aliquots of the anthocyanin extracts. The pH and the absorbance at 618 nm were monitored during the titration. The increase in absorbance was associated with a decomposition of the bisulphite addition product. When the solution was colourless, it was considered that all the anthocyanin was in the stable bisulphite addition product form.

Chapter 3

Malvidin-3-glucoside

Introduction

Malvidin-3-glucoside is the most important anthocyanin found in *Vitis vinifera* grapes. It serves as an ideal model compound for the development of techniques for the investigation of anthocyanins isolated from grapes and other pigments isolated from wine. A well defined molar absorbance coefficient is necessary for spectroscopic work on anthocyanins. It was proposed (Chapter 1) that the glycosyl-glucose (G-G) can provide a new method for the estimation of this absorbance coefficient. Since the molar absorbance coefficient for malvidin-3-glucoside has been reasonably well established (Table 1.1), the efficacy of G-G as a method for this coefficient may be analysed. The effect of ethanol, a non-aqueous solvent, on the molar absorbance coefficient is also of some interest.

At low concentrations and at wine pH (3.2 - 3.8), the hydration of anthocyanins in aqueous solutions prevents the formation of the coloured species of malvidin-3-glucoside. In Chapter 1, it was proposed that the spectrum of the coloured form of malvidin-3-glucoside at wine pH may be obtained using a continuous flow method that relies on a rapid mixing and pH change and thereby suppresses the hydration of malvidin-3-glucoside. The verification of the presence of the flavylium ion at wine pH would provide confidence in the reaction mechanisms that have proposed for the interchange of malvidin-3-glucoside species in wine.

Spectroscopic methods used previously for the estimation of hydration and ionisation constants of anthocyanins give little indication of the charge status of the anthocyanin at a particular pH. It was therefore proposed (Chapter 1) that high voltage paper electrophoresis (HVPE), which relies on charge to produce separations, may be used in conjunction with spectroscopic methods. The combination of these two methods should provide an improved understanding of the charge character of the individual malvidin-3-glucoside species. The methods developed may also be utilised to determine the charge and pH relationship for other anthocyanins or anthocyanin type pigments. Once the hydration and ionisation constants have been established, then the spectra of the various forms of malvidin-3-glucoside may be obtained.

Results

Molar absorbance coefficient

The estimated purity of the malvidin-3-glucoside sample isolated in this study using the ratio of its peak area to the total peak area after HPLC separation was 94%. The minor contaminants included the acetyl and *p*-coumaryl derivatives of malvidin-3-glucoside. The molar absorbance coefficient for malvidin-3-glucoside in aqueous solution estimated using the G-G assay (Table 3.1) was 27 958 (± 500).

Table 3.1: Estimation of the molar absorbance coefficient of malvidin-3-glucoside using the G-G assay. The absorbance and concentration of the eluent as well as the molar absorbance coefficient calculated for each sample replicate are shown.

Sample	Absorbance 520 nm	Conc. μmol dm^{-3}	ε
1	6.900	690	24 150
	7.760	776	26 896
2	6.060	606	27 611
	6.300	630	27 930
3	5.500	550	28 304
	5.840	584	29 766
4	6.160	616	28 450
	6.520	652	28 162
5	2.240	224	30 011
	2.360	236	28 297
mean (± s.e.)			27 958 (± 500)

A direct comparison of the spectra of malvidin-3-glucoside in 0.01 mol dm^{-3} HCl and 90% (v/v) aqueous ethanol indicates that in the ethanol malvidin-3-glucoside shows increased absorbance at a higher wavelength (Figure 3.1). With increasing ethanol concentration, the absorbance maximum both and shifts towards longer wavelengths (Figure 3.2b) and increases (Figure 3.2c). These data also show that increasing ethanol concentration there was a decline in absorbance at 520 nm with ethanol concentrations greater than 50%

(Figure 3.2a). As the concentration of HCl changes with the ethanol concentration, the absorbance of malvidin-3-glucoside was analysed in 0.01, 0.1 and 1 mol dm^{-3} HCl and 90% ethanol. There was no difference in absorbance observed.

A sigmoidal curve may be fitted (r^2 = 0.9976) to the data representing the change in the absorbance maximum with changing levels of ethanol (Figure 3.2b). By using this curve and extrapolation, it is possible to form an estimate of the absorbance maximum in 100% ethanol. Furthermore a sigmoidal curve may also be fitted (r^2 = 0.9494) to the absorbance measured at λ_{max}. Using this curve the maximum absorbance can be estimated λ_{max} in 100% ethanol. The absorbance of 19.64 µmol dm^{-3} malvidin-3-glucoside in 100% ethanol is 0.659. Using these values and the Beer-Lambert law (Equation 1.1), the molar absorbance coefficient estimate of malvidin-3-glucoside at 544 nm in 100% ethanol is approximately 33 550.

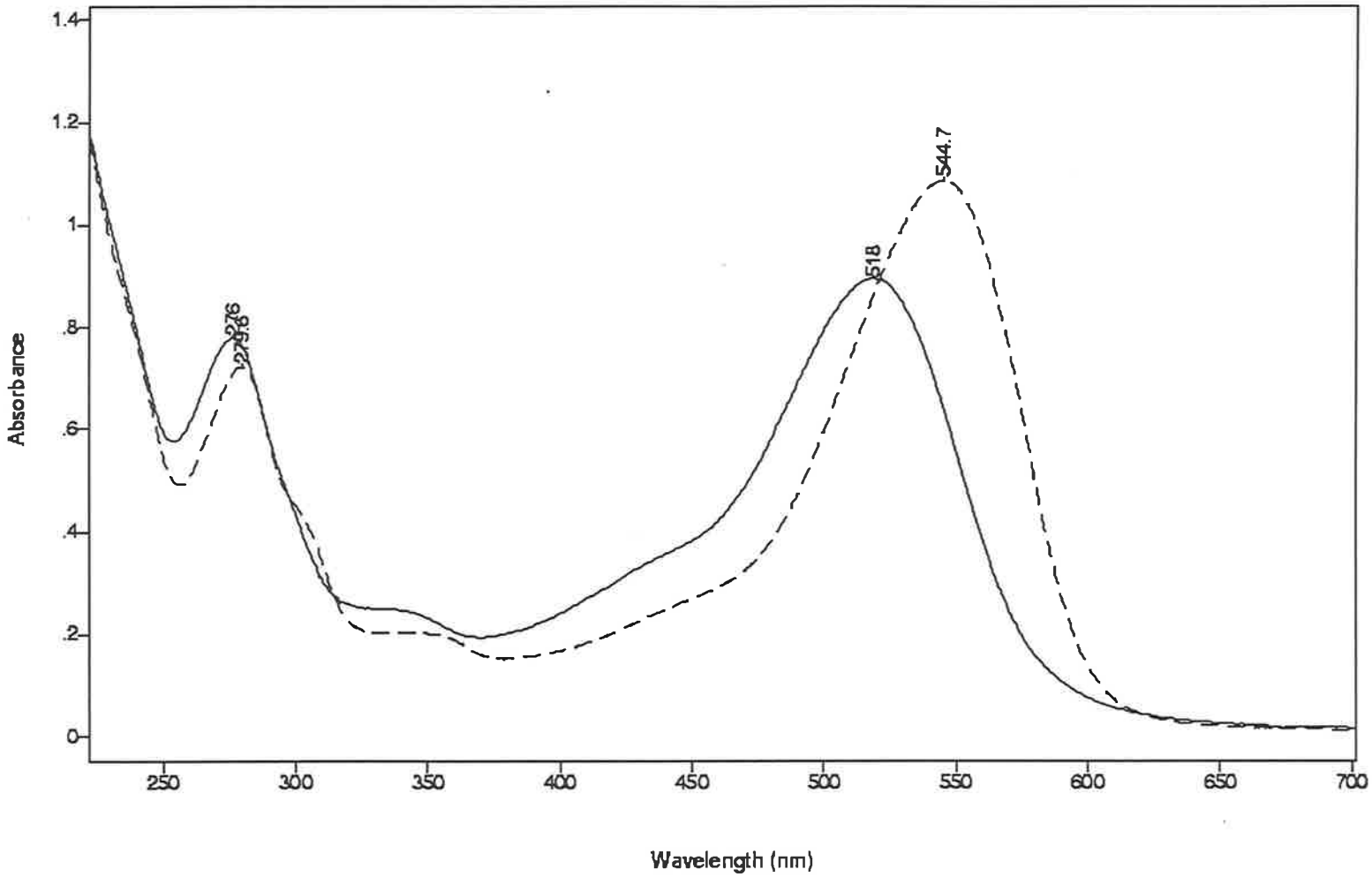

Figure 3.1: UV-visible spectrum of malvidin-3-glucoside in aqueous solution (solid line) and in acidified aqueous ethanol (dashed line).

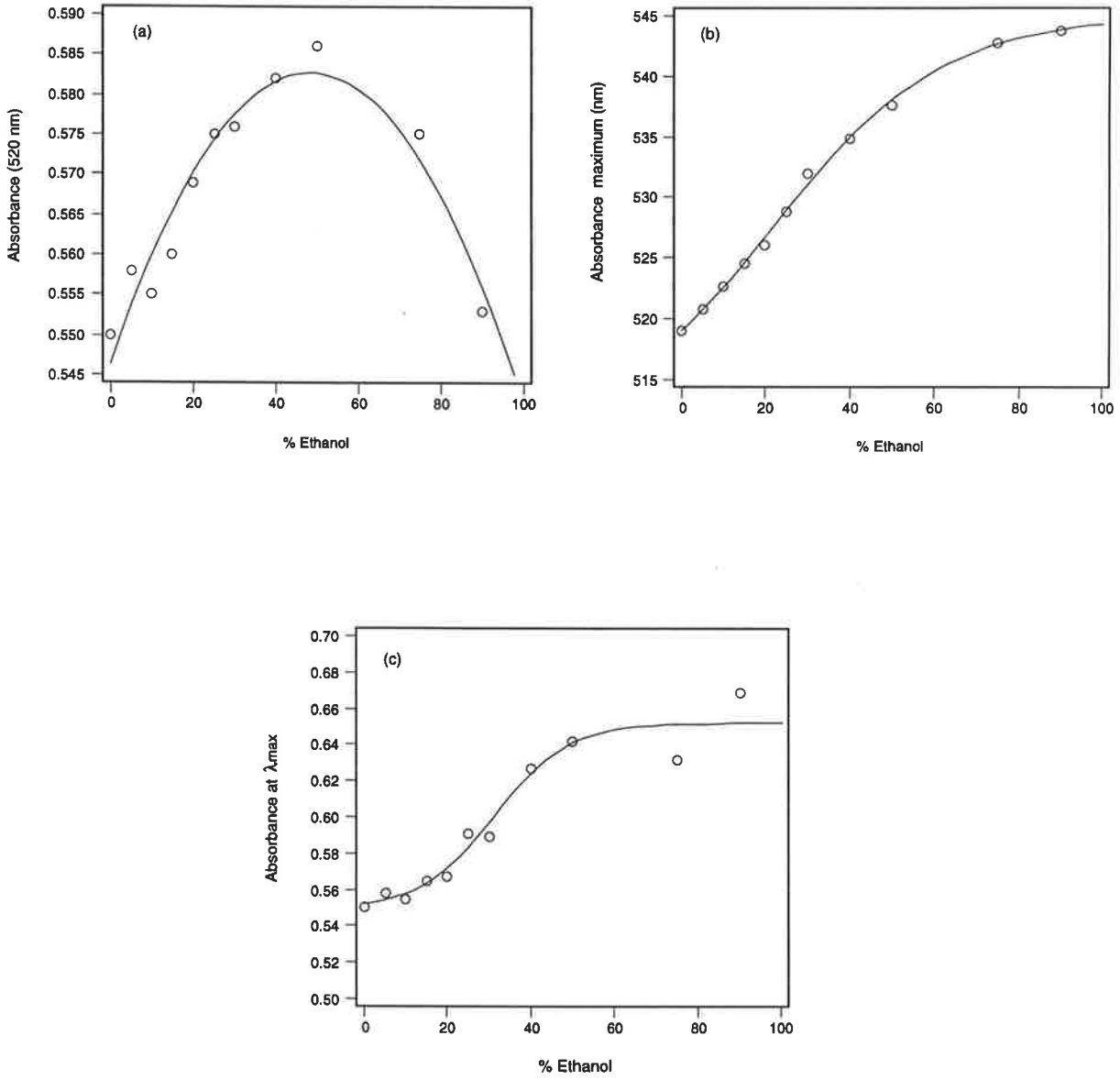

Figure 3.2: Change in absorbance of aqueous malvidin-3-glucoside solutions with an increasing concentration of ethanol; (a) absorbance measured at 520 nm verses the ethanol concentration fitted with a quadratic equation fitted (r^2 = 0.9227), (b) maximum absorbance (λ_{max}) compared with the ethanol concentration fitted with a sigmoid curve fitted (r^2 = 0.9976), (c) absorbance at maximum absorbance (λ_{max}) verses the ethanol concentration fitted with a sigmoid curve (r^2 = 0.9494).

Spectrum of the coloured species of malvidin-3-glucoside at wine pH

The analysis of the spectrum of malvidin-3-glucoside at wine pH was followed using the flow cell technique (Chapter 2). A solution of malvidin-3-glucoside at pH 0.7 and a citrate/phosphate buffer of pH 6.4 were rapidly mixed and pumped through the flow cell of a diode array spectrophotometer. The pH of the resulting mixture varied from pH 3.2 to 5.0, due to difficulties in achieving the necessary fine control of the pumps, and followed an essentially normal distribution, with a median of pH 4.2. There was no evidence that any new and significantly coloured species formed during the jump in pH of 0.7 to 4.2. At pH 4.2 the flow rates of 16 mL min^{-1} gave a flow cell retention time estimated to be less than 37.5 ms and the absorbance of malvidin-3-glucoside at 520 decreased rapidly (Table 3.2; Figure 3.4).

Table 3.2: Absorbance of the malvidin-3-glucoside at pH 0.7 compared with the average absorbance at 4.2 after mixing. The reaction time for the loss of colour is equivalent to the mixing time. The absorbances at 520 nm were adjusted according to the dilution.

pH	Flow Rates (mL min^{-1})		Dilution	Mixing	Abs 520 nm
	Pump A	Pump B		time (ms)	(Adjusted)
0.7	26.8	2	0.0694		4.822
4.2	8	8	0.5	37.5	1.191

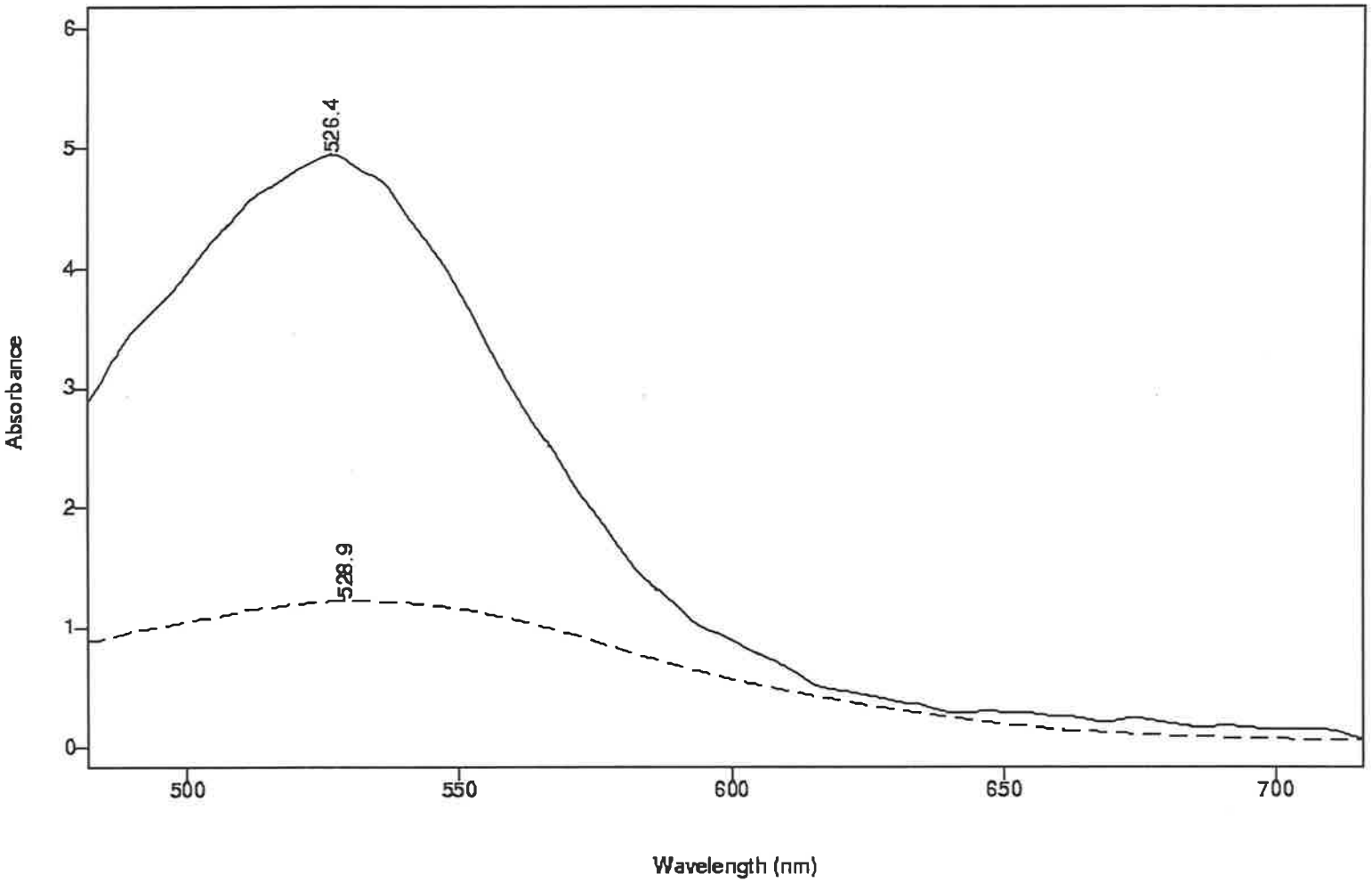

Figure 3.3: Spectra of malvidin-3-glucoside using the flow cell. The initial spectrum at pH 0.7 (solid line) and the spectrum at pH 4.2 approximately 37.5 ms later (dashed line). The spectra were adjusted for dilution.

Ionisation constants, hydration constants and UV-visible spectra

Three different buffers were used to examine three distinct pH regions. The buffers were; oxalate buffer for the pH range pH 1.4 to 4.5, citrate for pH 2.7 to 6.9 and pyrophosphate/oxalate buffer for pH 7.0 to 10.4. While the buffers were not optimised to present a complete mobility profile, the three buffer systems overlapped and therefore a pH profile was developed.

Using Equation 2.8, a curve can be fitted to the HVPE data for each of the three buffers used (Figure 3.4). Note that the plateau for zero charged species does not coincide with the zero mobility marker (Figure 3.4a). This is a consequence of the electro-osmotic flow of the buffer towards the cathode and the adsorption of the neutral species to the cellulose (Frahn and Mills, 1959). The fitted Equation 2.8 provides estimates of the three different pKa values (Table 3.3)

Table 3.3: Macroscopic pKa values for malvidin-3-glucoside at 25°C as derived using HVPE with the buffer for each determination indicated.

	Buffer	pKa
pKa_1	Oxalate	1.76 ± 0.07
pKa_2	Citrate	5.36 ± 0.04
pKa_3	Phosphate/oxalate	8.39 ± 0.07

While the pKa values may be estimated using Equation 2.8, the plateau regions correspond to the optimum pH for a particular ionisation state. It was estimated that the flavylium ion occurs at pH <1, the quinonoidal base at approximately pH 3.6, the anion at approximately pH 7.5 and the dianion at approximately pH 10.0. The colour of the spots on the HVPE electrophoretogram at these plateau regions were red for the quionoidal base, purple for the anion and blue for the dianion. For examples of these electrophoretograms see Appendix C.

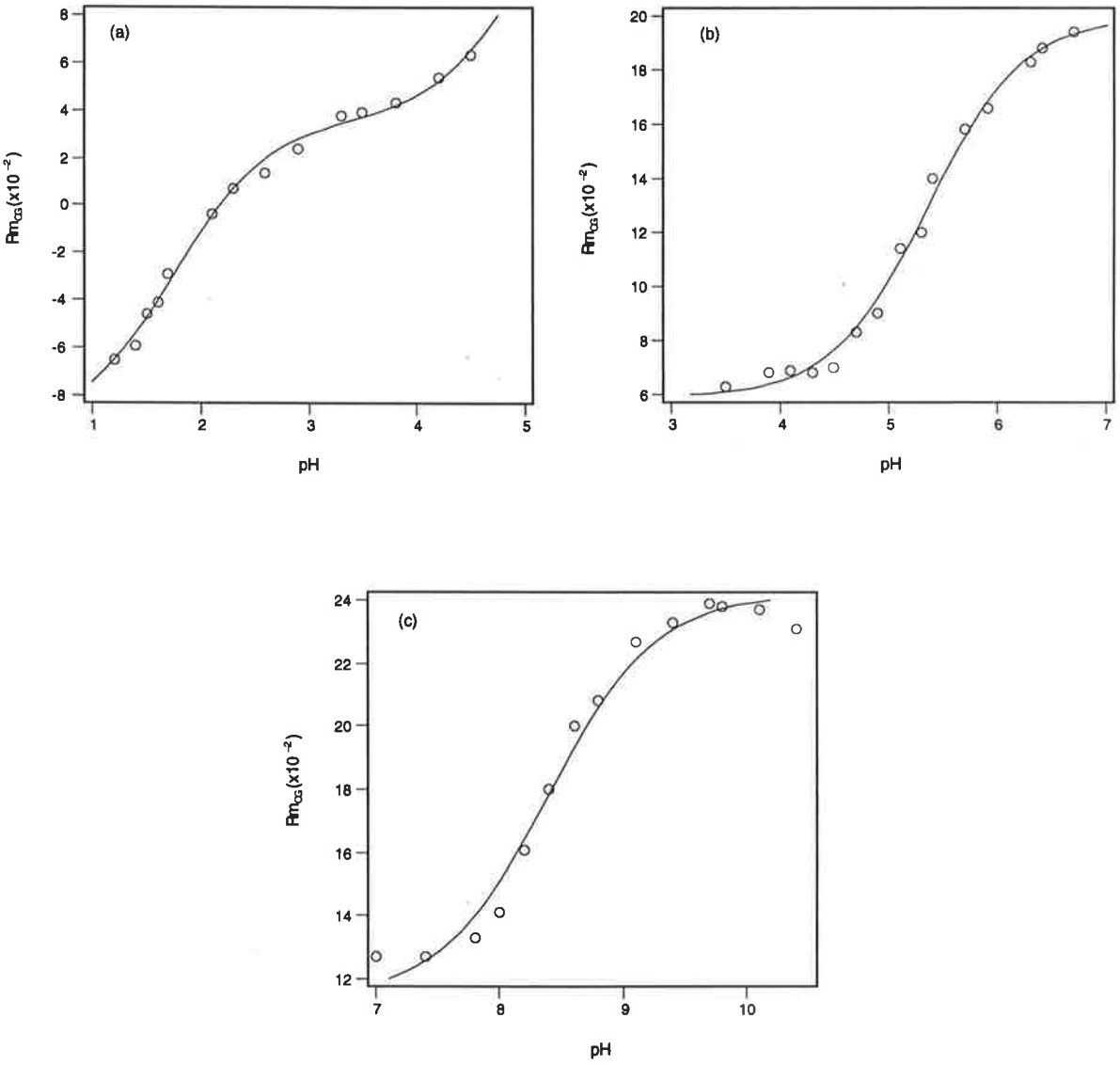

Figure 3.4: Relative mobility of malvidin-3-glucoside (Rm_{OG}) as a function of pH with Equation 2.8 fitted for the estimation of pKa values using HVPE. The three different pH ranges were defined by the three different buffers; (a) oxalate, (b) citrate, and (c) phosphate/oxalate. The coefficient of determination (r^2) for the three curves were (a) 0.9971, (b) 0.9839, and (c) 0.9839.

The HVPE data provided an optimal pH for the observation of the principle states of malvidin-3-glucoside, ie, pH 1 the flavylium ion, pH 3.0 for the uncharged quinonoidal form, pH 7.5 for the quinonoidal anion (A^-) and pH 10 for the quinonoidal dianion (A^{2-}). However, on analysing the spectroscopic data it was observed that only three coloured forms of malvidin-3-glucoside in the dilute solutions were observed. Thus, it was proposed that these coloured species represent the flavylium ion at low pH, and the two quinonoidal anions, A^- and A^{2-} at high pH values. At pH values greater than 1.0 there was a loss of colour associated with the hydration of malvidin-3-glucoside, as expected from previous research (Brouillard and Delaporte, 1977; Timberlake 1980). The proposed transient coloured quinonoidal base was not observed under these conditions.

The analytical wavelengths chosen were 520 nm for the estimation of the pK value for formation of the hemiketal/*cis*-chalcone, and 440 nm for the pK values associated with the development of the quinonoidal anion (A^-) and quinonoidal dianion (A^{2-}). The 575 nm wavelength was also used to calculate the pK values of the quinonoidal anions A^- and A^{2-}. By fitting the data to Equation 2.30 from the three analytical wavelengths (Figure 3.5), the macroscopic pK_{H1}, pK_{H2} and pKa_3 values were calculated (Table 3.4).

Table 3.4: Macroscopic pK_H and pKa_3 values for malvidin-3-glucoside at 25°C as derived using spectroscopic methods.

	Analytical wavelength	pK	Average
pK_{H1}	520 nm	2.66 ± 0.03	
pK_{H2}	440 nm	5.99 ± 0.05	
pK_{H2}	575 nm	5.79 ± 0.07	pK_{H2} = 5.90
pKa_3	440 nm	8.33 ± 0.11	
pKa_3	575 nm	8.08 ± 0.06	pKa_3 = 8.22

The combination of the spectroscopic and electrophoretic data permitted the spectra for the different species at their optimum pH to be recorded (Figure 3.6). Although the colourless hemiketal/*cis*-chalcone had a λ_{max} at 276 nm, there was also a small peak at 531 nm (Figure 3.6). It was proposed that this peak was due to a contribution of either the quinonoidal base or the quinonoidal anion, A^-. Furthermore, it was proposed that the quinonoidal anion (A^-) has two visible maxima at 444 nm and 578 nm (Table 3.5). The similarity between the

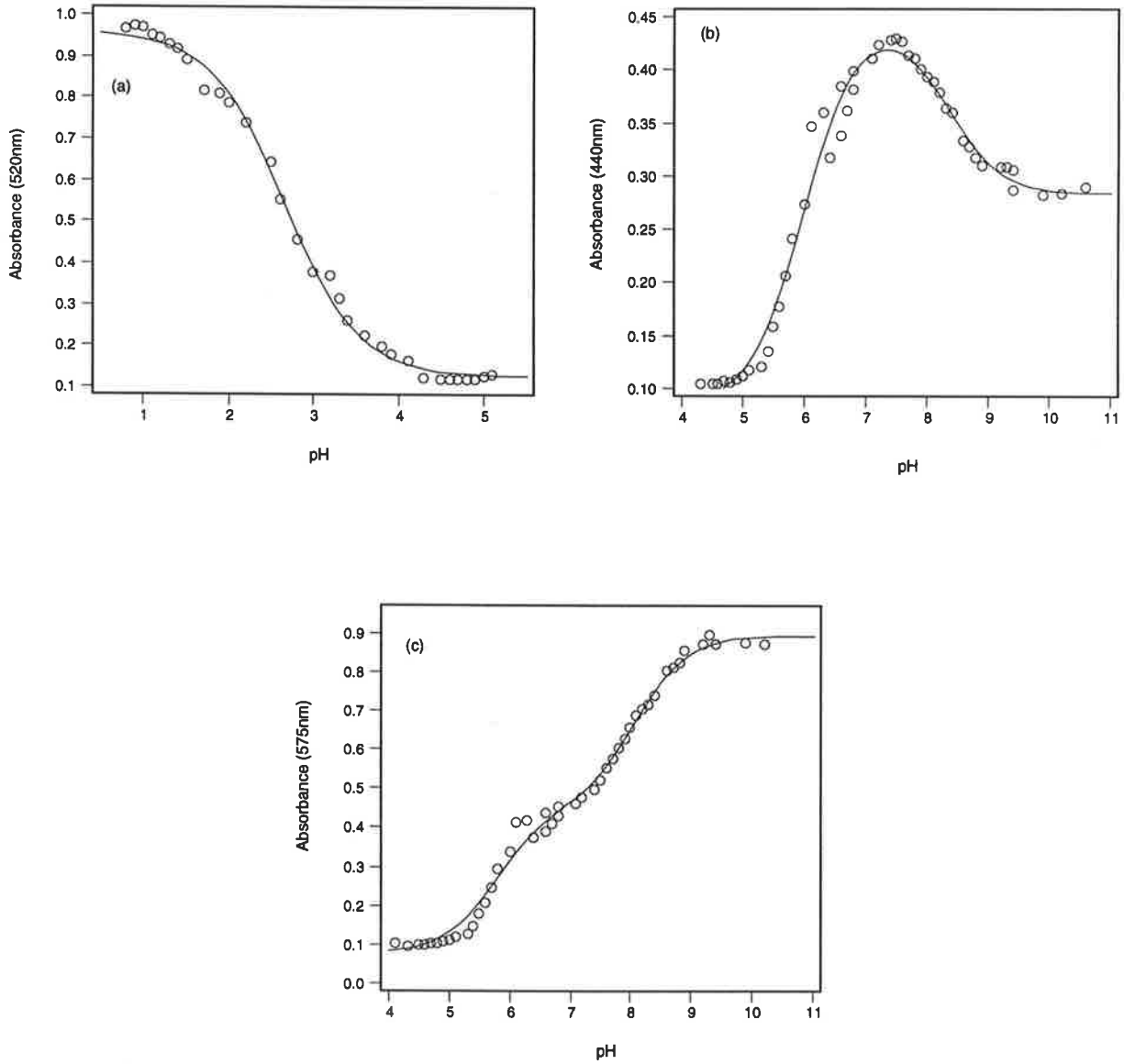

Figure 3.5: Absorbance of malvidin-3-glucoside as a function of pH with Equation 2.28 fitted for the estimation of hydration and ionisation constants by spectroscopic method. Three different pH ranges were used. The wavelengths used for the three pH ranges were; (a) 520 nm, (b) 440 nm, and (c) 575 nm. The coefficients of determination (r^2) were (a) 0.9957, (b) 0.9817, and (c) 0.9940.

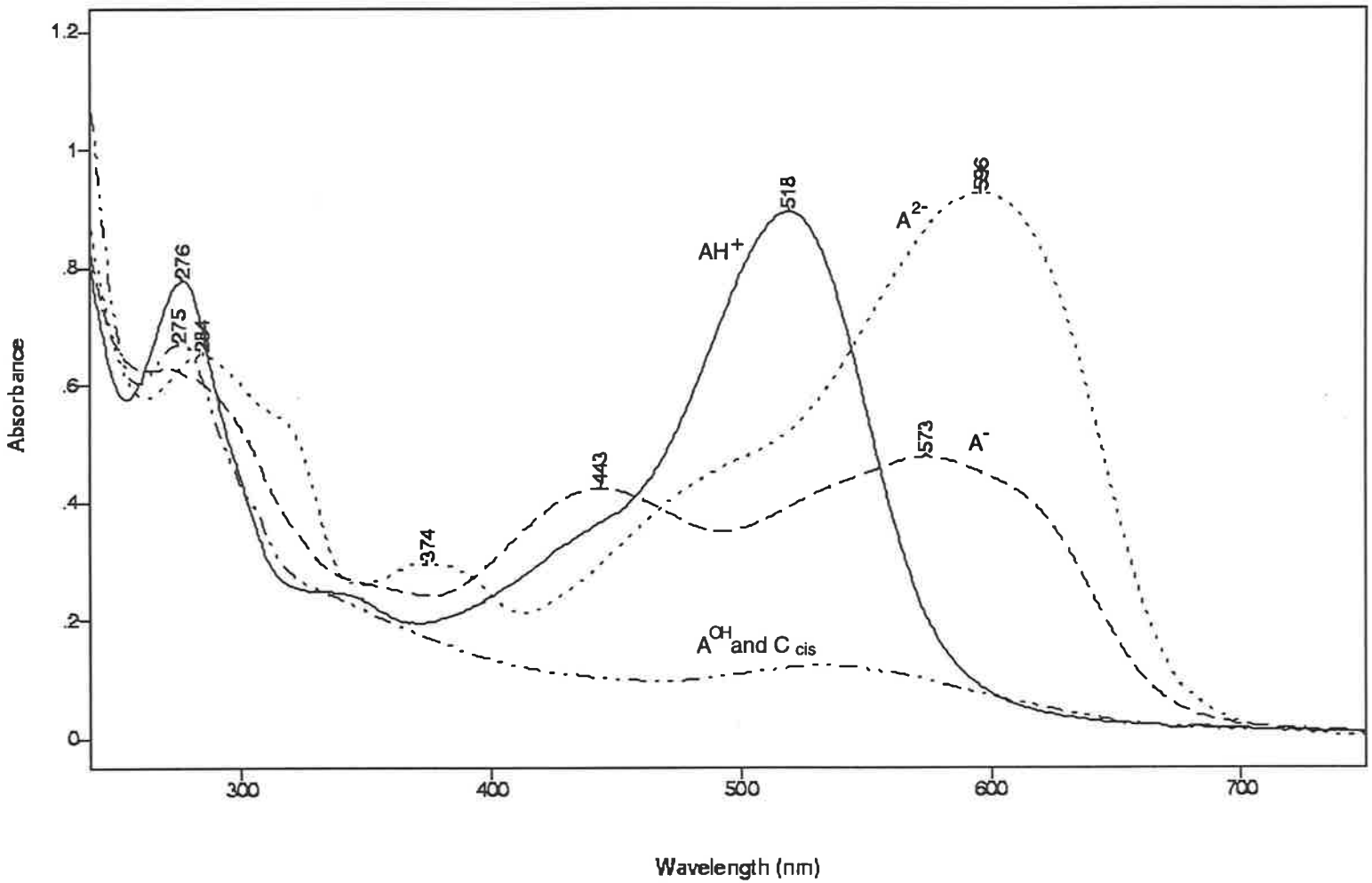

Figure 3.6: UV-visible spectra of the flavylium ion (AH^+), hydrated forms (hemiketal, A^{OH} and cis-chalcone C_{cis}), quinonoidal anion (A^-), and quinonoidal dianion (A^{2-}) of malvidin-3-glucoside at pH 0.7, 4.4, 7.2 and 10.0 respectively.

pK_{H2} values estimated at the two analytical wavelengths (575 nm and 440 nm), and also the closeness of the two pKa_3 values calculated at these same wavelengths, strongly suggests that the peaks at 444 nm and 578 nm belong to the same species.

Table 3.5: Different species of malvidin-3-glucoside with their corresponding maximal absorbances and the visible colour.

		pH	λ_{max}	visible colour
Flavylium ion	AH^+	1.0	276; 518	red
Hemiketal/*cis*-chalcone	$A^{OH}+C_{cis}$	4.4	276	colourless
Quinonoidal anion	A^-	7.2	272; 444; 578	purple
Quinonoidal dianion	A^{2-}	10.0	284; 374; 596	blue

The calculated pKa and pK_H values from HVPE and UV-visible spectroscopic experiments are combined and summarised in Figure 3.7. Using this data, a revised charge distribution (Figure 3.8) diagram for malvidin-3-glucoside of the ionic and neutral species found in aqueous solutions was compared with a similar diagram previously determined by Timberlake (1980). The principle difference regards the distribution of the flavylium ion and the quinonoidal base. The HVPE pKa estimates suggest that the maximum concentration of the flavylium ion occurs at a lower pH than indicated by Brouillard and Delaporte (1977), and Timberlake (1980).

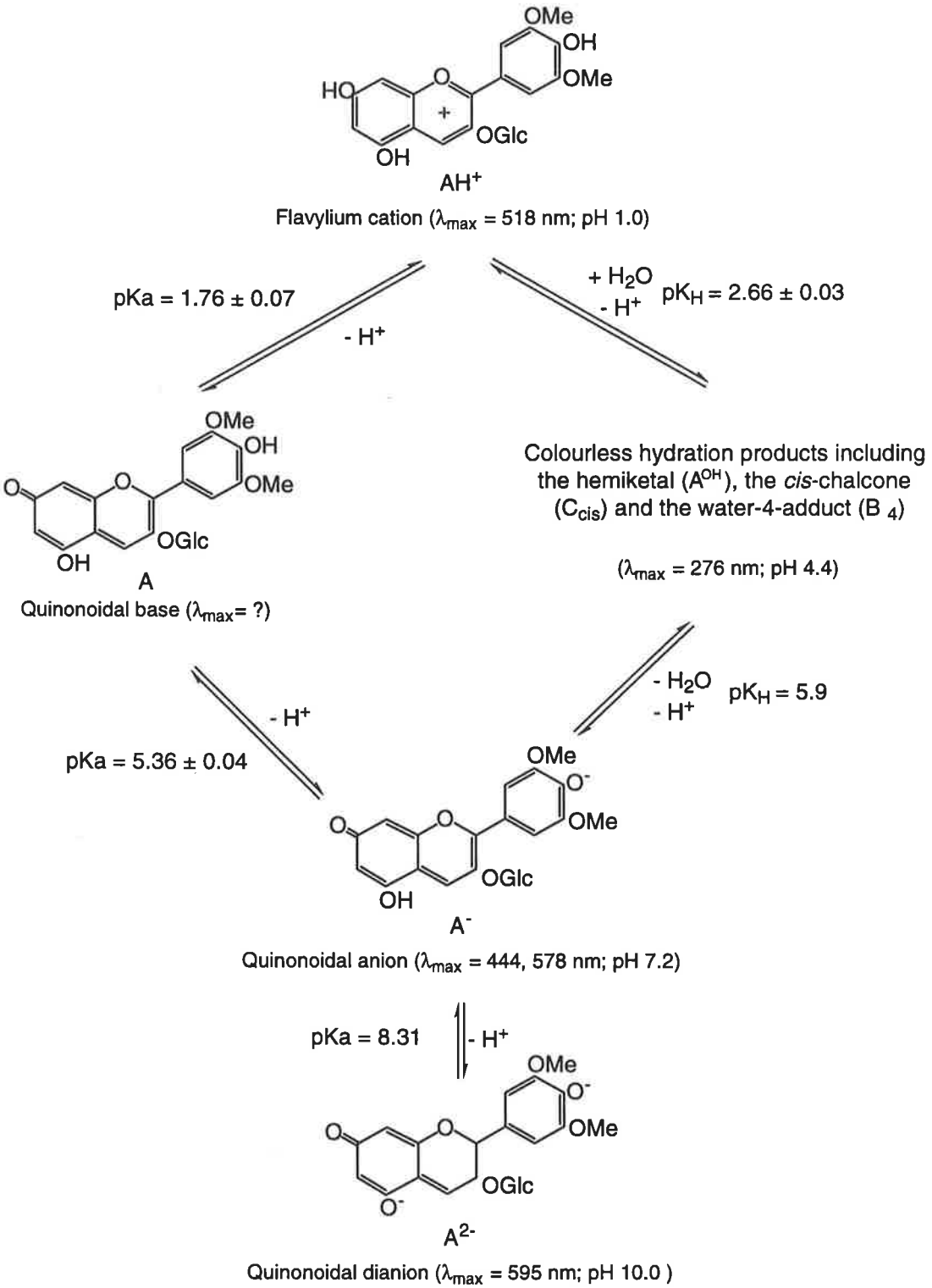

Figure 3.7: Structures of malvidin-3-glucoside as a function of pH. The macroscopic pKa and pK_H values of malvidin-3-glucoside in dilute solutions as calculated using HVPE and UV-visible spectrometry. The λ_{max} and the pH at which this occurs for each of the species of malvidin-3-glucoside has been included.

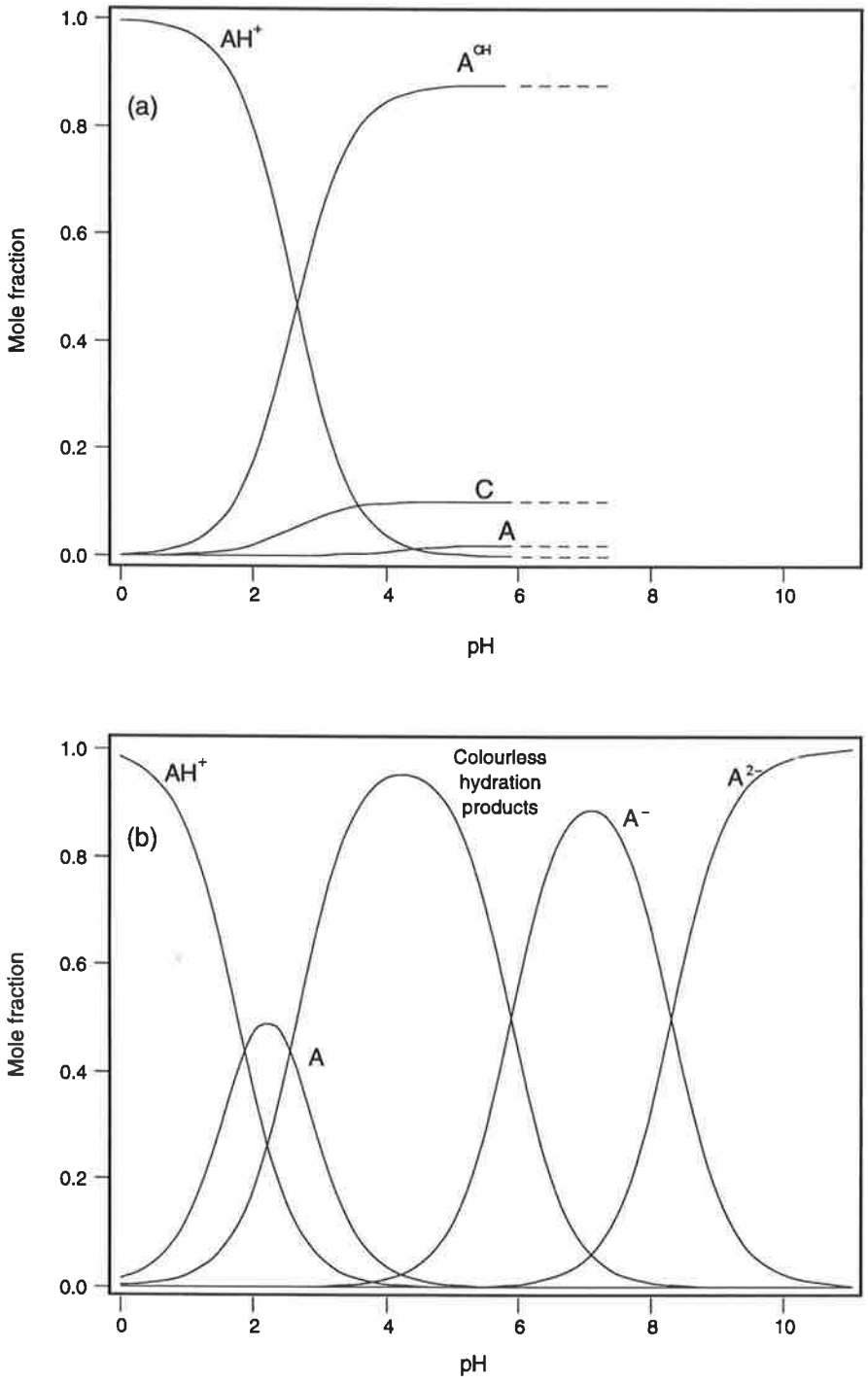

Figure 3.8: A comparison of charge distribution diagrams for malvidin-3-glucoside at 25°C. (a) The charge distribution diagram prior to the current investigations utilising pK values of pKa = 4.25, pK_H = 2.60. (Brouillard and Delaporte, 1977; adapted from Timberlake, 1980). (b) The revised distribution diagram using the pK values estimated by the HVPE and UV/Vis spectroscopy described in the text. The pK values used were pKa_1 = 1.76, pK_{H1} = 2.66, pK_{H2} = 5.9, and pKa_3 = 8.31. (Note AH^+ represents the flavylium ion, A the quinonoidal base, A^{OH} the hemiketal, C the chalcone, and, A^- the quinonoidal anion and A^{2-} the quinonoidal dianion.)

Discussion

Molar absorbance coefficient

The molar absorbance coefficient of malvidin-3-glucoside at pH 0.0 as calculated using the GG assay was 27 958 (± 500). This estimate agrees with the previously published estimates (Table 1.1) and validates the use of the G-G assay as an alternative method for the determination of the molar absorbance coefficient of anthocyanins. For the following work a molar absorbance coefficient of 28 000 will be used. In 100% ethanol, the molar absorbance coefficient of malvidin-3-glucoside$_{544}$ is approximately 33 550. This estimate is similar to the value calculated by Nagel and Wulf (1979) using methanol.

At pH 1 in aqueous solution malvidin-3-glucoside is almost fully ionised (Timberlake, 1980). However, the plateau in the absorbance maximum, observed at approximately 90% (v/v) acidified aqueous ethanol (Figure 3.2b), indicates that there is another red form of malvidin-3-glucoside that predominates. Therefore, there are two states of the malvidin-3-glucoside to be found as the concentration of ethanol increases. The one form of malvidin-3-glucoside is present in acidified aqueous solutions and has a λ_{max} of 519 nm and is thought to be the flavylium ion, while the other state exists in acidified ethanolic solution and has a λ_{max} of 544 nm. It should also be noted that malvidin-3-glucoside in 90% (v/v) acidified aqueous ethanol is resistant to changes in the concentration of HCl from 0.01 mol dm^{-3} to 1 mol dm^{-3}. It is well known that quinonoidal bases form under anhydrous conditions and thus, the alternative name for the quinonoidal base is the anhydrobase (Wawzonek, 1951) and unless kept anhydrous the quinonoidal base will form the hemiketal. Therefore, it is proposed that malvidin-3-glucoside$_{544}$ is the quinonoidal base.

The formation of chromenol ethers has been described (Wawzonek, 1951) whereby an alcohol reacts with the anthocyanin in a similar way to that of water with the anthocyanin to form the hemiketal. Thus, the reaction of ethanol with malvidin would yield an ethylketal. As

both the ethylketal and hemiketal are colourless, this study provided no evidence that malvidin-3-glucoside reacts with ethanol under the conditions used here.

The quinonoidal base of malvidin-3-glucoside has been described as blue by Timberlake (1980) and blue/violet by Liao *et al.* (1992). However, the data presented here suggests that the quinonoidal base, at least in ethanol, has a red colour. Evidence provided by Collins *et al.* (1950); Robertson and Whalley (1950) and Hirst (1927), indicates that it is not uncommon for neutral quinonones analogous to the malvidin-3-glucoside quinonoidal base to have a red colour (Figure 3.9).

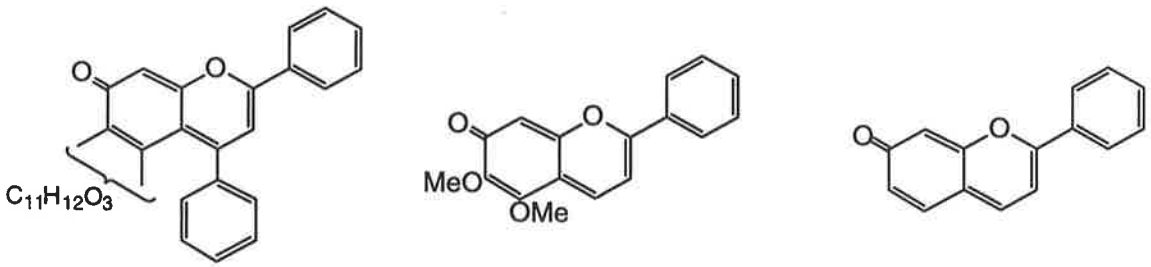

3.9a 3.9b 3.9c

Figure 3.9: Structures of three quinonoidal bases with a red colour; (3.9a) dracorubin (Collins *et al.,* 1950), (3.9b) dracorhodin (Robertson and Whalley, 1950) and (3.9c) the 7-hydroxyflavylium quinonoidal base (Hirst, 1927).

Spectrum of the aqueous quinonoidal base; rate of formation of the hemiketal

A rapid pH adjustment (37.5 ms) of malvidin-3-glucoside from pH 0.7 to 4.2, at 30°C, results in a loss of colour (Figure 3.3). The spectrum also shows that from pH 0.7 to pH 4.2 there is a slight bathochromic shift from 524 nm to 532 nm. The colour loss associated with the increase in pH is usually attributed to the formation of the hemiketal (Timberlake, 1980; Brouillard and Cheminat, 1988) and not the quinonoidal base. Therefore, the loss of colour observed is probably because of a loss of conjugation in the molecule associated with the formation of the hemiketal. This colour loss is the result of the quick conversion of the flavylium ion (pH 0.7) into the hemiketal, and therefore the spectrum of the quinonoidal base at pH 4.2 could not be measured. The concentration of water in aqueous solutions is usually very high (>50 mol dm^{-3}) and provides a considerable driving force for the hydration reaction.

The formation of the malvidin-3-glucoside hemiketal at 30°C is a rapid reaction, estimated to occur in less than 37.5 ms. This contrasts with 8.5 (± 0.1) x 10^{-2} s^{-1} ($t_{1/2}$ = 8.15 s) obtained by Brouillard and Delaporte, (1977) for malvidin-3-glucoside at 25°C using the pH jump method. The formation of the hemiketal does not follow first order kinetics. Brouillard and Delaporte, (1977) report the loss of colour at 517.5 nm due to a pH jump from pH 1 to 5 occurs as a three step process The first step occurs as fast as the pH jump whereby approximately 40% of colour is lost. These authors attribute this colour loss to formation of the quinonoidal base ($t_{1/2}$ = 1.47 x10^{-5}; Brouillard and Delaporte, 1977). The second phase of colour loss was much slower, and these authors proposed that the hemiketal was formed during this process. The third phase was associated with formation of the *trans*-chalcone. If comparable times are considered, the current experiment shows that approximately 75% of 520 absorbance was lost in 37.5 ms, which was considerably more than 40% observed by Brouillard and Delaporte (1977).

McClelland and Gedge (1980) observed a similar triphasic process when studying the hydration of the flavylium ion. However, these authors concluded the initial rapid colour loss was due to the formation of the C4 hydration product, and the second phase was due to the formation of the hemiketal via the flavylium ion, ie, the C4 hydration product was the kinetic product and the hemiketal the thermodynamic product.

An alternate explanation for the complex process involved in the hydration of the malvidin-3-glucoside involves the formation of malvidin-3-glucoside complexes. The colourless trans-chalcone is able to aggregate with coloured forms of malvidin-3-glucoside to form a co-pigmentation complex (Houbiers *et al.*, 1998). These types of self aggregation complexes may have a role in mediating the formation of the hemiketal.

The rapid hydration reaction may also affect the pKa calculations using spectroscopic methods. The technique for the determination of the pKa values using spectroscopic methods and temperature jump kinetics proposed by Brouillard and Delaporte, (1977) relies on the protonation reaction being faster than the hydration reaction. However, a faster rate of hydration than expected may interfere with this calculation and this emphasises the value of HVPE as an independent method for the estimation of pKa values. The rapid hydration reaction also indicates that it is possible to determine the hydration constants (pK_H) of malvidin-3-glucoside without the requirement for lengthy equilibration times.

Ionisation and hydration constants

In their recent publications, Pina (1998) and Amic *et al.* (1999) considered that the hydration and ionisation constants can be pooled in a single pK estimate

$$AH^+ \overset{K}{\rightleftharpoons} (A+B+C)+H^+ \qquad \text{(Equation 3.1)}$$

where K represents the overall acidity constant, AH^+ was the flavylium ion, A was the quinonoidal base, B was the pseudo-base (hemiketal and B4 hydration product), C was the chalcone (*cis*- and *trans*- chalcones) and H^+ the concentration of hydrogen ions calculated by pH. Amic *et al.* (1999) proposed that the pseudobase and the quinonoidal base were the thermodynamic and kinetic products respectively. However, this pooled estimate gives little information of the individual hydration and ionisation constants, and its validity is based on that ionisation and hydration being competing reactions with similar reaction rates.

The advantage of the use of HVPE is that it provides an independent method for the determination of the pKa values for the differently charged species of malvidin-3-glucoside. Brouillard and Delaporte (1977) used temperature jump experiments to estimate rate of proton transfer reactions, and thereby to estimate the pKa value. They proposed that the proton transfer reactions occur significantly faster than the hydration reaction of malvidin-3-glucoside. The time for the new equilibrium to be reached due to the temperature jump was called the relaxation time (t). The relaxation time is related to the reaction rates using the equation below,

$$\frac{1}{\tau} = k_a + k_{-a}([A]+[H^+]) \qquad \text{(Equation 3.2)}$$

where k_a was the rate of flavylium ion deprotonation, k_{-a} the rate of the quinonoidal base protonation, [A] the concentration of quinonoidal base at equilibrium, and $[H^+]$ the concentration of hydrogen ions. From Equation 3.2 it was possible to calculate the reaction

rates by plotting the inverse of the relaxation time against the concentration of the quinonoidal base plus the concentration of the hydrogen ions. The pKa constants for anthocyanins were estimated using the equation,

$$Ka = \frac{k_a}{k_{-a}} \qquad \text{(Equation 3.3)}$$

where pKa is the negative log of the Ka, k_a is the rate of flavylium ion deprotonation and k_{-a} was the rate of the quinonoidal base protonation. The spectral measures used by Brouillard and Delaporte (1977) for the pKa values requires both an understanding of the species involved in the equilibrium, and protonation constants much faster than the hydration constants.

The value obtained for the first dissociation constant using HVPE of 1.76 ± 0.07 is substantially different from that of 4.25 obtained by Brouillard and Delaporte (1977). The positive charge associated with the flavylium ion is considered to be stabilised as a combination of oxonium and carbonium ions (Wawzonek, 1951). The strong acidity of malvidin-3-glucoside may be rationalised on the basis that mesomeric forms of the anthocyanin structures can be written in which the cationic charge is accomodated on the oxygen atom(s) from which proton loss occurs (Figure 3.10). Thus, for the first pKa, malvidin-3-glucoside may be considered as a protonated quinonone (Figure 3.10a), rather than the benzopyrylium cation (Figure 3.10b).

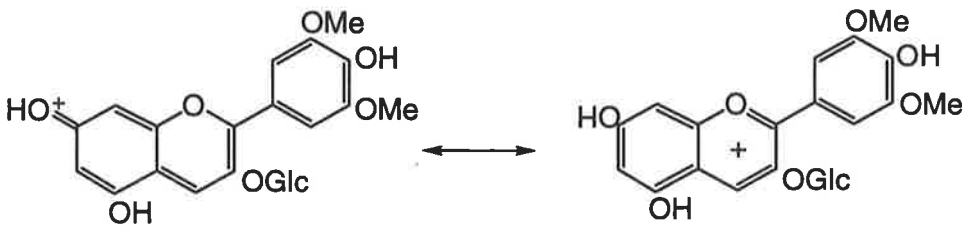

3.10a 3.10b

Figure 3.10: Two different mesomeric forms of the protonated malvidin-3-glucoside cation in solution. (3.10a) indicates protonation of the C7 oxygen. (3.10b) is the usual representation of the flavylium ion.

Only macroscopic pKa values can be calculated using HVPE and it is therefore not possible to determine microscopic protonation constants (ie, protonation constants at the molecular level). It is however expected that there are three overlapping microscopic pKa values representing the three different neutral quinonoidal species.

Each of the three quinonoidal species can form a quinonoidal anion, A^-. The experimental value of the macroscopic pKa_2 constant (5.36 ± 0.04) may be compared with theoretical estimates calculated using the principles outlined by Perrin *et al.* (1981). It is possible to use one quinonoidal base as a model for the formation of the quinonoidal anions (Figure 3.11).

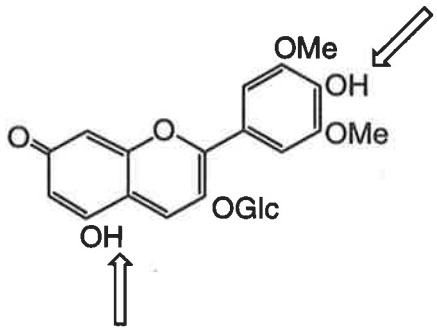

Figure 3.11: Structure of A7-quinonoidal base of malvidin-3-glucoside with the 4' and 5 hydroxyl groups indicated as potential sites for proton loss.

The C4' and C5 hydroxyl groups can form a vinyl quinonoidal species that can be considered to be analogous to a carboxylic acid. The pKa of a carboxylic acid is approximately 4.8 (Perrin *et al.*, 1981). There is a considerable degree of agreement between the predicted pKa and the pKa value obtained by HVPE.

An estimate for the dissociation constant, pKa_3, may be obtained using the Hammett and Taft equations according the procedures outlined by Perrin *et al.* (1981). A theoretical calculation pKa of the 4'-quinonoidal anion will be considered (Figure 3.12).

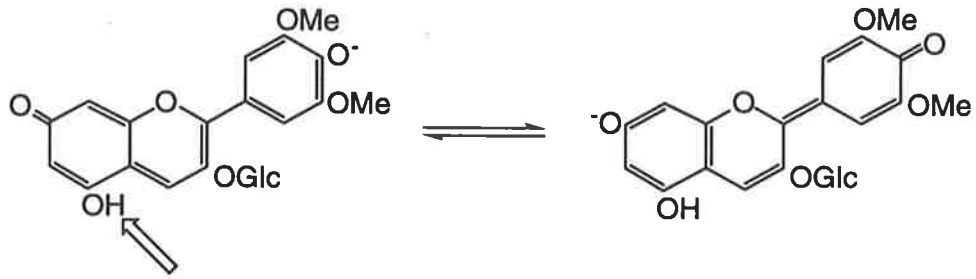

Figure 3.12: Two tautomers of the quinonoidal anion of malvidin-3-glucoside with the 5-hydroxy shown as the site for proton loss.

For the quinonoidal anion there are two models being the malvidin-3-glucoside ion with either the quinonone at carbon 7 or at carbon 4. For calculation using the Perrin procedure this can be simplified into two model compounds (see Figure 3.13a and 3.13b).

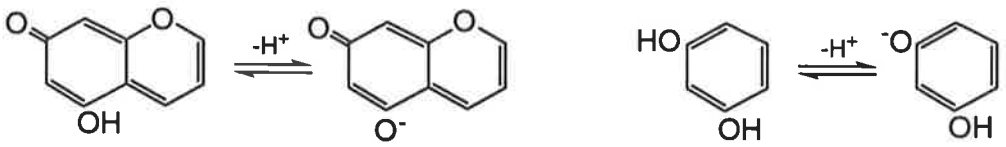

3.13a 3.13b

Figure 3.13: Two model compounds that can be used for the calculation of the pKa of the further ionisation of the quinonoidal anion.

Model compound 3.13a can be considered to be analogous to a carboxylic acid and therefore will have a pKa of approximately 4.8. It is possible to calculate the expected pKa of model compound 3.13b using the Hammett equation for phenols (Equation 3.4).

pKa phenol = 9.92 - 2.23 $\Sigma\sigma$ (Perrin *et al.*, 1981) (Equation 3.4)

σ for O^- = -0.47

pKa = 9.92 - 2.23(-0.47) = 11.0

Neither of these two models adequately explains the experimental pKa values obtained by HVPE (8.31) or spectroscopically (8.33 and 8.08). However, a calculation using a partial negative charge associated with the 4' and 7-oxo groups (Figure 3.14) is expected to give pKa that is closer to the experimental value. Similarly the pKa of the 4'-hydroxyl

group is expected to result from partial negative charge on both the 5 and 7 oxo groups, ie the charge is delocalised between the two non-protonated oxygens (Figure 3.14).

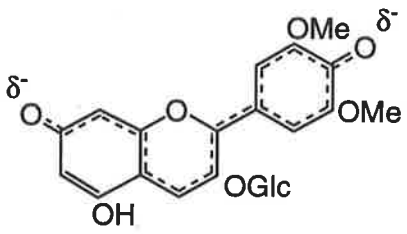

Figure 3.14: Structure of the quinonoidal anion of malvidin-3-glucoside indicating that the charge is evenly distributed between the non-protonated oxygens.

A similar explanation can be used for the derivation of the pKa values for the other quinonoidal anion tautomers. There is only one tautomer for the quinonoidal dianion A^{2-} expected (Figure 3.15).

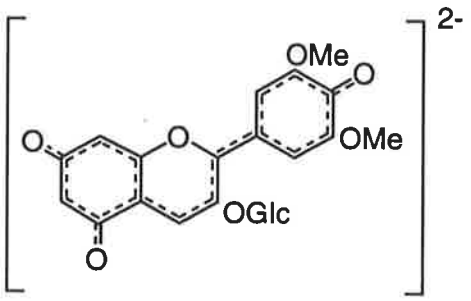

Figure 3.15: Structure of the quinonoidal dianion (A^{2-}) of malvidin-3-glucoside indicating charge delocalisation.

The flavylium ion exists at low pH only and the highest concentration of neutral species occurs at pH 3.60 (ie midway between pKa_1 and pKa_2). Therefore at wine pH (3.2 - 3.8), malvidin-3-glucoside is present as mainly neutral species.

Usually a single hydration constant has been used to describe the addition of water to the C2 position of theflavylium ion (Figure 3.16). The equilibrium between the hemiketal and *cis*-chalcone tautomeric reaction is rapid and it is not possible to differentiate between the two (Brouillard and Lang, 1990). The experimental estimate for the hydration constant,

pK_{H1}, obtained in this study (2.66 ± 0.03) was not significantly different from the estimate of 2.60 (± 0.02) obtained by Brouillard and Delaporte (1977) or 2.90 obtained by Timberlake (1980).

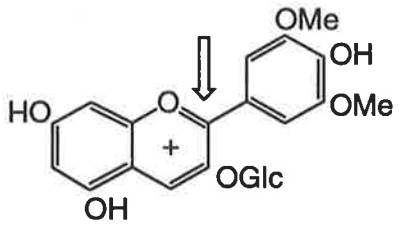

Figure 3.16: Structure of the flavylium ion of malvidin-3-glucoside indicating the position for the addition of water.

The existence of the uncharged quinonoidal base at pH 2.0 according to the HVPE data suggests that the macroscopic pK_{H1} calculated by the spectroscopic technique may represent a combination of the pKa_1 and pK_{H1} values. The 520 nm spectral data (Figure 3.6a) shows a minor plateau at pH 2.0, that may indicate the presence of two differing species. However, the data from the spectroscopic experiment was insufficient to accurately describe two different pK values.

The two estimates for pK_{H2} are 5.99 (± 0.05) and 5.79 (± 0.07) as determined from the spectral data calculated at 440 nm and 575 nm respectively. The similarity between the pK_{H2} values derived from the 440 nm and 575 nm data confirms that the species absorbing at these wavelengths are either the same or closely related. There are two possible explanations for the slightly lower value of the pK_{H2} measured at 575 nm. The difference in pK_{H2} between the two sets of measures may arise because of both the quinonoidal base and quinonoidal anion, A^-, forms contribute to this part of the spectrum, ie,

$$\bar{d} = d_0 + d_1 + d_2 \qquad \text{(Equation 3.5)}$$

where d_0 is the density attributable to the hemiketal, d_2 is the density of the quinonoidal base, A, and d_1 is the density of the quinonoidal anion, A^-. The calculation of the pK_H is only

valid if d_2 equals zero. The contribution of the absorbance of quinonoidal base under these conditions is unknown, however any augmentation will reduce the value of the macroscopic pK_{H2}. Another complicating factor for the determination of pK_{H2} is the multiple forms of the quinonoidal base and the quinonoidal anion A^-. Thus, at the microscopic level, multiple overlapping pKa and pK_H values are expected. However it only possible to observe the macro effects spectroscopically.

At pH 5.4 the hemiketal is still readily formed but at this pH there is only an extremely low concentration of the flavylium cation. Thus it is proposed that the quinonoidal base is able to form the hemiketal. Bunting (1979) reports that it is possible for the addition of water to the neutral base to form the hemiketal. It is proposed that the mechanism for the addition of water to the quinonoidal base is that the water molecule adds to the carbon 2 and subsequently loses a proton. This alters the electronic structure of the molecule and thereby changes the pKa of the oxygen on carbon 7. This oxygen then accepts a proton to form the neutral ion (Figure 3.17).

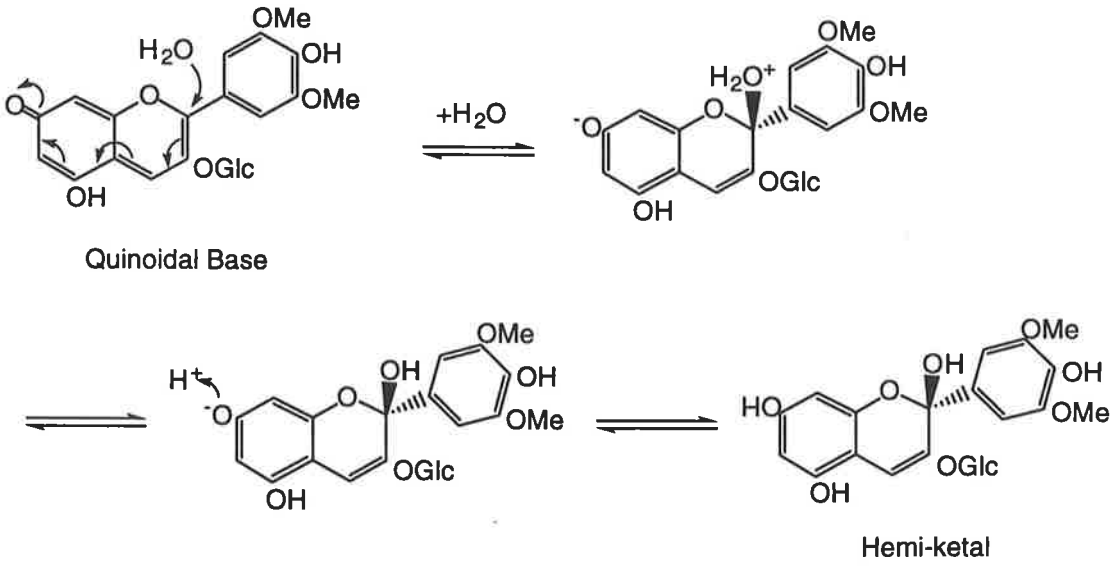

Figure 3.17: Proposed mechanism for the addition of water to the neutral quinonoidal base.

The mechanism for the formation of the quinonoidal anion from the hemiketal remains unknown. It is proposed that it is not a loss of water from the hemiketal that produces the

anion, but the hemiketal is in equilibrium with the quinonoidal base, and it is the quinonoidal base which loses the proton to form the anion. Thus the quinonoidal base is the active species for the loss of water to form the quinonoidal anion (Figure 3.18).

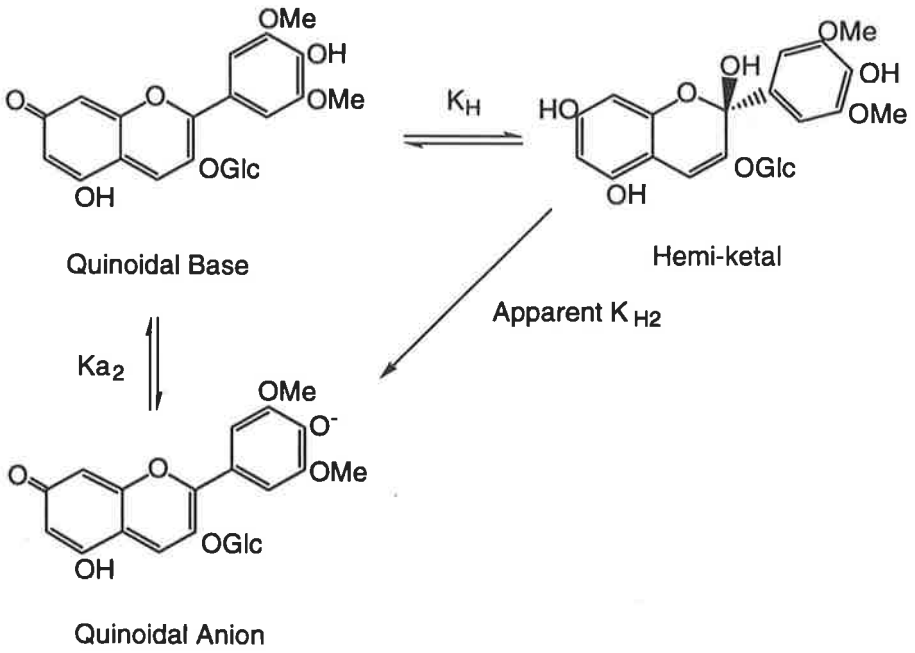

Figure 3.18: Formation of the quinonoidal anion (A^-) as the result of water loss by the hemiketal and subsequent ionisation.

Therefore, the macroscopic K_{H2} can be best described using the following equation,

$$K_{H2} = Ka_2 \times K_H \qquad \text{(Equation 3.6)}$$

Hence, it is the quinonoidal base and not the flavylium cation that is the species most involved in the hydration reactions. Furthermore, the addition of water to the quinonoidal base can be considered to be a Meisenheimer type reaction (Bunting, 1979). This also suggests that the addition of compounds such as bisulphite ion to the anthocyanin is via the quinonoidal base. This was further investigated in Chapter 7.

Other ionic and neutral molecular species of malvidin-3-glucoside have been predicted to occur in solutions (Brouillard and Cheminat, 1988). These include the C4 hydration product

or the water-4-adduct (B4). This is a colourless species analogous to the hemiketal. The addition occurs in the C4 position instead of the C2 position. There are two possible epimers of the water-4-adduct (Figure 3.19).

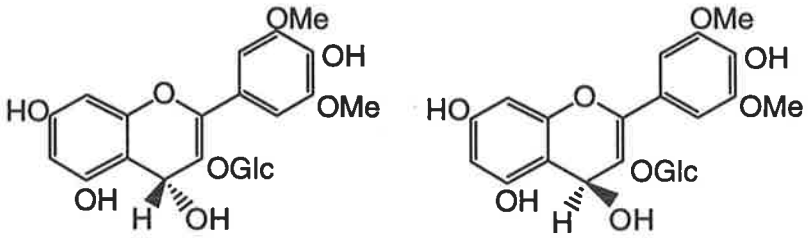

Figure 3.19: Two epimers of the water-4-adduct.

There is no way of differentiating spectroscopically between the colourless products and therefore the measured pK_H should be regarded as measuring the total concentration of colourless species. This can be described using the equations,

$$K_{H1} = \frac{([A^{OH}]+[B_4]+[C_{cis}]).\{H\}}{[AH^+]} \qquad \text{(Equation 3.7)}$$

and,

$$K_{H2} = \frac{[A^-].\{H\}}{([A^{OH}]+[B_4]+[C_{cis}])} \qquad \text{(Equation 3.8)}$$

Cheminat and Brouillard (1986), using NMR, provided direct evidence for the existence of the water-4-adduct of malvidin-3-glucoside. Furthermore, under the conditions used, Cheminat and Brouillard (1986) suggest that the concentration of the water-4-adduct, may be as high as 11% of the total anthocyanin at approximately pH 4-5 and 23°C. However, in their study of the anthocyanidins, McClelland and Gedge (1980) observed that while immediately after the addition of water, the water-4-adduct concentration was approximately two thirds of the hydration product, once equilibrium had been reached, the concentration of the water-4-adduct was minimal (<1%). With low concentrations of the

water-4-adduct at equilibrium (ie, 0.3% at pH 4.29), and a very short reaction time [the rate of water-4-adduct dehydration at pH 2.5 was 9.2×10^3 s^{-1} ($t_{1/2} = 7.5 \times 10^{-5}$ s)], McClelland and Gedge (1980) proposed that the water 4-adduct was the kinetic product of hydration only. Thus, the water-4-adduct is unstable and rapidly converted via the quinonoidal base into the hemiketal. However, at high pH the half life of the water-4-adduct increases, ($t_{1/2}$ = 66 s at pH 8.0) and therefore McClelland and Gedge (1980) propose that especially for kinetic studies, the importance of the water-4-adduct may increase with increasing pH.

In the current work possible effects of the water-4-adduct were ignored. It is unknown whether the experimental conditions used by Cheminat and Brouillard (1986) favoured the high concentration of the water-4-adduct observed, or McClelland and Gedge (1980) under estimated the importance of the water-4-adduct. The evidence from McClelland and Gedge (1980), suggests that the kinetic and thermodynamic energies of the C4 and the C2 hydration products are different. Therefore, it is very probable that the pK_H values for the two hydration products are different. Thus, the concentration of water-4-adduct may affect the macroscopic pK_H and therefore should be considered in future studies.

There are three isomers possible for the chalcone. These are the 2,3-*trans*-3,4-*cis*-chalcone, the 2,3-*trans*-3,4-*trans*-chalcone, and the 2,3-*cis*-3,4-*trans*-chalcone (Figure 3.20). The 2,3-*trans*-3,4-*cis*-chalcone is referred to as the *cis*- or E-chalcone, and the 2,3-*trans*-3,4-*trans*-chalcone and 2,3-*cis*-3,4-*trans*-chalcones are called the *trans*- or Z-chalcone. The hemiketal and *cis*-chalcone equilibrium (ie, ring opening and closing) reactions are very rapid (McClelland *et al.*, 1985) while the *cis*-chalcone to *trans*-chalcone conversion is slower (Brouillard and Lang, 1990).

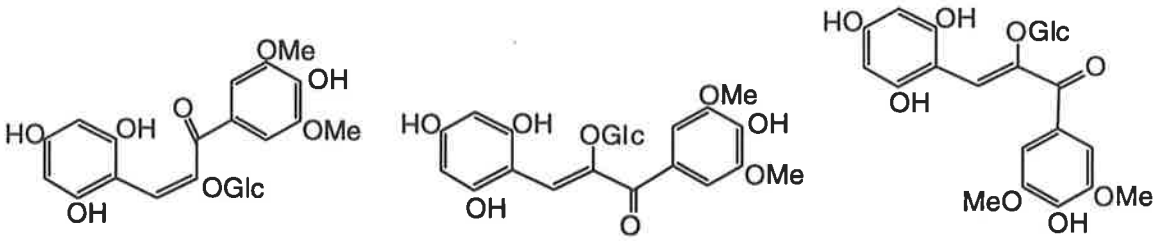

Figure 3.20: Three isomers of the chalcone of malvidin-3-glucoside; (3.20a) 2,3-*trans*-3,4-*cis*-chalcone, (3.20b) 2,3-*trans*-3,4-*trans*-chalcone, (3.20c) 2,3-*cis*-3,4-*trans*-chalcone.

Because the *cis*- and *trans*-chalcones of malvidin-3-glucoside co-exist (Houbiers and Santos, *unpublished* as cited by Figueiredo *et al.,* 1994), stabilisation of the *cis*-chalcone could be due to intramolecular hydrogen bonding (Santos *et al.*, 1993) It is proposed that there are two major tautomers of the *cis*-chalcone which may be stabilised by internal hydrogen bonding (Figure 3.21).

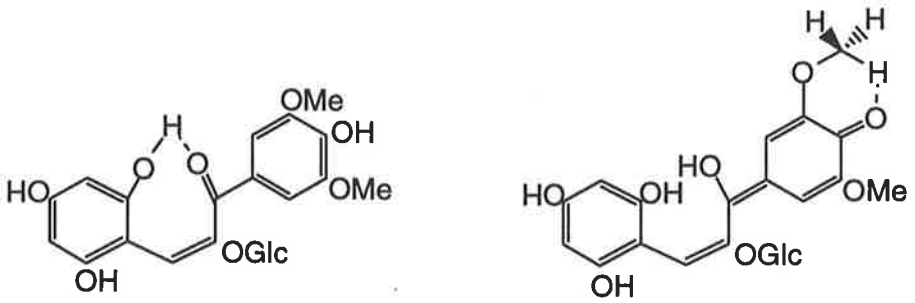

Figure 3.21: Two predicted principle tautomers of the *cis*- chalcone of malvidin-3-glucoside with internal hydrogen bonding indicated by a dashed line.

In this work it was considered that the *trans*-chalcone concentration was minimal. However, Santos *et al.* (1993) using proton NMR, observed that when equilibrium has been reached the concentration of the malvidin-3,5-diglucoside 2,3-*cis*-3,4-*trans*-chalcone is approximately 8%. Pina (1998) proposed that the rate of *trans*-chalcone formation and the concentration of the *trans*-chalcone should be accounted for when considering the macroscopic hydration constant. However, the *cis*- to *trans*- isomerisation rate as measured by Brouillard and Delaporte (1977) of 4.5×10^{-5} s^{-1} ($t_{1/2}$ = 4.28 h) implies that the

effect of the *trans*-chalcone on the macroscopic hydration constant in the current experiment was negligible.

The equilibrium between the *cis*- and *trans*- chalcone implies that when equilibrium is achieved the true pK_{H1} can be calculated using Equation 3.9,

$$K_{H1} = \frac{([A^{OH}]+[B_4]+[C_{cis}]+[C_{trans}]).\{H\}}{[AH^+]} \qquad \text{(Equation 3.9)}$$

and pK_{H2} estimated using Equation 3.10,

$$K_{H2} = \frac{[A^-].\{H\}}{([A^{OH}]+[B_4]+[C_{cis}]+[C_{trans}])} \qquad \text{(Equation 3.10)}$$

when the concentrations of A^{OH}, B_4, C_{cis} and C_{trans} represents the total concentration of colourless hydrated species. It is considered unlikely that the true pK_H values are substantially different from the macroscopic pK_H values obtained in this current work.

Ionised chalcones have a λ_{max} between 300 and 400 nm (McClelland and Gedge, 1980). The chalcone of the cyanidin-3,5-diglucoside has a λ_{max} of 377 nm (Mazza and Brouillard, 1987) When the pH of malvidin-3-glucoside was slowly increased to pH 10 to maximise the formation of the *trans*-chalcone, it was possible to show the presence of a peak at λ_{max} of 366 nm. It was proposed that this peak was the result of chalcone ionisation. This peak was absent from the spectra measured in the current experiment, and therefore there was no evidence for substantial concentrations of the ionised chalcone.

It is possible to estimate pKa values for the chalcone. If hydrogen bonding is ignored the pKa of these tautomers can be estimated, using the principles outlined by Perrin *et al.* (1981). Using the model compound 3,5-dimethoxy-4-hydroxybenzaldehyde, a pKa of approximately 7.6 can be estimated for the chalcone. Internal hydrogen bonding may decrease the acidity (Perrin *et al.*, 1981), and it is therefore predicted that the pKa of the *cis*-chalcone is greater than 7.6. Using kinetic data, McClelland and Gedge (1980)

estimated the pKa of 2-hydroxychalcone to be 9.0. These pKa values suggest that the concentration of the ionised chalcone of malvidin-3-glucoside is negligible at wine pH values (3.2 - 3.8).

The equilibria of anthocyanin species at high pH are poorly understood. Mazza and Brouillard (1987) observed that the ionised chalcone and the anionic quinonoidal base of cyanidin-3,5-diglucoside co-exist. The current data suggest that a similar situation exists for malvidin-3-glucoside. Interestingly, the reaction sequence (Equation 3.11) suggests that the interconvertability between the ionised chalcone and the anionic quinonoidal base may not be possible. This requires further investigation.

$$A^{2-} \rightleftharpoons A^{-} \rightleftharpoons A \rightleftharpoons A^{OH} \rightleftharpoons C_{cis} \begin{matrix} \rightleftharpoons C^{-}_{cis} \\ \rightleftharpoons C_{trans} \rightleftharpoons C^{-}_{trans} \end{matrix} \qquad \text{(Equation 3.11)}$$

Brouillard and Cheminat (1988) propose that the hemiketal can be ionised at the 2-hydroxyl group (Figure 3.22). However, hemiketals are very weak acids with expected pKa values similar to their hemiacetal analogues, ie glucose (pKa = 12.3; Perrin *et al.*, 1981) and fructose (pKa = 12.15; Perrin *et al.*, 1981), and therefore the hemiketal is not expected to ionise except at very high pH values (McClelland *et al.*, 1985).

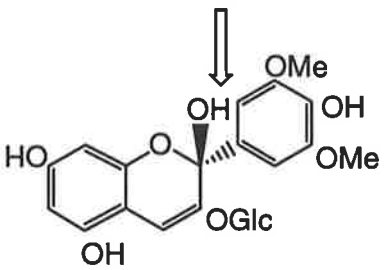

Figure 3.22: Indication of the 2-hydroxyl group of the hemiketal as a site for deprotonation.

Most spectroscopically observed kinetic studies use binary systems and therefore single wavelength monitoring is adequate. However, the equilibria involving malvidin-3-glucoside are extremely complex involving multiple species with different reaction kinetics. Kinetic

studies using UV-visible spectroscopic analysis of complex systems involving multiple species can only be performed using multiple analytical wavelengths. One of the deficiencies of the UV-visible spectral data currently available is that the spectrum of the quinonoidal base in aqueous solution remains unknown. An alternative method for the study of kinetic studies is NMR. Santos *et al.* (1993) proposed that NMR may have a role in the determination of rate constants in the range of 10^{-2} to 10^{-4} s^{-1} ($t_{1/2}$ = 70 s to 2 h). Cheminat and Brouillard (1986) proposed that spectral shift differences between the flavylium ion and the quinonoidal base of malvidin-3-glucoside could be detected. However, in a study of malvidin-3,5-diglucoside, Santos *et al.* (1993) were unable to detect any peaks specifically associated with the quinonoidal base. It is proposed that the keto oxygen of the quinonoidal base participates in rapid proton exchange with the hydroxyl groups, and therefore its is difficult to differentiate between the flavylium ion and the quinonoidal base using NMR.

The existing ideas regarding the colour of red wine must be reassessed in light of the new pH dependent charge distribution data of malvidin-3-glucoside (Figure 3.8). Certainly, the proposal by Brouillard and Delaporte (1977), and Timberlake (1980), that the concentration of the quinonoidal base is minimal at wine pH must be reconsidered. The results of the current study indicate that even at a low pH (pH 2.0) there is a considerable concentration of the malvidin-3-glucoside quinonoidal base. Furthermore, the results clearly indicate that at wine pH (3.2 - 3.8) there are only neutral species present (as determined by HVPE). The spectroscopic data show that the hemiketal/chalcone species dominate at wine pH and that malvidin-3-glucoside is almost colourless. However, red wine is not colourless. It is therefore proposed that the colour of wine is the result of an equilibrium between the coloured quinonoidal base and the colourless hemiketal/chalcone. This equilibrium may be mediated by effects such as co-pigmentation and self association.

Co-pigmentation is thought to control the extent of hydration reaction (Goto and Kondo, 1991, Mazza and Miniati, 1993). Asen *et al.* (1972) and Scheffeldt and Hrazdina (1978) propose that the co-pigmentation (and self association) effect on anthocyanins is due to the stabilisation of the more intensely coloured quinonoidal base (anhydrobase). The HVPE data provides evidence that the uncharged quinonoidal base, is at a maximum

concentration at approximately pH 3.5. Interestingly, Brouillard *et al.* (1989) determined the optimal pH for co-pigmentation between malvidin-3,5-diglucoside and chlorogenic acid as pH 3.6. Similarly, Levengood (1996) found the optimum pH for co-pigmentation in wine to be pH 3.3. This is consistent with co-pigmentation associations being optimised for the species with zero charge.

While the spectra of the flavylium ion, the quinonoidal anions, A^-, and dianion, A^{2-}, and the spectra of the colourless hydrated species are known, the spectrum of the neutral quinonoidal base still remains elusive. In the next chapter (Chapter 4) the spectroscopic and electrophoretic properties of malvidin-3-(*p*-coumaryl)glucoside are investigated. Furthermore, using these methods it was possible to obtain the spectrum of the malvidin-3-(*p*-coumaryl)glucoside quinonoidal base under aqueous conditions.

The results from this chapter indicate that neutral species of malvidin-3-glucoside are important to the overall chemistry of the wine, whereas previously it was thought that the ratio of the relatively stable flavylium ion and the more reactive hemiketal and chalcones were important to wine colour expression. As mentioned earlier, the data presented here implies that the non-charged quinonoidal base is of greater importance than the flavylium ion to the colour of wine. By virtue of its uncharged state, the quinonoidal base is expected to participate in different reactions than the flavylium ion.

Chapter 4

Malvidin-3-(*p*-coumaryl)glucoside

Introduction

Malvidin-3-(*p*-coumaryl)glucoside, usually accounts for less than 10% of total anthocyanins in *V. vinifera* (Ribereireau-Gayon 1973) although in some varieties it may be the dominant anthocyanin pigment (Bakker and Timberlake, 1985). Very little is known regarding the basic chemical properties of malvidin-3-(*p*-coumaryl)glucoside and therefore an investigation was warranted. To perform these studies a new method was developed for the isolation of malvidin-3-(*p*-coumaryl) glucoside. This technique utilises the preferential extraction of malvidin-3-(*p*-coumaryl) glucoside by isoamyl alcohol from a 1% sulphur dioxide extract of grape skin. With a sufficiently pure sample, it is possible to investigate the properties of malvidin-3-(*p*-coumaryl)glucoside using the methods developed for malvidin-3-glucoside.

Koeppen and Basson (1966) determined a molar absorbance coefficient at 538 nm for malvidin-3-(*p*-coumaryl)glucoside of 30 200 in acidic methanol. This was compared with values obtained using the glycosyl-glucose (G-G) assay. Furthermore, the effect of ethanol on the absorbance of malvidin-3-(*p*-coumaryl)glucoside was also investigated.

Estimates of the ionisation and hydration constant for malvidin-3-(*p*-coumaryl)glucoside were obtained using a combination of high voltage paper electrophoresis (HVPE) and UV-visible spectroscopy. These results were compared to those obtained previously for malvidin-3-glucoside. Utilising these results the spectra of some of the different forms of malvidin-3-(*p*-coumaryl)glucoside could be obtained.

Results

Molar absorbance coefficient

The malvidin-3-(*p*-coumaryl)glucoside isolated had a purity of 94% as determined by the integrated area by HPLC. The contaminants included malvidin-3-glucoside as well as some other minor unidentified compounds. The molar absorbance coefficient at 520 nm for malvidin-3-(*p*-coumaryl)glucoside was 25 683 ± 233 (Table 4.1). For further work a molar absorbance coefficient of 25 700 was used. In ethanol it has an absorbance maximum at 542 nm with a molar absorbance coefficient of 30 840 ± 380, which is approximately 1.2 fold greater than the molar absorbance coefficient in aqueous solution. The spectra of aqueous malvidin-3-(*p*-coumaryl)glucoside and in acidified 90% aqueous ethanol are shown in Figure 4.1.

Table 4.1: Estimation of the molar absorbance coefficient (ε) of malvidin-3-(*p*-coumaryl)-glucoside using the G-G assay. The absorbance and concentration of the eluent as well as the molar absorbance coefficient calculated for each sample replicate are shown.

Sample	Absorbance 520 nm	Conc. μmol dm^{-3}	ε
1	11.160	439.5	25 393
2	11.040	433.6	25 461
3	11.960	466.9	25 616
4	13.760	531.5	25 889
5	15.400	597.7	25 765
6	14.960	576.0	25 972
mean (± s.e.)			25 683 (± 233)

The pH verses absorbance data indicates that malvidin-3-(p-coumaryl)glucoside is only completely positively charged at a pH value less than 0.2 (Figure 4.2). The plateau region at approximately pH 1.0 does not correspond to the formation of the hemi-ketal and it is therefore proposed that this plateau is the result of the formation of the quinonoidal base. This will be discussed later.

Upon the addition of ethanol, malvidin-3-(*p*-coumaryl)glucoside shows similar spectral changes to malvidin-3-glucoside. There was an increase in the absorbance at 520 nm up to 30% ethanol. When more ethanol is added there is a slight decline in the absorbance, not as large as observed with malvidin-3-glucoside. With increasing ethanol concentration, malvidin-3-(*p*-coumaryl)glucoside exhibits an absorbance shift towards longer wavelengths (Figure 4.3), and an increase in the maximum absorbance. This was similar to the effects observed with malvidin-3-glucoside. At low ethanol concentrations, however, malvidin-3-(*p*-coumaryl)glucoside was not fully ionised at pH 0.7, and therefore there was no lower plateau observable in Figure 4.3a. The plateau region at 540 nm (Figure 4.3b) was first observed at 60% ethanol, and thus it is proposed that malvidin-3-(*p*-coumaryl)glucoside formed the quinonoidal base under slightly less hydrophobic conditions than malvidin-3-glucoside.

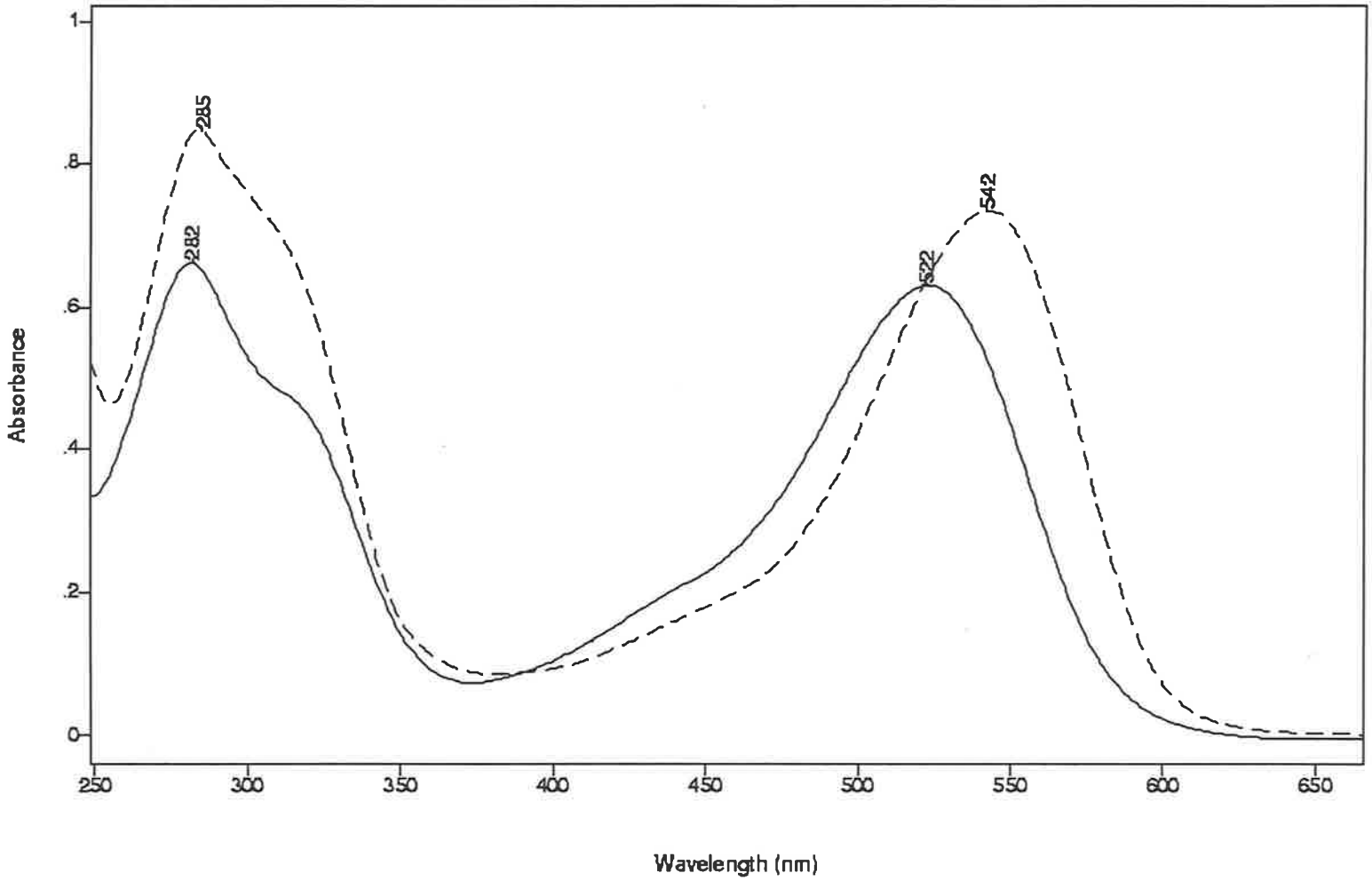

Figure 4.1: UV-visible spectrum of malvidin-3-(*p*-coumaryl)glucoside in aqueous solution (solid line) and in 90% (v/v) acidified aqueous ethanol (dashed line).

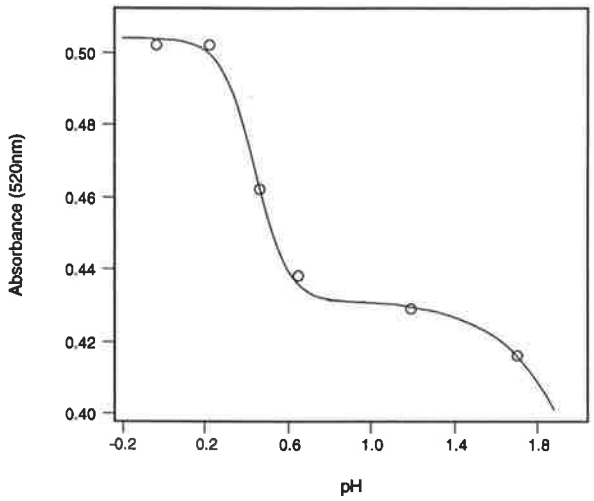

Figure 4.2: Absorbance of malvidin-3-(*p*-coumaryl)glucose with increasing pH. A proposed curve was fitted to indicate the plateau at approximately pH 1.

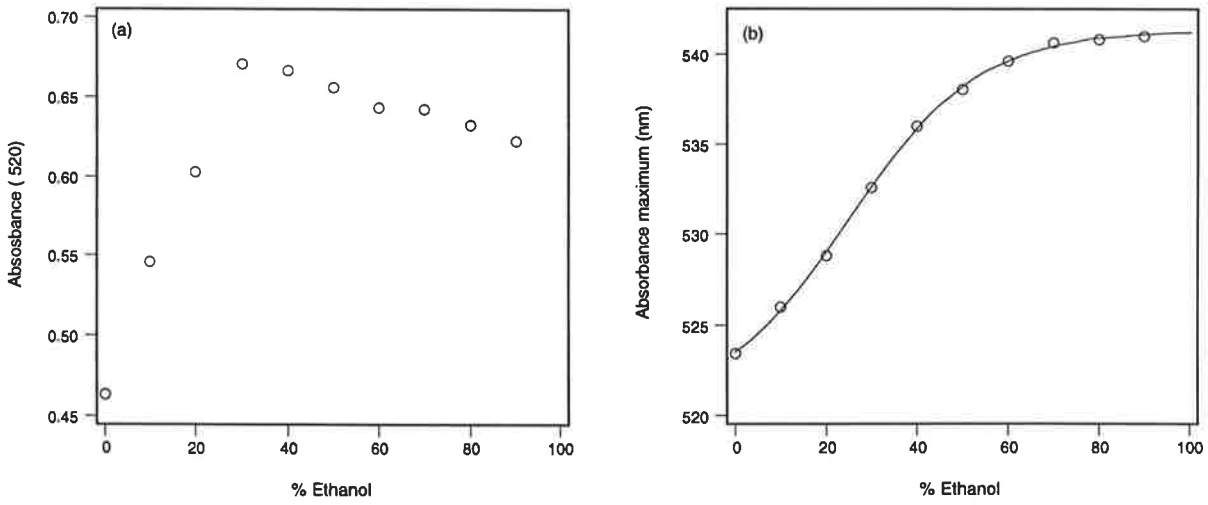

Figure 4.3: Change in absorbance of aqueous malvidin-3-(*p*-coumaryl)glucoside solutions with different concentrations of ethanol, (a) the absorbance measured at 520 nm compared to ethanol concentration, (b) the maximum absorbance (λ_{max}) verses ethanol concentration with a sigmoid curve fitted ($r^2 = 0.9995$).

Ionisation constants, hydration constants and UV-visible spectra

The adsorption of malvidin-3-(*p*-coumaryl)glucoside to the paper under most of the buffer systems attempted, confined the use of HVPE to the 0.1 mol dm^{-3} oxalate buffer. The oxalate buffer could only be used in a limited pH range of 1.2 - 4.9. By fitting the pKa curve (Equation 2.14), it was possible to estimate two pKa values (Figure 4.4). These were a pKa_1 of 0.90 ± 0.07 and a pKa_2 of 4.45 ± 0.03.

An initial survey of the spectroscopic data indicated that there are five plateaus representing five different forms of malvidin-3-(*p*-coumaryl)glucoside. The spectra of these forms are shown in Figure 4.5. A summary of the pH corresponding with each form and their absorbance maxima is presented in Table 4.2.

Table 4.2: Different species of malvidin-3-(*p*-coumaryl)glucoside with their corresponding maximal absorbances and the pH at which this occurs.

		pH	λ_{max}
Flavylium ion	A^+	0.3	283,523
Quinonoidal base	$A^0_{(aq)}$	1.9	282,527
Hemiketal	A^{OH}	5.0	282
Quinonoidal anion	A^-	7.3	295,448,581
Quinonoidal dianion	A^{2-}	11.0	359,595

The two peaks in the visible spectrum at 448 and 581 nm for the quinonoidal anion, A^-, are consistent with the data presented previously for malvidin-3-glucoside. In this experiment a plateau was detected at pH 1.9 and the charge of the species detected was neutral at this pH (Figure 4.6) and therefore it is proposed that this represents the quinonoidal base of malvidin-3-(*p*-coumaryl)glucoside. The transition between the initial plateau and the plateau at pH 1.9 can be therefore attributed to pKa_1. A second plateau at pH 5 is due to the hemiketal and *cis*-chalcone. Two more plateaus at pH 7.4 and 11.0 represent the quinonoidal anion, A^-, and quinonoidal anion, A^{2-}, respectively.

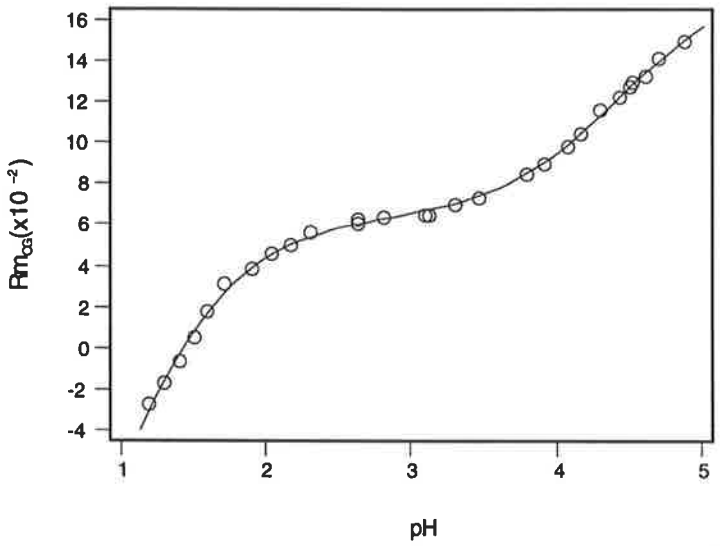

Figure 4.4: Relative mobility of malvidin-3-(*p*-coumaryl) glucoside (Rm_{OG}) as a function of the pH with fitted for the estimation of pKa values using HVPE.The buffer used for the HVPE was an oxalate buffer. The coefficient of determination (r^2) for the fitted line was 0.9990.

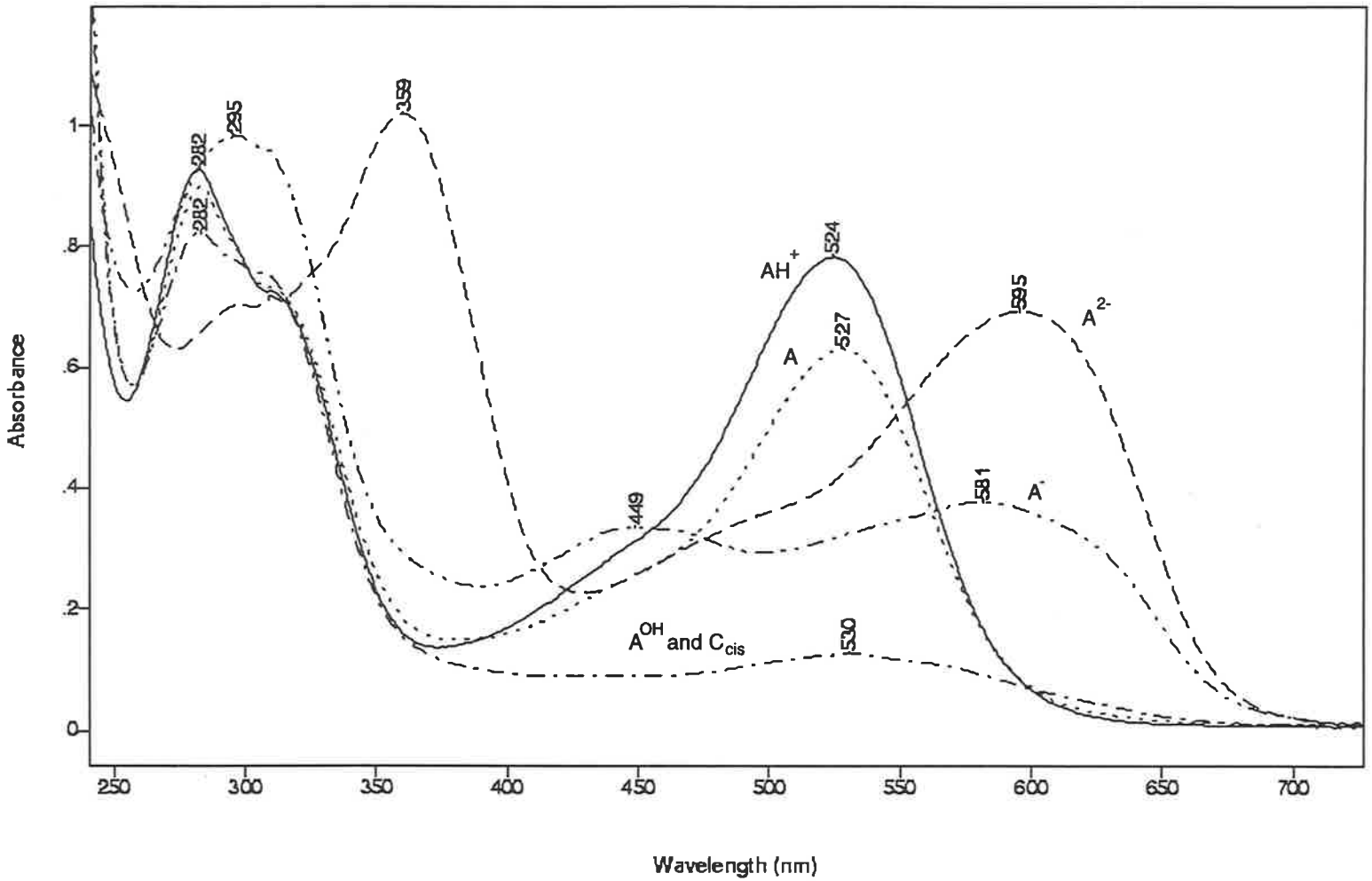

Figure 4.5: UV-visible spectra of the flavylium ion (AH^+), quinonoidal base (A), hydrated forms (hemiketal, A^{OH} and cis-chalcone C_{cis}), quinonoidal anion (A^-), and quinonoidal dianion (A^{2-}) of malvidin-3-(*p*-coumaryl)glucoside at pH 0.0, 1.9, 5.0, 7.4 and 10.0 respectively.

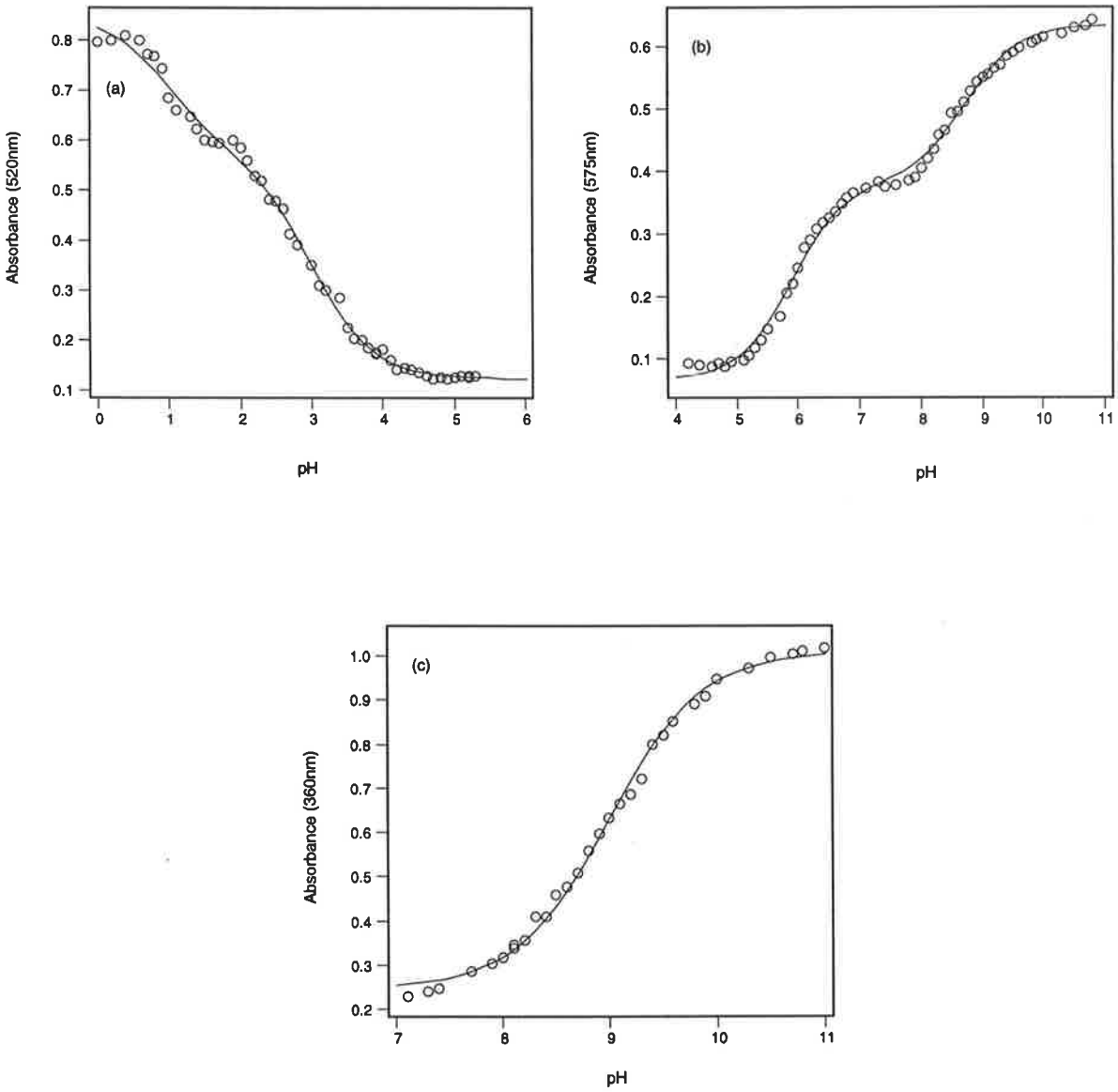

Figure 4.6: Absorbance of malvidin-3-(*p*-coumaryl)glucoside as a function of pH with Equation 2.28 fitted for the estimation of hydration and ionisation constants by spectroscopic method. Three different pH ranges were used. The three different wavelengths used for the three pH ranges were, (a) 520 nm, (b) 575 nm, and (c) 360 nm. The coefficients of determination (r^2) for the three curves were (a) 0.9963, (b) 0.9968 and (c) 0.9965.

The three analytical wavelengths chosen for the calculation of the pK_H and pKa_3 values were 520 nm, 575 nm and 360 nm. The 520 nm and 575 nm wavelengths were chosen because they correspond to the flavylium ion, A^+, and the quinonoidal dianion, A^{2-}. An analytical wavelength of 360 nm was selected to confirm the peak at 359 nm resulted from the quinonoidal dianion, A^{2-}, and not another species such as the quinonoidal trianion, A^{3-}.

Using these three analytical wavelengths and fitting the pK curve to the spectroscopic data (Equation 2.28), it was possible to determine the pKa_1, pK_{H1}, pK_{H2} and pKa_3 values (Table 4.3). Notice the similarity of the pKa_3 values calculated using the 360 nm and 575 nm wavelengths. It is therefore proposed that malvidin-3-(*p*-coumaryl)glucoside dianion has spectral maxima 359 nm and 595 nm.

Table 4.3: pK values of malvidin-3-(*p*-coumaryl)glucoside as determined using UV-visible spectrometry

	Analytical wavelength	pK value	Average
pKa_1	520 nm	0.98 ± 0.10	
pK_{H1}	520 nm	3.01 ± 0.04	
pK_{H2}	575 nm	5.90 ±0.04	
pKa_3	360 nm	8.90 ± 0.02	
pKa_3	575 nm	8.82 ± 0.04	pKa_3 = 8.86

The ionisation and hydration constants for malvidin-3-(*p*-coumaryl)glucoside as calculated using HVPE and UV-visible spectrometry are summarised in Figure 4.7. An average pKa_1 value of 0.94 was estimated using both spectroscopic (520 nm) and electrophoretic data. The average value for pKa_3 of 8.86 was derived using spectroscopic data at the two analytical wavelengths of 330 nm and 575 nm. The estimated pKa and pK_H values were used to calculate the contribution of each of the different forms of malvidin-3-(*p*-coumaryl)glucoside to the visible spectrum at any pH value. This is graphically shown in Figure 4.8.

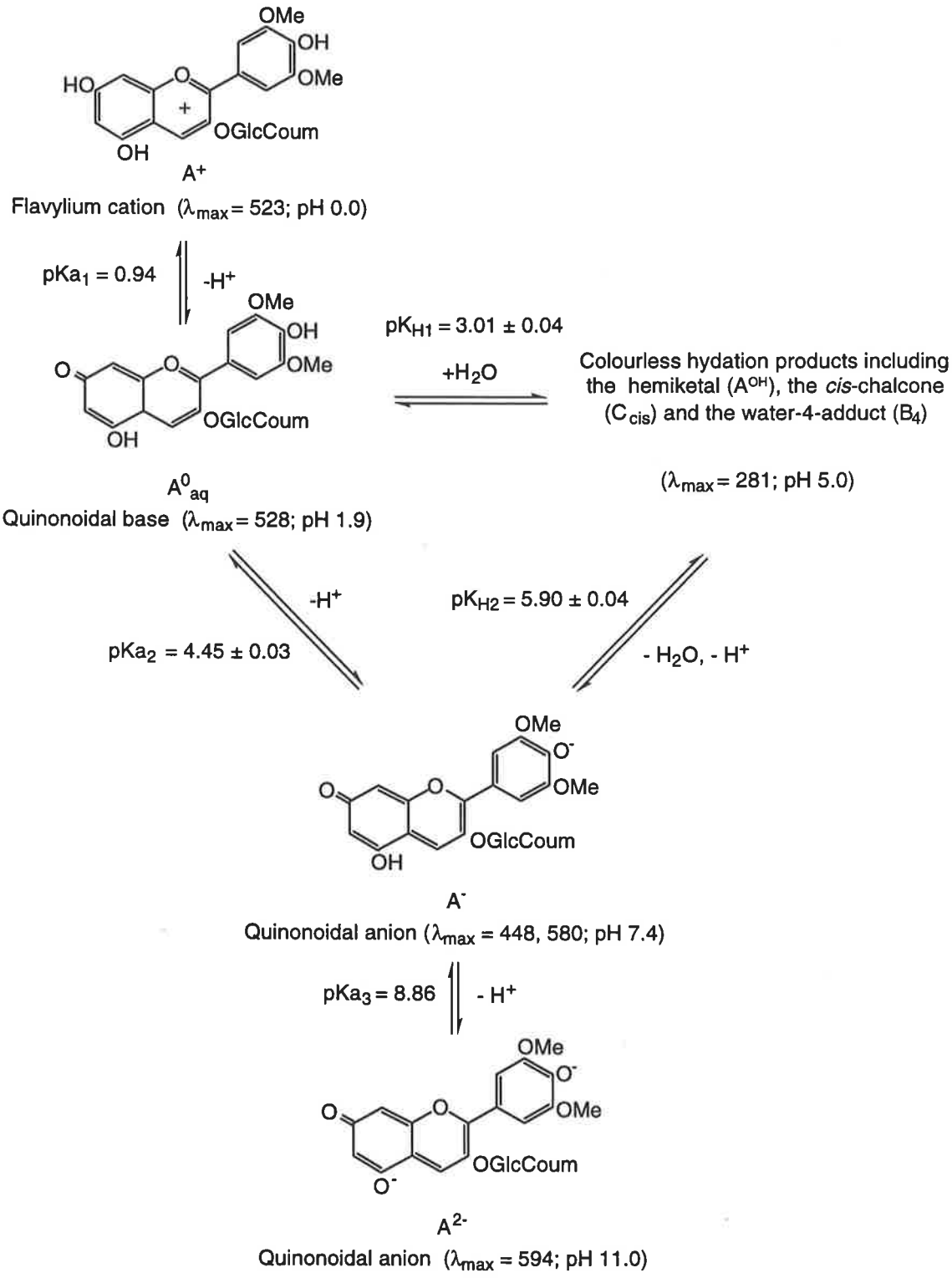

Figure 4.7: Structures of malvidin-3-(*p*-coumaryl)glucose as a function of pH. The macroscopic pKa and pK_H values of malvidin-3-(*p*-coumaryl)glucoside in dilute solutions as calculated using HVPE and UV/Vis spectrometry. The λ_{max} and the pH at which this occurs for each of the species of malvidin-3-(*p*-coumaryl)glucose have been included.

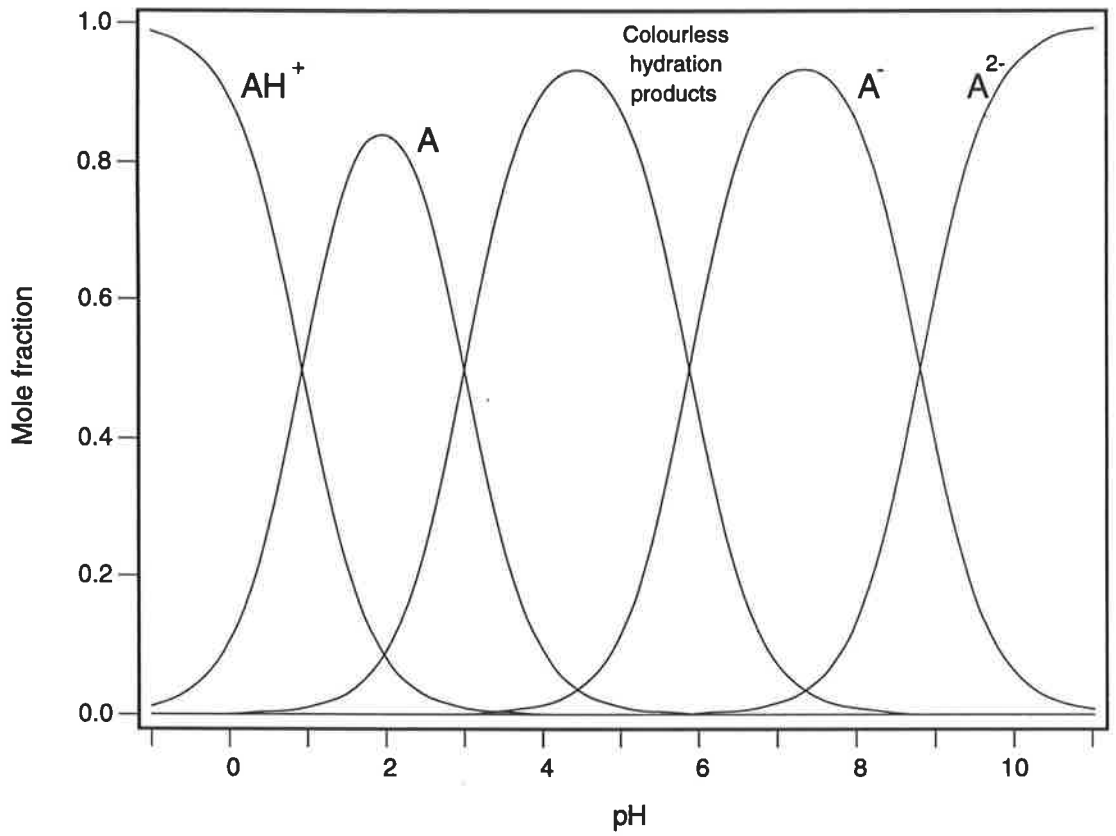

Figure 4.8: Proposed charge distribution diagram for malvidin-3-(*p*-coumaryl)glucoside at 25°C. The pK values used were; $pKa_1 = 0.94$, $pK_{H1} = 3.01$, $pKa_2 = 4.45$, $pK_{H2} = 5.90$, and $pKa_3 = 8.86$. (Note AH^+ represents the flavylium ion, A the quinonoidal base, A^- the quinonoidal anion and A^{2-} the quinonoidal dianion.)

Discussion

The methods used previously for the isolation of malvidin-3-(*p*-coumaryl)glucoside have proven inadequate to isolate sufficient quantities for detailed research. In this study sulphur dioxide and isoamyl alcohol solvent extraction were used as a novel procedure for the differential separation of anthocyanins. The solubility of anthocyanins in isoamyl alcohol is altered by the presence of the sulphur dioxide solution. Two mechanisms may be proposed for the effect of the sulphur dioxide solution in allowing the preferential extraction of malvidin-3-(*p*-coumaryl)glucoside. The differential partitioning of anthocyanins utilising isoamyl alcohol and differing concentrations of dilute hydrochloric acid (Willstätter and Zollinger, 1916; Levy and Robinson, 1931), is related to the pKa values of the individual anthocyanins. Thus, the sulphur dioxide solution may have the optimum pH for malvidin-3-(*p*-coumaryl)glucoside isolation. Alternatively, it may be proposed that the sulphur dioxide solution may improve anthocyanin separation by altering the solubility of the respective anthocyanins via the formation of the bisulphite addition product. These proposals require further investigation.

The molar absorbance coefficient at 520 nm for malvidin-3-(*p*-coumaryl)glucoside in aqueous solution is 25 683 (± 233). In ethanol malvidin-3-(*p*-coumaryl)glucoside has a higher molar absorbance coefficient compared to aqueous solutions with a bathochromically shifted maximum absorbance. This is similar to the situation with malvidin-3-glucoside. The molar absorbance coefficient calculated in acidified ethanol (30 840 ± 380) is similar to the previously published estimate of 30 200 in acidic methanol (Koeppen and Basson, 1966).

When ethanol is added to an acidic solution of malvidin-3-(*p*-coumaryl)glucoside, a plateau of the sigmoidal curve fitted to the absorbance values was observed at 60-70% ethanol (Figure 4.3). It is proposed that this plateau is associated with the formation of the quinonoidal base. In contrast, the equivalent plateau for malvidin-3-glucoside was found only at concentrations of ethanol greater than 90%. Thus, the quinonoidal base of malvidin-3-(*p*-coumaryl)glucoside forms under less hydrophobic conditions than malvidin-3-

glucoside and it is therefore proposed that acylation by *p*-coumaric acid contributes towards the stability of the quinonoidal base.

The ethanol dehydration of the flavylium ion gives the spectrum of the neutral quinonoidal base ($A_{ethanol}$) with a maximal absorbance that is at least 1.2 times greater higher than that of the original flavylium ion, while the pH data shows a neutral quinonoidal base (A_{aq}) with a maximum absorbance that is approximately 0.80 times less than the flavylium ion. It is proposed that there are two forms of the quinonoidal base with two distinct molar absorbance coefficients. These forms are planar ($A_{ethanol}$) and folded (A_{aq}). Under anhydrous conditions the neutral quinonoidal base remains planar, and interactions between the electrons of the aromatic acid and the anthocyanin base are expected to be minimal. However, under aqueous conditions the quinonoidal base can fold such that there is an intra-molecular association between the anthocyanin base structure and the aromatic acid, and this inhibits the formation of the hemi-ketal. The molar absorbance coefficient of the quinonoidal base under these conditions will be influenced by the interaction of the electrons between the quinonoidal base and the *p*-coumaric acid. Furthermore, hydrogen bonding can occur between the aqueous solvent and the quinonoidal oxygen. Thus, it is expected that under these conditions there is a greater de-localisation of the electrons from the quinonoidal base and this results in the decreased absorbance observed when compared with the quinonoidal base under anhydrous conditions.

The spectral data (Figure 4.6) show that there are two distinct pK constants at pH values less than 4 with a plateau at pH 1.9. A similar plateau, albeit at the slightly lower pH of 1.0, was detected in experiments whereby the pH of a malvidin-3-(*p*-coumaryl)glucoside solution has been increased from pH 0.7 (Figure 4.2). The difference in pH values of these two experiments can be attributed to hysteresis. It is proposed that the lower pK value represents the transition from the flavylium ion towards the quinonoidal base (ie pKa_1). The second pK value depicts the hydration of the quinonoidal base to produce the hemi-ketal/chalcone (ie pK_{H1}). It was therefore possible to calculate pKa_1 and pK_{H1} using spectral data.

The pK_{H1} of malvidin-3-(*p*-coumaryl)glucoside is 3.01 (± 0.03) compared with a value for malvidin-3-glucoside of 2.66 (± 0.03). These results provide evidence that intra-molecular association of the aromatic *p*-coumaric acid and the neutral quinonoidal base hinders the formation of the hemi-ketal and therefore the *cis*-chalcone. In contrast, the apparent pK_{H2} (5.90) for malvidin-3-(*p*-coumaryl)glucoside is similar to the previous estimates for malvidin-3-glucoside (pK_{H2} = 5.90). Thus, the *p*-coumaryl group has little effect on the loss of water from the hemi-ketal.

The presence of the aromatic acyl group increases the pKa_3 (8.86) values when compared with previous estimates for malvidin-3-glucoside (pKa_3 = 8.22). Using the methods outlined by Perrin *et al.* (1981) it is possible to employ the Hammet equation to equate an estimate of the protonation constant for an ester-linked *p*-coumaric acid. The pKa_3 value obtained is 9.85. It is therefore expected that the anthocyanin portion (malvidin-3-glucoside; pKa_3 = 8.22) and the *p*-coumaric acid ester portion of the molecule to have overlapping pKa values. The apparent pKa_3 calculated may represent two different apparent micro-protonation constants (ie, pKa_3 and pKa_4). Alternatively, it can be proposed that the *p*-coumaryl group actively participates in the ionisation of the molecule, and therefore the value obtained for pKa_3 represents only a single protonation constant. There is currently insufficient evidence to confirm that there are two separate protonation values.

In dilute aqueous solution, the visible spectrum of five different forms malvidin-3-(p-coumaryl)glucoside can be detected with varying pH. This contrasts with malvidin-3-glucoside where the quinonoidal base is not clearly observable as a separate species. Thus, the visible spectral data portrays the structural transformation of the flavylium ion, via the quinonoidal base, the hemi-ketal/chalcone and the quinonoidal anion, A^-, to the quinonoidal dianion, A^{2-}. These results also confirm the observations in the previous chapter that the neutral species are important to wine colour.

In spectral studies of co-pigmentation, Figueiredo *et al.* (1996a), were able to show that the quinonoidal base forms at low pH values (~2.1 - 3.5). These authors considered that the cornerstone of colour stabilisation and variation rests of the formation of the quinonoidal base at low pH values. The results presented here demonstrate that it is possible to

observe the spectrum of the malvidin-3-(*p*-coumaryl)glucoside quinonoidal base at low pH values in the absence of co-pigments.

Intermolecular copigmentation is responsible for the stability of anthocyanins containing two or more aromatic acyl groups (Brouillard, 1981). It is thought that two aromatic acyl groups are required to sandwich and thereby stabilise the anthocyanin-chromophore. However, in copigmentation studies, it has been found that anthocyanins participating in inter- or intra-molecular associations show a red shift accompanied by a small decrease in the molar absorbance coefficient which indicates that the complexed forms exhibit a slightly less intense colouration than the corresponding free flavylium cations (Brouillard and Dangles, 1993; Figueiredo *et al.,* 1996b). The results presented in this chapter demonstrates that the quinonoidal form of malvidin-3-(*p*-coumaryl)glucoside in aqueous solutions displays both a slight bathochromic shift and a slight decrease in the molar absorbance coefficient, and therefore a single aromatic acyl group can contribute towards the stabilisation of the chromophore.

There are two possible mechanisms by which the *p*-coumaric acid suppresses the hydration of the quinonoidal base. The association of the *p*-coumaric acid with the malvidin C ring leads to a sufficient charge density delocalisation, and thereby deactivates the C2 carbon (Figure 4.9a). The alternate mechanism is similar to the theory of co-pigmentation as proposed by Goto and Kondo (1991), where the anthocyanin exists naturally as loose dimers or clusters and the aromatic acyl group helps stabilise these hydrophobic units (Figure 4.9b). Alternatively the stabilising effect of the *p*-coumaric acid may involve a combination of both mechanisms.

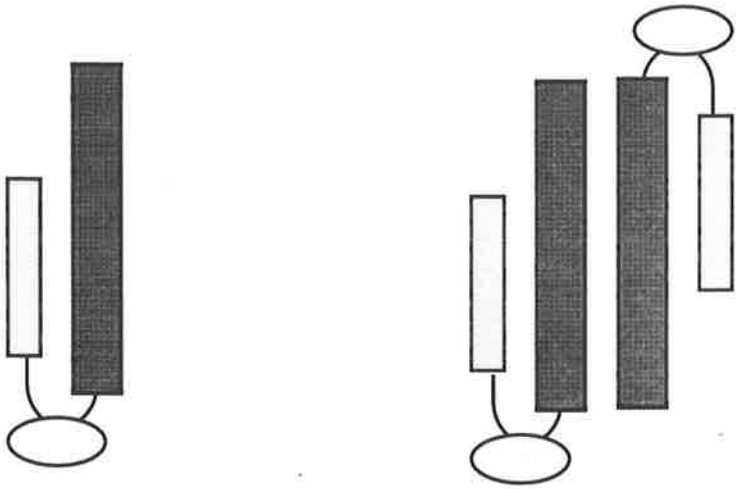

4.9a 4.9b

Figure 4.9: Two alternative methods of stabilisation of the quinonoidal base of malvidin-3-(*p*-coumaryl)glucoside; (4.9a) charge density delocalisation, (4.9b) hydrophobic co-pigmentation type dimers. The malvidin unit and the *p*-coumaryl acyl group are represented by the large rectangle and the smaller rectangle respectively, and the glucoside is depicted by the oval.

The difference in molar absorbance coefficients and absorbance maxima of the malvidin-3-(*p*-coumaryl)glucoside quinonoidal base between the aqueous and ethanol solutions, suggests that water molecules are not only important for the formation of the co-pigmentation complex but also may actually participate in the co-pigmentation complex. Thus water not only provides a medium within which co-pigmentation occurs but it also actively partakes in the co-pigmentation phenomenon. Further research into how the aromatic acyl group influences the quinonoidal base will improve our understanding of the chemistry of co-pigmentation and how co-pigmentation influences wine colour.

As was described in Chapter 3 in wines where malvidin-3-glucoside is the dominant chromophore, the colour depends on the concentrations of the coloured quinonoidal base and the colourless hemi-ketal and chalcone species. The observation that intra-molecular co-pigmentation helps stabilise the chromophore of malvidin-3-(*p*-coumaryl)glucoside suggests that in wines with low pigment concentrations, malvidin-3-(*p*-coumaryl)glucoside will exhibit greater colour than the non-acylated malvidin-3-glucoside. However, in wines with high concentrations of anthocyanins, where the effects of self-association become important, or in wines with high concentrations of molecules that are capable of participating

in co-pigmentation, the advantage of *p*-coumaryl group in promoting the colour of wine is lost. It is therefore proposed that in the absence of suitable co-pigments, the *p*-coumaryl acylation of malvidin-3-glucoside may be important to the colour of young wines containing low concentrations of anthocyanins.

Chapter 5

Vitisin A

Introduction

Vitisin A is one of a group of recently discovered C-4 vinyl wine pigments. In preliminary of the current work, vitisin A was identified in a number of Australian wines. Although the relative contribution of this pigment to the colour of red wine at 520 nm is estimated to be low (1-6%), it was thought that vitisin A may be a compound to provide a template for the further investigation of the properties of other wine pigments.

This chapter describes the isolation of vitisin A, and its identification using both mass spectrometry (Bakker *et al.*, 1997; Bakker and Timberlake, 1997; Fulcrand *et al.*, 1998) and comparison to the synthetic product of pyruvic acid and malvidin-3-glucoside (Fulcrand *et al.*, 1998). The isolation of vitisin A using a combination of ion exchange and reverse phase chromatography produced sufficient quantities for further investigation. The molar absorption coefficient of vitisin A was determined using the G-G assay. Furthermore, the estimation of the ionisation and hydration constants using a combination of high voltage paper electrophoresis (HVPE) and UV-visible spectrometry were estimated allow for the identification of the most important forms of vitisin A at wine pH. Infra red spectrometry were used to investigate the structure of vitisin A

To be able to understand the synthesis of vitisin A during the wine making process, a knowledge of the mechanisms for its synthesis is required. These mechanisms are discussed in this chapter.

Results

Mass spectral studies of vitisin A

The mass spectral data confirmed that the compound isolated form wine and under investigation was vitisin A. The positive ion mass spectrum of vitisin A had major ions with m/z of 561.3 and 399.2 (Figure 5.1a). The ion with m/z 399.2 corresponds to the aglycone and m/z 561.2 (M^+) represents the glycoside of vitisin A (Figure 5.3). MS/MS shows a single daughter ion for 561.3 at 398.9. Although this will be discussed later, these mass values are in agreement with those obtained for vitisin A by Bakker *et al.* (1997) and Bakker and Timberlake (1997).

The negative ion mass spectrum produced major peaks at m/z 559.4, 515.6, 353.4, 339.4, 325.4, and 311.2 (Figure 5.1b). The expected daughter ion representing the aglycone of vitisin A (397 amu) was not observed. The negative ion mass spectrum shown here in Figure 5.4b also contained a daughter ion with a mass of 515 which corresponds to the parent ion losing a carboxylic acid (559 - 44) as described by Fulcrand *et al.* (1998). This provides evidence for the presence of a carboxylic acid. The further loss of 162 mass units from the ion with m/z of 515 to give an ion with m/z 353 was due to the loss of the glucose moiety.

As a means of monitoring the number of hydroxyl groups, vitisin A was acylated using acetic anhydride and perchloric acid. Using ionspray ionisation mass spectrometry in the positive ion mode, the acetylated vitisin A shows a major signal at m/z of 813.4 (Figure 5.2). Loss of the acetylated glucose (330 amu) yields an ion m/z 483.2. Further sequential loss of two acetyl groups yields m/z 441.2 and 399.2 respectively, where the ion with m/z 399.2 represents the vitisin A aglycone.

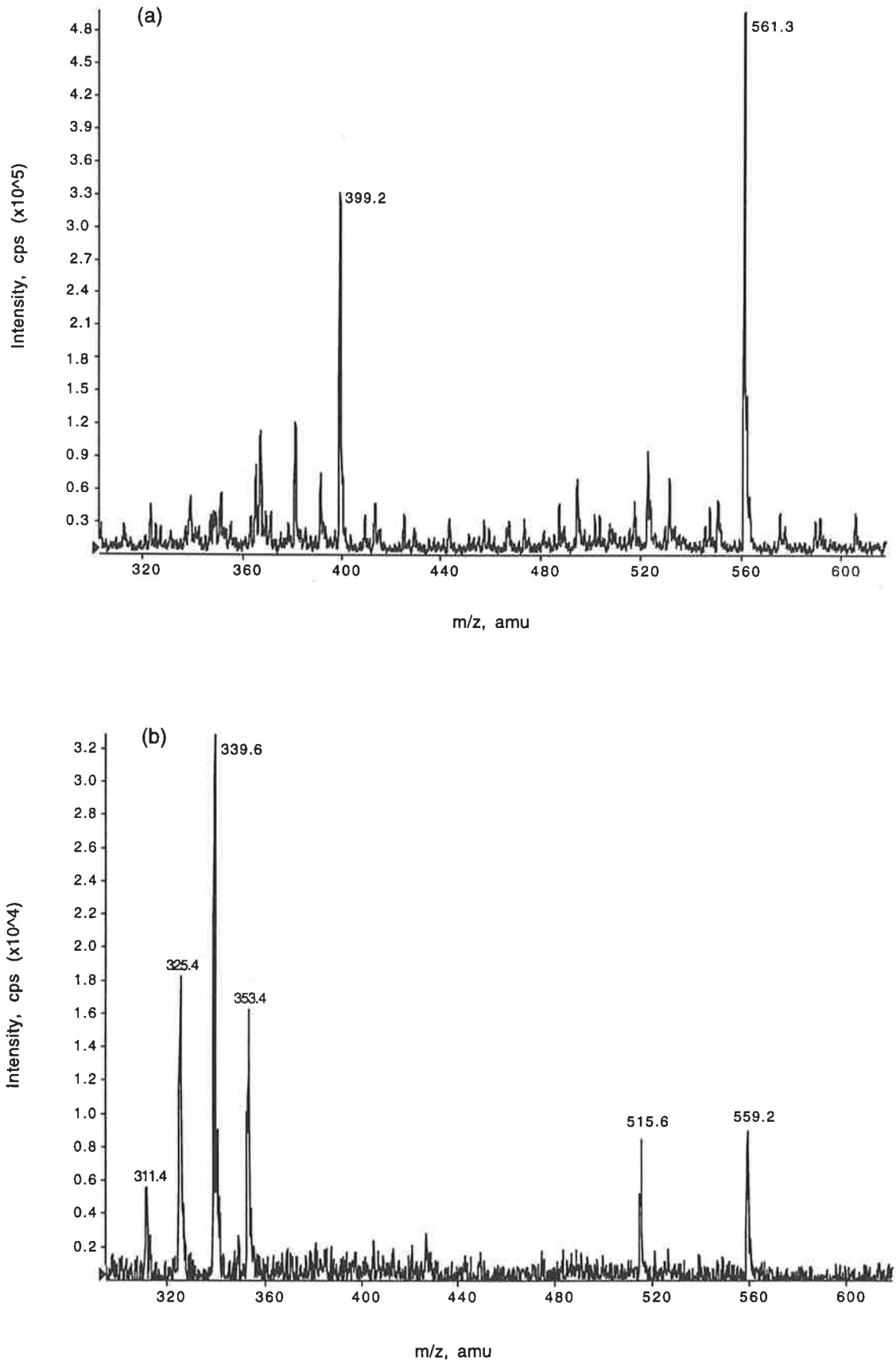

Figure 5.1: Positive ion (a) and negative ion (b) mass spectra of vitisin A

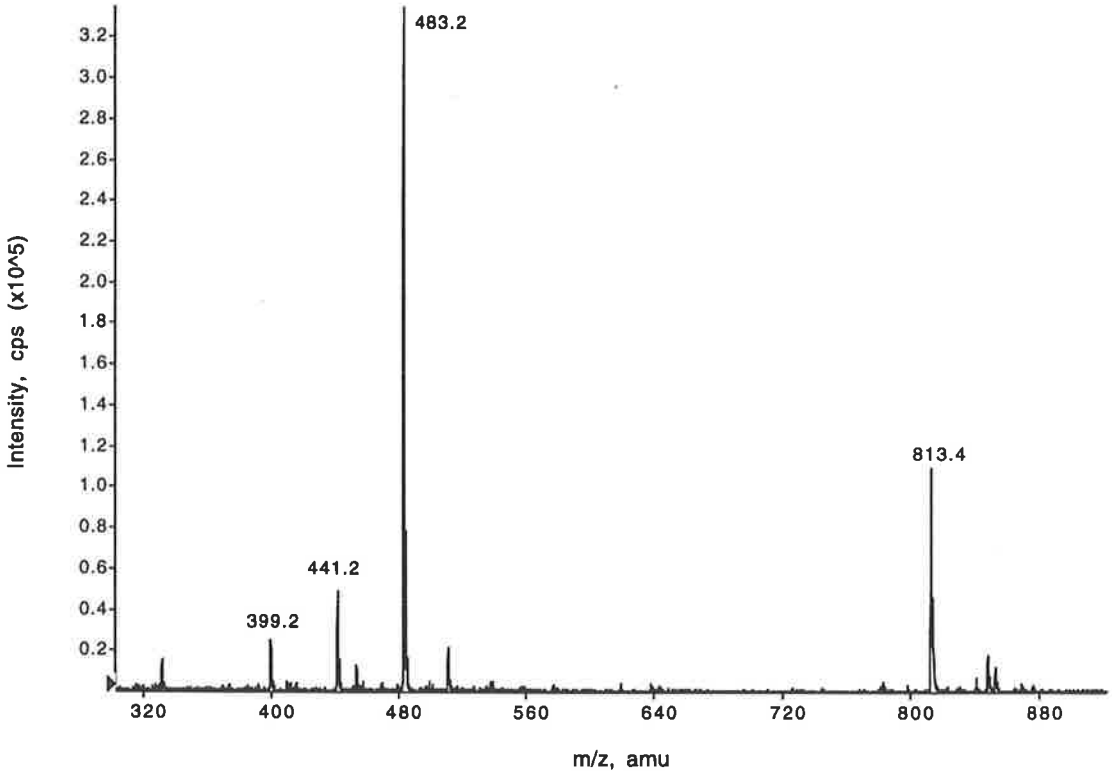

Figure 5.2: The mass spectrum of acetylated vitisin A.

Synthesis of vitisin A

Vitisin A was synthesised using malvidin-3-glucoside and pyruvic acid under aerobic conditions for 6 h. Yields of vitisin A are given as equivalents of malvidin-3-glucoside. An initial amount of 2.105 mg (4.23 μmol) malvidin-3-glucoside in 10 mL reaction mixture gave a yield of 0.786 mg (1.58 μmol) vitisin A or 37.3%. The coloured product had identical diode array UV-visible spectrum as the natural product (Figure 5.3).

An initial mass of 194.1 μg (0.392 μmol) malvidin-3-glucoside in 10 mL reaction mixture yielded 84.8 μg (0.172 μmol) vitisin A when exposed to oxygen but only 35.9 μg (0.072 μmol) vitisin A whilst protected by nitrogen gas. Thus, the exclusion of oxygen by use of a nitrogen gas during the synthesis greatly reduces the yield of vitisin A to 42% of the non blanketed control over an 8 hour period. However, after subsequent exposure to oxygen the synthesis proceeded rapidly and within 2 hours, the yield (80.6 μg or 0.163 μmol) was approximately the same as the control.

In another experiment copper sulphate was used to catalyse the synthesis of vitisin A. After 4 hours in the presence of copper, 2.05 mg (4.15 μmol) malvidin-3-glucoside in 10 mL of reaction mixture yielded 0.19 mg (38.5 μmol), or a yield of 9.3%, compared with the control which yielded 0.14 mg (28 μmol) or a yield of 6.8%. Thus, the added copper produced 1.4 times the vitisin A compared with the control.

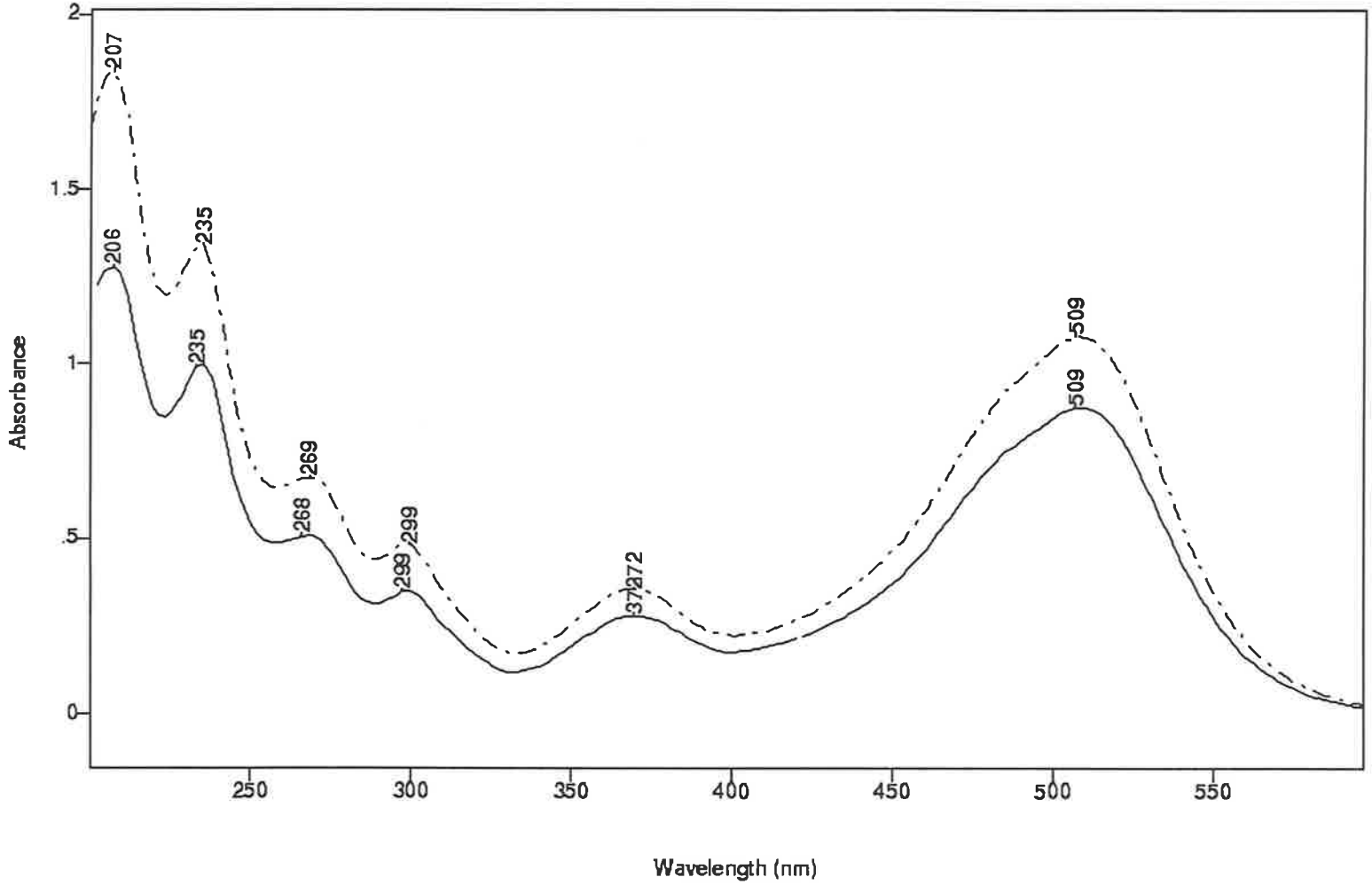

Figure 5.3: Spectrum of vitisin A synthetic product (solid line) compared with the spectrum of natural product (dotted line). Both spectra were obtained using HPLC diode array spectrophotometer.

Molar absorbance coefficient

After the isolation of vitisin A from wine, using a combination of sulphoxyethyl cellulose cation exchange and Sephadex LH 20 chromatography, two methods - thin layer chromatography and C18 reverse phase column chromatography - were used for its final purification. Whilst thin layer chromatography allowed for the isolation of small quantities (µg) of high purity vitisin A, the column method yielded mg quantities. The sample purified using the C18 reverse phase chromatography was used to calculate the molar absorption coefficient. The final purity of vitisin A was 96.6% (area at 280 nm) according to HPLC. The molar absorbance coefficient calculated using the G-G assay at pH 0.0 was 24 863 ± 1 807 (Table 5.1)

Table 5.1: Estimation of the molar absorbance coefficient (ε) of vitisin A using the G-G assay. The absorbance and concentration of the eluent as well as the molar absorbance coefficient calculated for each sample replicate are shown.

Sample	Absorbance 520 nm	Conc. µmol dm^{-3}	ε
1	1.000	42.40	23 585
2	1.020	39.02	26 140
mean (± s.e.)			24 863 (± 1 807)

The absorbance at 520 nm of vitisin A rapidly increases with increasing ethanol concentration and then fluctuates (Figure 5.4a). The λ_{max} in 90% ethanol was 537 nm. When the absorbance was measured at 537 nm, one plateau was observed between 50% and 60% ethanol and another plateau at 90% ethanol (Figure 5.4b). Three spectra were then recorded at different concentrations of ethanol representing three states of vitisin A (Figure 5.5). The absence of a plateau at low ethanol concentrations suggests that vitisin A was not fully ionised at pH 0.0.

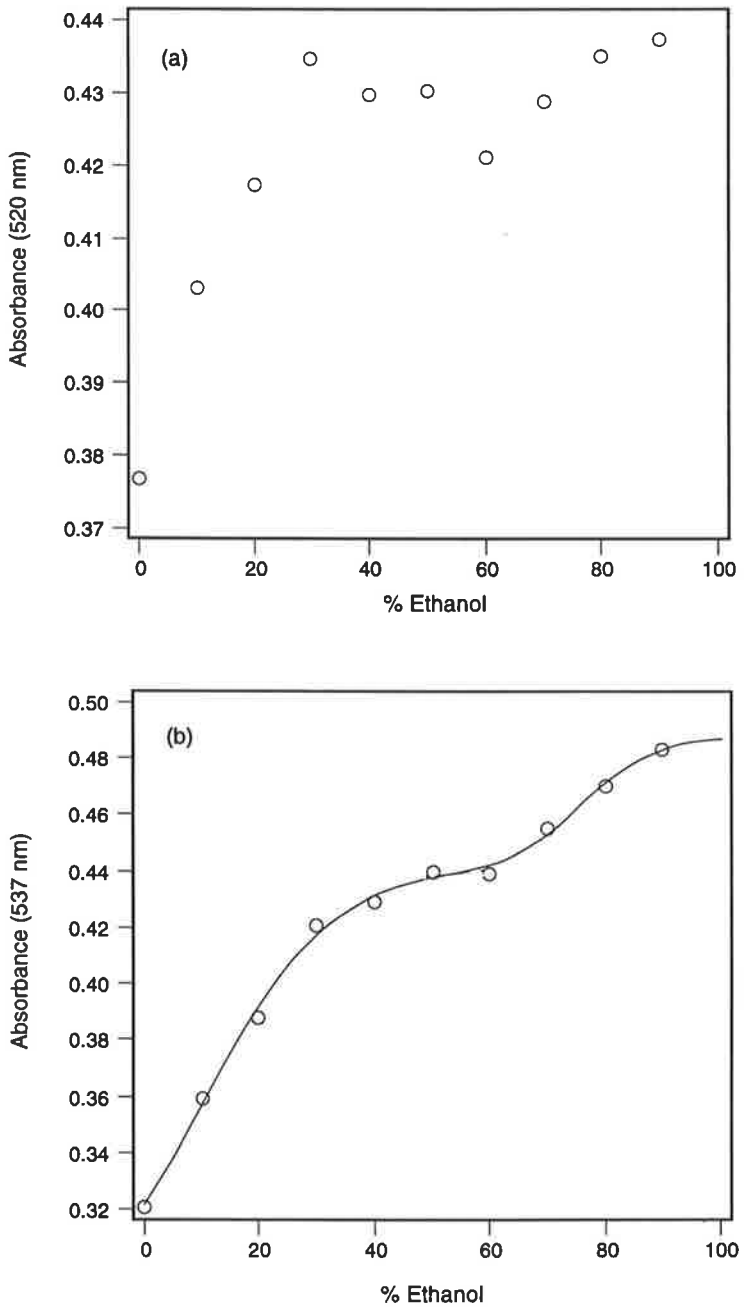

Figure 5.4: Absorbance at (a) 520 nm and (b) 537 nm of vitisin A with increasing concentrations of ethanol. The initial aqueous solution had a pH of 0.0. A curve was fitted to the 537 nm absorbance graph to indicate the two plateaus at 50-60% ethanol and 100% ethanol.

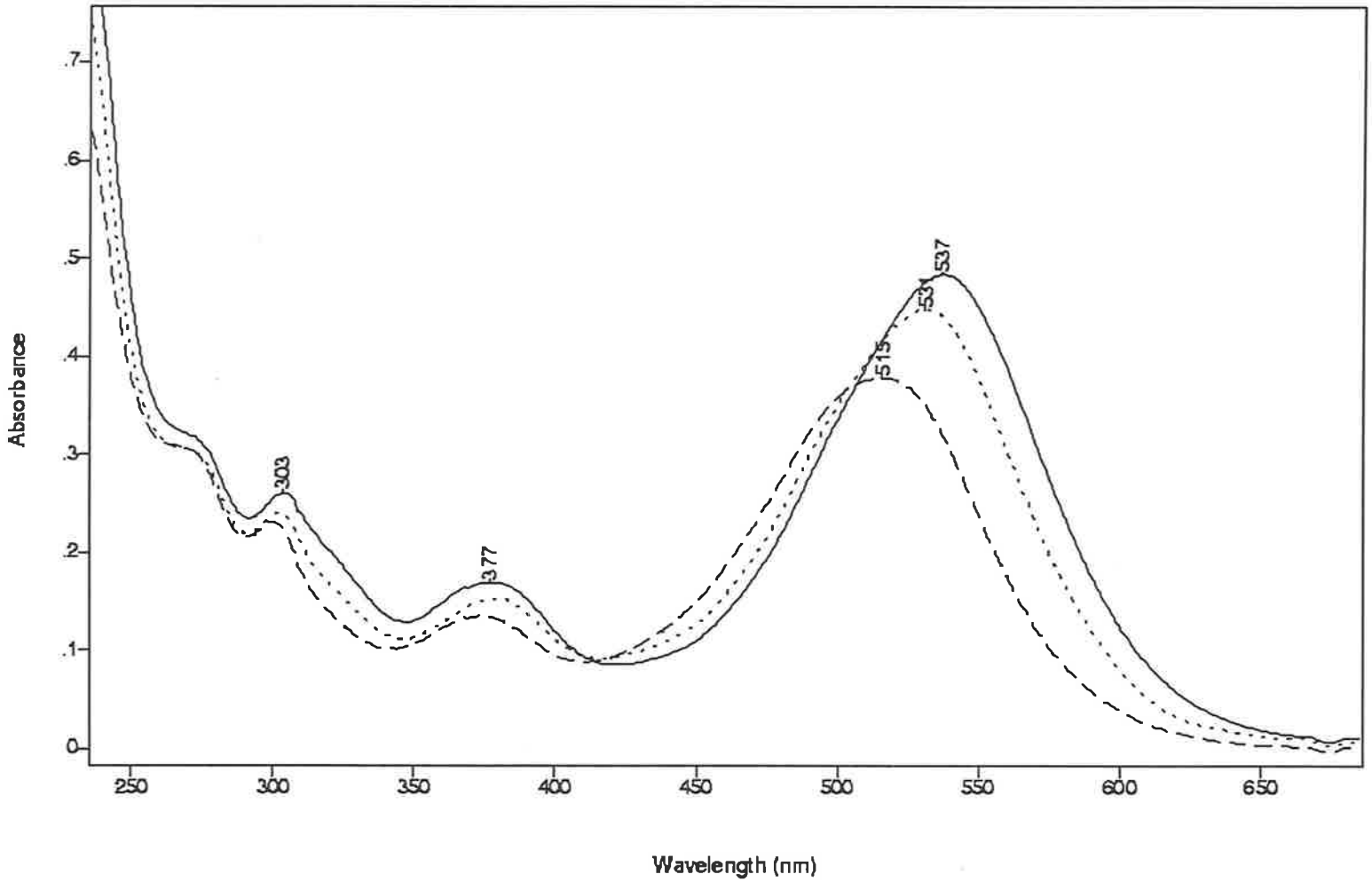

Figure 5.5: UV-visible spectra of vitisin A in acidified aqueous solution with 0% (dashed line), 60% (dotted line) and 90% (solid line) (v/v) aqueous ethanol.

Ionisation constants, hydration constants and UV-visible spectra

HVPE was used for the determination of the apparent protonation constants for vitisin A. These data are summarised in Figure 5.6. A single apparent pKa was determined for the oxalate buffer system and two pKa values could be determined using the citrate buffer system. A fourth pKa estimate was calculated using the phosphate-oxalate buffer. Above pH 9.8 the compound undergoes decomposition and, as a result, the last two points were omitted from the calculation. The pKa values are summarised in Table 5.2.

Table 5.2: Apparent pKa values for vitisin A derived using HVPE with the buffer for each determination indicated.

	Buffer	pKa
pKa_1	Oxalate	0.95 ± 0.10
pKa_2	Citrate	3.56 ± 0.06
pKa_3	Citrate	5.38 ± 0.07
pKa_4	Phosphate/oxalate	8.84 ± 0.06

The apparent hydration constants for vitisin A were estimated using UV-visible spectroscopy. A probable ionisation constant was also observed by this method. The data from three analytical wavelengths used for the calculation of the apparent pKa and pK_H constants are summarised in Figure 5.7. A wavelength of 544 nm was used as an analytical wavelength because the indications were that at this wavelength there were maximal differences between the flavylium ion and the quinonoidal base. This allowed the estimation of the apparent pKa_1 using spectroscopic methods. The pK_{H1} estimate was the average calculated using the citrate and phosphate buffer systems and the two analytical wavelengths of 544 nm and 510 nm. The pK_{H2} value was the average of the two analytical wavelengths of 510 and 599 nm using phosphate buffer. The apparent pKa_1 and pK_H constants are summarised in Table 5.3.

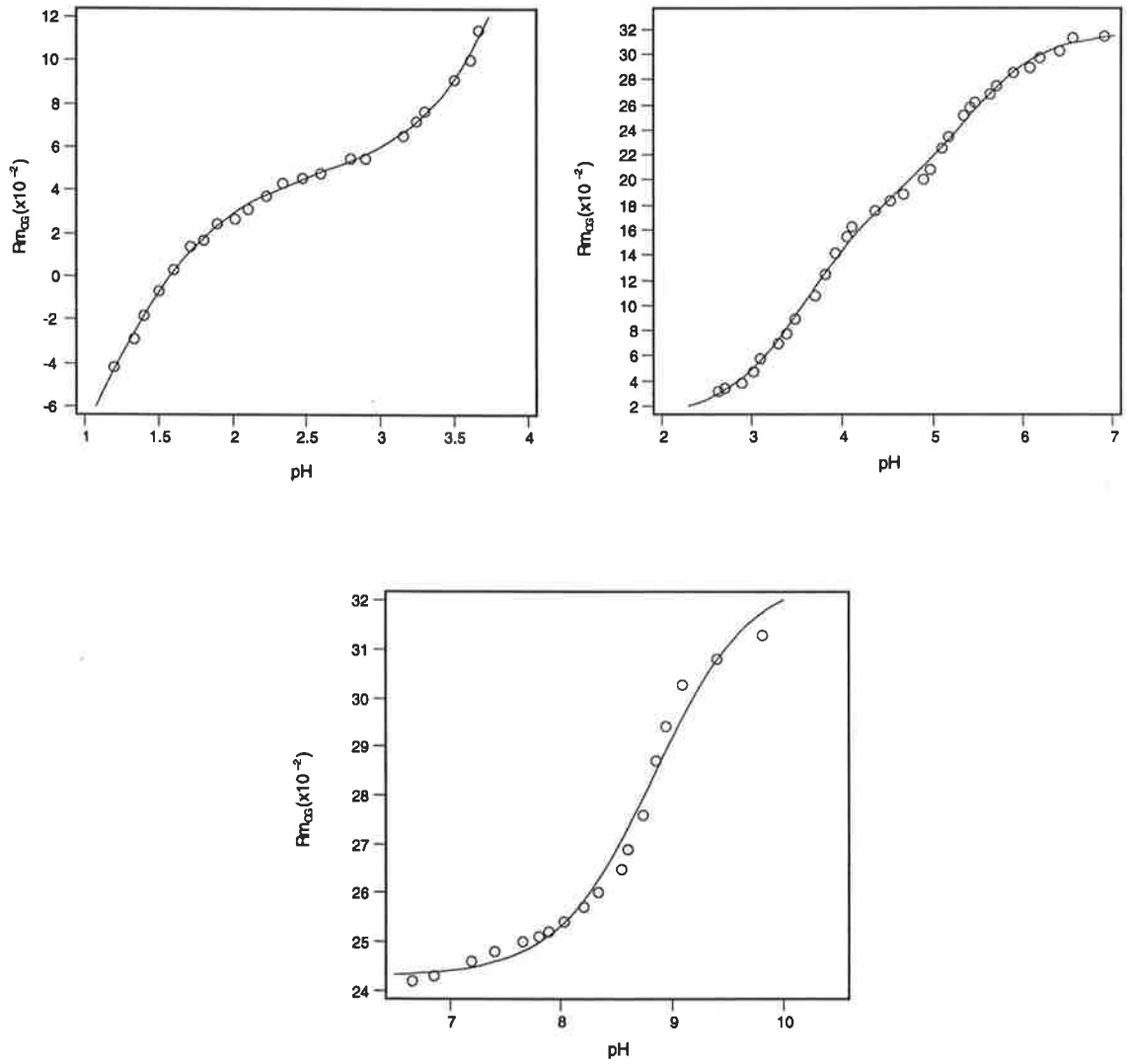

Figure 5.6: Relative mobility of vitisin A (Rm_{OG}) as a function of pH with Equation 2.8 fitted for the estimation of pKa values using HVPE. Three different pH ranges were defined by the three different buffers; (a) oxalate, (b) citrate, and (c) phosphate/oxalate. The coefficients of determination (r^2) for the three curves were (a) 0.9980, (b) 0.9977, and (c) 0.9814.

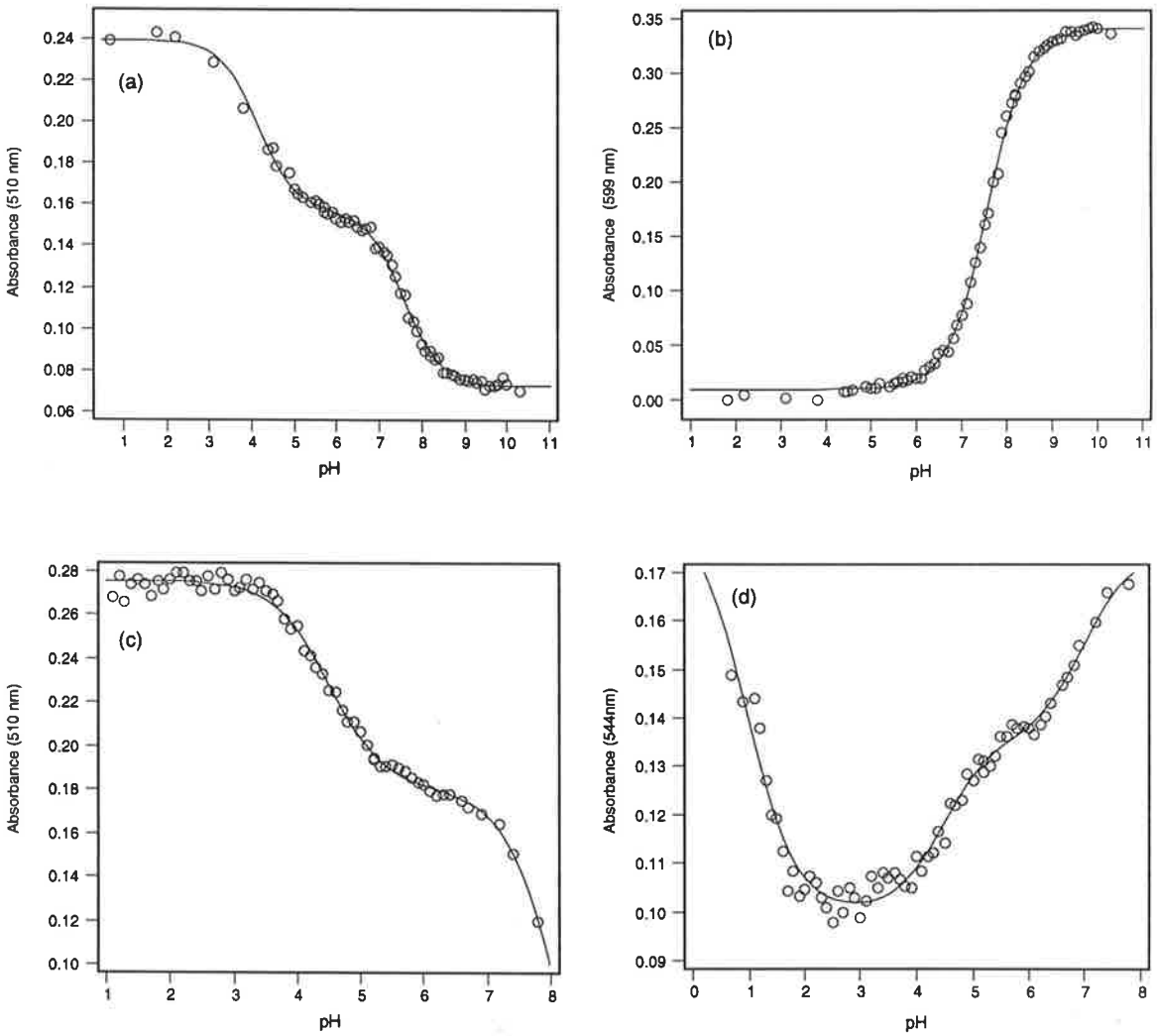

Figure 5.7: Absorbance of vitisin A as a function of pH with Equation 2.28 fitted for the estimation of hydration and ionisation constants by spectroscopic method (Equation 2.28). Two pH ranges were defined by the buffer systems; sodium pyrophosphate (a, b) and citrate (c, d). The wavelengths used were; (a) 510 nm, (b) 599 nm, (c) 510 nm and (d) 544 nm. The coefficient of determination (r^2) estimates for each of the fitted lines were (a) 0.9976, (b) 0.9990, (c) 0.9948 and (d) 0.9744

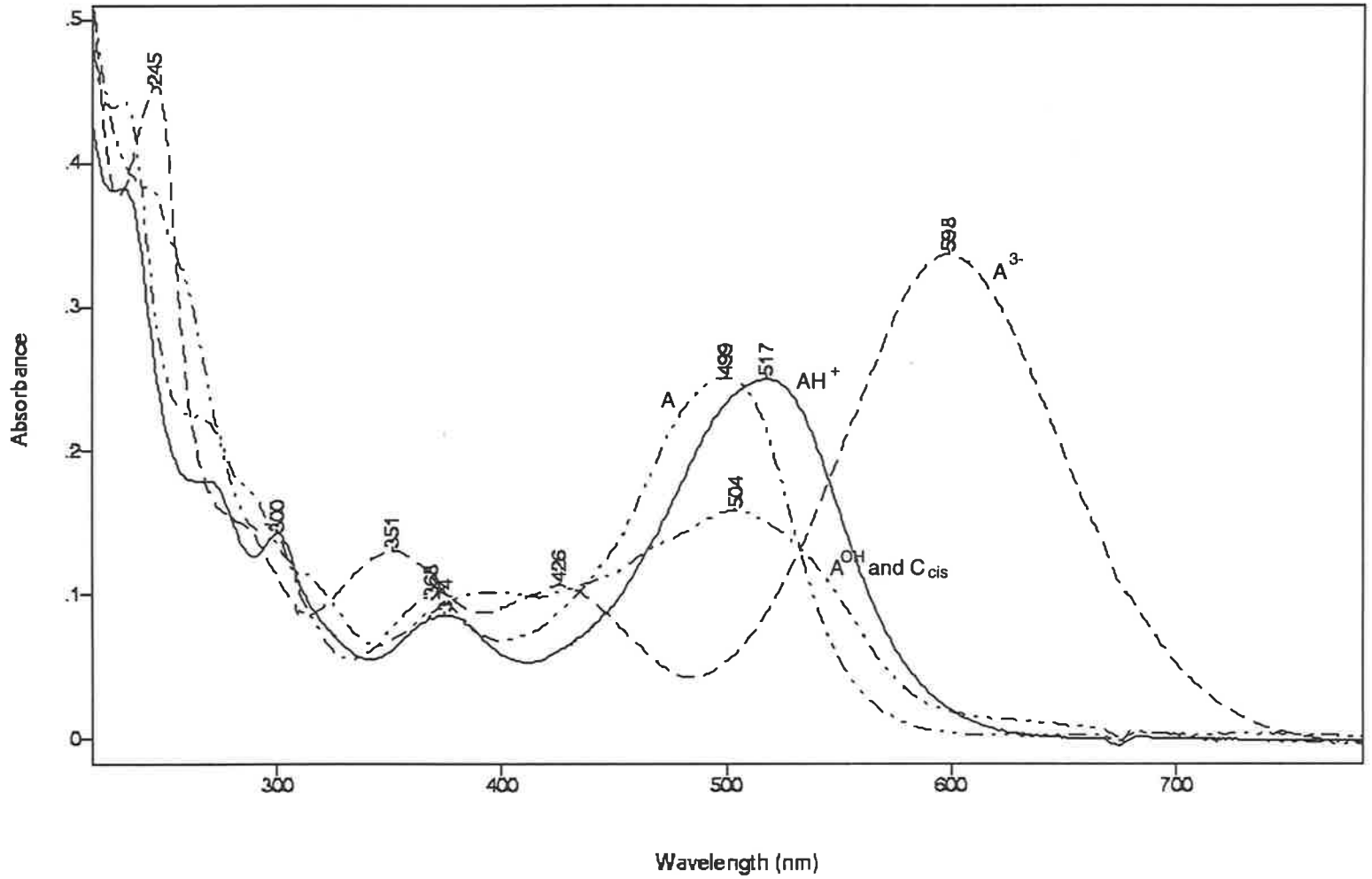

Figure 5.8: UV-visible spectra of the flavylium ion (AH^+), quinonoidal base (A), hydrated forms (hemiketal, A^{OH} and cis-chalcone C_{cis}), and quinonoidal trianion (A^{3-}) of vitisin A at pH 0.0, 2.2, 5.8, and 10.3 respectively.

Table 5.3: Apparent pKa and pK_H values of vitisin A as determined using UV-visible spectrometry.

	Buffer	Analytical wavelength	pK value	Average
pKa_1	citrate	544 nm	0.98 ± 0.10	
pK_{H1}	citrate	544 nm	4.48 ± 0.08	
pK_{H1}	citrate	510 nm	4.51 ± 0.03	
pK_{H1}	phosphate	510 nm	4.15 ± 0.04	pK_{H1} = 4.36
pK_{H2}	phosphate	510 nm	7.57 ± 0.02	
pK_{H2}	phosphate	599 nm	7.58 ± 0.01	pK_{H2} = 7.58

The UV-visible spectra of the different forms of vitisin A are shown in Figure 5.8. Table 5.4 list the maxima of each of the different spectra shown. It was not possible to obtain the spectrum of the quinonoidal anion, A^-, because of the similarity between pKa_2 and pK_{H1}. Furthermore it was not possible to measure the spectrum of the quinonoidal dianion, A^{2-} because of the similarity between the pK_{H2} and pKa_4. The difference between pK_{H1} (4.36) and pK_{H2} (7.58) suggests that hemi-ketal and cis-chalcone show a wide range of pH stability. The hemi-ketal/chalcone form of vitisin A has a λ_{max} of 503 nm. This absorbance maximum is intermediate between the quinonoidal base and the quinonoidal anion A^{3-}.

Table 5.4: Different species of vitisin A with their corresponding maximal absorbances.

		pH	λ_{max}
Flavylium ion	AH^+	0.0	513, 375, 300, 270, 233
Quinonoidal base	$A^0_{(aq)}$	2.2	499, 368, 298, 267, 232
Hemi-ketal/*cis*-Chalcone	$A^{OH}+C_{cis}$	5.8	505, 396, 318, 292, 258, 247
Quinonoidal trianion	A^{3-}	10.4	599, 426, 351, 288, 246

There were four ionisation constants estimated using HVPE. However, only one hydration constant could be identified using UV-visible spectroscopy at low pH. This suggested that vitisin A is normally hydrated under aqueous conditions. This will be discussed later.

The ionisation and hydration constants for vitisin A as calculated using HVPE and UV-visible spectrometry are summarised in (Figure 5.9). An average of pKa_1 was estimated using both spectroscopic (544 nm in citrate buffer) and electrophoretic data, the average

value for for pK_{H1} was derived using spectroscopic data using both the citrate and phosphate buffers and an average for pK_{H2} was calculated using the phosphate buffer at 510 nm and 599 nm. The estimated pKa and pK_H values were used to calculate the contribution of each of the different forms of vitisin A to the visible spectrum at any pH value. This is graphically shown in Figure 5.10.

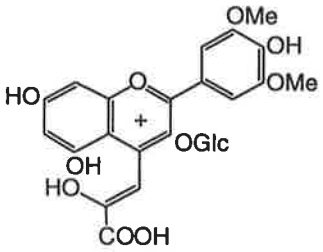

Flavylium cation, A^+ (λ_{max}= 513 nm, pH 0.0)

$pKa_1 = 0.97$ $-H^+$

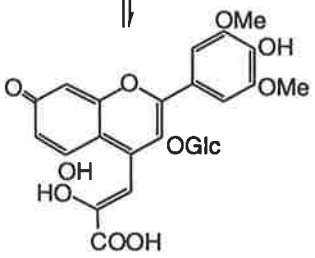

Quinonoidal base, A^0 (λ_{max} = 498 nm, pH 2.2)

$pKa_2 = 3.56 \pm 0.06$ $-H^+$

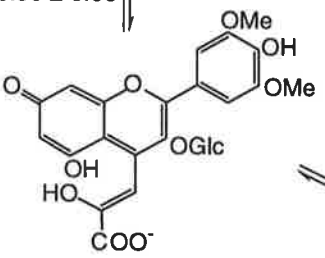

pK_{H1}= 4.37

$-H_2O$

Quinonoidal anion, A^-

Hydration products including the hemiketal (A^{OH}) and the *cis*-chalcone (C_{cis})

(λ_{max} = 503 nm, pH 5.8)

$pKa_3 = 5.38 \pm 0.07$ $-H^+$

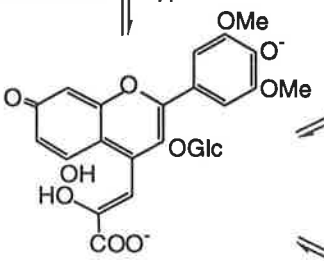

$+H_2O$
$+H^+$

pK_{H2}= 7.58

$pKa_4 = 8.84 \pm 0.06$

$+H^+$

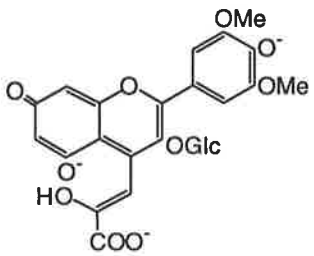

Quinonoidal anion, A^{3-} (λ_{max} = 599 nm, pH 10.3)

Figure 5.9: Structures of vitisin A as a function of pH. The macroscopic pKa and pKH values of vitisin A in dilute solutions as calculated using HVPE and UV/Vis spectrometry. The λ_{max} and the pH at which this occurs for each of the species of vitisin A has been included.

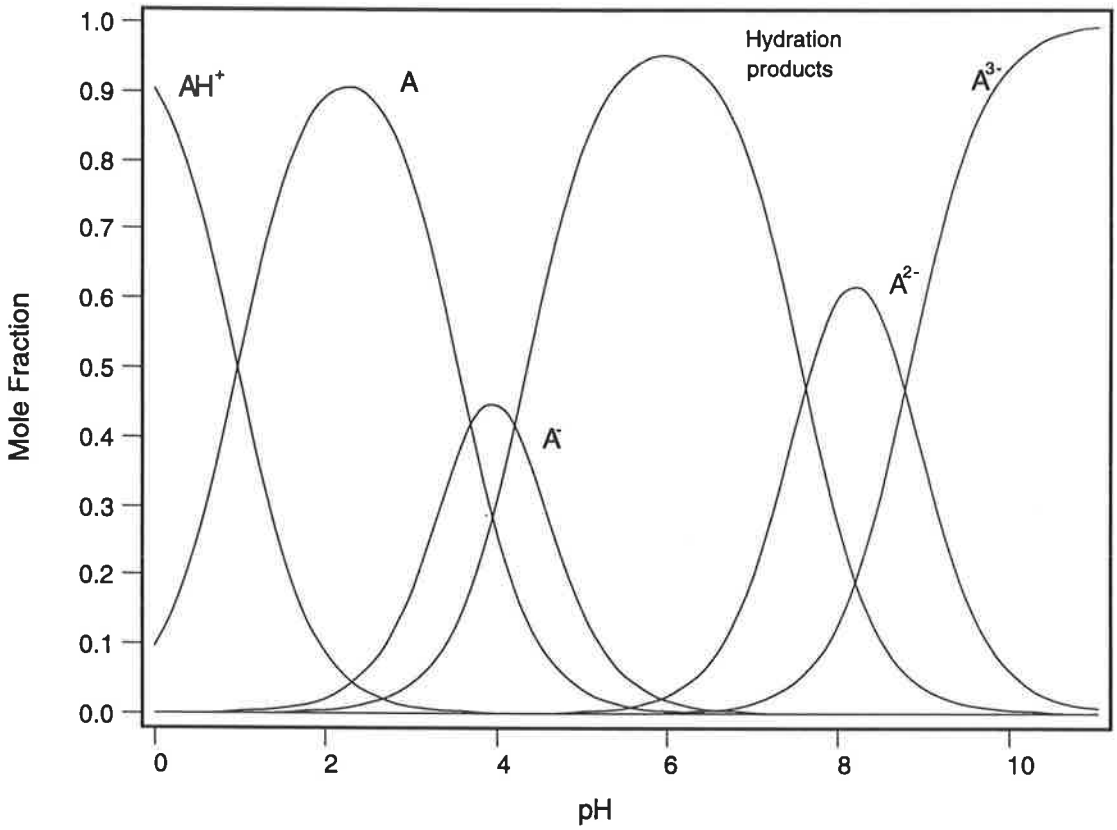

Figure 5.10: Proposed charge distribution diagram for vitisin A utilising pK values estimated using HVPE and UV-visible spectrometry as described in the text. The pK values employed were $pKa_1 = 0.97$, $pKa_2 = 3.56$, $pK_{H1} = 4.37$, $pK_{H2} = 7.58$ and $pKa_4 = 8.84$. (Note AH^+ represents the flavylium ion, A is the quinonoidal base, A^- is the quinonoidal anion, A^{2-} is the quinonoidal dianion and A^{3-} is the quinonoidal trianion.)

Infra-red spectral data

To provide addition data on the structure of vitisin A the infrared spectrum of vitisin A was compared with those of malvidin-3-glucoside, *p*-hydroxyphenylpyruvate and pyruvic acid. The spectra obtained by diffuse reflectance infrared spectroscopy for the carbonyl region (1800-1600 cm^{-1}) of malvidin-3-glucoside, *p*-hydroxyphenylpyruvate, pyruvic acid and vitisin A are shown in Figure 5.15. The peaks of interest were summarised in Table 5.5.

Table 5.5: Major infra-red peaks in the carbonyl region (1800-1600 cm^{-1}) for malvidin-3-glucoside, *p*-hydroxyphenylpyruvate, pyruvic acid and vitisin A. A minor peak or shoulder is indicated by sh.

Compound	Peaks (cm^{-1})
malvidin-3- glucoside	1720 sh, 1641
p-hydroxyphenylpyruvate	1760 sh, 1693, 1603
pyruvate	1778 sh, 1732, 1657, 1602 sh
vitisin A	1736, 1657, 1624, 1600 sh

The infra red spectrum of malvidin-3-glucoside has two bands in the carbonyl region being a major band at 1641 cm^{-1} and a shoulder at 1720 cm^{-1}. The 1641 cm^{-1} absorbance band has been attributed to arise from the aryl-conjugated heterocyclic atom of the flavylium ion (Ribéreau-Gayon and Josien, 1960). This band is thought to result from the ring stretching frequency (ie ring breathing). The small to medium band at 1700-1720 cm^{-1} of malvidin-3-glucoside was also observed by Ribéreau-Gayon and Josien (1960).

Pyruvic acid has a major peak at 1732 cm^{-1}, a smaller peak at 1657 cm^{-1}, a shoulder at 1778 cm^{-1} and a small shoulder at 1602 cm^{-1}. The major band at 1732 cm^{-1} is consistent with the result published by Randall *et al.* (1949) of 1745 cm^{-1}. It should be noted that saturated carboxylic acids show a C=O frequency band between 1725 and 1700 cm^{-1} and $\alpha\beta$-unsaturated carboxylic acids show a band between 1715 and 1690 cm^{-1} (Williams and Fleming, 1989). However, whilst the α-carbon of pyruvic acid is unsaturated, the carbonyl on the α–carbon interacts with the carboxyl carbonyl resulting in a carbonyl band with a higher frequency.

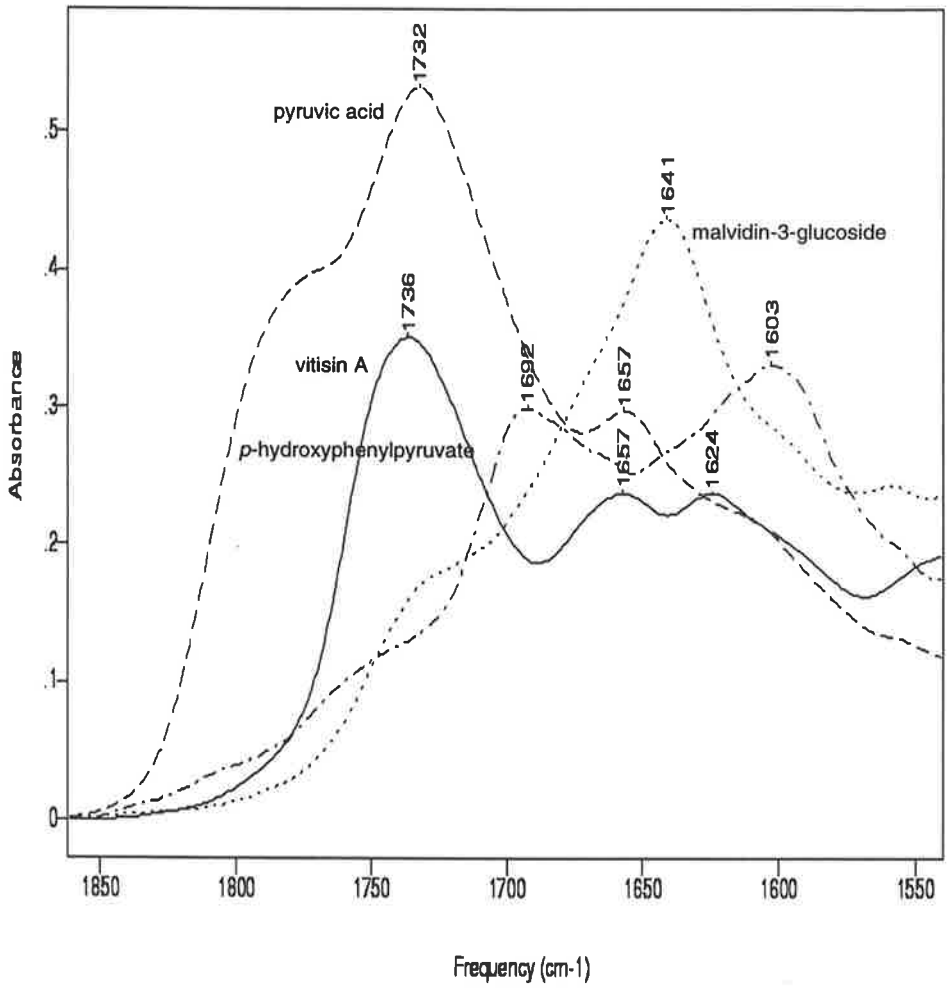

Figure 5.11: Carbonyl region of the infrared spectra of pyruvic acid (dashed line), vitisin A (solid line), malvidin-3-glucoside (dotted line) and *p*-hydroxyphenylpyruvate (dash-dotted line).

The enolic tautomer of pyruvic acid can form internal hydrogen bonds, which would significantly decrease the frequency of the carbonyl (Bellamy, 1975) and it is proposed that the band at 1656 cm^{-1} represents this enolic tautomer. Furthermore, it is proposed that the shoulder at 1778 cm^{-1} in the spectrum of pyruvic acid is the result of inter carboxylic acid hydrogen bonding. The band from a carboxylic acid dimer corresponds to a frequency approximately 45 cm^{-1} higher than the band from the monomer (Bellamy, 1975). Pyruvic acid also shows a shoulder at 1602 cm^{-1} final band which is indicative of the carboxylate ion (Williams and Fleming, 1989).

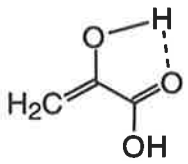

5.17a

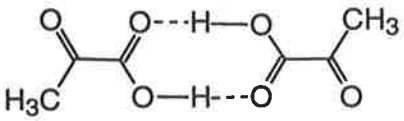

5.17b

Figure 5.12: (5.12a) The enolic form of pyruvic acid showing hydrogen bonding and (5.12b) the carboxylic acid dimer as a result of intermolecular hydrogen bonding.

Para-hydroxyphenylpyruvate shows an absorbance maximum at 1694 cm^{-1} which is consistent with the main isomer being an aryl cinnamic acid (Bellamy, 1975), and the pyruvic acid group for the $\alpha\beta$-unsaturated enolic form. A major band of *p*-hydroxyphenylpyruvate at 1602 cm^{-1} indicates a relatively high concentration of the carboxylate ion.

Vitisin A showed three major bands in the mid infra-red carbonyl region with peaks at 1736 1657 and 1624 cm^{-1} and a shoulder at 1600 cm^{-1}. The infra-red spectrum of vitisin A shows no evidence of a typical anthocyanin band at approximately 1641 cm^{-1} as exhibited by malvidin-3-glucoside. Vitisin A has three bands at that are similar to pyruvic acid; 1736 and 1657 cm^{-1} and the shoulder at 1600 cm^{-1}. Neither pyruvic acid, malvidin-3-glucoside nor *p*-hydroxyphenyl pyruvate show a major band at 1624 cm^{-1}. The 1624 cm^{-1} band may be due to ring breathing frequency of an anthocyanin, but the 1736 cm^{-1} carbonyl is a much stronger band, and therefore the 1624 cm^{-1} band appears less important.

Discussion

The mass spectral data was used for the preliminary confirmation that the pigment isolated was vitisin A. Both the positive and negative ion mass spectra were used for the identification of the pigment. However, the structural identification of vitisin A was made complicated because there were two different isomers proposed (Figure 1.6); one by Bakker and Timberlake (1997), and Bakker *et al.* (1997), and the other by Cheynier *et al.* (1997) and Fulcrand *et al.* (1998).

The positive ion mass spectrum acquired in this study shows two major ions with a m/z 561.3 and 399.2 (Figure 5.1a). These values agree with a molecular ion (M^+) of 561 and a fragment of m/z 399 obtained by Bakker and Timberlake (1997) using fast atom bombardment mass spectrometry. The negative ion mass spectrum for vitisin A obtained in this study shows major ions with a m/z of 559.4 (M^+), 515.6, 353.4, 339.4 (base peak), 325.4 and 311.2 (Figure 5.1b). However, Fulcrand *et al.* (1998) only observed three of these ions, m/z 559.2 (M^-), 515.2, and 353.2 (base peak), using ion spray mass spectrometry in the negative ion mode. The negative ion mass spectrum contains a daughter ion with a mass of 515 which corresponds to the parent ion losing a carboxylic acid (559 - 44) as described by Fulcrand *et al.* (1998). The ion m/z 353 results from the loss of both the carboxylic acid (m/z 44) and the glucose (m/z 162) from the parent ion (m/z 559) (Figure 5.13).

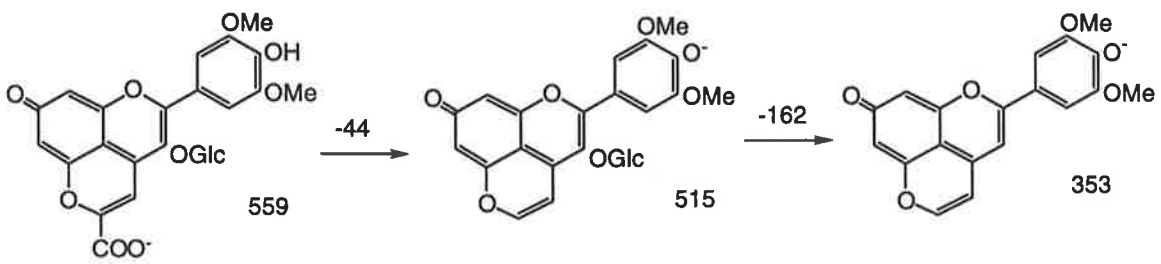

Figure 5.13: Proposed structures representing one series of negative ions from the ion spray mass spectrum of vitisin A.

The conditions for mass spectrometry used in this experiment favoured the formation of three ions m/z 339.4, 325.4 and 311.2 that were not observed by Fulcrand *et al.* (1998). It is proposed that loss of an oxygen occurs, probably in the 7 position as a result of the ionisation energy. The deglycosylated fragment that remains has a m/z 339. This undergoes further mass loss to form ion fragments with m/z of 325 and 311 (Figure 5.14).There is no evidence that these ions are not derived from vitisin A and this highlights that changes in the conditions used for mass spectrometry can alter the spectrum obtained.

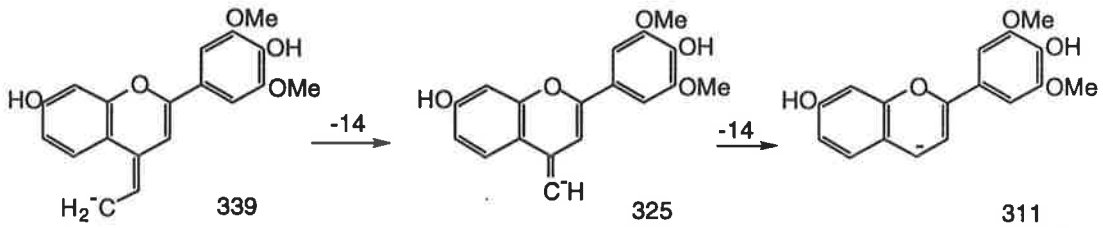

Figure 5.14: Proposed structures representing the second series of negative ions from the ion spray mass spectrum of vitisin A.

The identity of the pigment in this study was confirmed to be vitisin A by its synthesis. Vitisin A may be synthesised using pyruvic acid and malvidin-3-glucoside as precursors (Cheynier *et al.*, 1997; Fulcrand et al., 1998; Romero and Bakker, 1999). These mechanisms for the formation of vitisin A will be discussed later.

The spectrum of the flavylium ion of vitisin A has a absorbance maximum of 513 nm. This λ_{max} is slightly shifted to shorter wavelength than the equivalent ions of malvidin-3-glucoside (518 nm) and malvidin-3-(*p*-coumaryl)glucoside (523 nm). The similarity between the spectra of the different compounds suggests that the absorbance of positively charged malvidin chromophore is only slightly influenced by the presence of adducts. The molar absorbance coefficient for vitisin A of 24 863 (± 1807) at 520 nm (1 mol dm^{-3}) is similar that of to malvidin-3-glucoside (27 958 ± 514) and malvidin-3-(*p*-coumaryl)glucoside (25 683 ± 233). The difference between the absorbance coefficients of malvidin-3-glucoside, malvidin-3-(*p*-coumaryl)glucoside and vitisin A is relatively small and

therefore a single coefficient can be used for the determination of total anthocyanin concentration in wine as has been suggested by Somers and Vérette (1988).

The apparent pKa values and pK_H values for vitisin A obtained in this study are different than those predicted from the structures presented by either Cheynier *et al.* (1997) and Fulcrand *et al.* (1998), or Bakker and Timberlake (1997) and Bakker *et al.* (1997). It is proposed that in aqueous solutions vitisin A is a malvidin-3-glucoside pyruvic acid adduct with a three ring structure and can be identified as malvidin-3-glucose-4-(2-keto propionic acid) (Figure 5.15).

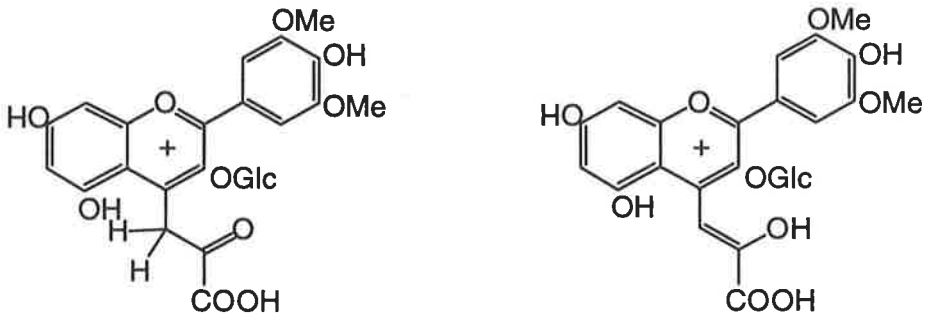

5.15a 5.15b

Figure 5.15: Proposed structure of the flavylium ion of the vitisin A in aqueous solutions according to pKa values showing the (5.15a) keto and (5.15b) enolic tautomers.

An examination of the carbonyl region of the mid infra-red (1800-1600 nm) of vitisin A supports the proposal that 'fourth ring' vitisin A is open. Vitisin A shows a peak at 1736 cm^{-1} and 1657 cm^{-1} with a shoulder at 1680 cm^{-1} which is consistent a structure with an open D-ring that exists with both the enolic and keto tautomers of malvidin-3-glucose-4-(2-keto propionic acid). The D ring closed structure of the pyruvic acid adduct of malvidin-3-glucoside, proposed by Cheynier *et al.* (1997), is expected to have major C=O band of the aryl cinnamic acid similar to that of *p*-hydroxy phenyl pyruvate at 1694 cm^{-1}. The structure for vitisin A, as proposed by Bakker and Timberlake (1997), can be considered to contain an α,β-unsaturated, β-hydroxy aldehyde with major band expected at approximately 1670 -1645 cm^{-1} (Bellamy, 1975) and no band at 1736 cm^{-1}. Vitisin A has a

major band at 1736 cm^{-1} band that is similar to the major band of pyruvic acid (1732 cm^{-1}). Thus, it can be proposed that vitisin A has a carboxylic acid group with an α-ketoenol substituent.

The vitisin A band at 1657 cm^{-1}, also evident in pyruvic acid, when compared with the usual band for $\alpha\beta$-unsaturated carboxylic acids at 1705-1690 cm^{-1} indicates that the carboxylic acid participates in internal hydrogen bonding. It is not possible for the carboxylic acid of a closed D-ring structure for to engage in internal hydrogen bonding (Figure 5.16). It should also be noted that the pKa values of vitisin A indicated that the carboxylic acid group of the hemiketal and the chalcone are ionised. Only a minor band representing a carboxylate ion (1600 cm^{-1}) could be detected and therefore it is proposed that the contribution of the hemiketal, chalcone or the anion (A^-) to this infra-red spectrum was minimal. Thus, the 1657 cm^{-1} and 1600 cm^{-1} bands provides further evidence that, at low pH, vitisin A exists as a tricyclic and not a tetracyclic compound.

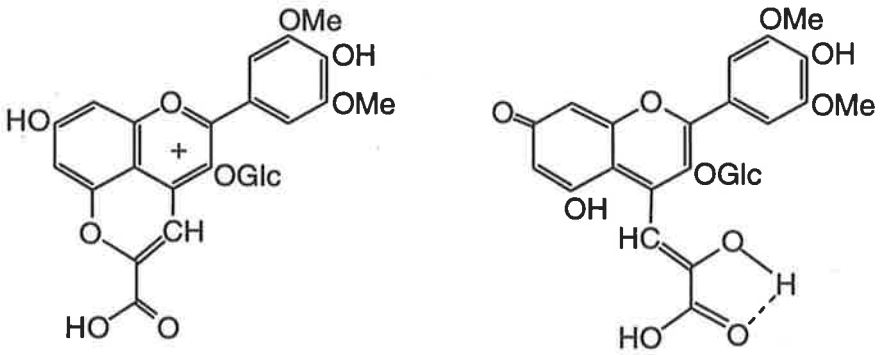

5.16a 5.16b

Figure 5.16: Internal hydrogen bonding shown by vitisin A. (5.16a) structure of the pyruvic acid adduct of malvidin-3-glucoside as proposed by Fulcrand *et al.* (1998) has no hydrogen bonding involving the carboxylic acid group. (5.16b) proposed structure of vitisin A showing hydrogen bonding between the C2" hydroxyl and the carboxylic acid group.

Using NMR to elucidate the structure of Vitisin A, Bakker *et al.* (1997) experienced difficulties in obtaining the spectrum of the flavylium ion and quinonoidal species because there were five different isomers present in the solution. The most stable isomer was the

chalcone and therefore the spectrum of the chalcone is the most reliable. Bakker *et al.* (1997) utilised both proton and carbon NMR to describe the structure of the chalcone. However, the C^{13} NMR although not unambiguous, does not fit their initially predicted structure for the chalcone but rather describes the chalcone as the malvidin-3-glucoside chalcone with an $\alpha\beta$-unsaturated α-hydroxy carboxylic acid on the 4 position. Furthermore, the α-hydroxyl group participates in a rapid keto-enol tautomerism. This is consistent with the structure for the chalcone of vitisin A as proposed in this study.

The NMR measurements by both Fulcrand *et al.* (1998) and Bakker and Timberlake (1997) were performed in dimethyl sulphoxide (DMSO) with trifluoroacetic acid added. These authors describe closed ring products for vitisin A. The acetylation of vitisin A in acetic anhydride, yielded a mass spectrum that indicated a closed ring structure. This evidence strongly suggests that dehydration of vitisin A readily occurs in non-aqueous solvents. With increasing ethanol concentration, the absorbance at 537 nm (Figure 5.5), indicates that there are two plateaus at 50-60% ethanol and approximately 100% ethanol. It is therefore proposed that these plateaus represent the quinonoidal base and closed ring quinonoidal base structures of vitisin A respectively (Figure 5.17), ie vitisin A is dehydrated to give the four ringed structure.

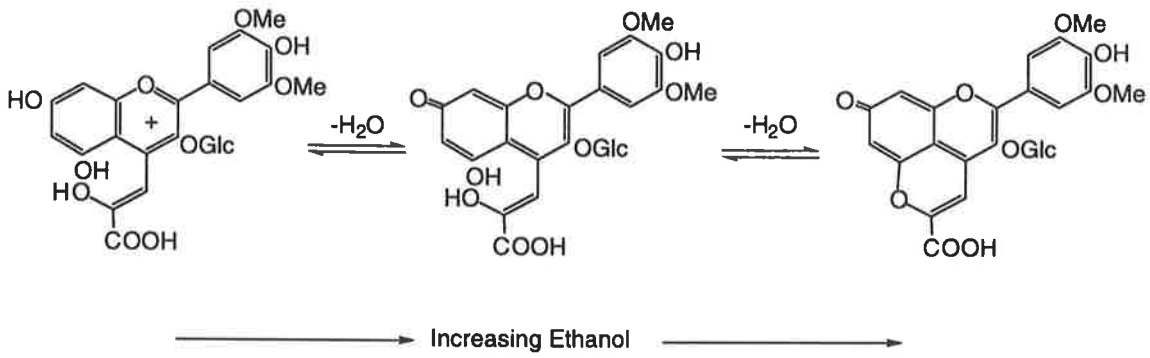

Figure 5.17: Proposed equilibrium of vitisin A observed when ethanol is added to acidified aqueous vitisin A.

The pKa_1 of 0.97, is in the range expected for proton loss from the flavylium ion (Chapter 3; Figure 5.18). The spectroscopic method and the electrophoretic method both provide

similar estimates for the pKa_1 value, 0.98 ± 0.1 and 0.95 ± 0.1, respectively. This value suggests that the compound is a stronger acid than proposed by Cheynier *et al.* (1997). While the pKa_1 is lower than that of malvidin-3-glucoside it is identical to malvidin-3-(*p*-coumaryl)glucoside. The pyruvate group attached to carbon 4 may participate in electron sharing and therefore helps in delocalising the charge associated with the C ring.

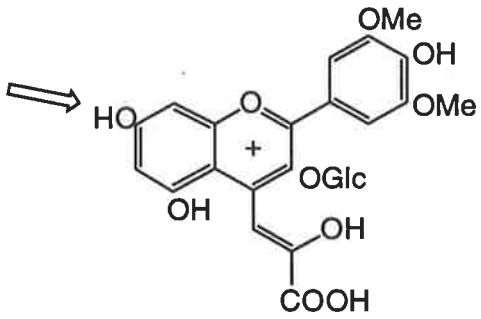

Figure 5.18: Structure of vitisin A flavylium ion with the C7 hydroxyl group indicated as a potential site for deprotonation.

Dehydration of the vitisin A resulting in ring closure would require the estimation of an additional pK_H value. There is no evidence that at very low pH, vitisin A is either a closed or open ring structure. However closely overlapping pKa and pK_H values would make the identification of a closed ring structure difficult using these methods.

The pKa_2 has been estimated using HVPE as 3.56 ± 0.06. There are two micro protonation constants expected for the loss of the proton from the carboxylic acid. The keto and enol tautomers (Figure 5.19) forms will, theoretically, have different pKa values. Conditions in aqueous solution or the wine matrix will influence the macro protonation constant. The final apparent pKa will depend on which tautomer predominates.

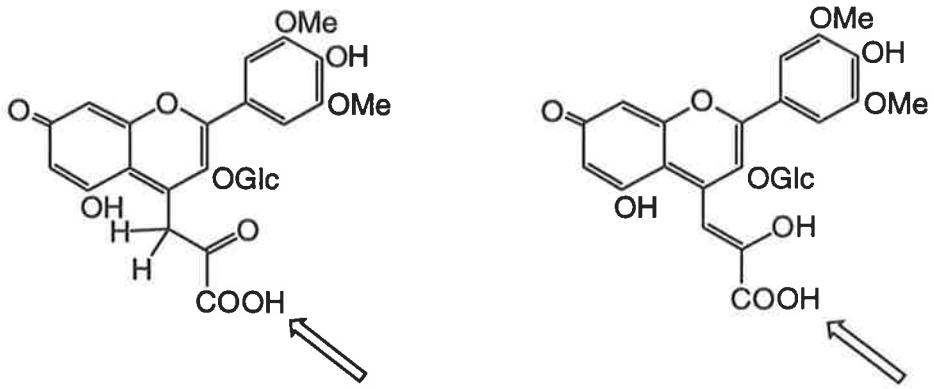

5.19a 5.19b

Figure 5.19: Structures of (5.19a) the keto and (5.19b) enol tautomers of the vitisin A quinonoidal base with the carboxylic acid groups indicated as the probable sites for deprotonation.

Various methods can be used to provide an estimate for the pKa of the keto and enol tautomers. The pKa of pyruvic acid is 2.49 (Kortüm *et al.*, 1961), and therefore the keto tautomer is expected to have a similar pKa value. The pKa of enol can be estimated using the equation for estimating the pKa of an aromatic acrylic acid (ArHC=C(R)COOH) using the methods outlined by Perrin *et al.* (1981). Thus, the pKa of can be estimated where R is a hydroxyl group using the formula,

$$pKa \text{ aryl acrylic acid} = 4.45 - 3.48\sigma \text{ (Perrin } et\ al.\text{, 1981)} \qquad \text{(Equation 5.2)}$$

$$\sigma \text{ for OH} = 0.13$$

$$pKa = 4.45 - (3.48 \times 0.13) = 4.0$$

The pKa estimate for the enolic form of vitisin A is 4.00. If both of the tautomers contribute equally then an average of these two estimates (ie 2.49 and 4.00) is 3.71. The experimental value for vitisin A of 3.56 ± 0.06, is lower than the pooled estimate, and therefore it is proposed that the keto tautomer contributes more towards the pKa_2, than the enol tautomer.

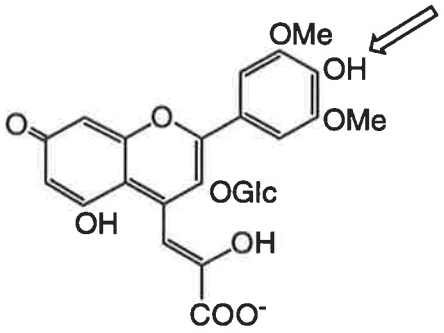

Figure 5.20: Structure of vitisin A anion (A^-) with the C4" hydroxyl group indicated as a potential site for deprotonation.

The vitisin A quinonoidal anion is analogous to the quinonoidal base of malvidin-3-glucoside and therefore deprotonation is expected to be from similar hydroxyl groups (Figure 5.20). Thus, the pKa_3 can be considered as analogous to the pKa_2 of malvidin-3-glucoside and malvidin-3-(*p*-coumaryl)glucoside. The expected site of deprotonation is shown in Figure 5.20. The revelant pKa values for vitisin A and malvidin-3-glucoside, 5.38 ± 0.07 and 5.36 ± 0.04 respectively, are surprisingly similar. However, the pKa value of malvidin-3-(*p*-coumaryl) glucoside, (4.45 ± 0.03) is much lower. An electron dense substitution group on carbon 4 would be expected to have a role in lowering the pKa in a similar manner as the *p*-coumaric acid folding and thereby protecting the carbon 4 of malvidin-3-(*p*-coumaryl)glucoside. However, the negative charge associated with the pyruvate group negates this effect and consequently raises the pKa again.

At wine pH (3.2 - 3.8) vitisin A is predominantly in the neutral and anionic ion states, and not cationic as suggested by Bakker and Timberlake (1997) and Bakker *et al.* (1997). Furthermore the spectrum of vitisin at wine pH of 3.6 has a λ_{max} of 498 nm, and therefore vitisin A is expected to contribute towards the brick red colour of an aged wine.

While it was not possible to obtain the spectrum of the quinonoidal base of malvidin-3-glucoside in aqueous solution, the neutral form of malvidin-3-(*p*-coumaryl)glucoside had a λ_{max} of 528 nm. The wavelength of the quinonoidal base of malvidin-3-(*p*-coumaryl) glucoside is intermediate between the flavylium ion and the anionic ions. In contrast, the quinonoidal base of vitisin A has a λ_{max} of 498 nm, and this absorbance maximum is

distinct from the cationic and hydrated states of vitisin A. This makes study of the properties of the quinonoidal base of vitisin A easier than either malvidin-3-glucoside or malvidin-3-(*p*-coumaryl)glucoside.

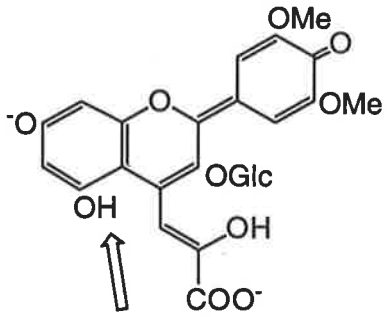

Figure 5.21: Structure of vitisin A dianion (A^{2-}) with the C5 hydroxyl group indicated as a potential site for deprotonation.

The pKa_4 value of vitisin A is expected to be equivalent to the pKa_3 values of malvidin-3-glucoside and malvidin-3-(*p*-coumaryl)glucoside. The expected site of deprotonation is shown in Figure 5.21. The ability for pyruvic acid group to participate in electron delocalisation will increase the pKa of vitisin A when compared with malvidin-3-glucoside. It was found that the pKa_4 of vitisin A is 8.84 (± 0.06) is greater than pKa_3 of malvidin-3-glucoside (8.31). What is surprising is the similarity of the pKa values of vitisin A and malvidin-3-(*p*-coumaryl)glucoside (pKa_3 = 8.86). This suggests that the *p*-coumaric acid has a very similar effect on electron delocalisation as the pyruvic acid moiety on carbon 4.

The spectrum of the fully ionised vitisin A has a similar λ_{max} (599 nm) to both malvidin-3-glucoside (596 nm) and malvidin-3-(*p*-coumaryl)glucoside (594 nm). This suggests a very similar electronic configuration for all three species.

The hydration of vitisin A occurs in the C2 position (Figure 5.22). While it has been suggested that C4-substitution may prevent hydration, although Brouillard *et al.* (1982) provided evidence that C4-substitution does not prevent the hydration of anthocyanins and the structure of the vitisin A chalcone has been described by Bakker *et al.* (1997) using NMR.

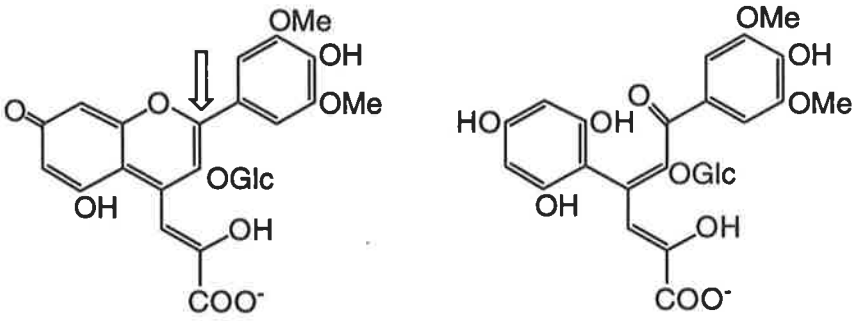

5.22a 5.22b

Figure 5.22: (5.22a) Hydration at the C2 carbon leads to the formation of the hemi-ketal and subsequent ring opening results in (5.22b) the chalcone

The pK_{H1} of vitisin A is 4.37 and is greater than that of either malvidin-3-glucoside (pK_{H1} = 2.66) or malvidin-3-(*p*-coumaryl)glucoside (pK_{H1} = 3.01). The greater hydration constant for vitisin A is consistent with the expectation that C4-substituted anthocyanins are more resistant to hydration at lower pH values than simple anthocyanins. In dilute aqueous solutions it is possible to estimate the percent contribution of the hemi-ketal/chalcone of vitisin A to the colour of wine at pH 3.5 using the equation,

$$pH = pKa + \log\frac{\alpha}{1-\alpha} \qquad \text{(Equation 5.3)}$$

where α is the degree of dissociation (Clark, 1928). Using the pK_{H1} estimate of 4.37 (± 0.02) at a wine pH of 3.5 there is only approximately 12% of vitisin A in the hydrated form. Under similar conditions, malvidin-3-glucoside has 87% in the hydrated state.

The hemi-ketal and chalcone are probably anionic because of the carboxylic acid function. It is however difficult to predict whether the chalcone remains in the *cis*-isomer or converts to the *trans*-isomer. Hydrogen bonding may favour the *cis*-tautomer, but the *trans*-tautomer may be a low energy state as with malvidin-3-glucoside.

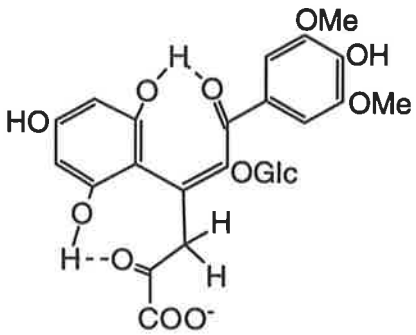

5.23a

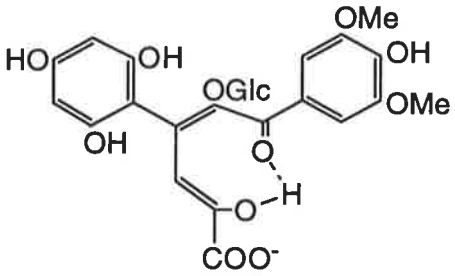

5.23b

Figure 5.23: Proposed internal hydrogen bonding shown by vitisin A chalcones. (5.23a) *cis*-chalcone may show hydrogen bonding between the C2 oxygen and the C9 hydroxyl group on the A ring of the as well as between the C2" oxygen and C5 hydroxyl group. (5.23b) *trans*-chalcone may exhibits hydrogen bonding between the C2 oxygen and the C2" hydroxyl of the enolic isomer.

That a high amount of red colour is associated with the hydrated forms of vitisin A (Figure 5.8) is unexpected. There are two possible explanations. Either the concentrations of quinonoidal anion and dianion have been underestimated at pH 5.8 or the chalcone itself contributes to the visible spectrum. The enolic form of the chalcone exhibits a high degree of conjugation, and therefore it is possible that the chalcone is coloured. Further investigation is required.

The second hydration constant, pK_{H2}, of vitisin A of 7.58 (± 0.01) is substantially greater than that of either malvidin-3-glucoside (5.9) or malvidin-3-(*p*-coumaryl)glucoside (5.9 ± 0.4). There is little data published regarding the dehydration of anthocyanins at high pH. Therefore, it is not known whether the high pK_{H2} value is the result of C4-substitution or specific to vitisin A.

The synthesis of vitisin A involves not only the addition of pyruvic acid to malvidin-3-glucoside but also an oxidative step (Figure 5.24). It can be shown that the synthesis under conditions that minimise aerobic oxidation gives a lower yield of vitisin A than in the presence of oxygen. Similarly, Blackburn *et al.* (1957) reported that the reaction of dimethylaniline with the flavylium base to form a C4-substituted anthocyanin type pigments requires the presence of oxygen. These oxidation reactions usually occur via two

single electron oxidation reactions and are catalysed by transition metal ions. When synthesising vitisin A, the yield of vitisin A was increased by the addition of a copper sulphate ($CuSO_4$) catalyst.

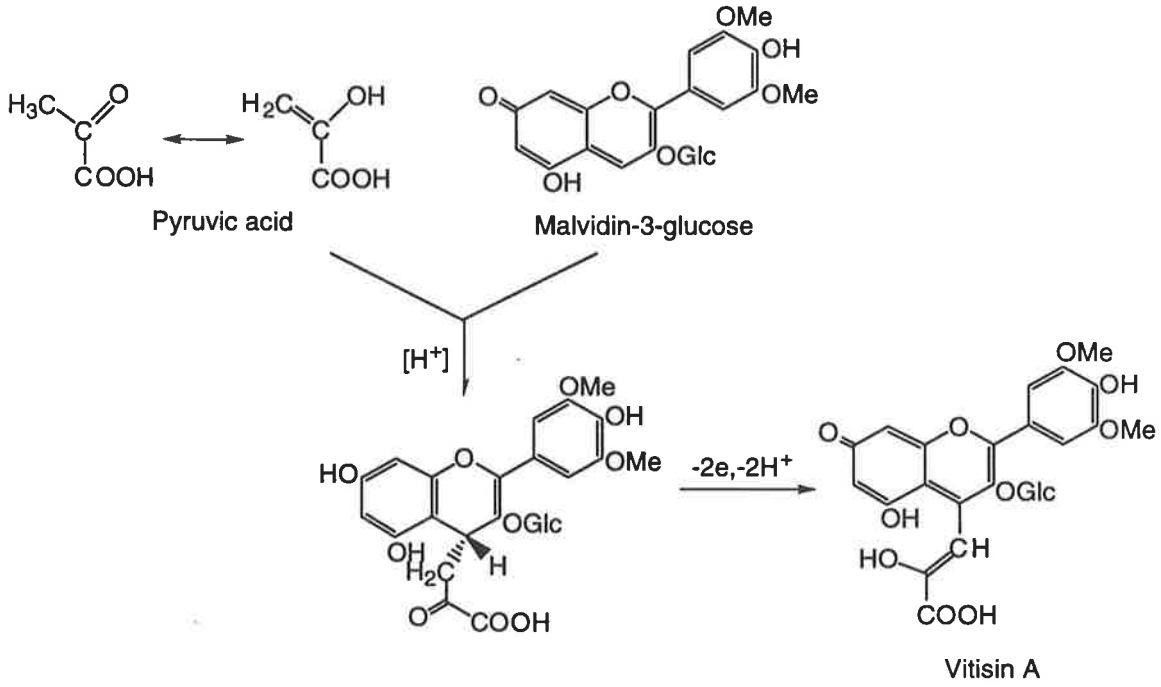

Figure 5.24: Reaction of malvidin-3-glucoside and enol tautomer of pyruvic acid yields 4-pyruvyl(3-glucosyl)flav-2-ene. This must undergo a further oxidation step to form vitisin A.

At wine pH (3.6) the hemi-ketal and the quinonoidal base are expected to be the predominant forms of malvidin-3-glucoside, and therefore it can be proposed that these are implicated in the synthesis of vitisin A. Wizinger and Luthiger (1953), and Blackburn *et al.* (1957) condensed dimethylanaline diarylethylenes and malonic acid with flavylium perchlorate to synthesise stable C4-substituted anthocyanins. These authors note that it is the neutral quinonoidal base and not the flavylium ion which is the active species for these synthesis reactions.

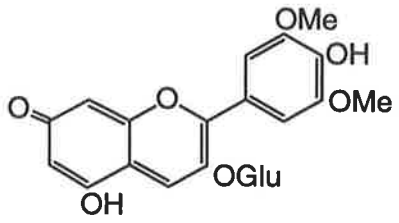

5.25a

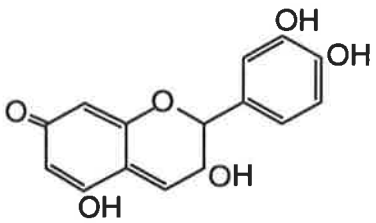

5.25b

Figure 5.25: Note the structural similarity between (5.25a) the malvidin-3-glucoside quinonoidal base and (5.25b) 3,3',4',5-tetrahydroxy flavanol quinone methide.

There is high structural analogy between the quinonoidal base and the flavanol quinone methide (Figure 5.25). Quinone methides show a high degree of conjugation, have a labile π-electron bond system and have the capacity for the delocalisation of electrons (Volod'kin and Ershov, 1988). They readily undergo oxidation-reduction reactions and nucleophilic substitution reactions (Volod'kin and Ershov, 1988). The reactions that quinone methides participate in are specific to the particular quinone methide and therefore it is difficult to predict the reactions in which the quinonoidal base may participate. The α-carbon of a quinone methide can act as an electron acceptor, and the quinoidal oxygen can act as an electron donor. It is therefore proposed that the quinonoidal base of malvidin-3-glucoside can be partially oxidised to form the stabilised free radical, and this free radical may be involved in the formation of wine pigments. Thus, the partial oxidation of malvidin-3-glucoside may occur prior to the addition of the pyruvic acid, or at least whilst pyruvic acid is being added to the malvidin moiety. A possible mechanism for the synthesis of vitisin A is outlined in Figure 5.26.

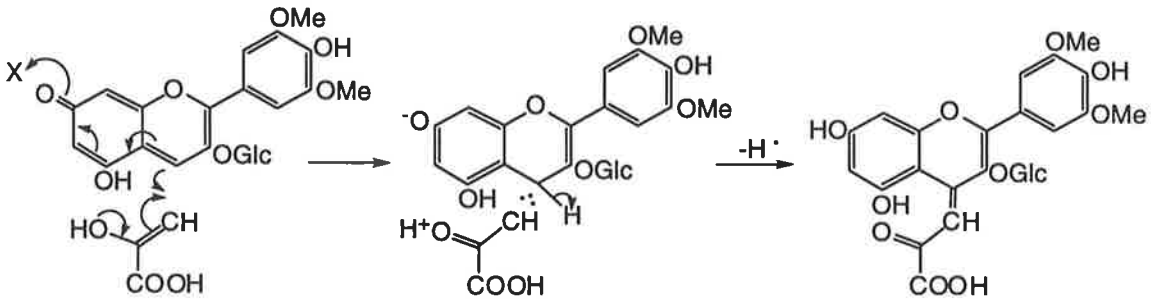

Figure 5.26: Possible mechanism for the formation of vitisin A. The loss of an electron as pyruvic acid is added to malvidin-3-glucoside creates an unstable intermediate (where X is an electron acceptor). This intermediate loses a hydrogen radical (H·) to create vitisin A.

It is proposed that *in vitro,* oxygen is the oxidative species that promotes vitisin A production, and that the formation of C4-substituted anthocyanins *in vitro* may be restricted without the presence of an appropriate catalyst. The importance of oxygen for the formation of vitisin A in wine will be examined further in the next chapter.

Chapter 6

Formation of vitisin A in wine

Introduction

A number of pigments have now been identified in wine (Fulcrand *et al.*, 1996b; Bakker *et al.*, 1997; Bakker and Timberlake, 1997; and Benabdeljalil, 1998), however little is known regarding their formation. An examination of the factors associated with the production of vitisin A in wine may provide a general understanding regarding the formation of pigments in wine. To date, it remains unknown as to whether vitisin A is the product of fermentation or maturation or both. In this chapter, a number of factors are investigated that were thought to influence vitisin A production during both fermentation and maturation.

Vitisin A can be synthesised by the reaction between pyruvic acid and malvidin-3-glucoside in the presence of an oxidant (Chapter 5). Vitisin A formation has been measured in model solutions (Romero and Bakker, 1999; 2000). The concentration of vitisin A has been measured in red wines during maturation by Bakker *et al.* (1998). However, there have been no reports regarding when vitisin A synthesis actually occurs. From a winemaking point of view it is important to establish the time of vitisin A synthesis during fermentation or maturation. Vitisin A synthesis can then be related to the concentration of constituents within the wine including malvidin-3-glucoside and pyruvic acid.

The final vitisin A concentration in wine depends on both synthesis and degradation of this compound. This chapter investigates both vitisin A synthesis and the long term stability of vitisin A.

Results

Synthesis of vitisin A during fermentation

Vitisin A, pyruvate and malvidin-3-glucoside concentrations of four replicate wines were monitored by HPLC. The results are summarised in Figure 6.1. The modified logistic equation (Equation 2.40) was fitted to the means of the four replicates (Figure 6.1). Using this equation it was possible to calculate the time of most rapid vitisin A and pyruvic acid production, malvidin-3-glucoside extraction, and sugar utilisation.

The yeast counts determined during the stationary phase of yeast growth at 18° Brix are shown in Table 6.1. A statistical comparison of the plates colony numbers using Anova showed that there was no significant difference between the four replicates at the 5% level. Furthermore, there was no evidence of foreign yeasts or bacteria.

Table 6.1: Yeast counts of four replicate wines measured at 18° Brix.

Replicate	A	B	C	D
Cell no. $x10^7$	7.37± 0.32	8.67 ± 1.36	6.20 ± 0.29	8.00 ± 0.48

Any increase in the concentration of pyruvic acid ceases at approximately 76 hours after initiation of the fermentation (Figure 6.1b) and the increase in the concentration of vitisin A ends at approximately 80 hours after the initiation of fermentation (Figure 6.1a). The increase in the concentration of vitisin A stops even though there are still high levels of both pyruvate and malvidin-3-glucoside in the wine must. The time for the maximum production rates of pyruvate and vitisin A, estimated using Equation 2.40, were at 45.6 hours and 52.1 hours respectively. The maximum rate of malvidin-3-glucoside extraction from the skins was estimated using Equation 2.40 to be 14.7 hours. The maximum rates for glucose and fructose utilisation determined using Equation 2.40 occurred at approximately 54.9 hours and 79.5 hours respectively.

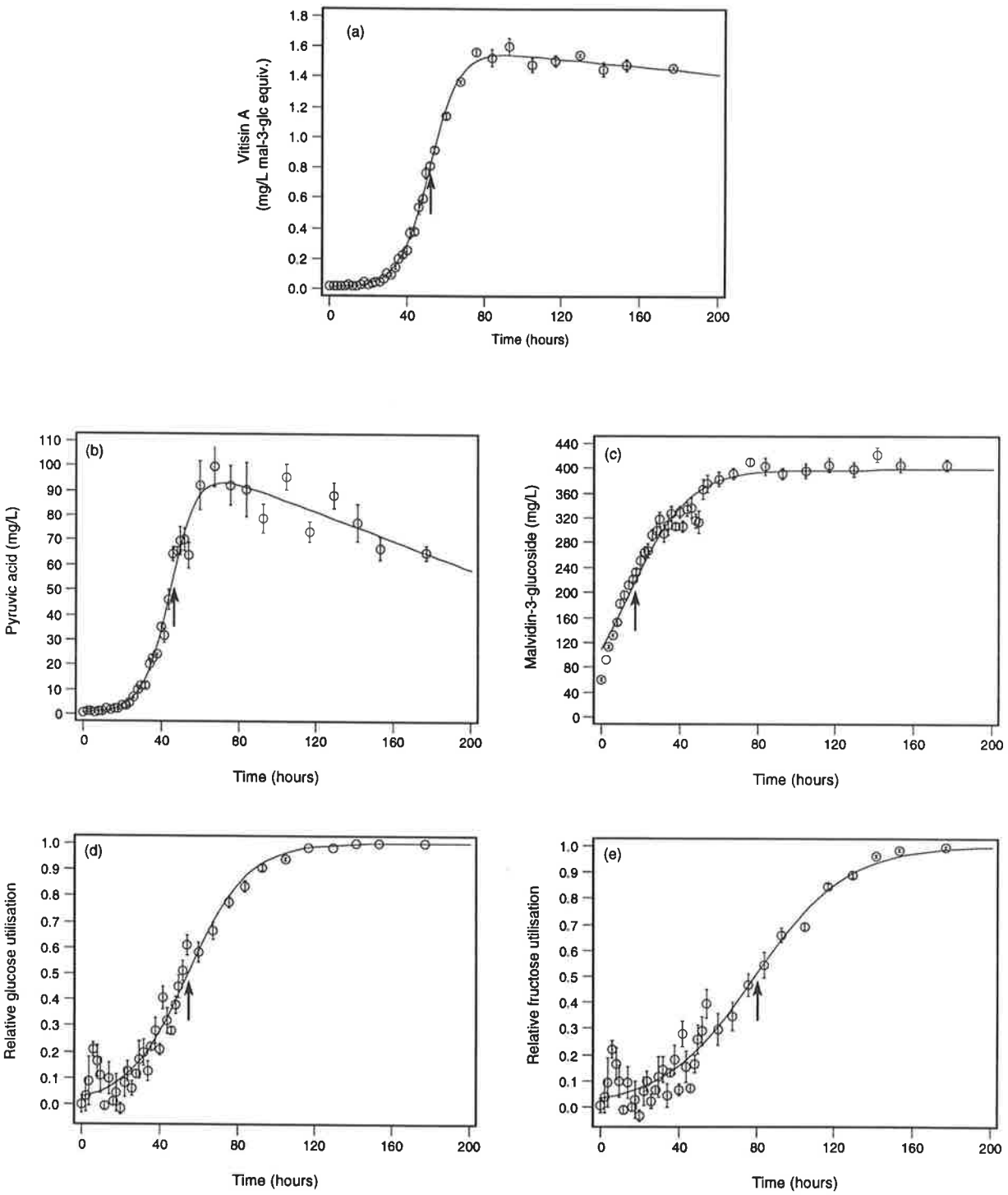

Figure 6.1: Vitisin A synthesis during fermentation. (a) The change in vitisin A concentration in wine during fermentation. (b) The change in pyruvate concentration, measured as pyruvic acid, in wine during fermentation. (c) The change in malvidin-3-glucoside concentration in wine during fermentation. (d) The relative utilisation of glucose in wine during fermentation. (e) The relative utilisation of fructose in wine during fermentation. Each point represents the mean of four replicates and the vertical bars represent the standard error. The modified logistic equation (Equation 2.40) fitted to the mean data with estimated coefficients of determination (r^2) equal to (a) 0.9982, (b) 0.9819, (c) 0.9589, (d) 0.9719 and (e) 0.9565. The maximum production, extraction or utilisation of compounds calculated from the logistic curves (indicated by an arrow) occurred at (a) 52.1 hours, (b) 45.6 hours, (c) 14.7 hours (d) 54.9 hours, and (e) 79.5 hours.

A correlation matrix was generated to compare the concentrations of vitisin A, pyruvate, and malvidin-3-glucoside, as well as the relative glucose utilisation (G_u) and relative fructose utilisation (F_u) over the 180 hours of the experiment. There was significant positive correlation between all the factors measured at the 0.1% level (Table 6.2).

Table 6.2 Correlation matrix for the wines comparing the concentrations of pyruvate, vitisin A, malvidin-3-glucoside, and the relative glucose utilisation (G_u) and relative fructose utilisation (F_u). The different relationships were analysed using regression analysis for significance comparisons. All were significant at the 0.1% level.

Variable	Pyruvate	Vitisin A	Mal-3-glc	G_u	F_u
Pyruvate	1				
Vitisin A	0.9224	1			
Mal-3-glc	0.8033	0.7825	1		
G_u	0.8415	0.9533	0.7635	1	
F_u	0.6737	0.8635	0.6455	0.9878	1

Apparent oxygen concentration during fermentation and its relationship to the formation of vitisin A

A fermentation on a sample of defrosted grapes was carried out where vitisin A, pyruvate and malvidin-3-glucoside and apparent oxygen concentrations of three replicate wines were monitored. The concentration profiles of pyruvic acid and vitisin A were similar to those obtained previously. The relative glucose utilisation was also similar to that observed earlier. A difference was however observed in the extraction rate of malvidin-3-glucoside deemed to be because the wine was made from frozen berries, and under these conditions the extraction of malvidin-3-glucoside was enhanced.

The data (Figure 6.2) indicate that the apparent oxygen levels are depleted early in the ferment, between 40 and 80 hours there is a slight increase, and from 88 to 140 hours there is a decline in the apparent oxygen concentration. There is a final increase in the apparent oxygen concentration towards the end of fermentation. Pressing of the wines off skins was performed at 160 hours. After pressing the apparent oxygen concentration rose to 7.23 (± 0.38) mg/L and after 6 hours post pressing the concentration had declined to 5.28 (± 0.27) mg/L. The vitisin A concentration 6 hours after pressing was 0.914 (± 0.011) mg/L, and 3 days after pressing the concentration had reached 0.960 (± 0.015) mg/L.

The estimated time of the maximum production rates for pyruvate and vitisin A were at 59.3 hours, and 77.8 hours respectively. The greatest rate of glucose utilisation occurred at approximately 72.7 hours.

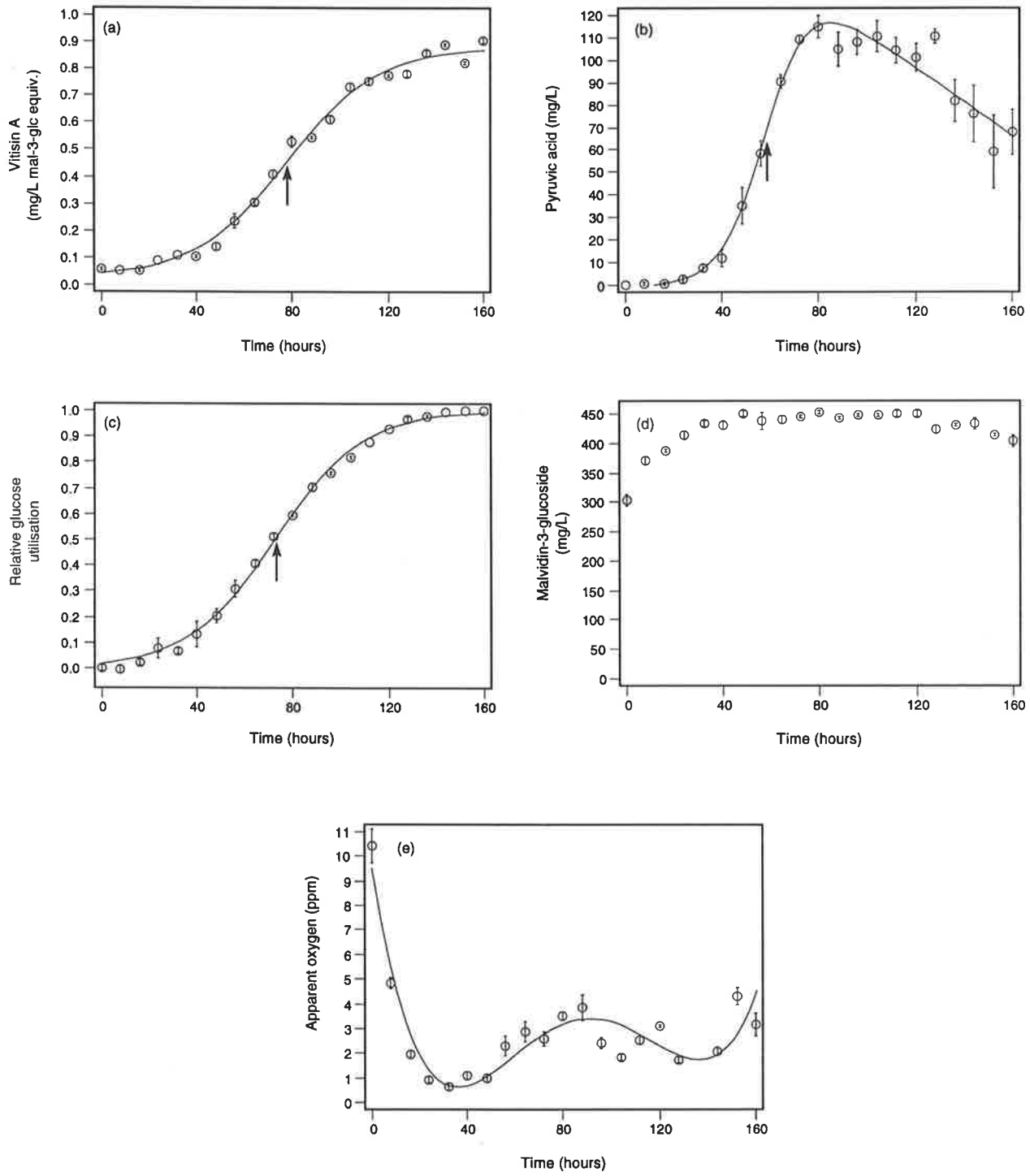

Figure 6.2: Apparent oxygen concentration and vitisin A synthesis during fermentation. (a) The change in vitisin A concentration in wine during fermentation. (b) The change in pyruvate concentration, measured as pyruvic acid, in wine during fermentation. (c) The relative utilisation of glucose in wine during fermentation. (d) The change in malvidin-3-glucoside concentration in wine during fermentation. (e) The change in apparent oxygen concentration in wine during fermentation. Each point represents the mean of three replicates and the vertical bars represent the standard error. The modified logistic equation (Equation 2.40) was fitted to the vitisin A, pyruvic acid and relative glucose utilisation mean data with estimated coefficients of determination (r^2) equal to (a) 0.9930, (b) 0.9795, (c) 0.9978. The maximum production, extraction or utilisation of compounds calculated from the logistic curves (indicated by an arrow) occurred at (a) 77.8 hours, (b) 59.3 hours, (c) 72.7 hours. The apparent oxygen concentration was fitted with a four factor polynomial with a coefficient of determination of 0.8729.

Formation of vitisin A in wines post fermentation

Eleven wines made from different regions representing the 1997 vintage were measured for the malvidin-3-glucoside and vitisin A concentrations after pressing and after six months of maturation (Table 6.3). The initial concentrations of pyruvic acid, both free and bound were also measured after pressing (Table 6.3). The correlation coefficients and regression analysis calculated an the results are summarised in Table 6.4.

The initial malvidin-3-glucoside was significantly correlated with final malvidin-3-glucoside at the 0.1% significance level. However, no correlation could be determined between malvidin-3-glucoside and vitisin A concentrations. There was a significant positive correlation (0.1%) between initial vitisin A and final vitisin A concentrations.

The pyruvate concentration of the wine was measured as pyruvic acid. Pyruvate is significantly positively correlated with both the initial vitisin A, and the final vitisin A concentrations, but significantly negatively correlated with initial malvidin-3-glucoside concentration. There was a significant correlation (at the 0.1% level) between free and bound pyruvate, but no correlation was observed between the vitisin A concentration and bound pyruvate concentration.

Table 6.3: Concentration (means ± s.e.) of malvidin-3-glucose [mal-3-glc], vitisin A, and pyruvate (both total and bound measured as pyruvic acid) for 11 wines from different regions representing the 1997 vintage. The initial concentrations were measured at pressing and the final concnetrations were measured after six months of aging. The concentration of malvidin-3-glucose degraded [Mal-3-glc (deg)] was defined by initial malvidin-3-glucose concentration minus final malvidin-3-glucose concentration. The concentration of vitisin A synthesised [vitisin A (syn)] was described by final vitisin A concentration minus the initial vitisin A concentration.

Site	Mal-3-glc (initial) mg/L	Mal-3-glc (final) mg/L	Mal-3-glc (deg) mg/L	Vitisin A (initial) mg/L	Vitisin A (final) mg/L	Vitisin A (syn) mg/L	Pyruvate (initial free) mg/L	Pyruvate (initial bound) mg/L
1	416 ± 10	265 ± 11	152 ± 4	2.70 ± 0.02	5.02 ± 0.42	2.32 ± 0.41	11.2 ± 1.3	0.9 ± 0.1
2	447 ± 12	223 ± 1	225 ± 11	4.10 ± 0.35	3.31 ± 0.06	-0.79 ± 0.33	5.2 ± 1.2	0.6 ± 0.2
3	367 ± 9	199 ± 9	168 ± 9	2.44 ± 0.13	2.97 ± 0.21	0.53 ± 0.08	8.5 ± 1.8	0.6 ± 0.2
4	391 ± 17	253 ± 2	138 ± 16	3.17 ± 0.09	3.81 ± 0.06	0.64 ± 0.03	16.6 ± 1.9	0.7 ± 0.2
5	307 ± 8	217 ± 7	90 ± 1	2.78 ± 0.08	3.72 ± 0.07	0.94 ± 0.07	23.4 ± 3.4	3.5 ± 0.3
6	360 ± 6	258 ± 4	102 ± 2	2.77 ± 0.17	3.73 ± 0.36	0.95 ± 0.19	19.6 ± 2.8	3.1 ± 0.2
7	564 ± 23	331 ± 16	233 ± 7	3.80 ± 0.30	5.52 ± 0.45	1.73 ± 0.15	15.9 ± 2.7	1.5 ± 0.3
8	354 ± 1	284 ± 11	70 ± 15	2.55 ± 0.01	1.70 ± 0.09	-0.85 ± 0.13	21.1 ± 2.4	5.8 ± 0.4
9	311 ± 10	215 ± 7	96 ± 4	5.67 ± 0.27	6.60 ± 0.05	0.93 ± 0.30	46.6 ± 6.2	6.0 ± 0.9
10	292 ± 10	191 ± 1	101 ± 9	4.44 ± 0.20	5.54 ± 0.26	1.10 ± 0.13	35.5 ± 2.4	4.2 ± 0.2
11	251 ± 8	176 ± 5	74 ± 6	2.74 ± 0.08	3.26 ± 0.07	0.52 ± 0.15	35.7 ± 4.8	6.9 ± 1.3

Table 6.4: Correlation matrix for the 1997 vintage wines comparing the concentrations of initial malvidin-3-glucoside (M_0), final malvidin-3-glucoside at six months (M_f), the amount of malvidin-3-glucoside lost in six months (-M) initial vitisin A (V_0), vitisin A at six months (V_f), the amount of vitisin A synthesised in six months (+V), initial total pyruvate (P) and the initial pyruvate bound to metabisulphite (P_B). The different factors were analysed using regression analysis for significance comparisons (* is significant at the 5% level, ** significant at the 1% level and *** significant at the 0.1% level).

Variable	M_0	M_f	-M	V_0	V_f	+V	P	P_B
M_0	1							
M_f	0.8120***	1						
-M	0.8806***	0.4385*	1					
V_0	-0.0026	-0.1100	0.0852	1				
V_f	0.1069	0.0619	0.1143	0.7365***	1			
+V	0.1625	0.2144	0.0761	-0.0203	0.6613***	1		
P	-0.6329***	-0.3869*	-0.6604***	0.5374**	0.4758**	0.1067	1	
P_B	-0.6743***	-0.3517*	-0.7528***	0.2409	0.0714	0.1624	0.8602***	1

Effect of sulphur dioxide as an oenological treatment on the formation of vitisin A during maturation

A series of wines containing different concentrations of sulphur dioxide added at crushing were measured after pressing for vitisin A, malvidin-3-glucoside and pyruvic acid concentrations. The sulphur dioxide concentrations determined at pressing reflect the impact of the different initial treatments (Table 6.5). There was a sequential increase in the concentration of sulphur dioxide measured at pressing corresponding to the amount of sulphur dioxide added prior to fermentation.

Table 6.5: Sulphur dioxide (mg/L) added to the grapes at crushing and the subsequent free and bound sulphur dioxide concentration (mg/L) calculated at the pressing of the wine.

SO_2 added	SO_2 (free)	SO_2 (bound)
0	0.1 ± 0.1	2.5 ± 0.3
50	1.1 ± 0.4	13.9 ± 0.5
100	3.3 ± 0.1	29.6 ± 0.4
200	9.7 ± 0.1	70.3 ± 3.5

After pressing, each of the wines were divided and one portion was inoculated with malo-lactic bacteria. Vitisin A, malvidin-3-glucoside pyruvic acid and malic acid concentrations each of the wines were then monitored. The changes in malic acid concentration indicates the progress of malolactic fermentation. In the absence of deliberate malolactic inoculation, spontaneous malolactic fermentation occurred in all those wines in which the SO_2 levels added at crushing were less than 50 mg/L (Figure 6.3d). For those wines deliberately inoculated, malolactic fermentation proceeded in all wines except that wine in which 200 mg/L SO_2 was added at crushing. In this latter wine, malolactic fermentation was significantly delayed (Figure 6.4d). The decline in pyruvate concentration of the inoculated wines and of the two non inoculated wines initially containing 0 mg/L and 50 mg/L SO_2 is concomitant with a decline in malic acid (Figure 6.3c, d; Figure 6.4c, d). It was therefore proposed that this loss of pyruvate was the result of malolactic fermentation.

During the maturation period, vitisin A was synthesised in all of the non-inoculated wines (Figure 6.3a) and in the inoculated wine with an initial SO_2 addition of 200 mg/L (Figure 6.4a). Vitisin A synthesis ceased in all of the wines at the end of the maturation period. This also applied to the two non-inoculated wines that had an initial SO_2 addition of 100 mg/L and 200 mg/L, which potentially contained sufficient pyruvate (Figure 6.3c) and malvidin-3-glucoside (Figure 6.3b) for continued vitisin A synthesis.

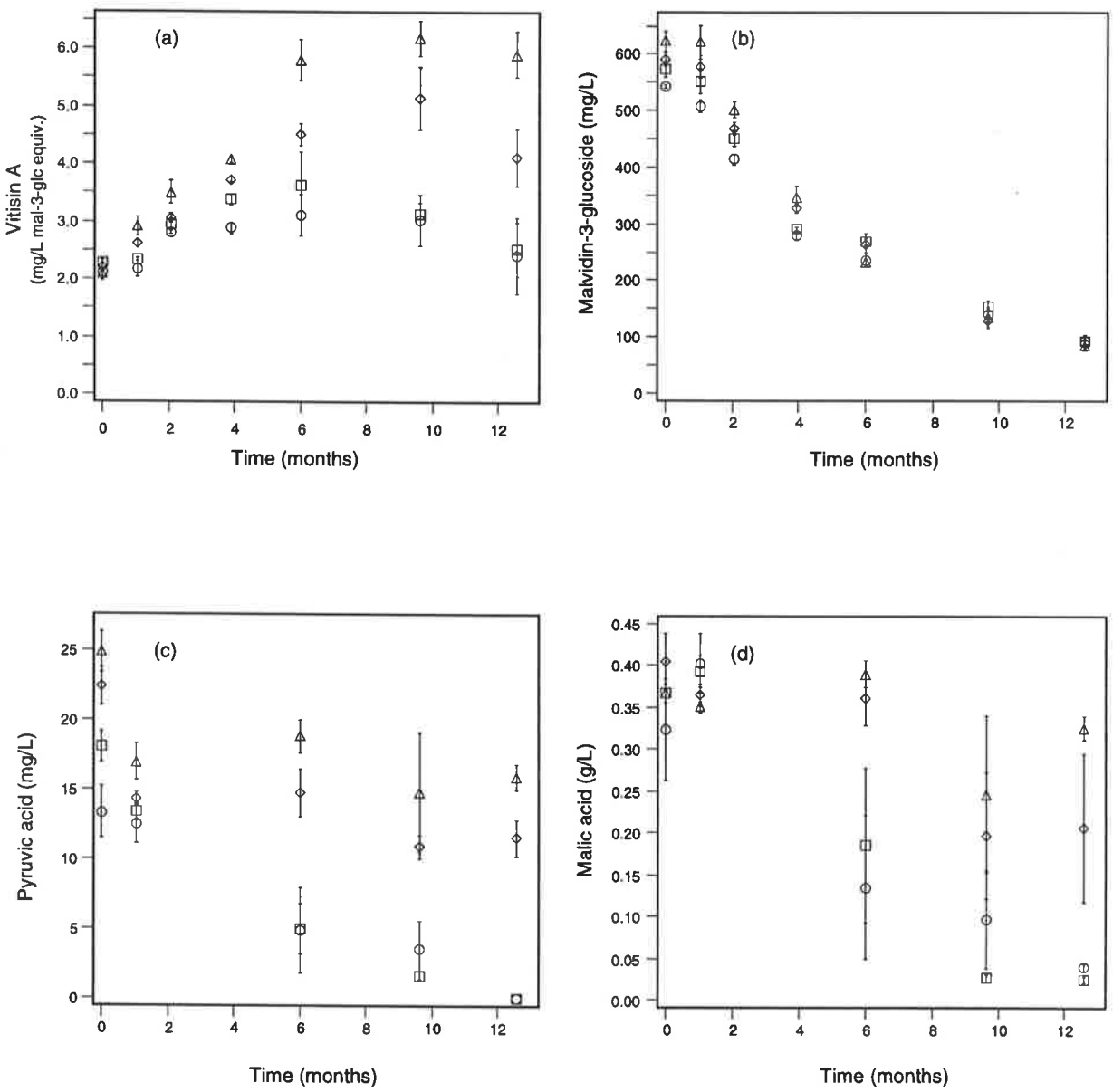

Figure 6.3: Change in the concentrations of vitisin A, malvidin-3-glucoside, pyruvic acid and malic acid post fermentation in wines where that were not inoculated with malolactic bacteria. The different concentrations of sulphur dioxide were 0 mg/L (○), 50 mg/L (□), 100 mg/L (◇), and 200 mg/L (△).

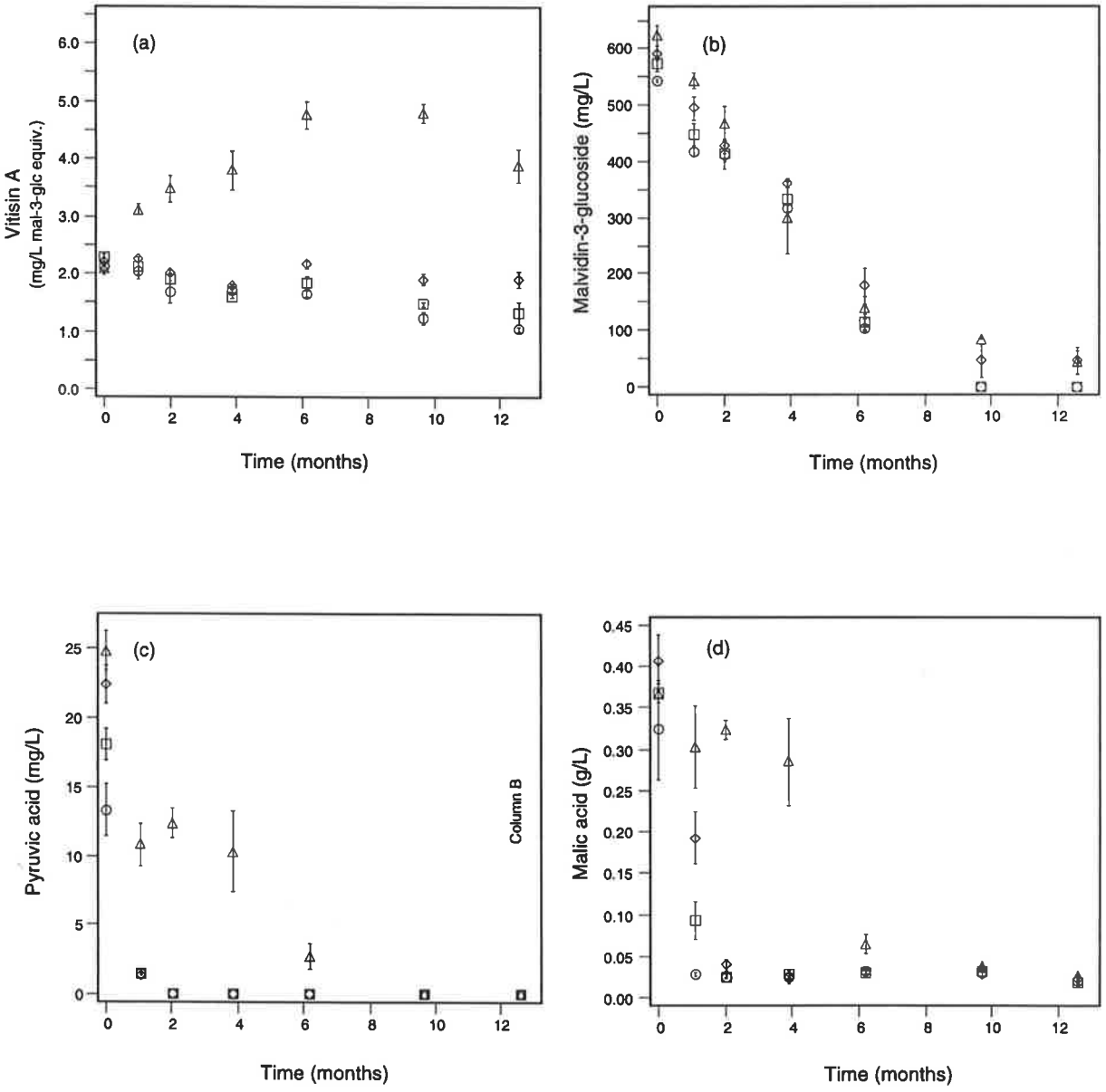

Figure 6.4: Change in the concentrations of vitisin A, malvidin-3-glucoside, pyruvic acid and malic acid post fermentation in wines where that were inoculated with malolactic bacteria. The different concentrations of sulphur dioxide were 0 mg/L (○), 50 mg/L (□), 100 mg/L (◇), and 200 mg/L (△).

Oxidative stability of vitisin A and its longevity in wine

The relative degradation of malvidin-3-glucoside and vitisin A in model wine solution under oxidative conditions is shown in Figure 6.5. The stability constants (rates of degradation) are recorded in Table 6.6. Malvidin-3-glucoside degradation rate is significantly greater than that of vitisin A under these conditions (Table 6.6).

Table 6.6: Rate of oxidative loss of pigments (± standard error) at 20°C in model wine solutions.

	Malvidin-3-glucoside	Vitisin A
k ($month^{-1}$)	0.808 (± 0.102)	0.016 (± 0.005)
$t_{1/2}$	25.8 days	50.0 months

In the series of wines spanning 40 years, malvidin-3-glucoside can be measured in wines up to 8 years old and vitisin A can be measured even after 41 years of maturation (Figure 6.6a, b). It is possible to estimate K values for these wines using Equation 2.29 (Table 6.7).

Table 6.7: Rate of loss of pigments (± standard error) from a series of wines obtained from a single vineyard.

	Malvidin-3-glucoside	Vitisin A
k ($year^{-1}$)	0.443 (± 0.057)	0.065 (± 0.007)
$t_{1/2}$	1.6 years	10.7 years

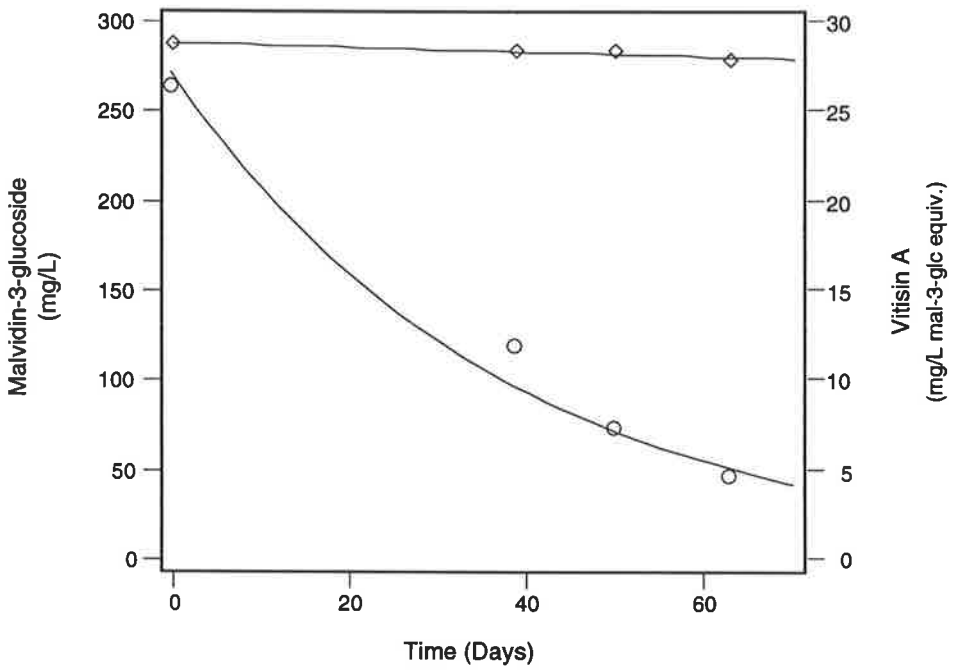

Figure 6.5: The relative degradation of malvidin-3-glucoside (○) and vitisin A (◇) in model wine solutions exposed to oxygen. Equation 2.43 was fitted to the data with coefficients of determination for malvidin-3-glucose and vitisin A of 0.7986 and 0.9990 respectively.

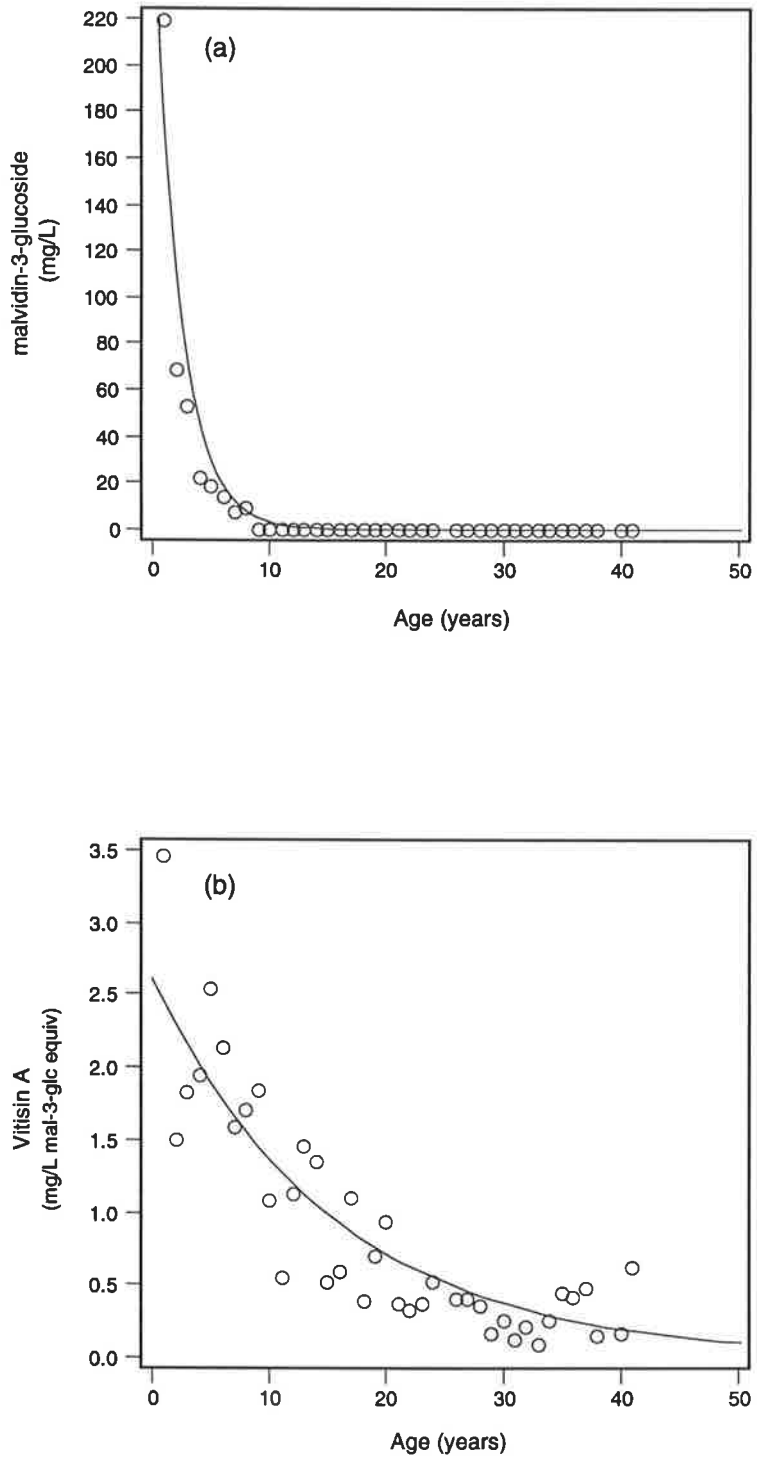

Figure 6.6: Concentration of malvidin-3-glucoside (a) and vitisin A (b) in a series of Shiraz wines obtained from a single vineyard. An first order kinetic curve (Equation 2.43) was fitted with coefficients of determination (r^2) for malvidin-3-glucoside and vitisin A of 0.939 and 0.7990 respectively.

Discussion

The synthesis of vitisin A during wine fermentation

Yeast are capable of obtaining energy for metabolism and growth from grape-derived glucose and fructose both aerobically and anaerobically. Glucose and fructose are degraded via glycolysis to yield pyruvate. Pyruvate is further catabolised to yield energy. The pyruvate degradation proceeds either aerobically or anaerobically. The aerobic pathway utilises the mitochondrial tri-carboxylic acid (TCA) cycle (Pronk *et al.*, 1994). The alternative pathway occurs under anaerobic and limited oxygen conditions, whereby the pyruvate is converted by a series of cytoplasmic enzymes into ethanol.

The final concentration of pyruvate in the wine depends on many factors including the efficiency of the enzymes involved in the glycolysis reaction in producing pyruvate, the efficiency of enzymes degrading pyruvate, the loss of pyruvate from the yeast cell, and the ability of the yeast cell to reabsorb or scavenge lost pyruvate. Enzyme regulation, especially down stream product regulation, and shortage of NAD are important in regulation of the glycolysis reaction, and therefore the pyruvate concentration in the cell. Using a synthetic medium, Michnick *et al.* (1997), noted that pyruvate accumulation occurred during the stationary phase of fermentation until approximately 50% of glucose was metabolised. After this initial accumulation, the pyruvate level may decline depending on the yeast strain.

Examination of the sugar usage as a measure of yeast activity shows an initial lag phase followed by a period of high metabolic activity (Figure 6.1d and 6.1e). During this early stage one would expect that the low pyruvate concentration in the ferment would limit vitisin A synthesis. However, following this lag phase, the rate of consumption of glucose and fructose increases, and there was an associated rapid production of pyruvic acid. During this stage the rate of synthesis of vitisin A was at its highest.

The correlations between the concentration of vitisin A, pyruvate, malvidin-3-glucoside and the relative concentration of glucose and fructose were all significant (Table 6.2). It is therefore not possible to predict that one factor was more important than another in the production of vitisin A. However, the modified logistic equation (Equation 2.40) gave an indication of the relative effects of the various factors in terms of maximum reaction rates. The greatest coincidence was that of the timing of the highest rate of vitisin A production (52.1 hours) and that of greatest glucose utilisation (54.9 hours). The maximum pyruvate release occurred 6.5 hours prior to the highest rate of vitisin A production. The highest rates of malvidin-3-glucoside extraction (14.7 hours) and fructose degradation (79.5 hours) were least related to that of the maximum rate of vitisin A production. It is therefore proposed that the malvidin-3-glucoside concentration in the fermenting wine was non-limiting for vitisin A synthesis.

After the initial phase of rapid pyruvic acid production, at approximately 80 hours after the initiation of fermentation, the concentration of pyruvic acid in the ferment declined. Associated with the decline in pyruvate concentration was a cessation in the increase in the vitisin A concentration. During the final stages of fermentation, the yeast metabolised the remaining sugar and probably utilised some of the free pyruvic acid. However, at the end of fermentation the pyruvate and malvidin-3-glucoside concentrations are still sufficient for synthesis of vitisin A, but the rates of formation observed were slow. The relatively high concentration of malvidin-3-glucoside and pyruvate, and the low rate of vitisin A synthesis suggests that there is another agent required for the formation of vitisin A. As noted in the previous chapter, the synthesis of vitisin A involves an oxidation reaction.

There is little recorded information regarding the concentration of oxygen in the must as it undergoes fermentation. An oxygen meter was used for the estimation of the apparent oxygen concentration during fermentation. The results indicate that the yeast depletes the oxygen concentration early during fermentation. The initial lag phase during fermentation is associated with the yeast becoming acclimatised to the must conditions. Oxygen is required by the yeast as it undergoes multiplication and acclimatisation (Pronk *et al.*, 1994). The concentration of oxygen remains low during fermentation due to the presence of a carbon dioxide gas cover. It is proposed that an increase in the apparent oxygen

concentration towards the end of fermentation is due to an influx of oxygen because the carbon dioxide production declines as the fermentation slows. When the oxygen concentration begins to increase towards the end of fermentation, or even after pressing, there is no rapid increase in vitisin A production even though the malvidin-3-glucoside and pyruvic acid levels are high (Figure 6.2). This suggests that oxygen is not the sole oxidative catalyst that promotes vitisin A production.

The fermentative stage of most interest is that which occurs between 40 and 120 hours when the apparent oxygen concentration reaches a maximum concentration and declines (Figure 6.2e). Most of the vitisin A production occurred between 40 and 120 hours and the maximum rate of formation was at approximately 77.8 hours. The oxidative processes occurring in this time requires further investigation.

Formation of vitisin A in wine during maturation

Somers (1980) proposed that reactions occurring during maturation were important to the second phase of wine colour development. The experiments described in the current work investigate vitisin A as a model for the formation of C4 compounds after fermentation. The experiments described above show that the precursors for the synthesis of vitisin A are present in relatively high concentrations at the end of fermentation. It is thought that the concentration of malvidin-3-glucoside declines after fermentation (Somers, 1980). However, little is known regarding the fate of either pyruvate or vitisin A after fermentation.

In the eleven wines examined from the 1997 vintage no statistically significant correlation between the concentrations of vitisin A and malvidin-3-glucoside could be found. However, a significant negative correlation between pyruvate and malvidin-3-glucoside existed (Table 6.4). This negative relationship may obscure the relative importance of either pyruvate or malvidin-3-glucoside to the synthesis of vitisin A during maturation.

Pyruvate forms an addition complex with the bisulphite ion, and pyruvate may therefore exist in either free or bound forms within the wine. It is proposed that this pool of bound pyruvate serves as a pool of pyruvate that can be released during maturation. This

pyruvate is then free to react with malvidin-3-glucoside to form vitisin A. However, there was no significant correlation in this study between the bound pyruvate and vitisin A concentrations (Table 6.4). The apparent equilibrium constant of pyruvate, (K_P) of 1.82 x 10^{-4} at pH 3.6 (Burroughs and Sparks, 1973b,c) is smaller than that of acetaldehyde (K_A = 1.45 x 10^{-6}; Burroughs and Sparks, 1973b,c) and malvidin-3-glucoside (K_M = 6 x 10^{-5}; Burroughs, 1975) which indicates that that sulphur dioxide is bound less tightly by pyruvate than by either acetaldehyde or malvidin-3-glucoside. Furthermore, the bound pyruvate and free pyruvate are expected to be readily interchangeable in a dynamic equilibrium. Thus, it can be proposed that the concentration of total pyruvate should be more important than free or bound.

The synthesis of vitisin A also requires an oxidant (Chapter 5). It was pointed out previously that the synthesis of vitisin A during fermentation was, at least in part, inhibited by an insufficient concentration of oxidants. The lack of suitable oxidants may also limit vitisin A production during maturation. Vitisin A and malvidin-3-glucoside have similar molar absorbance coefficients. It is therefore possible to express vitisin A as malvidin-3-glucoside equivalents and be confident that they would be of a similar concentration. If 1 mol of pyruvate can yield 1 mol of vitisin A, then 1 mg of pyruvic acid can yield in excess of 6 mg of vitisin A. Thus, in the eleven wines analysed from the 1997 vintage, the initial concentration of pyruvic acid was far in excess for the amount of vitisin A synthesised (Table 6.3). Furthermore, in all wines there was an excess of malvidin-3-glucoside required for the concentration of vitisin A synthesised during maturation (Table 6.3). There was, however, no correlation between the initial pyruvate concentration and the amount of vitisin A formed over the six month period (Table 6.3). This suggests that either the reaction of pyruvic acid and malvidin-3-glucoside is very slow, or another factor or catalyst was required for the reaction. It was therefore proposed that an oxidant was limiting for the formation of vitisin A after fermentation as well as during fermentation.

The eleven wines of the 1997 vintage investigated, showed a significant positive correlation between final vitisin A and initial vitisin A concentrations (Table 6.4). This suggests that either the processes occurring during fermentation are more important than

those after fermentation for the synthesis of vitisin A, or the factors limiting vitisin A synthesis during fermentation are still limiting vitisin A production after fermentation.

The addition of sulphur dioxide is one way by which the winemaker may influence fermentation. In the study that examined the wines made utilising different concentrations of sulphur dioxide whilst crushing the grapes, the initial pyruvic acid concentration was higher in the wines made with higher sulphur dioxide levels (Figure 6.3c; Figure 6.4c). The potential for vitisin A synthesis was greater with a higher pyruvic acid concentration. In this experiment the effect of malolactic fermentation was also examined. Malolactic bacteria were able to utilise the pyruvic acid and, as a consequence of malolactic bacteria activity, vitisin A production ceased (Figure 6.3; Figure 6.4). High concentrations of sulphur dioxide inhibited malolactic fermentation (Figure 6.3d; Figure 6.4d) and thereby increased the concentration of vitisin A in wine. Thus, sulphur dioxide can be used to increase the vitisin A concentration by increasing the initial concentration of pyruvate and by inhibiting malolactic bacteria that consume pyruvate.

After approximately 6 months of maturation, in the wines made without malolactic bacteria inoculation, the production of vitisin A ceases even though there was sufficient malvidin-3-glucoside and pyruvate for continued synthesis (Figure 6.3). This was especially noticeable in the wines made with the high initial sulphur dioxide concentrations of 100 mg/L and 200 mg/L. It has been described previously that during vitisin A synthesis oxidation is required. It was therefore proposed that in these wines the limiting factor for vitisin A synthesis was an insufficient concentration of suitable oxidants.

The final vitisin A concentration in wine is the end result of production and loss via degradation. The role of sulphur dioxide in relation to the concentration of vitisin A in an aged wine is complex. There is some evidence that sulphur dioxide acts as an anti-oxidant by prevent the degradation of vitisin A. In the experiment examining the role of sulphur dioxide in vitisin A formation, and where malolactic fermentation proceeded rapidly (ie, 0 mg/L, 50 mg/L and 100 mg/L SO_2; Figure 6.4), the loss of vitisin A was inhibited by higher sulphur dioxide levels. However, in a similar experiment, Bakker *et al.* (1998) were unable to show any effect of higher sulphur dioxide levels on vitisin A degradation.

By acting as an anti-oxidant, sulphur dioxide may inhibit vitisin A production. Dallas and Laureano (1994a) observed that sulphur dioxide can prevent the formation of C4-substituted pigments. However, in the presence of sulphur dioxide and absence of malo-lactic fermentation, the synthesis of vitisin A is actually higher with a greater concentration of sulphur dioxide when the two wines 100 mg/L is compared with 200 mg/L (Figure 6.3a). When these two wines are compared, Figure 6.3c indicates that sulphur dioxide increases the concentration of pyruvate in wine, and thereby shifting the equilibrium towards greater vitisin A synthesis. This data (Figure 6.3) also suggests that sulphur dioxide is not very effective in preventing certain oxidative type reactions such as the formation of vitisin A. Alternatively sulphur dioxide plays a positive role in providing a source of oxidants for vitisin A formation during maturation. It is well known that that sulphur dioxide binds with carbonyl compounds both present in the juice and formed during fermentation (Burroughs, 1981). These adducts pass into the wine, where through progressive break down, the carbonyl compounds are released. Some of these carbonyl containing compounds may act as oxidants and have a positive role in vitisin A formation.

Longevity of vitisin A in wine

The long term colour stability of wines depends on the stability of the pigments within the wine. Under normal storage conditions, it has been observed that vitisin A is more stable than malvidin-3-glucoside in wine with k values of 0.026 $month^{-1}$ for vitisin A and 0.104 $month^{-1}$ for malvidin-3-glucoside, or half lives ($t_{1/2}$) of 26.7 months and 6.7 months, respectively (Bakker *et al.*, 1998). The results presented in this chapter for model wine solutions confirm that vitisin A is more stable to oxidation than malvidin-3-glucoside wine with k values of 0.014 $month^{-1}$ for vitisin A and 0.808 $month^{-1}$ for malvidin-3-glucoside, or half lives ($t_{1/2}$) of 50 months and 28.5 days. The k value estimated in this study for vitisin A is similar to that reported by Bakker *et al.* (1998). However, the k value estimates suggest that malvidin-3-glucoside is somewhat less stable in the oxidative conditions of the model solutions than in wine.

The degradation of both vitisin A and malvidin-3-glucoside observed in this study and by Bakker *et al.* (1998) for wine and model solutions follows first order kinetics. The 40 year series of wines gave stability constant (k) estimates for malvidin-3-glucoside and vitisin A were 0.443 $year^{-1}$ and 0.065 $year^{-1}$ or half lives ($t_{1/2}$) of 1.6 years and 10.7 years respectively. The stability of vitisin A and malvidin-3-glucoside are far greater in these wines than in either the wines investigated by Bakker *et al.* (1998) or the model solutions used in this study. Thus, it is proposed that factors within wine matrix may either increase or decrease the stability of vitisin A and malvidin-3-glucoside. The nature of these factors require further investigation.

Chapter 7

Isolation of wine pigments

Introduction

Various authors have proposed an extensive range of pigments that occur in wine (Chapter 1). The exact identity of many of the pigments in wines remains unknown, one of the problems being that they are difficult to isolate. Many of these wine pigments are resistant bleaching by the bisulphite ion (Somers, 1971). The resistance of anthocyanins to bisulphite bleaching indicates that these compounds are C4-substituted, ie, they cannot form the anthocyanin-bisulphite addition product (Timberlake and Bridle, 1968) This chapter discusses development of methods for the separation of pigments according to their resistance to the addition of the bisulphite ion.

The ionisation and hydration constants of C4-substituted pigments may be estimated using vitisin A as a model compound. However, vitisin A contains a carboxylic acid group. It is thought that most C4-substituted pigments do not have a carboxylate group and therefore the pKa value at approximately 3.6 will be absent in most C4-substituted pigments. The carboxylic acid group may also influence the hydration constants. It is therefore proposed that all bisulphite resistant pigments without carboxyl groups are cationic at very low pH (<0.5) or neutral at low pH (1.5 - 4.5). In contrast, grape anthocyanins in the presence of bisulphite form sulphonic acids, whilst, substituted pigments, do not. Sulphonic acids are strong acids, and therefore it is proposed that anthocyanin bisulphite addition products are anionic except at extremely low pH values. Thus, because of the charge difference between the anthocyanin bisulphite addition products and the C4-substituted pigments, separation of these two groups of compounds is possible using molecular charge.

To develop methods for the purification of anthocyanins, the properties of the bisulphite-addition products required further investigation. This required the study of both the charge state and pH stability of the bisulphite-addition products. With this information, a technique for the isolation of pigments using ion exchange was developed.

Results

HVPE

Using HVPE, the anthocyanins in grape extracts and wine were separated in a bisulphite buffer. The chromatograms were fumed with concentrated hydrochloric acid to disrupt the colourless bisulphite-addition product to reveal the coloured pigments. The chromatograms were then observed under UV light (254 nm) where the monomeric anthocyanins exhibited fluorescence. This makes the monomeric anthocyanins easily discernible from other pigments (Figure 7.1). These anthocyanins, as their bisulphite-addition products were anionic at pH 4.2 in the metabisulphite buffer. There was clear separation of the anthocyanins into two bands. The mass spectroscopic analysis combined with HPLC identification using UV-visible diode array reveals that the faster band, Rm_{OG} = 0.39, consists primarily of malvidin-3-glucoside and malvidin-3-*(*acetyl)glucoside, while the slower band Rm_{OG} = 0.34 represents the malvidin-3-*(p*-coumaryl) glucoside. It was not possible to get further separation of the malvidin-3-glucoside and malvidin-3-*(*acetyl)glucoside under these conditions.

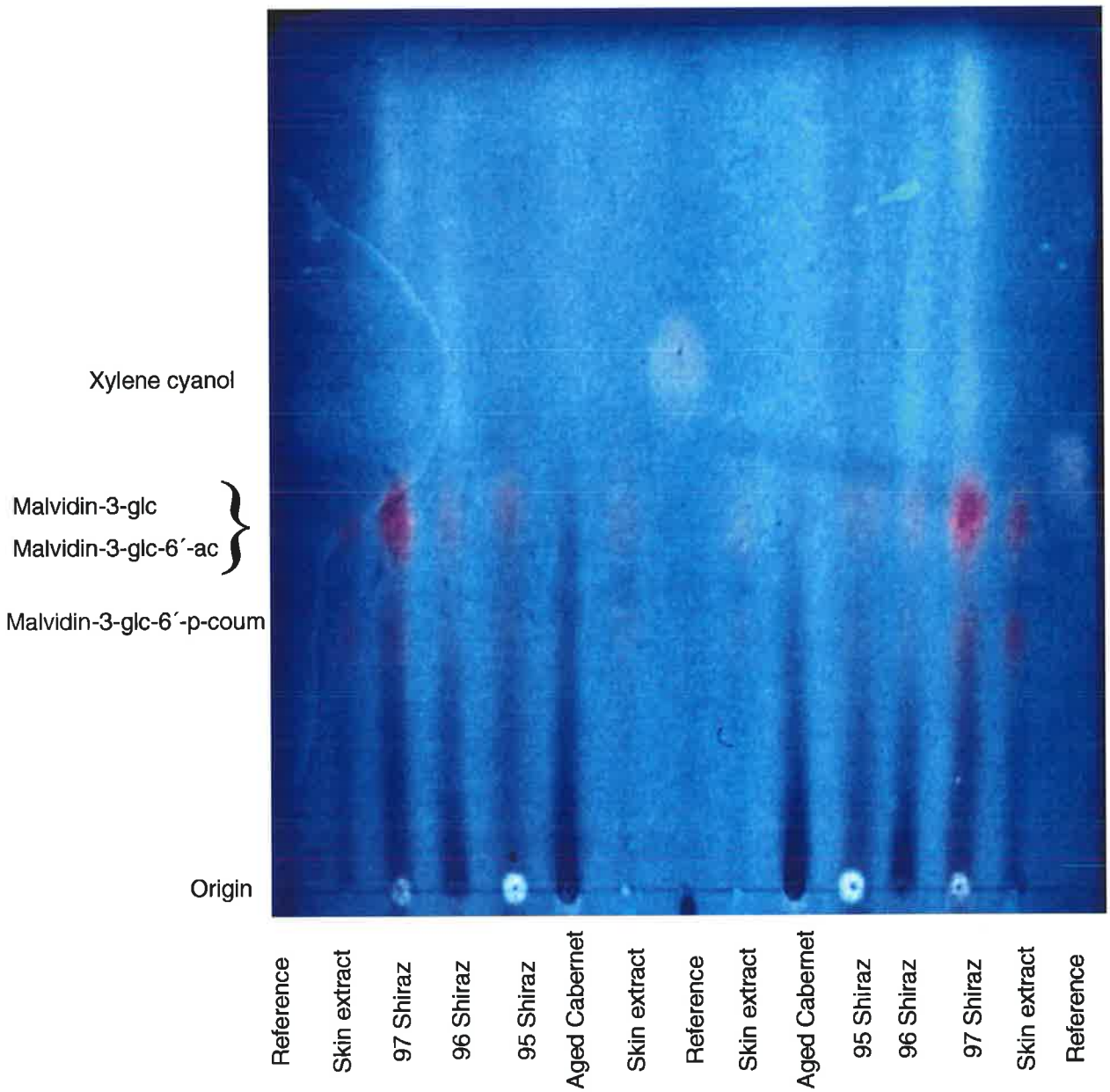

Figure 7.1: High voltage paper electrophoretogram of grape skin extract and wine samples. Xylene cyanol is an anionic standard with a relative mobility (Rm_{OG}) of 0.54. (The photo was taken under UV light at 254 nm).

pH stability of the bisulphite-addition complex

The pH stability of the bisulphite-addition product was measured spectrophotometrically (Figure 7.2). The bisulphite addition product is colourless and in bisulphite solution the anthocyanins remains colourless at pH values where the bisulphite addition product is stable. The two analytical wavelengths used were 520 nm for low pH and 618 nm for high pH. The pH stability of the bisulphite complex was increased with increasing concentrations of bisulphite under both acid and alkaline conditions (Figure 7.2). Thus, the optimum pH stability was achieved under high bisulphite concentrations. At a concentration of 100 mmol dm^{-3} potassium metabisulphite, the bisulphite-addition product was stable between pH 2 and pH 8 while at the lower concentration of 1 mmol dm^{-3} potassium metabisulphite, the bisulphite addition complex was stable between pH 3 and pH 7.

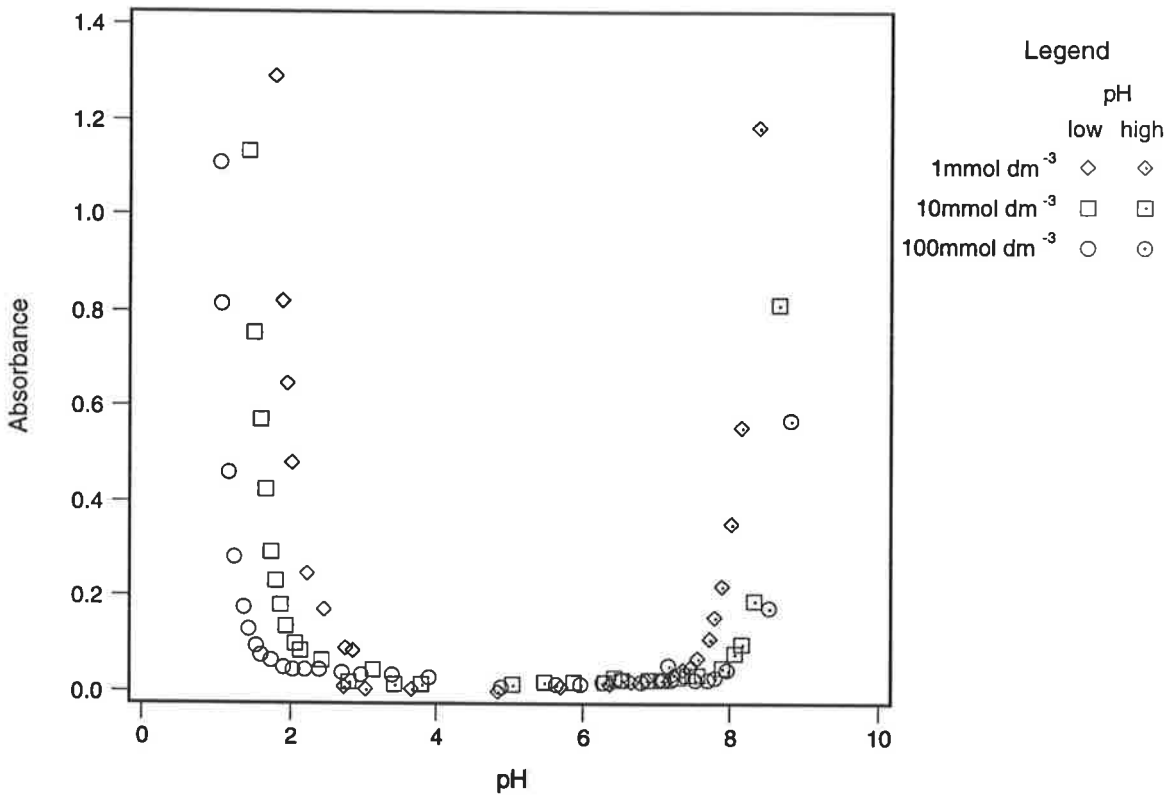

Figure 7.2: Absorbance of malvidin-3-glucoside bisulphite addition product as a function of pH with various concentrations of potassium metabisulphite. When stable, the bisulphite addition product is colourless (ie, the absorbance equals zero) and at excessively low or high pH values the bisulphite addition product is disrupted and a coloured product is observed. The absorbance at low pH was measured at 520 nm and high pH at 618 nm. (See legend for explanation of symbols.)

Bisulphite-addition product formation as a means of purification of wine pigments

The separation of pigments from both wine and grape marc extracts using cation exchange in the presence of a bisulphite buffer yielded crude extracts containing C4-substituted pigments. These pigment extracts were not purified further but investigated directly using HPLC and mass spectrometry. The HPLC chromatograms of the samples measured at both 520 and 280 nm indicated that the pigment samples were free of phenolic contaminants.

Using mass spectrometry, a number of pigments were identified in both the grape marc and wine samples (Table 7.1). The grape marc samples were injected into the mass spectrometer via a desalting column. The mass spectrum of this injection for this sample is shown in Figure 7.3. The mass spectrum contains pigment A as well as (*p*-coumaryl)vitisin A. Furthermore, it is proposed that the pigments with the masses of m/z 805.4, 847.4, 951.4, 1093.4, 1135.4, 1239.6, 1381.6, 1423.4, 1527.6, and 1669.4 belong to the group of oligomeric pigments whereby an anthocyanin linked in the C4 position via a vinyl linkage to either a catechin or procyanidin (Francia-Aricha *et al.,* 1997). No attempt was made to quantify any of these pigments.

Compared with the grape marc sample, the wine lacked a number of large mass oligomeric pigments (Table 7.1). Furthermore, the wine sample contained some smaller pigments not evident in the grape marc sample.

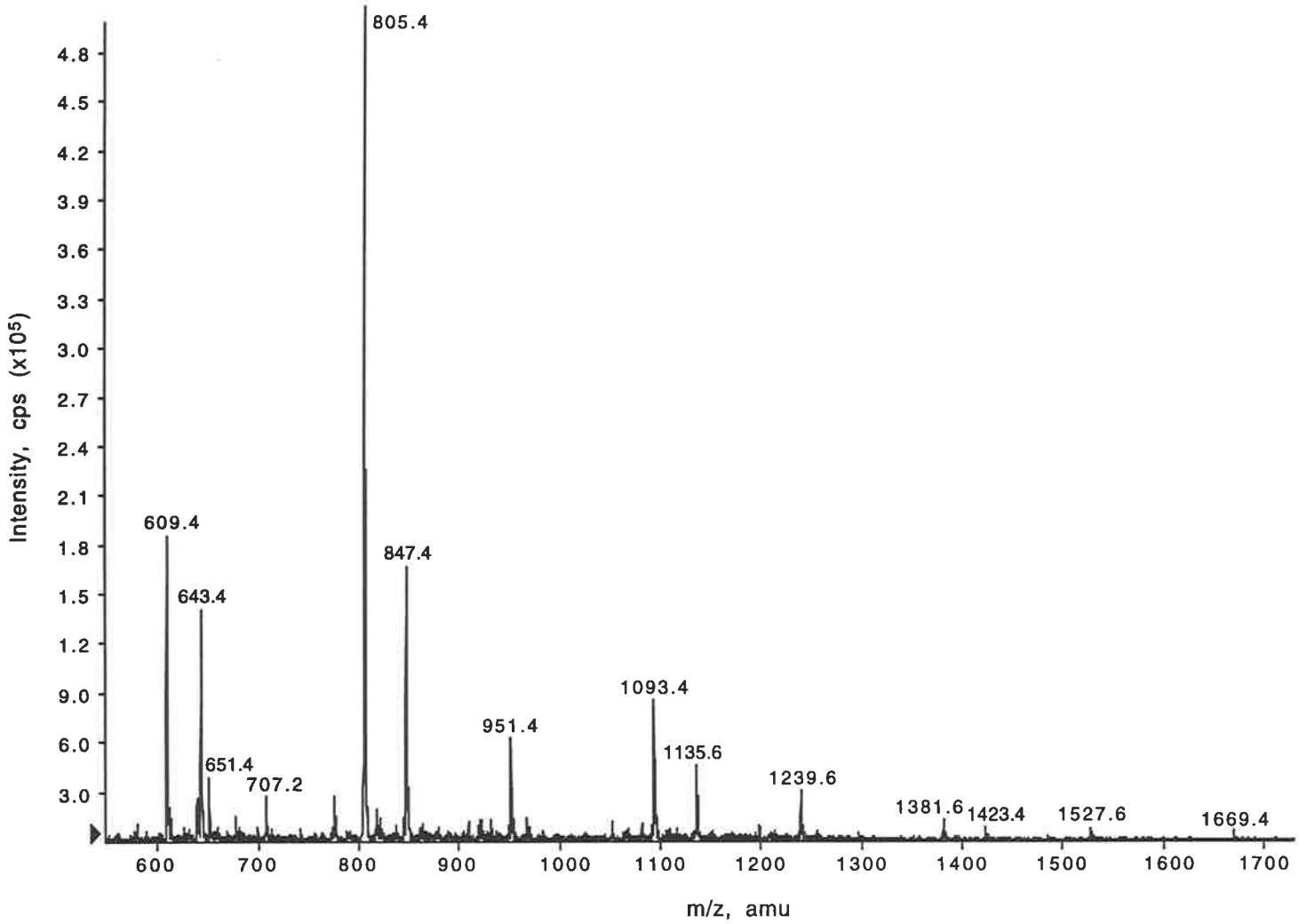

Figure 7.3: The direct injection ion spray mass spectrum of the coloured fraction isolated from grape marc (See Table 7.1)

Table 7.1: Mass of pigments isolated from grape marc and wine accompanied by the proposed pigment that each mass represents (Note, catechin represents either catechin or epicatechin)

Marc (m/z)	Wine (m/z)	Compound
609.4	609.4	pigment A
-	639.4	3''-*O*-methyl- pigment A
651.4	651.4	(acetyl)pigment A
-	855.6	(*p*-coumaryl)pigment A
707.2	707.2	(*p*-coumaryl)vitisin A
805.4	805.4	malvidin-3-glucose-4-vinyl-catechin
847.4	-	malvidin-3-(acetyl)glucose-4-vinyl-catechin
951.4	951.4	malvidin-3-(*p*-coumaryl)glucose-4-vinyl-catechin
1093.4	1093.4	malvidin-3-glucose-4-vinyl-catechin-catechin
1135.4	-	malvidin-3-(acetyl)glucose-4-vinyl-catechin-catechin
1239.6	-	malvidin-3-(*p*-coumaryl)glucose-4-vinyl-catechin-catechin
1381.6	-	malvidin-3-glucose-4-vinyl-catechin-catechin-catechin
1423.4	-	malvidin-3-(acetyl)glucose-4-vinyl-catechin-catechin-catechin
1527.6	-	malvidin-3-(*p*-coumaryl)glucose-4-vinyl-catechin-catechin-catechin
1669.4	-	malvidin-3-glucose-4-vinyl-catechin-catechin-catechin-catechin

The grape marc sample was also analysed using LC/MS (Figure 7.4 and Figure 7.5). The mass spectra taken from the LC/MS (Figure 7.4) show that the peaks A and C with different retention times have an identical parent ion with a mass of m/z 805 (Figure 7.5). Therefore, it is proposed peaks A and C represent two isomers of the same compound, ie, malvidin-3-glucose-4-vinyl-catechin and malvidin-3-glucose-4-vinyl-epicatechin. Similarly, LC/MS peaks B and D (Figure 7.4) have an identical parent ion with a mass of m/z 847 (Figure 7.5). It is proposed that peaks B and D represent malvidin-3-(acetyl)glucose-4-vinyl-catechin and malvidin-3-(acetyl)glucose-4-vinyl-epicatechin. The identity of the compound represented by peak E was unknown. Peak F (Figure 7.4) contains a fragment with m/z of 609 (Figure 7.5) and therefore it is proposed that this peak represents pigment A.

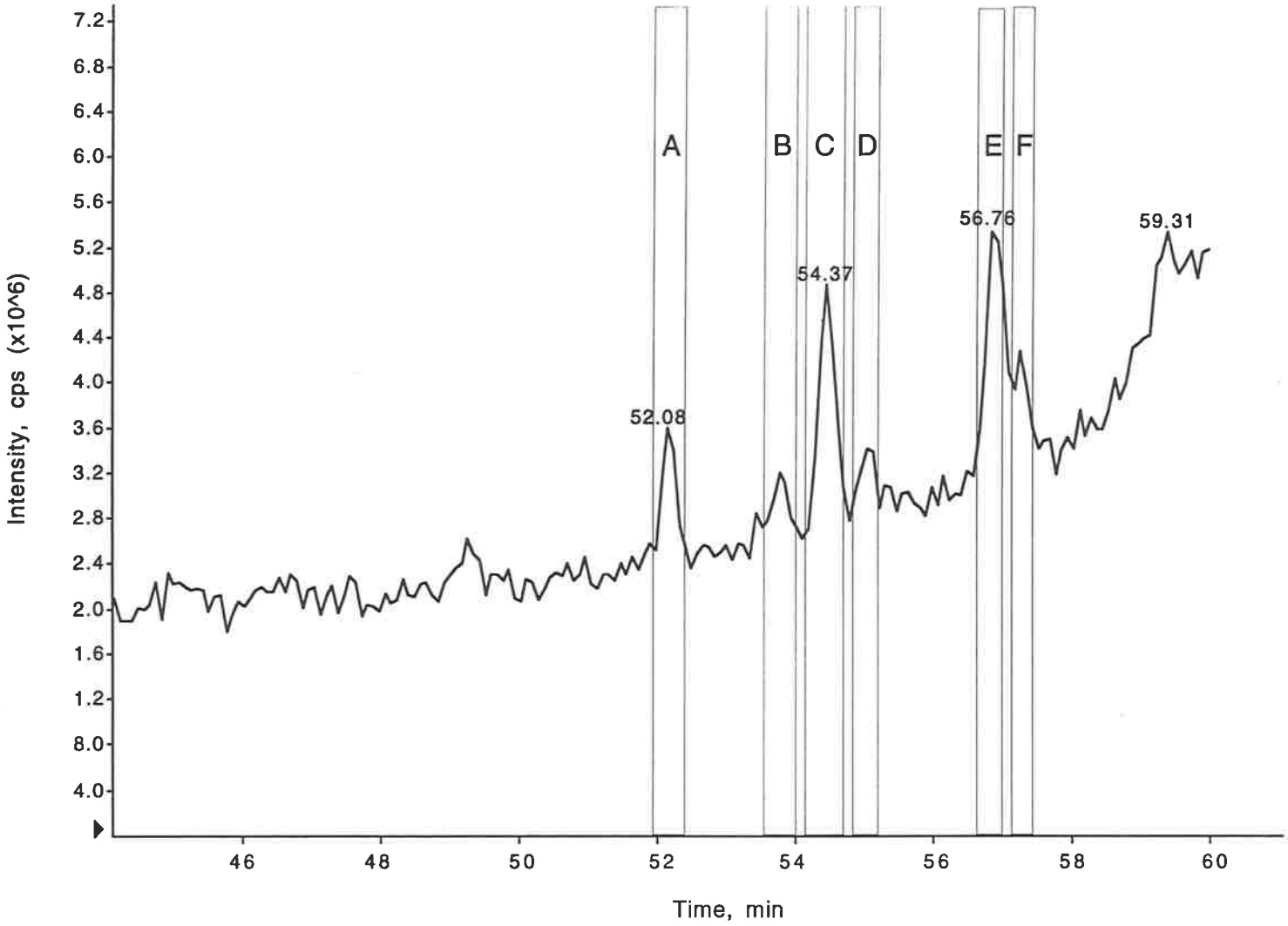

Figure 7.4: The LC/MS of the grape marc sample indicating the peaks of interest. The mass spectra of each of the marked peaks are represented in Figure 7.5

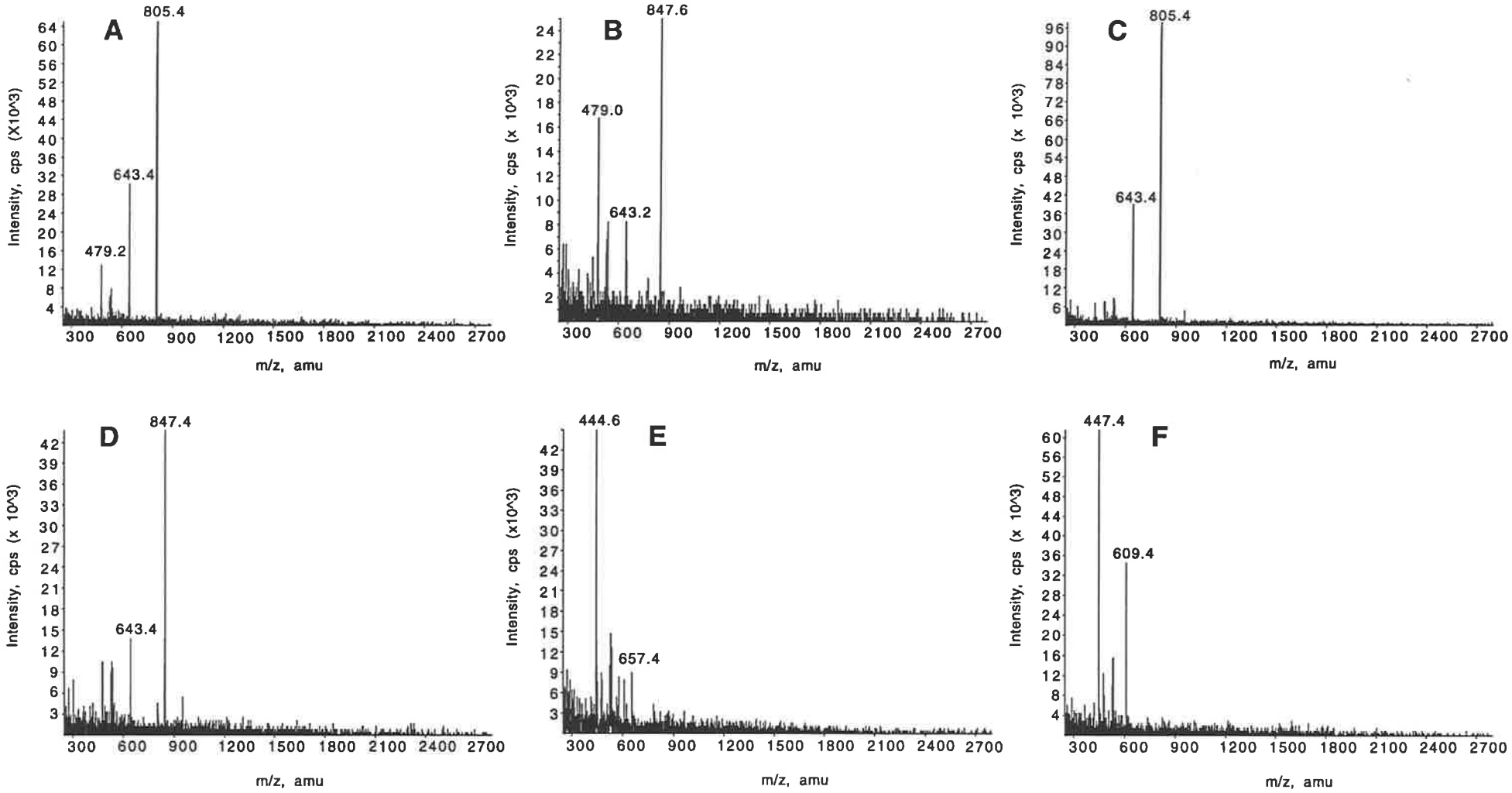

Figure 7.5: Mass spectra taken from the LC/MS (Figure 7.4). (A) and (C) have an identical parent mass of 805 m/z and it is proposed that these mass spectra identify the presence of two isomers of malvidin-3-glucose-4-vinyl-catechin. Similarly, (B) and (D) have an identical parent mass of 847 m/z and it is proposed that these mass spectra identify the presence of two isomers of malvidin-3-(acetyl)glucose-4-vinyl-catechin. (E) represents an unidentified compound. (F) contains a mass of 609 m/z and it proposed that this spectrum represents pigment A.

Discussion

Properties of the anthocyanin bisulphite addition product

The HVPE results confirm that at pH 4.2 the anthocyanin bisulphite addition complex has a negative charge associated with it, ie, the bisulphite addition product is anionic (Figure 7.6). Although HVPE could not separate malvidin-3-glucoside and malvidin-3-acetyl glucoside, these compounds could be separated from malvidin-3-(*p*-coumaryl)glucoside. The separation of the anthocyanins to give clearly identifiable products suggests that HVPE has the potential to be developed for use as a method for the isolation and identification of anthocyanins. This method is currently being investigated for identification of anthocyanins from plant material.

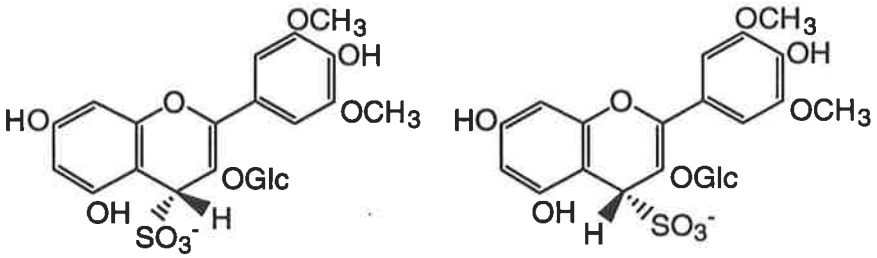

Figure 7.6: Two stereoisomers of the bisulphite addition product at pH 4.2

A suitable pH for stability of the bisulphite addition complex is between pH 3 and pH 7. However, the results presented here clearly show that the concentration of bisulphite influences the pH equilibrium. The pKa of sulphurous acid (aqueous SO_2) and the bisulphite ion HSO_3^- is 1.77 (Schmidt and Siebert, 1975). The disruption of the bisulphite addition complex occurs at a pH of approximately 2 and below (Figure 7.2). It is therefore proposed that at low pH, there is a competition between the anthocyanin cation and the hydrogen cation to bond to the bisulphite ion.

$$ASO_3^- + H^+ \rightleftharpoons HSO_3^- + AH^+$$ (Equation 7.1)

Under acid conditions a higher bisulphite concentration prevents the dissociation of the bisulphite addition product (ie, by forcing the equilibrium, Equation 7.1, towards the left).

There are two equilibria that should be considered when studying the stability of the bisulphite addition product under alkaline conditions. The equilibrium between the bisulphite (HSO_3^-) and sulphite (SO_3^{2-}) ions in solution has a pKa 7.21 (Schmidt and Siebert, 1975). The pKa of malvidin-3-glucoside of interest in alkaline solutions is pKa_3, (8.31), where the quinonoidal anion A^- and quinonoidal dianion A^{2-} are in equilibrium. The dissociation of the bisulphite addition product occurs at approximately pH 8 (Figure 7.2). It is therefore proposed that the bisulphite anthocyanin addition product is in equilibrium with the sulphite ion and the malvidin-3-glucoside dianion.

$$ASO_3^- + 3OH^- \rightleftharpoons A^{2-} + 3H_2O + SO_3^{2-}$$ (Equation 7.2)

The higher the concentration of bisulphite the greater concentration of the sulphite ion and the more stable the bisulphite addition product (ie forces the Equation 7.2 to the left).

Under aqueous conditions between pH 3 and pH 7 (Figure 7.2) where the bisulphite addition complex is stable, malvidin-3-glucoside is predominantly in its non-charged quinonoidal state. Thus, the addition of bisulphite ion (HSO_3^-) to the anthocyanin neutral base (A) is represented by the following equation,

$$A + HSO_3^- \rightleftharpoons ASO_3^-$$ (Equation 7.3)

In a similar pH range in aqueous solutions, the quinonoidal base of malvidin-3-glucoside undergoes hydration reactions to form a colourless hemi-ketal.

$$A + H_2O \rightleftharpoons AOH$$ (Equation 7.4)

The binding constant for the bisulphite and malvidin-3-glucoside is 1.2 x 10^{-4} at pH 4.0 (Burroughs, 1975) and this indicates that bisulphite is not strongly bound to the anthocyanin. It can therefore be concluded that there is a competitive process between water and the bisulphite ion (Brouillard and Hage-Chahine, 1980) for the anthocyanin as illustrated in Equation 7.5.

$$AOH + HSO_3^- \rightleftharpoons ASO_3^- + H_2O$$ (Equation 7.5)

In aqueous solutions, minimum concentrations of the bisulphite ion are required to maintain the anthocyanin-bisulphite complex. Thus, the separation on the basis of charge of the anthocyanin bisulphite addition products from C4-substituted anthocyanins can only be carried out in the presence of a bisulphite buffer. This is an important factor for the development of methods for the separation of anthocyanins based on the charge of the bisulphite addition product, such as anion exchange chromatography.

Isolation of wine pigments using bisulphite

A series of pigments were isolated from wine and grape marc. From the mass spectra a number of smaller pigments were identified, including, *p*-coumaryl-vitisin A, pigment A (Figure 7.7a), and acetyl-pigment A, and *p*-coumaryl-pigment A. Another pigment with a m/z of 30 greater than pigment A was also observed. A m/z of 30 represents an *O*-methyl group. Para-vinylguaiacol has been identified in wine (Rapp and Mandery, 1986) and originates from the degradation of ferulic acid, a naturally occurring compound in grapes, by an identical process to the degradation of *p*-coumaric acid (Steinke and Paulson, 1964) as described in Chapter 1. It is therefore proposed that the new compound was 3"-*O*-methyl-pigment A (Figure 7.7b) resulting from the reaction of *p*-vinylguaiacol and malvidin-3-glucoside by a similar mechanism to that leading to the formation of pigment A.

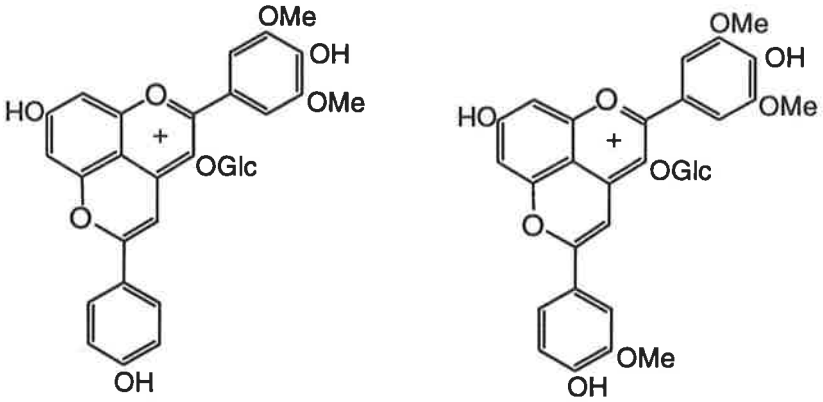

Figure 7.7: Two simple pigments isolated from wine, (7.7a) pigment A as described by Fulcrand *et al.* (1996) and (7.7b) 3"-*O*-methyl-pigment A.

A number of pigments were also identified in both the wine and marc samples. It is proposed that the pigments with the masses of *m/z* 805.4, 847.4, 951.4, 1093.4, 1135.4, 1239.6, 1381.6, 1423.4, 1527.6, and 1669.4, belong to the group of pigments described by Francia-Aricha *et al.* (1997), whereby an anthocyanin linked in the C4 position via a vinyl linkage to either a catechin or procyanidin (Figure 7.8d). As these pigments are built up from a few flavonoid molecules they can be described as oligomeric. The LC/MS of this sample clearly showed that there are two isomers of each of the 805.4 and 847.4 *m/z* compounds. It is proposed that these isomers represent the catechin and epicatechin isomers of malvidin-3-glucose-vinyl-catechin and malvidin-3-(acetyl)glucoside-vinyl-catechin respectively.

All of the pigments identified were C4-substituted and similar in structure to vitisin A. This method for pigment extraction is designed for the isolation of C4-substituted pigments, and any pigment that can form bisulphite-addition products will not be isolated by this method. For example pigments with an interflavan linkage to the C6 or C8 positions of the anthocyanin such as malvidin-3-glucoside-8-catechin (Figure 7.8b; mass MH^+ = m/z 781; Remy *et al.*, 2000) or polymeric pigments with an acetaldehyde bridge (Figure 7.8c; Timberlake and Bridle, 1967b) such as the catechin-ethyl-malvidin-3-glucoside (mass MH^+

= *m/z* 809; Bakker *et al.* 1993) have a non-substituted C4 carbon. It is therefore proposed that these pigments can form bisulphite addition products. Different techniques need to be developed for the study of these compounds, and to determine their relevance to the colour of wine.

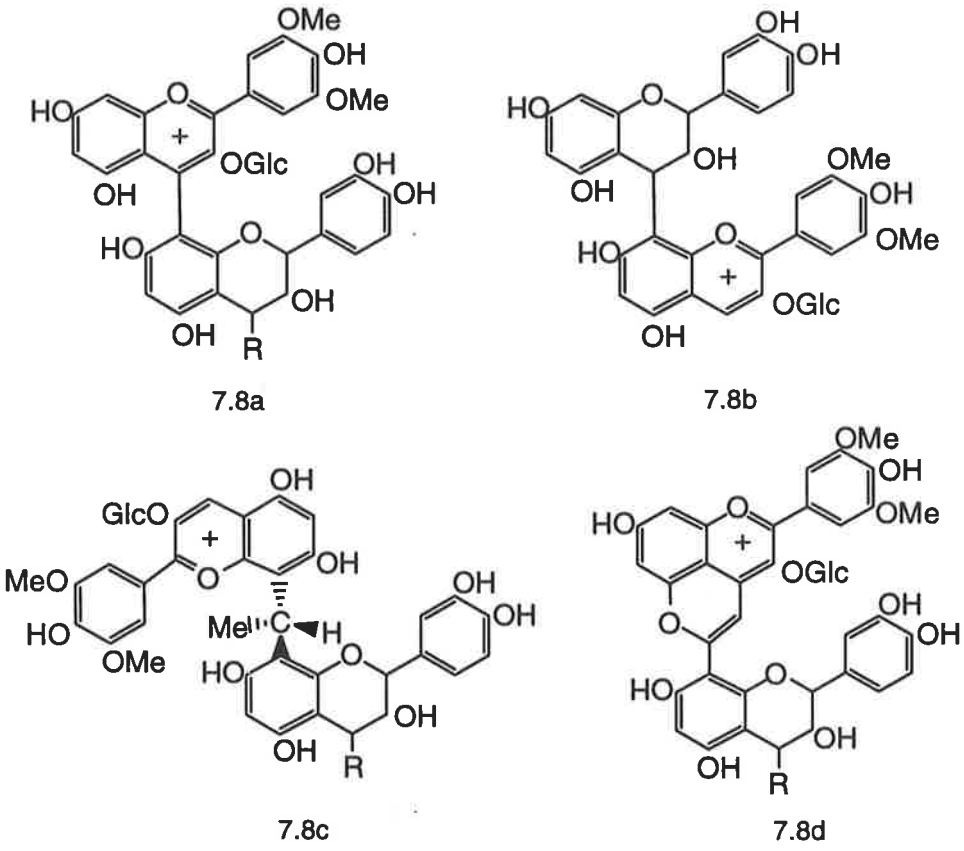

Figure 7.8: Four different types of pigments resulting from the polymerisation of malvidin-3-glucoside and catechin or procyanidin; (7.8a) interflavan linked as proposed by Somers (1971), (7.8b) interflavan linked as proposed by Remy *et al.*, (2000), (7.8c) ethyl linked as proposed by Timberlake and Bridle (1967b) and (7.8d) vinyl linked as proposed by Francia-Aricha *et al.* (1997).

It is interesting to note that none of the interflavan linked C4-substituted polymeric pigments (Figure 7.8a) as proposed by Somers (1971) were identified in either the grape marc extract or wine in this study. This does not prove their non-existence but it suggests that in this case their concentration within the samples examined is very low.

The mechanism for the separation of the various pigments using the sulphoxyethyl cellulose column is not fully understood. Malvidin-3-glucoside, malvidin-3-(*p*-coumaryl)-glucoside and vitisin A are all reasonably strong acids with pKa_1 values of 1.76, 0.94 and 0.95 respectively. Malvidin-3-glucoside and malvidin-3-(*p*-coumaryl)glucoside were absorbed to the sulphoxyethyl cellulose and yet vitisin A was not (Chapter 5). Furthermore, the *p*-coumaryl vitisin A was retained on the sulphoxyethyl cellulose column (Table 7.1) while the vitisin A was not. It is therefore proposed that the difference in retention is due to a difference in hydrophobicity rather than charge. The addition of the bisulphite ion to malvidin-3-glucoside not only alters the charge characteristic of this compound but also changes its solubility and the ability of the anthocyanin to engage in hydrophobic bonding. The cationic or hydrophobic material retained on the column was removed using sodium chloride and the use of acid was deliberately avoided. However the material retained on the column generally exhibited high hydrophobicity in the sodium chloride solution and therefore 50% methanol was a requirement.

There are differences in the types of pigments in grape marc and in wine samples (Table 7.1). These results suggest that while the smaller pigments remain in the wine, the larger pigments are lost into the marc portion. It is known that the physico-chemical adsorption of anthocyanins to yeast cell walls is an important mechanism for the loss of anthocyanins during fermentation (Vasserot *et al.,* 1997). Furthermore, the cell wall matrix of the grape skins may adsorb these larger pigments in a similar fashion to the absorption of pigments to the cellolose of the chromatographic paper during HVPE. Thus, the larger pigments exhibit greater interaction with yeast proteins and grape skins and thereby are lost from the wine.

This study positively identified a number of simple and oligomeric pigments in wine. Any future studies on wine pigments should include these pigments but to do this samples of pure pigments are required. The techniques developed in this study, utilising a bisulphite buffer solution in conjunction with ion exchange, will enable these pigments to be isolated from either wine or grape marc extracts.

Chapter 8

General discussion and directions for future research

Introduction

The red colour of wine depends on the anthocyanin and anthocyanin derived pigments. Malvidin-3-glucoside is the main anthocyanin found in wines made from *Vitis vinifera* cv. Shiraz. The other major red wine pigments are derived from malvidin-3-glucoside. There are three main pigments isolated from *Vitis vinifera* cv. Shiraz grape skins. These were malvidin-3-glucoside, and its acetylated derivatives, malvidin-3-(acetyl)glucoside and malvidin-3-(*p*-coumaryl) glucoside. The wine fermentation and maturation process increased the diversity of red pigments, such that these pigments can be divided into three main categories; grape derived anthocyanins, simple and oligomeric wine pigments.

Grape derived anthocyanins

An understanding of malvidin-3-glucoside and of factors that influence its colour is essential to the study of wine pigment chemistry. With an understanding of the chemistry influencing the colour of malvidin-3-glucoside it is then possible to examine the effect of substitution groups on this molecule and thus consider all the pigments derived from malvidin-3-glucoside. The effects of solvents, pH, molecular substitutions and sulphur dioxide are all considered in this thesis. These are, however, not the only factors that may influence the colour of malvidin-3-glucoside. For example, another field receiving considerable attention by other researchers research is co-pigmentation (Mazza and Brouillard, 1990; Goto and Kondo, 1991; Mistry, *et al.*, 1991; Liao *et al.*, 1992).

One of the most important findings described in this thesis was the revision of the protonation constants as described in Chapter 3. The previous method used for the calculation of pKa values entails the use of temperature jump experiments (Brouillard and Delaporte, 1977). This research was performed without a knowledge of the charge state of the anthocyanins at which the pH was measured, nor was the spectrum of the quinonoidal base known correctly. The previous estimate for the pKa_1 of 4.25, indicated an important role for the flavylium ion at wine pH (3.2 - 3.8). However, the revised estimate for the pKa_1

of 1.76 (Chapter 3) suggests that in red wine, the concentration of the flavylium ion is negligible.

From the studies in Chapter 3 it is now proposed that at wine pH (3.2 - 3.8), malvidin-3-glucoside has a neutral charge and therefore the colour of red wine may be attributed to the quinonoidal base. It was not possible to obtain the UV-visible spectrum of the neutral malvidin-3-glucoside quinonone in aqueous solution in this study. While it is important to obtain the spectrum of the malvidin-3-glucoside quinonoidal base, it is proposed that the spectrum of the malvidin-3-(*p*-coumaryl)glucoside quinonoidal base in aqueous solution (Figure 4.5) can serve as an approximation. This spectrum of the quinonoidal base, and the revised pKa values provides an opportunity for recalculating the kinetics for the formation of the various states of malvidin-3-glucoside.

At low concentrations of malvidin-3-glucoside and malvidin-3-(*p*-coumaryl)glucoside at wine pH of 3.2 to 3.8, the hemiketal and chalcone are dominant, and therefore these solutions are essentially colourless (Table 8.1). It is therefore possible to propose that the colour of wine, especially young wine where the grape derived anthocyanins predominate, is the result of the equilibrium of the quinonoidal base with the hemiketal and chalcone species.

Table 8.1: Effect of group substitution on the apparent pKa_1, pK_{H1} and pK_{H2} values of malvidin-3-glucoside.

	pKa_1	pK_{H1}	pK_{H2}
Malvidin-3-glucoside	1.76	2.66	5.90
Malvidin-3-(*p*-coumaryl) glucoside	0.94	3.01	5.90
Vitisin A	0.97	4.37	7.58

From this study it is now known that the quinonoidal base/hemiketal/chalcone equilibrium can be influenced by solvent effects such as the addition of ethanol (Chapter 3 and 4). Furthermore, the presence of *p*-coumaric acid acylation can promote the quinonoidal base in preference to both the flavylium ion and the hemiketal/chalcone (Table 8.1). This is especially noticeable when the species distribution diagrams of malvidin-3-glucoside and malvidin-3-(*p*-coumaryl)glucoside are compared (Figure 3.8 and 4.8). The effect of the *p*-

coumaric acid in stabilising the quinonoidal base is a clear demonstration of intramolecular co-pigmentation. The effects of intramolecular co-pigmentation, intermolecular co-pigmentation and self association are thought to be similar (Chapter 1). Thus, it is proposed that that the effects of self association and intermolecular co-pigmentation may be interpreted as an alteration of the equilibrium between the quinonoidal base and the hemiketal/chalcone. This requires further investigation.

The work described in this thesis also examined the effect of pH on malvidin-3-glucoside and malvidin-3-(*p*-coumaryl)glucoside beyond the pH range of wine. Previous to this study, the second pK_H value of malvidin-3-glucoside and malvidin-3-(*p*-coumaryl)glucoside had not been described and moreover no second pK_H values for any anthocyanins had been published. Furthermore, the correct spectra for the quinonoidal anions, A^- and A^{2-}, of malvidin-3-glucoside and malvidin-3-(*p*-coumaryl)glucoside were unknown due to the incorrect charge allocation of these species. This extra data supports the proposal that the quinonoidal base is important to the colour of wine.

The apparent pKa and pK_H estimates for malvidin-3-glucoside can be used as a model compound for the calculation of protonation and hydration constants for other anthocyanins by using methods presented by Perrin *et al.* (1981). Therefore, this research is not only relevant to malvidin-3-glucoside, but also to a large number of other simple anthocyanins. Furthermore, the pKa and pK_H estimates for malvidin-3-(*p*-coumaryl)glucoside and vitisin A can be used to estimate the effects of acylation by a cinnamic acid or the effects of C4-substitution. Certainly it is now possible to reassess previous studies on anthocyanins. This is, however, beyond the focus of this thesis.

It is proposed that future research into grape anthocyanins should consider attempt to measure the spectrum of the malvidin-3-glucoside quinonoidal base and confirm that this spectrum is similar to that of the malvidin-3-(*p*-coumaryl) glucoside quinonoidal base. The spectral data and the new pKa estimates obtained in this thesis may be used to re-examine the reaction mechanisms and reaction kinetic data involving anthocyanins. Furthermore, the effect of co-pigmentation needs to be re-investigated with regard to these pKa estimates.

Simple and oligomeric wine pigments

Timberlake and Bridle (1968) described that C4-substituted anthocyanins are resistant to both hydration and bisulphite addition and this lead to the proposal by Somers (1971) that C4-substituted anthocyanins may constitute a pool of stable pigments within wine. There is however little experimental evidence for the presence of the pigments as proposed by Somers (1971) in wine. Thus, the identification of C4-substituted pigments is important for the understanding of the long term stability of wine colour.

The most easily identifiable of these C4-substituted pigments, is vitisin A. Vitisin A is an pigment in wine that is the result of the addition of pyruvic acid to the C4 position of malvidin-3-glucoside. Contrary to the results of previous authors (Bakker *et al.*, 1997; Bakker and Timberlake, 1997; Cheynier *et al.*, 1997a; Fulcrand *et al.*, 1998), a single structure may be used to describe vitisin A. The evidence in Chapter 5 indicates that this compound is not a 4 ringed pigment at wine pH (3.2 - 3.8) as was previously proposed by Bakker *et al.* (1997), Bakker and Timberlake (1997) and Fulcrand *et al.*, (1998). Vitisin A is a three ringed malvidin-3-glucose-4-α,β-vinyl-β-hydroxy-β-R type anthocyanin where R is a carboxylic acid.

In addition to vitisin A and its acetyl and *p*-coumaryl derivatives, a number of C4-substituted pigments were recognised in both wine and gape marc extracts (Chapter 7). These pigments could all be identified as vinyl C-4 substituted pigments, some of which were simple and others complex. Many of these pigments are present in wine in low concentrations. However, as a group these pigments may prove to be very important to wine colour and therefore wine colour stability. Currently it is very difficult to estimate the relative contribution of each of these pigments to wine colour. New methods need to be developed for the routine quantification of these compounds. These new methods may include improvements to HPLC, or the development of new techniques such as capillary electrophoresis.

While these vinyl C-4 substituted pigments provide a pool of colour stable compounds, is this colour desirable? The colour of vitisin A at wine pH is brick red (λ_{Max} = 501), and therefore it may be proposed that the tawny colour of aged wine may be attributed to the presence of these stable pigments. However, in younger wines these pigments will still contribute to the total pool of pigments and therefore may be considered as important pigments in the overall expression of wine colour.

Using the structural analogy between vitisin A and the other C4 vinyl pigments it can be proposed that the C4 vinyl pigments possess only 3 rings in aqueous solution at wine pH (Figure 8.1). This proposal requires further investigation. HVPE proved useful for structural elucidation of vitisin A by allowing the estimation of its pKa values. However, the possibility of using HVPE to estimate pKa values of the oligomeric pigments, and thereby to establish the structure of these compounds in aqueous solutions is probably limited because these compounds tend to absorb strongly to cellulose support. Therefore, new methods may need to be developed to confirm this proposal.

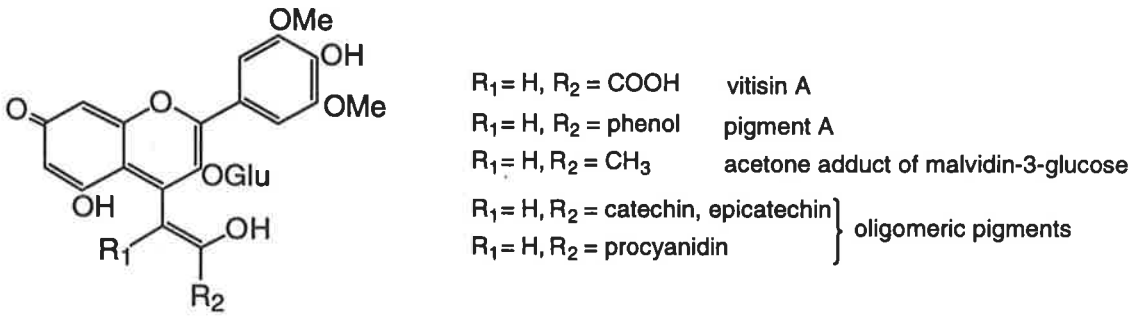

Figure 8.1: Proposed structure of C4 vinyl pigments in wine.

Although the evidence regarding the equilibria of the C4 vinyl pigments in aged wine requires further research, it is possible to extrapolate from the data presented for vitisin A. The protonation and hydration constants from vitisin A (Table 8.1) suggest that, in wine, C4 vinyl pigments exist primarily as the coloured quinonoidal base (ie, the pK_H is sufficiently high that formation of the hemi-ketal is restricted at wine pH). Vitisin A is unusual in that it contains a carboxylic acid, and therefore at wine pH exists in a combination of the quinonoidal base and quinonoidal anion (Figure 8.2). Both the pKa_1 and the pK_{H1} of vitisin

A, were calculated spectroscopically, and therefore the calculation of these constants for the other C4-substituted compounds should be possible. The establishment of pK_{H1} will indicate whether these compounds are hydrated at wine pH (3.2 - 3.8). It is proposed that because the inductive effects of the carboxylate ion are absent in vinyl C4-substituted pigments other than vitisin A, the pK_{H1} of these compounds is greater that that of vitisin A. Therefore in aged wine, where the concentration of grape derived anthocyanins is negligible, the C4 vinyl pigments should contribute significantly towards the colour of wine.

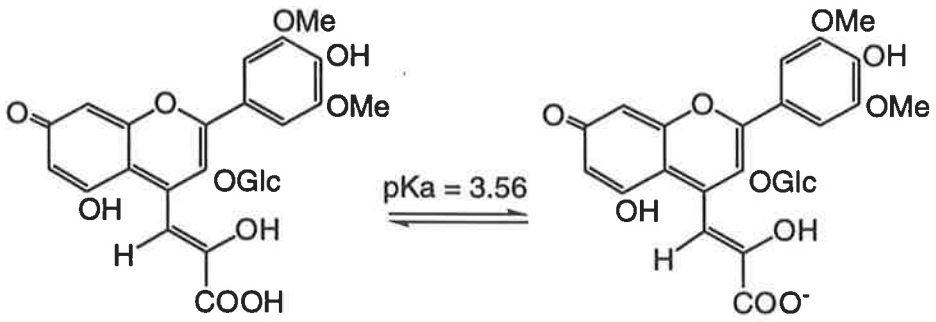

8.2a 8.2b

Figure 8.2: Equilibrium of vitisin A at wine pH (3.2 - 3.8) involves two principle species; (8.2a) the quinonoidal base and (8.2b) the quinonoidal anion.

The concentration of many of the wine pigments is very low, and may be too low for successful isolation from wine. Grape marc extract may serve as an alternative source of many of these compounds. The method utilising bisulphite addition and ion exchange developed during this study proved useful in obtaining extracts of these compounds. However, due to the lengthy procedures involved in extracting these compounds, synthesis may provide a more effective method for obtaining sufficient amounts of the compounds for further research. The methods developed by Fulcrand *et al.*, (1996b), Francia-Aricha *et al.*, (1997), Benabdeljalil, (1998), and Fulcrand *et al.*, (1998), can be used for the synthesis of many of the wine pigments.

The formation of these C4-substituted compounds are interesting because they not only depend on the presence of the anthocyanin, (ie, malvidin-3-glucoside) and a molecule that can undergo an addition reaction, but also on an oxidation step (Chapter 5). Vitisin A

synthesis relies on the presence of pyruvic acid and malvidin-3-glucoside. Pigment A and B formation depend on *p*-vinyl phenol and malvidin-3-glucoside. The synthesis of the malvidin-3-glucoside-4-vinyl type compounds requires vinyl-catechins or vinyl-procyanidins, and malvidin-3-glucoside. The synthesis of vinyl-catechins and vinyl-procyanidins necessitates acetaldehyde reaction with either (epi)-catechin or procyanidin. In addition, the synthesis of vitisin A, and presumably the synthesis of the other C4-substituted pigments, is dependent on the concentration of an as yet unidentified oxidant or oxidants. The evidence presented in this thesis suggests that this oxidation process required for the synthesis of wine pigments can occur both during fermentation and post fermentation (Chapter 6). It is proposed that the greatest rate of vitisin A synthesis occurs during fermentation, because this is when concentration of the required oxidants is their greatest. The results from Chapter 6 indicate that oxidants are released into the wine as a consequence of yeast activity. It is unknown, however, whether the oxidants are the direct result of yeast metabolism or from the breakdown of grape tissue.

Oxidation reactions occurring during fermentation and the presence of endogenous oxidants during maturation have significant implications for wine. These oxidative reactions may have consequential influences upon wine attributes other than pigment formation, such as flavour Moreover these reactions may be important for wine maturation. The concentration of the oxidants, the reactions in which they participate, and the overall significance of oxidation reactions to wine require further investigation.

From the results presented in this thesis, it is proposed that future research into C-4 vinyl pigments should develop improved HPLC separation techniques to quantify these pigments and thereby establish the importance of the various pigments in wine. The isolation of the pigments from red wine should be continued, and methods should be developed for the synthesis of these compounds. With pure pigment samples, structural and spectral analysis will be possible. These analyses should include the estimation of pKa and pK_H values. Furthermore, it may be possible to verify that these C-4 vinyl pigments have a 3-ringed structure and not a 4 ringed structure at wine pH.

The results from this study also suggest that oxidative compounds are released during fermentation, and endogenous oxidants are present after bottling. These oxidants have been implicated in the formation of C-4 vinyl pigments during the winemaking process. Future research is required into the importance of these oxidative processes.

Appendix A

Grams/32 programs

These two short programs were written specifically for the Grams/32 software (Galactic Industries Corp.; New Hampshire, USA) to calculate the absorbance at a particular wavelength.

Quickpoint calculator file

```
' enter the wavelength, x (nm)
      input "Enter an x value:", x
' calculate the absorbance at the wavelength x
      y = #s(x)
' print the wavelength with the corresponding absorbance
      print: x, y
      end
```

Multipoint calculator file

```
' enter a file name
      input "enter name:", name
' define the wavelengths x1, x2, x3,....,xn
      x1 = wavelength 1
      x2 = wavelength 2
      x3 = wavelength 3
' calculate the absorbance (y) at x
' where #s= amplitude (absorbance) at x
      y1 = #s(x1)
      y2 = #s(x2)
      y3 = #s(x3)
' line print by attached printer
      lprint; name
      lprint ; x1, y1
      lprint; x2, y2
      lprint; x3, y3
      end
```

Appendix B

Predicted pKa values of vitisin A

The pKa values for the two different structures of vitisin A proposed by Bakker *et al.* (1997) and Fulcrand *et al.* (1998) were estimated according to the methods presented b y Perrin *et al.* (1981).

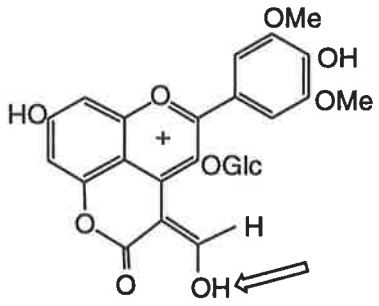

Figure B.1: Structure of vitisin A indicating the proton of interest.

The estimation of the pKa of vitisin A as proposed by Bakker *et al.* (1997; Figure B.1) requires a suitable model. Due to the conjugation between the ketone and the hydroxyl group the compound can be considered as a carboxylic acid.

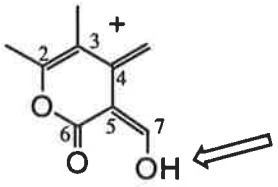

Figure B.2: Structure of vitisin A fragment indicating the proton of interest.

The pKa of a carboxylic acid is approximately 4.8 (Perrin *et al.*, 1981). The conjugation of the hydroxyl group to the ring (ie, the C5-C7 double bond of Figure B.2) for vitisin A provides a means for the unsaturated ring to participate in the acidity of the hydroxyl group. Therefore, the hydroxyl group can be considered to be directly connected to the ring structure. The C4 carbon of vitisin A can be considered to have a δ+ charge. There is however an odd number of conjugated atoms between C4 and the proton of interest, and this will increase the pKa of this fragment. Furthermore, the C2 and C3 carbons, with a δ+ and charge δ- charge respectively, reinforce the δ+ charge of the C4 carbon. Thus, the expected pKa of vitisin will be increased through inductive effects.

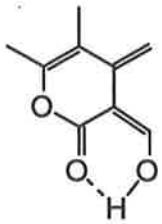

Figure B.3: Internal hydrogen bonding of the vitisin A fragment.

The number of carbons between the hydroxyl group and the ketone, affect the ability for internal hydrogen bonding. A six membered ring is optimal for hydrogen bonding, and therefore will further decrease the acidity.

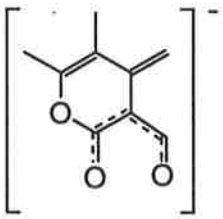

Figure B.4: Resonance stabilises the negative ion the vitisin A fragment.

The possibility of electron sharing between the oxygen groups by resonance will increase the acidity of this compound. Vinylogous carboxylic acids have a pKa between 0.89 and 5.12 (Perrin *et al.*, 1981). However, the effects of inductive effects from the C2, C3 and C4 carbons as well as the effect of hydrogen bonding means that the pKa of vitisin A as proposed by (Bakker *et al.*, 1997) will lie in the upper part of the range, ie 4-5.

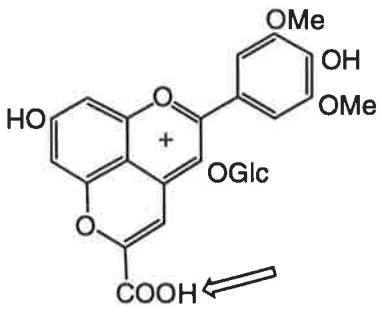

Figure B.5: Structure of vitisin A as proposed by Fulcrand *et al.* (1998) indicating the proton of interest.

Vitisin A as proposed by Fulcrand *et al.* (1998) contains a carboxylic acid (Figure B.5) that can be considered as an aryl acrylic acid, ArHC=C(R)COOH. Using the Taft equation for an aryl acrylic acid,

pKa aryl acrylic acid = 4.45 - 3.48 * σ (Perrin *et al.*, 1981) (Equation B.1)

where σ for OH = 0.13

pKa = 4.45 - 3.48 * 0.13 = 4.0

The estimated pKa of the proton of interest for vitisin A as proposed by Fulcrand *et al.* (1998) is 4.0.

Appendix C

HVPE electrophoretograms

The electrophoretograms (Figure C.1) may show different relative mobilities (RM_{OG}) than those indicated in the text (Chapters 3 - 5). Improvements in the technique have been made since the submission of this thesis and it being returned for revision. This has been achieved by adding a small amount of 1,4-dioxan to the buffer (approximately 1% v/v). It is known that trace metal contamination in the paper can lead to streaking of polyanions in the electrophoretic system at high pH (Seiffert and Agranoff, 1965), and therefore it is thought that the dioxan acting by a similar mechanism improves separation at low pH. Although the relative mobilities using this improved technique were slightly different to the ones reported previously, there was no impact on the apparent pKa values obtained.

The data (Figure C.1) clearly indicates that malvidin-3-glucoside, malvidin-3-(*p*-coumaryl)glucoside and vitisin A are cationic at pH 1.2 and at pH 2.5 malvidin-3-glucoside, malvidin-3-(*p*-coumaryl)glucoside are anionic, whilst vitisin A is neutral. At pH 3.6, which is within the pH range of wine (pH 3.2 - 3.8), the electrophoretograms show that at this pH malvidin-3-glucoside, malvidin-3-(*p*-coumaryl)glucoside are neutral whilst vitisin A is anionic. At higher pH values of pH 7.2 and pH 10.0 both malvidin-3-glucoside, and vitisin A are anionic. The greater mobility of vitisin A pH 7.2 and pH 10.0 indicates a greater charge/mass ratio, which is consistent with a greater anionic charge associated with vitisin A at these pH values (Chapter 5).

Although there is some loss of colour when the electrophoretograms (Figure C.1) due to drying and photographing, the red colouration of the quinonoidal forms of malvidin-3-glucoside, malvidin-3-(*p*-coumaryl)-glucoside at pH 3.6 are clearly observable. The orange colour of vitisin A at pH 3.6 is less well defined and in Figure C.1 is appears red. At the higher pH values of pH 7.2 malvidin-3-glucoside quinonoidal anion appears purple and at pH 10.0 the quinonoidal dianion appears dark blue whilst the quinonoidal dianion of vitisin A at 7.2 appears blue and the quinonoidal trianion of vitisin A at pH 10.0 appears light blue.

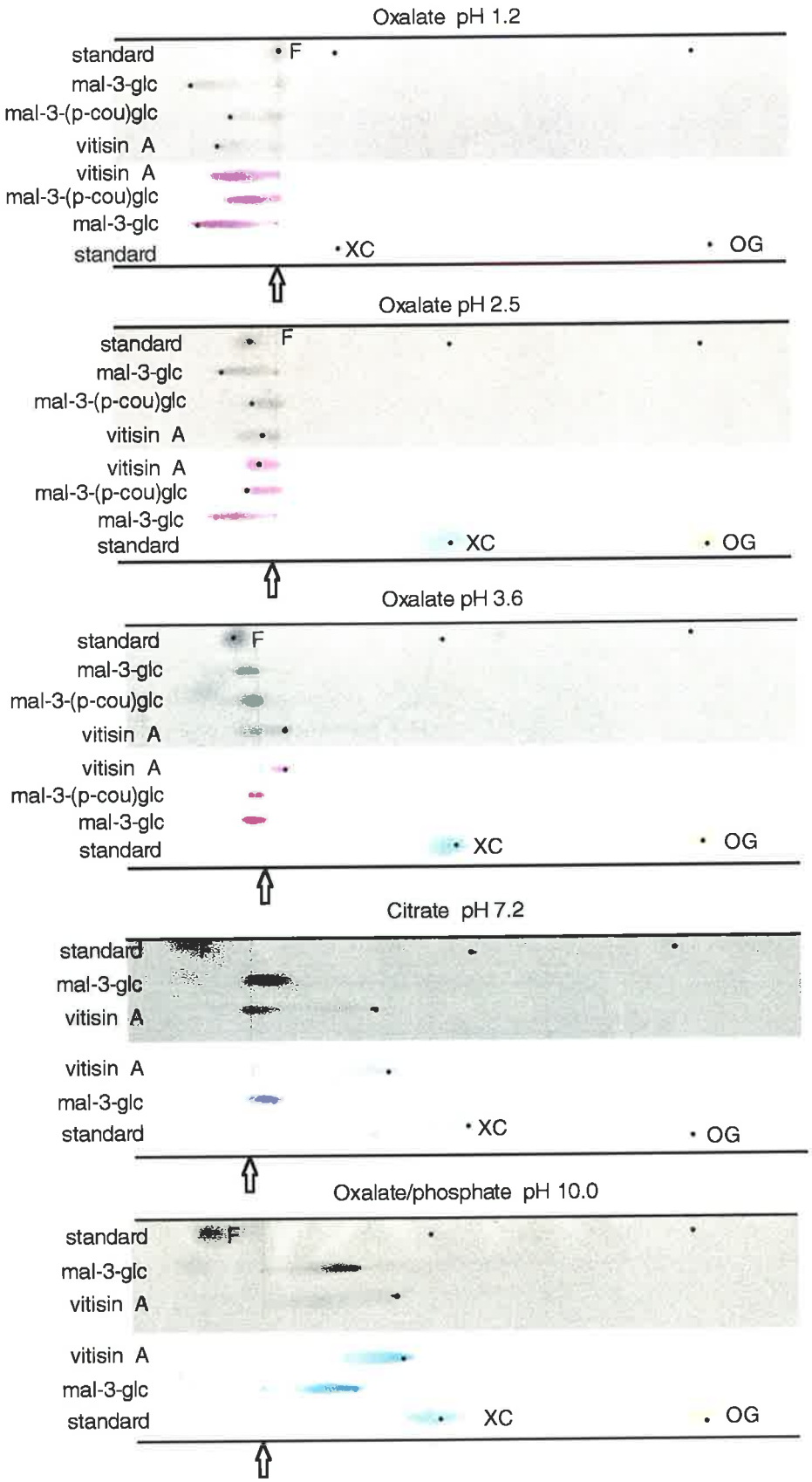

Figure C.1: HVPE electrophoretograms in oxalate buffer (pH 1.2, 2.5, 3.6), citrate buffer (pH 7.2), and oxalate/phosphate buffer (pH 10.0). The top half of each electrophoretogram is stained with silver nitrate (Treveyan, 1950) to reveal the neutral standard fructose (F). XC and OG are the anionic standards xylene cyanol and orange G respectively, and the arrow indicates the origin. Points (•) indicate the location of the greatest concentration of either standard or compound of interest.

References

Adams, J. B. and Woodman, J. S. (1973) "Thermal degradation of anthocyanins with particular reference to the 3-glycosides of cyanidin. II. The anaerobic degradation of cyanidin-3-rutinoside at 100 °C and pH 3.0 in the presence of sodium sulphite." *J. Sci. Fd Agric.* **24**: 763-768.

Aguín, M. L., Vindevogel, J. and Sandra, P. (1993) "Utilisation of the bisulphite addition reaction for the separation of neutral aldehydes by capillary electrophoresis." *Chromatographia* **37**(7/8): 451-454.

Albert, A. and Serjeant, E. P. (1971) *Ionization constants of Acids and Bases* (T. & A. Constable Ltd., Edinburgh, UK).

Allen, M. (1996) "A curious brew." *Chemistry in Britain* **1996**(May): 35-37.

Amic, D., Davidovic-Amic, D. and Beslo, D. (1999) "Prediction of pK values, half lives, and electronic spectra of flavylium salts from molecular structure." *J. Chem. Inf. Comput. Sci.* **1999**(39): 967-973.

Asen, S., Stewart, R. and Norris, K. (1972) "Co-pigmentation of anthocyanins in plant tissues and its effect on color." *Phytochem.* **11**: 1139-1144.

Bakker, J. and Timberlake, C. (1985) "The distribution of anthocyanins in grape skin extracts of port wine cultivars as determined by high performance liquid chromatography." *J. Sci. Fd. Agric.* **36**: 1315-1324.

Bakker, J. and Timberlake, C. F. (1997) "Isolation, identification, and characterisation of new color-stable anthocyanins occurring in some red wines." *J. Agric. Food Chem.* **45**: 35-43.

Bakker, J., Preston, N. W. and Timberlake, C. F. (1986) "The determination of anthocyanins in aging red wines: Comparison of HPLC and spectral methods." *Am. J. Enol. Vitic.* **37**(2): 121-126.

Bakker, J., Picinelli, A. and Brindle, P. (1993) "Model wine solutions: Colour and composition changes during ageing." *Vitis* **32**: 111-118.

Bakker, J., Bridle, P., Honda, T., Kuwano, H., Saito, N., Terahara, N. and Timberlake, C. F. (1997) "Identification of an anthocyanin occurring in some red wines." *Phytochem.* **44**(7): 1375-1382.

Bakker, J., Bridle, P., Bellworthy, S. J., Garcia-Viguera, C., Reader, H. P. and Watkins, S. J. (1998) "Effect of sulphur dioxide and must extraction on colour, phenolic composition and sensory quality of red table wine." *J. Sci. Fd Agric.* **78**: 297-307.

Baranowski, E. and Nagel, C. (1983) "Kinetics of malvidin-3-glucoside condensation in wine model systems." *J. Food Sci.* **48**: 419-429.

Baumes, R., Cordonnier, R., Nitz, S. and Drawert, F. (1986) "Identification and determination of volatile constituents in wines from different cultivars." *J. Sci. Food Chem.* **37**: 927-943.

Beechey, R. B. and Ribbons, D. W. (1972). "Oxygen electrode measurements" In *Methods in Microbiology,* Vol. 6B, pp 25-53. Edited by J. R. Norris and D. W. Ribbons. (Academic Press, London)

Bellamy, L. J. (1975) *The infra-red spectra of complex molecules* (Chapman and Hall, London, UK) 433p.

Benabdeljalil, C. (1998) "*Valorisation de la matiere colorante des marcs des raisin: mise en evidence de nouveaux pigments.*", PhD. Thesis, Universite Mohammed V, Faculte des Sciences, Rabat, Morocco.

Benabdeljalil, C., Cheynier, V., Fulcrand, H., Hakiki, A., Mosaddak, M. and Moutounet, M. (2000) "Mise en evidence de nouveaux pigments formes par reaction des anthocyanes avec des metabolites de levure." *Sciences des Aliments* **20**: 203-220.

Berké, B., Chèze, C., Vercauteren, J. and Deffieux, G. (1998) "Bisulphite addition to anthocyanins: revisited structures of colourless adducts." *Tetrahedron Letters* **39**: 5771-5774.

Blackburn, M., Sankey, G. B., Robertson, A. and Whalley, W. B. (1957) "Reactions of flavylium salts with dimethylaniline and malonic acid." *J. Chem. Soc.* **1957**: 1573-1576.

Brouillard, R. (1981) "Origin of the exceptional colour stability of the *Zebrina* anthocyanin." *Phytochem.* **20**: 143-145.

Brouillard, R. and Cheminat, A. (1988) "Flavonoids and plant colour." In *Plant Flavonoids in Biology and Medicine II. Biochemical, Cellular, and Medicinal Properties,* Proceedings of a Meeting on Plant Flavonoids in Biology and Medicine, Strasbourg, France, pp 93-96, Edited by V. Cody, E. Middleton, J. B. Harborne and A. Beretz (Liss, New York, USA)

Brouillard, R. and Dangles, O. (1993). "Flavonoids and flower colour." In *The flavonoids: Advances in research since 1986.,* pp 565-588. Edited by J. Harborne. (Chapman and Hall; New York, USA; London, UK)

Brouillard, R. and Delaporte, B. (1977) "Chemistry of anthocyanin pigments. 2. Kinetic and thermodynamic study of proton transfer, hydration, and tautomeric reactions of malvidin 3-glucoside." *J. Am. Chem. Soc.* **99**(26): 8461-8468.

Brouillard, R. and Dubois, J. (1977) "Mechanism of the structural transformations of anthocyanins in acidic media." *J. Am. Chem. Soc.* **99**(5): 1359-1364.

Brouillard, R. and Hage-Chahine, J. E. (1980) "Chemistry of anthocyanin pigments. 6. Kinetic and thermodynamic study of hydrogen sulphite addition to cyanin, Formation of a highly stable Meisenheimer-Type adduct from a 2-phenylbenzopyrylium salt." *J. Am. Chem. Soc.* **102**: 5375-5378.

Brouillard, R. and Lang, J. (1990) "The hemiacetal-*cis*-chalcone equilibrium of malvin, a natural anthocyanin." *Can. J. Chem.* **68**: 755-761.

Brouillard, R., Iacobucci, G. A. and Sweeney, J. G. (1982) "Chemistry of anthocyanin pigments. 9. UV-Visible spectrophotometric determination on the acidity constants of apigenin and three related 3-deoxyflavylium salts." *J. Am. Chem. Soc.* **104**(26): 7585-7590.

Brouillard, R., Mazza, G., Saad, Z., Albrecht-Gary, A. and Cheminat, A. (1989) "The copigmentation reaction of anthocyanins: A microprobe for the structural study of aqueous solutions." *J. Am. Chem. Soc.* **111**: 2604-2610.

Bunting, J. W. (1979). "Heterocyclic pseudobases" *Advances in Heterocyclic Chemistry,* **25:** 1-82.

Burroughs, L. F. (1975) "Determining free sulphur dioxide in red wine." *Am. J. Enol. Vitic.* **26**(1): 25-29.

Burroughs, L. F. (1981) "Dissociable products formed with sulphur dioxide in wine." *J. Sci. Food Agric.* **32**: 1140-1144.

Burroughs, L. F. and Sparks, A. H. (1973a) "Sulphite-binding power of wines and ciders. I. Equilibrium constants for the dissociation of carbonyl bisulphite compounds." *J. Sci. Fd. Agric.* **24**: 187-198.

Burroughs, L. F. and Sparks, A. H. (1973b) "Sulphite-binding power of wines and ciders. II. Theoretical consideration and calculation of sulphite-binding equilibria." *J. Sci. Fd Agric.* **24**: 199-206.

Burroughs, L. F. and Sparks, A. H. (1973c) "Sulphite-binding power of wines and ciders. III. Determination of carbonyl compounds in a wine and calculation of its sulphite binding power." *J. Sci. Fd Agric.* **24**: 207-217.

Cabrita, L., Fossen, T. and Andersen, O. M. (2000) "Colour and stability of the six common anthocyanidin 3-glucosides in aqueous solutions." *Food Chem.* **68**: 101-107.

Cavin, J. F., Andioc, V., Etievant, P. X. and Divies, C. (1993) "Ability of wine lactic acid bacteria to metabolise phenol carboxylic acids." *Am. J. Enol. Vitic.* **44**(1): 76-80.

Chatonnet, P., Dubourdieu, D., Boidron, J. and Lavigne, V. (1993) "Synthesis of volatile phenols by *Saccharomyces cerevisiae* in wines." *J. Sci. Food Agric.* **62**: 191-202.

Chatonnet, P., Dubourdieu, D. and Boidron, J. N. (1995) "The influence of *Brettanomyces/Dekkera* sp. yeasts and lactic acid bacteria on the ethylphenol content of red wines." *Am. J. Enol. Vitic.* **46**(4): 463-468.

Chatonnet, P., Viala, C. and Dubourdieu, D. (1997) "Influence of polyphenolic components of red wines on the microbial synthesis of volatile phenols." *Am. J. Enol. Vitic.* **48**(4): 443-448.

Cheynier, V., Fulcrand, H., Sarni, P. and Moutounet, M. (1997a) "Reactivity of phenolic compounds in wine: diversity of mechanisms and resulting products." Proceedings *In Vino Analytica Scientia*, Bordeaux, France. pp 143-154.

Cheynier, V., Fulcrand, H., Sarni, P. and Moutounet, M. (1997b) "Application des techniques analytiques à l'étude des composés phénoliques et de leurs réactions au cours de la vinification." *Analysis* **25**(3): M14-M20.

Cheynier, V., Doco, T., Guyot, S., Le Roux, E., Souquet, J. M., Rigaud, J. and Moutounet, M. (1997c) "ESI-MS analysis of polyphenolic oligomers and polymers." *Analusis* **25**(8): 32-37.

Clark, W. M. (1928) *The determination of hydrogen ions* (Bailliere, Tindall and Cox., London, UK) 171p

Collins, D. A., Haworth, F., Isarasena, K. and Robertson, A. (1950) "The pigments of "Dragons Blood" resin. Part I. Dracorubin." *J. Chem. Soc.* **1950**: 1876-1881.

Dallas, C. and Laureano, O. (1994a) "Effects of pH, sulphur dioxide, alcohol content, temperature and storage time on colour composition of a young Portuguese red table wine." *J. Sci. Fd Agric.* **65**: 477-485.

Dallas, C. and Laureano, O. (1994b) "Effect of SO_2 on the extraction of individual anthocyanins and colored matter of three Portuguese grape varieties during winemaking." *Vitis* **33**: 41-47.

De Sapio, R., (1978) *Calculus for the life sciences* (W. H. Freeman and Company, San Francisco, USA) 740p

Donner, S.C. (1997) "Agrocins from agrobacteria." PhD Thesis, The University of Adelaide, Australia.

Escribano-Bailón, T., Dangles, O. and Brouillard, R. (1996) "Coupling reactions between flavylium ions and catechin." *Phytochem.* **41**(6): 1583-1592.

Figueiredo, P., Lima, J. C., Santos, H., Wigland, M., Brouillard, R., Maçanita, A. L. and Pina, F. (1994) "Photochromism of the synthetic 4',7-dihydroxyflavylium chloride." *J. Am. Chem. Soc.* **116**: 1249-1254.

Figueiredo, P., Elhabiri, M., Saito, N. and Brouillard, R. (1996a) "Anthocyanin intramolecular interactions. A new mathematical approach to account for the remarkable colorant properties of the pigments extracted from *Matthiola incana*." *J. Am. Chem. Soc.* **118**: 4788-4793.

Figueiredo, P., Elhabiri, M., Toki, K., Saito, N., Dangles, O. and Brouillard, R. (1996b) "New Aspects of Anthocyanin complexation. Intramolecular copigmentation as a means for colour loss?" *Phytochem.* **41**(1): 301-308.

Fong, R. A., Kepner, R. E. and Webb, A. D. (1971) "Acetic-acid-acylated anthocyanin pigments in the grape skins of a number of varieties of *Vitis vinifera*." *Am. J. Enol. Vitic.* **3:** 150-155.

Francia-Aricha, E. M., Guerra, M. T., Rivas-Gonzalo, J. C. and Santos-Buelga, C. (1997) "New anthocyanin pigments formed after condensation with flavonols." *J. Agric Food Chem.* **45**: 2262-2266.

Frayne, R. F. (1986) "Direct analysis of the major organic components in grape must and wine using high performance liquid chromatography." *Am. J. Enol. Vitic.* **37**(4): 281-287.

Fulcrand, H., Doco, T., Es-Safi, N., Cheynier, V. and Moutounet, M. (1996a) "Study of acetaldehyde induced polymerisation of flavan-3-ols by liquid chromatography-ion spray mass spectrometry." *J. Chromatog. A* **752**: 85-91.

Fulcrand, H., dos Santos, P., Sarni-Manchado, P., Cheynier, V. and Favre-Bonvin, J. (1996b) "Structure of new anthocyanin-derived wine pigments." *J. Chem. Soc. Perkin Trans. I.* pp735-739.

Fulcrand, H., Benabdeljalil, C., Rigaud, J., Cheynier, V. and Moutounet, M. (1998) "A new class of wine pigments generated by reaction between pyruvic acid and grape anthocyanins." *Phytochem.* **47**(7): 1401-1407.

García-Viguera, C., Brindle, P. and Bakker, J. (1994) "The effect of pH on the formation of coloured compounds in model solutions containing anthocyanins, catechin and acetaldehyde." *Vitis* **33**: 37-40.

Cheminat, A. and Brouillard, R. (1986) "PMR investigation of 3-*O*-(β-D-glucosyl)malvidin structural transformations in aqueous solutions." *Tetrahedron Letters* **27**(37): 4457-4460.

Goto, T. and Kondo, T. (1991) "Structure and molecular stacking of anthocyanins-flower colour variation." *Agnew. Chem. Int. Ed. Eng.* **30**: 17-33.

Gueffroy, D., Kepner, R. and Webb, A. (1971) "Acylated anthocyanin pigments in Vitis vinifera grapes: identification of malvidin-3-(6-*p*-coumaroyl) glucoside." *Phytochem.* **10**: 813-819.

Harborne, J. (1989). "General procedures and measurement of total phenolics." In *Methods in Plant Biochemistry,* Vol. 1, pp 1-28. Edited by J. Harborne. (Academic Press Limited, London, UK)

Haslam, E. (1980) "*In Vino Veritas* : Oligomeric procyanidins and the aging of red wines." *Phytochem.* **19**: 2577-2582.

Hirst, E. L. (1927) "Derivatives of Orcinol. Part I." *J. Chem. Soc.* **1927**: 2490-2495.

Hoshino, T., Matsumoto, U. and Goto, T. (1981) "Self-association of some anthocyanins in neutral aqueous solution." *Phytochem.* **20**(8): 1971-1976.

Houbiers, C., Lima, J. C., Macanita, A. L. and Santos, H. (1998) "Color stabilisation of malvidin-3-glucose: self aggregation of the flavylium cation and copigmentation with the z-chalcone form." *J. Phys. Chem. B* **102**: 3578-3585.

Hrazdina, G. and Franzese, A. (1974) "Structure and properties of the acylated anthocyanins from *Vitis* species." *Phytochem.* **13**: 225-229.

Iland, P. G., Cynkar, W., Francis, I. L., Williams, P. J. and Coombe B. G. (1996) "Optimisation of total and red-free glycosyl glucose in black berries of Vitis vinifera" *Aust. J. Grape Wine Res.* **2:** 171-178

Iland, P., Ewart, A. and Sitters, J. (1993) *Techniques for chemical analysis and stability tests of grape juice and wine* (Patrick Iland Wine Promotions, Campbelltown, South Australia) 65p

Johnson, T. and Morris, J. (1996) "Circular dichroism and spectroscopic studies of *Vitis vinifera* cv. Cabernet Sauvignon and *Vitis rotundifolia* cv. Noble Red wine liquid chromatographic fractions." *Am. J. Enol. Vitic.* **47**(3): 323-328.

Jokl, V. (1964a) "Studium der Komplexverbindungen in lösung mittels Papier-elektrophorese. I. Electrophoretische beweglikeit und zusammensetzung der Komplexe." *J. Chromatog.* **13**: 451-458.

Jokl, V. (1964b) "Studium der Komplexverbindungen in lösung mittels Papier-elektrophorese. II. Electrophoretische beweglikeit und stabilität der einkernigen Komplexe." *J. Chromatog.* **14**: 71-78.

Jokl, V. (1972) "Papierelektrophorese von metallionen in EDTA Ligendpuffern. I. Theoretische behandlung." *J. Chromatog.* **71**: 523-531.

Josien, M. L., Fusen, N., Labas, J. M. and Gregory, T. M. (1953) "An infrared spectroscopic study of the carbonyl stretching frequency in a group of *ortho* and *para* quinones." *J. Chem. Phys.* **21**(2): 331-340.

Jurd, L. (1969) "Review of the polyphenol condensation reactions and their possible occurrence in the aging of wines." *Am. J. Enol. Vitic.* **20**: 191-195.

Koeppen, B. H. and Basson, D. S. (1966) "The anthocyanin pigments of Barlinka grapes." *Phytochem.* **6**: 183-187.

Kortüm, G., Vogel, W. and Andrussow, K. (1961) *Dissociation constants of organic acids in aqueous solution.* For the, 'International Union of Pure and Applied Chemistry. Commission on Electrochemical Data', (Butterworths, London, UK) 547p

Kristiansen, K. (1984) "Biosynthesis of proanthocyanidin in barley: genetic control of the conversion of dihydroquercetin to catechin and procyanidins." *Carlsberg Res. Commun.* **49**: 503-524.

Levengood, J. S. (1996) "*A survey of copigmentation in Cabernet Sauvignon*", Masters Thesis University of California, Davis, USA

Levy, L. and Robinson, R. (1931) "Experiments on the synthesis of anthocyanin. Part IX. Synthesis of oxycoccicyanin chloride. Observations on the distribution numbers of the anthocyanins." *J. Chem. Soc.* **1931**: 2715-2722.

Levy, L. F., Posternak, T. and Robinson, R. (1931) "Experiments on the synthesis of the anthocyanins. Part VIII. A synthesis of oenin chloride." *J. Chem. Soc.* **1931**: 2701-2715.

Liao, H., Cai, Y. and Haslam, E. (1992) "Polyphenol interactions. Anthocyanins: co-pigmentation and colour changes in red wines." *J. Sci. Fd Agric.* **59**: 299-305.

Markakis, P. (1960) "Zone electrophoresis of anthocyanins." *Nature* **187**: 1092-1093.

Markham, R. and Smith, J. D. (1951) "Structure of ribonucleic acid." *Nature* **168**: 406-408.

Markham, R. and Smith, J. D. (1952) "The structure of ribonucleic acids." *Biochem. J.* **52**: 552-557.

Mazza, G. and Brouillard, R. (1987) "Color stability and structural transformations of cyanidin 3,5-diglucoside and four 3-deoxyanthocyanins in aqueous solutions." *J. Agric. Food Chem.* **35**: 422-426.

Mazza, G. and Brouillard, R. (1990) "The mechanism of co-pigmentation of anthocyanins in aqueous solutions." *Phytochem.* **29**(4): 1097-1102.

Mazza, G. and Miniati, E. (1993) *Anthocyanins in fruits, vegetables and grains.* (CRC Press, Boca Raton, USA) 262p

McClelland, R. A. and Gedge, S. (1980) "Hydration of the flavylium ion." *J. Am. Chem. Soc.* 102: 5838-5848.

McClelland, R., Devine, D. and Sørensen, P. (1985) "Hemiacetal formation with a phenol nucleophile: Simple proton transfers as rate limiting steps." *J. Am. Chem. Soc.* **107**: 5459-5463.

Michnick, S., Roustan, J. L., Remize, F. and Barre, P. (1997) "Modulation of glycerol and ethanol yields during alcoholic fermentation in *Saccharomyces cerevisiae* strains over expressed or disrupted for *GPD1* encoding glycerol 3-phosphate dehydrogenase." *Yeast* **13**: 783-793.

Mistry, T., Cai, Y., Lilley, T. and Haslam, E. (1991) "Polyphenol interactions. Part 5. Anthocyanin co-pigmentation." *J. Chem. Soc. Perkin Trans. II.* pp1287-1296.

Nagel, C. and Wulf, L. (1979) "Changes in the anthocyanins, flavonoids and hydroxycinnamic acid esters during fermentation and aging of Merlot and Cabernet Sauvignon." *Am. J. Enol. Vitic.* **30**(2): 111-116.

Niketic-Aleksic, G. K. and Hrazdina, G. (1972) "Quantitative analysis of the anthocyanin content in grape juices and wines." *Lebensm. Wiss. u. Technol.* **3**(5): 163-165.

Perrin, D. D., Dempsey B. and Serjeant, E. P. (1981) *pKa Prediction for organic acids and bases.* (Chapman and Hall, London, UK) 146p

Pina, F. (1998) "Thermodynamics and kinetics of flavylium salts revisited." *J. Chem. Soc. Faraday Trans.*, **94**(15): 2109-2116.

Pronk, J. T., Wenzel, T. J., Luttik, M. A. H., Klaasen, C. C. M., Scheffers, W. A., Steensma, H. Y. and van Dijken, J. P. (1994) "Energetic aspects of glucose metabolism in a pyruvate-dehydrogenase-negative mutant of *Saccharomyces cerevisiae*." *Microbiology* **140**: 601-610.

Randall, H. M., Fowler, R. G., Fuson, N. and Dangl, J. R. (1949) *Infrared determination of organic structures* (D. Van Nostrand Co. Inc., New York, USA) 239p

Rapp, A. and Mandery, H. (1986) "Wine Aroma." *Experientia* **42**: 873-884.

Remy, S., Fulcrand, H., Labarbe B., Cheynier, V., and Moutounet, M. (2000) "First confirmation in red wine of products resulting from the direct anthocyanin-tannin reactions." *J. Sci. Food Agric.* **80**: 745-751

Revilla, I., Pérez-Magariño, S., González-SanJosé, M. L. and Beltrán, S. (1999) "Identification of anthocyanin derivatives in grape skin extracts and red wines by liquid chromatography with diode array and mass spectrometric detection." *J. Chromatogr. A.* **847**: 83-90.

Ribéreau-Gayon, P. (1973). "The chemistry of red wine colour." In *Chemistry of Winemaking,* pp 50-87. Edited by A. Webb. (American Chemical Society, Washington D. C., USA)

Ribéreau-Gayon, P. and Josien, M. L. (1960) "Contribution à l'étude des anthocyannes par spectrométrie infrarouge." *Bull. Soc. Chim. France* **1960**: 934-937.

Robertson, A. and Whalley, W. B. (1950) "The pigments of "Dragon's Blood" resin. Part II. A synthesis of dracorhodin." *J. Chem. Soc.* **1950**: 1882-1884.

Robinson, G. and Robinson, R. (1931) "A survey of anthocyanins. I." *Biochem.* **25**: 1687-1705.

Romero, C. and Bakker J. (1999) "Interactions between grape anthocyanins and pyruvic acid, with effect of pH and acid concentration on anthocyanin composition and colour in model solutions." *J. Agric. Food Chem.* **47**: 3130-3139.

Romero, C. and Bakker, J. (2000) "Effect of acetaldehyde and several acids on the formation of vitisin A in model wine anthocyanin and colour evolution." *Int. J. Food Sci. Tech.* **35**: 129-140.

Rossotti, F. J. C. and Rossotti, H. (1961) *The Determination of Stability constants and other equilibrium constants in solution.* McGraw-Hill Book Company, New York, USA

Ryder, M. H., Tate, M. E. and Jones, G. J. (1984) "Agrocinopine A, a tumor-inducing plasmid-coded enzyme product, is a phosphodiester of sucrose and L-arabinose." *J. Biol. Chem.* **259**(15): 9704-9710.

Santos, H., Turner, D., Lima, J., Figueiredo, P., Pina, F. and Maçanita, A. (1993) "Elucidation of the multiple equilibria of malvin in aqueous solution by one- and two-dimensional NMR." *Phytochem.* **33**(5): 1227-1232.

Scheffeldt, P. and Hrazdina, G. (1978) "Co-pigmentation of anthocyanins under physiological conditions." *J. Food Sci.* **43**: 517-520.

Schmidt, M. and Siebert, W. (1975) "The chemistry of sulphur", In *The chemistry of Sulphur Selenium, Tellurium and Polonium.* Edited by M. Schmidt, W. Siebert, and K. W. Bagnell, As part of the series *Comprehensive Inorganic Chemistry, Chapter 23,24* (Pergamon Press, Oxford, UK)

Schneider, A., Gerbi, V. and Redoglia, M. (1987) "A rapid HPLC method for separation and determination of major organic acids in grape musts and wines." *Am. J. Enol. Vitic.* **38**(2): 151-155.

Seiffert, U.B. and Agranoff, B.W. (1965) "Isolation and separation of inositol phosphates from hydrolysates of rat tissue." *Biochim. Biophys. Acta* **98**: 574-581

Somers, T. (1966) "Grape phenolics: The anthocyanins of *Vitis vinifera* , variety Shiraz." *J. Sci. Fd Agric.* **17:** 215-219.

Somers, T. (1971) "The polymeric nature of wine pigments." *Phytochem.* **10**: 2175-2186.

Somers, T. C. (1980) "Pigment phenomena - from grapes to wine." Proceedings *1880-1980 University of California, Davis, Grape and Wine Centenary*, pp 254-257, University of California, Davis, USA

Somers, T. and Evans, M. (1977) 'Spectral evaluation of young red wines: anthocyanin equilibria, total phenolics, free and molecular SO_2, "Chemical Age".' *J. Sci. Fd Agric.* **28**: 279-287.

Somers, T. and Vérette, E. (1988). "Phenolic composition of natural wine types." In *Modern Methods of Plant Analysis,* Vol. 6 pp 219-257. Edited by H. Linskens and J. Jackson (Springer Verlag, Berlin, Heidelberg, Germany)

Somers, T. C. and L.G., Wescombe. (1982) "Red wine quality: The critical role of SO_2 during vinification and conservation." *Aust. Grapegrower & Winemaker* **220**: 68, 70, 72, 74.

Spagna, G. and Pifferi, P. G. (1992) "Purification and separation of oenocyanin anthocyanins on sulphoxyethylcellulose." *Food Chem.* **44**: 185-188.

Steinke, R. D. and Paulson, M. C. (1964) "The production of steam-volatile phenols during the cooking and alcoholic fermentation of grain." *J. Agric. Food Chem.* **12**(4): 381-387.

Tate, M. E. (1968) "Separation of myoinositol pentaphosphates by moving paper electrophoresis (MPE)." *Anal. Biochem.* **23**: 141-149.

Tate, M. (1981) " Determination of ionization constants by paper electrophoresis." *Biochem. J.* **195**: 419-426.

Tate, M. E., Ellis, J. G., Kerr, A., Tempe, J., Murray, K. E. and Shaw, K. J. (1982) "Agropine: A revised structure." *Carbohydr. Res.* **104**: 105-120.

Theander, O. (1957) "Paper ionophoresis of aldehydes and ketones in the presence of hydrogen sulphite." *Acta Chem. Scan.* **11**: 717-723.

Timberlake, C. F. (1980) "Factors affecting red wine colour: the use of a 'coloration' constant in evaluating red wine color." Proceedings *1880-1980 University of California, Davis. Grape and Wine Centenary*, pp 240-244, University of California, Davis, USA

Timberlake, C. and Bridle, P. (1967a) "Flavylium salts, anthocyanidins and anthocyanins I. Structural transformations in acid solutions." *J. Sci. Fd Agric.* **18**: 473-478.

Timberlake, C. and Bridle, P. (1967b) "Flavylium salts, anthocyanidins and anthocyanins II. Reactions with sulphur dioxide." *J. Sci Fd Agric.* **18**: 479-485.

Timberlake, C. F. and Bridle, P. (1968) "Flavylium salts resistant to sulphur dioxide." *Chem. and Ind.* **1968**: 1489.

Trevelyan, W. E., Proctor, D. P. and Harrison, J. S. (1950) "Detection of sugars on paper chromatograms." *Nature* **166**: 444-445.

van Buren, J., Bertino, J. and Robinson, W. (1968) "The stability of wine anthocyanins on exposure to heat and light." *Am. J. Enol. Vitic.* **19**: 147-154.

Vasserot, Y., Caillet, S. and Maujean, A. (1997) "Study of anthocyanin adsorption by yeast lees. Effect of some physico-chemical parameters." *Am. J. Enol. Vitic.* **48**(4): 433-437.

Volod'kin, A. A. and Ershov, V. V. (1988) "Stable methylenequinones." *Russ. Chem. Rev. (Engl. Transl.)* **57**(4): 336-349.

Wawzonek, S. (1951). "Chromenols, chromenes and benzopyrylium salts the anthocyanins." In *Heterocyclic compounds,* Vol. 2, pp 277-342, Edited by R. C. Elderfield. (John Wiley and Sons Inc., New York, USA)

Williams, D. H. and Fleming, I. (1989) *Spectroscopic methods in organic chemistry* (McGraw-Hill Book Co., London, UK) 264p

Willstätter, R. and Zollinger, E. H. (1916) "XVI. Über die Farbstoffe der Weintraube und der Heidelbeere, II." *Annalen* **412**: 195-216.

Wizinger, R. and Luthiger, A. (1953) "Über eine einfache Synthese von Flavyliumfarbsalzen." *Helv. Chim. Acta* **36**(2): 526-530.

Wulf, L. W. and Nagel, C. W. (1978) "High pressure liquid chromatographic separation of anthocyanins of Vitis vinifera." *Am. J. Enol. Vitic.* **29**(1): 42-49.